Molecular Mechanisms of the Rapid and Weight Loss-Independent Beneficial Cardiovascular Effects of Roux-en-Y Gastric Bypass Surgery

Dissertation

zur

Erlangung der naturwissenschaftlichen Doktorwürde

(Dr. sc. nat.)

vorgelegt der

Mathematisch-naturwissenschaftlichen Fakultät

der

Universität Zürich

von

Petia Ivanova Doytcheva

aus Bulgarien

Promotionskomitee

Prof. Dr. Thomas A. Lutz (Vorsitz)

Prof. Dr. Arnold von Eckardstein

Prof. Dr. Christian Wolfrum

Prof. Dr. Bart Staels

Dr. Elena Osto

Zürich, 2016

Table of contents

1. Summary

Obesity is one of the major disease epidemics of the modern world because if its high prevalence – approximately 10% of the global population is obese, and approximately 30% is overweight – and because of its high association with cardiovascular disease and mortality. Currently the only effective anti-obesity treatment to induce sufficient weight loss and to decrease associated cardiovascular disease and mortality is bariatric, or gastrointestinal surgery. The current "gold standard" bariatric procedure is Roux-en-Y gastric bypass (RYGB), where a small part of the stomach is directly connected to the distal small intestine while the rest of the stomach and the proximal small intestine are bypassed, resulting in restriction of food intake and in an altered nutrient flow through the gastrointestinal tract. Presently it is not known whether the beneficial effects of RYGB on energy metabolism and the cardiovascular system are entirely mediated by weight loss, or there are also other weight-independent mechanisms involved. We hypothesized that RYGB surgery improves obesity-induced endothelial and high-density lipoprotein (HDL) dysfunction rapidly and independently of weight loss through glucagon-like peptide-1 (GLP-1) and c-jun N-terminal kinase (JNK) dependent mechanisms. To test this hypothesis, we performed RYGB surgery in diet-induced obese rats and studied *ex vivo* endothelial function and *in vitro* HDL functional properties 8 days after surgery; weight-dependent and -independent effects were assessed using sham-operated ad libitum-fed and sham-operated body weight-matched control groups. The roles of GLP-1 and JNK in mediating the beneficial cardiovascular effects of RYGB were assessed using *in vivo* pharmacological agonists and/or antagonists of GLP-1 and JNK. In addition, we assessed the *in vitro* HDL functional properties of RYGB patients before and shortly after RYGB surgery. We demonstrate that in rats RYGB improves endothelial function and HDL endothelial protective properties independently of weight loss within 8 days after surgery; in humans HDL protective properties improve within 2 weeks and 3 months after surgery. The effect on endothelial function was mediated by GLP-1 receptor-dependent JNK2 inhibition in aorta, and the effect on HDL function was mediated by GLP-1 receptor-independent mechanisms. These results highlight novel roles of GLP-1 and JNK2 in the restoration of obesity-induced endothelial dysfunction after RYGB. This knowledge could be exploited in the future to develop new non-invasive anti-obesity treatments that mimic the weight loss-independent effects of RYGB.

2. Zusammenfassung

Adipositas (Fettleibigkeit) zählt wegen ihrer Häufigkeit – etwa 10 % der Weltbevölkerung sind adipös und circa 30 % sind übergewichtig – und wegen des häufigen Auftretens kardiovaskulärer Begleiterkrankungen zu den grössten Epidemien der Moderne. Eine gastrointestinale Operation ist die derzeit einzig effektive Behandlung, die sowohl genügend Gewichtsreduktion, als auch eine Verringerung des kardiovaskulären Risikos induziert. Der aktuelle Goldstandard ist der Roux-en-Y-Magenbypass (RYMB), der zu einer Verminderung der Nahrungsaufnahme und einem veränderten Nahrungsmittelfluss durch den Gastrointestinaltrakt führt. Bisher ist nicht bekannt, ob die positive Effekte des RYMB auf Metabolismus und kardiovaskuläres System einzig durch den Gewichtsverlust vermittelt werden, oder ob zusätzlich andere gewichtsunabhängige Mechanismen beteiligt sind. Wir stellten die Hypothese auf, dass nach einem RYMB adipositasinduzierte HDL- und Endotheldysfunktion verbessert werden und dass dies schnell und unabhängig von einem Gewichtsverlust aufgrund GLP-1 und JNK-abhängiger Mechanismen geschieht. Um diese Behauptung zu testen untersuchten wir Endothelfunktion und HDL-Eigenschaften in RYMB-operierten adipösen Ratten 8 Tage nach dem Eingriff. Gewichtsabhängige und –unabhängige Effekte wurden mit Hilfe von placebooperierten gewichtsangepassten Kontrolltieren beurteilt. Die Rollen von GLP-1 und JNK bei der Vermittlung der positiven Effekte des RYMB wurden *in vivo* mittels Einsatz pharmakologischer Agonisten und/oder Antagonisten betrachtet. Zusätzich wurde HDL bezüglich seiner funktionellen Eigenschaften in RYMB-Patienten vor und nach dem Eingriff analysiert. Wir konnten zeigen, dass RYMB in Ratten Endothelfunktion und HDL-Beschaffenheit unabhängig von einem Gewichtsverlust innerhalb von 8 Tagen nach Operation verbessert. Im Patienten verbesserten sich die HDL-Eigenschaften innerhalb von 2 Wochen bis 3 Monaten nach RYMB. Der Effekt auf die Endothelfunktion wurde in Aortae durch GLP-1-rezeptorabhängige JNK2-Inhibierung vermittelt, während der Effekt auf HDL unabhängig vom GLP-1-Rezeptor stattfand. Diese Ergebnisse zeigen neue Rollen für GLP-1 und JNK2 in der Wiederherstellung der Endothelfunktion von Adipositaspatienten nach RYMB auf. In Zukunft könnten diese Erkenntnisse genutzt werden, um neue nichtinvasive Therapien der Adipositas mit vergleichbaren Effekten eines RYMB zu entwickeln.

3. Introduction

3.1 Prevalence of obesity

Obesity, defined as a body mass index (BMI, calculated as the weight in kilograms divided by the height in squared meters) over 30 kg/m^2 (normal BMI between 18-24.9 kg/m^2), is one of the major health epidemics of the contemporary world [1]. The worldwide prevalence of adult overweight (BMI between 25-29.9 kg/m^2) and obesity combined has increased from 28.8% in 1980 to 36.9% in 2013 for men, and from 29.8% in 1980 to 38% in 2013 for women, which corresponds to a total increase of 27.5% over three decades [1]. In 2014, the global prevalence of obesity was 10.8% for men and 14.9% for women [2]. BMI increases with age, reaching a peak of 60% overweight and 25% obese men at 55 years of age, and a peak of 64.5% overweight and 31.3% obese women at 60 years of age in developed countries [1]. The statistics for childhood and adolescent overweight and obesity in developed countries are also staggering – the overweight prevalence has increased from 16.9% in 1980 to 23.8% in 2013 for boys, and from 16.2% to 22.6% for girls; the total increase in children overweight and obesity has been estimated at 47.1% over the last three decades [1]. Similar age-related patterns are also observed in developing countries; in fact, 62% of the world`s obese individuals are estimated to live in developing countries [1].

3.2 Obesity, cardiovascular disease, and mortality

Besides the increase in prevalence, obesity and overweight are a major health concern because of the associated higher mortality, and in particular higher cardiovascular mortality in both men and women. The relative risk of death is 2 to 3 times higher for obese [3], and 20% to 40% higher for overweight individuals [3] compared with individuals with normal weight. This mortality risk increases with BMI in all age groups [3, 4], all racial and ethnic groups [4] and for all causes of death [3-6], but a higher BMI is most strongly associated with death from cardiovascular disease [3, 5]. In fact, each 5 kg/m2 increase in BMI is associated with a 30% higher overall mortality and a 40% higher cardiovascular mortality [5]. Excess weight alone is estimated to account for 7.7% of deaths in men and 11.7% of deaths in women [4]. This association between BMI and mortality is strongest in younger individuals with no history of smoking or chronic disease [3, 4, 6, 7], where excess weight accounts for 18.1% and 18.7% of premature deaths in men and women respectively [4]. Indeed, it has been estimated that in young obese individuals - the group with the highest obesity-

associated mortality risk - median survival is reduced by up to 13-20 years in men, and by up to 5-8 years in women [7].

The strong correlation of obesity with cardiovascular mortality could be explained by the association of obesity with classical cardiovascular risk factors such as hypertension, dyslipidemia, and type 2 diabetes. BMI is linearly associated with systolic and diastolic blood pressure [5, 8, 9], and a BMI above 25 kg/m2 accounts for 34% of hypertension in men and 62% of hypertension in women [9]. Total blood cholesterol also increases with BMI [8]. In contrast, BMI is inversely associated with high density lipoprotein (HDL) levels [5, 8], and thus it is positively associated with the ratio of non-HDL to HDL cholesterol [5]. Both hypertension and dyslipidemia, alone or in combination, are associated with BMI in men and women, in all racial and ethnic groups, and in most age groups, especially in younger individuals [8]. Increased blood pressure alone accounts for 31% of the risk for coronary artery disease (CAD) and 65% of the risk for stroke; overweight and obesity are both associated with CAD and cerebrovascular disease [10]. In fact, the relative risk for CAD and stroke increases with 27% and 18% respectively for each 5 kg/m2 increase in BMI [10]. In addition, obesity is associated with a 40% increased mortality from ischemic heart disease [5], and with a >90% increased risk of heart failure [11]. The risk of heart failure increases with 5% for men and 7% for women for each 1 kg/m2 increase in BMI, and obesity alone accounts for 11% of heart failure in men and 14% of heart failure in women [11]. Finally, obesity is strongly associated with type 2 diabetes, which itself is an independent cardiovascular risk factor [5, 12]; the relative risk for type 2 diabetes is 7 times higher in obese and 3 times higher in overweight individuals compared with individuals with normal weight [12].

3.3 Treatment of obesity

Considering the high prevalence of obesity and overweight and their strong association with cardiovascular disease and mortality, lifestyle and medical weight loss interventions to treat or prevent obesity-associated cardiovascular disease have been extensively investigated. Currently there are three major options to treat obesity – lifestyle interventions such as diet and exercise; pharmacological treatments to reduce food intake, reduce fat absorption, or increase energy expenditure; and restrictive or malabsorptive gastrointestinal surgery, also known as bariatric surgery.

3.3.1 Intensive lifestyle intervention

There have been many studies investigating the efficacy of lifestyle interventions to reduce body weight and to ameliorate cardiovascular risk factors. Very-low-calorie diets, for example, can lead to a mean weight reduction of 22.6%-25.5%, with 98% of subjects losing at least 10% of their initial weight in the short term [13]. After a three-year follow-up, 53% of subjects maintain a weight loss of 5% of their initial weight, and 35% maintain a weight loss of 10% or more of their initial weight [13]. After a five-year follow-up, 29% of subjects maintain a weight-loss of 4.5%-6.6% of their initial weight [14]. Combination of diet and exercise leads to a higher weight loss and weight loss maintenance after five years, where average weight loss is 12.5% [14]. In fact, the combination of diet and exercise leads to a 20% greater initial weight loss and a 20% greater weight loss maintenance after one year [15]. Finally, the Look AHEAD Study, which is the longest randomized controlled study on intensive lifestyle intervention on weight management, showed that a combination of diet and exercise leads to a mean weight loss of 4.7% after eight years, with 50% of subjects maintaining a weight loss of 5% of their initial weight, and 26.9% of subjects maintaining a weight loss of 10% or more of their initial weight [16].

Although lifestyle diet and exercise interventions only lead to an average weight loss of 5%-10% in the long term, it has been shown that this amount of weight loss is clinically relevant, because it leads to reduced plasma glucose levels, blood pressure, total cholesterol and low-density lipoprotein (LDL) levels, and to increased HDL levels [17]. These changes in cardiovascular risk factors are directly proportional to the total amount of weight loss [18]. More specifically, every kilogram of body weight lost is associated with a 0.015 mmol/L decrease in triglycerides, a 0.05 mmol/L decrease in total cholesterol, and a 0.02 mmol/L decrease in LDL [19]; the effect on HDL is not so clear as HDL levels decrease by 0.007 mmol/L per kg when subjects are actively losing weight, and increase by 0.009 mmol/L per kg when weight loss is maintained [19]. Blood pressure is also significantly decreased already at six months after the start of lifestyle intervention, and is directly proportional to the amount of weight loss; the risk of hypertension is decreased by 65% after three years in subjects that successfully maintain their weight loss [20]. Intensive lifestyle intervention also leads to prevention of type 2 diabetes – weight loss leads to decreased fasting glucose levels and decreased glucose and insulin levels after an oral glucose tolerance test, and to a 58%

decreased risk of type 2 diabetes [21, 22]. In fact, lifestyle intervention is more effective in preventing the incidence of type 2 diabetes in overweight subjects than treatment with the anti-diabetic drug metformin, which leads to only a 31% decreased risk of type 2 diabetes [22]. Finally, intensive lifestyle intervention can also lead to a partial remission of type 2 diabetes by 11.5% after one year and by 7.3% after four years [23].

However, despite these beneficial effects of lifestyle intervention-induced weight loss on cardiovascular risk factors, the Look AHEAD and the Finnish Diabetes Prevention studies showed that intensive diet and exercise intervention do not reduce overall cardiovascular mortality in obese subjects with type 2 diabetes after a ten-year follow-up [24, 25]; another study confirmed the lack of effect on mortality with lifestyle intervention after a twenty-year follow-up [26].

3.3.2 Pharmacological therapy

Anti-obesity pharmacological treatment is currently recommended as an adjunct therapy in obese individuals who are not able to achieve a clinically relevant body weight loss of 5%-10% with lifestyle intervention alone. Examples of currently approved drugs for long-term obesity treatment in the US or Europe include orlistat, a lipase inhibitor; lorcaserin, a serotonin receptor agonist; phentermine/topiramate combination therapy; and liraglutide, a glucagon-like peptide-1 (GLP-1) analogue. The following paragraphs discuss the effects on weight loss and cardiovascular risk markers of some of these currently available anti-obesity drugs.

Orlistat is a pancreatic/gastric lipase inhibitor that blocks intestinal digestion and absorption of approximately 30% of ingested fat, therefore reducing dietary fat intake [27-31]. When combined with a hypocaloric diet (a 600 kcal/day deficit), it leads to a mean body weight loss of 5.9%-10.2% after one year, compared with a mean body weight loss of 4.6%-6.6% after placebo treatment [27-31]. Of these, 54.2%-72.8% of orlistat-treated subjects lose more than 5% of their initial body weight compared with 40.9%-45.1% of placebo-treated subjects, and 38.3%-41%% of orlistat-treated subjects lose more than 10% of their initial body weight compared with 18.8%-24.8% of placebo-treated subjects [28-30]. Two years after start of treatment, 57.1% of orlistat-treated subjects maintain a body weight loss of more than 5% compared with 37.4% of placebo-treated subjects, and 28.2%-34.1% of

orlistat-treated subjects maintain a body weight loss of more than 10% compared with 17.5%-18.6% of placebo-treated subjects [27, 28, 30]. After four years of treatment, 52.8% of orlistat-treated subjects maintain a body weight loss of more than 5% compared with 37.3% of placebo-treated subjects, and 26.2% of orlistat-treated subjects maintain a body weight loss of more than 10% compared with 15.6% of placebo-treated subjects [31]. Therefore, orlistat is not only able to induce a greater body weight loss when compared to diet alone, but also to more successfully maintain this body weight loss in the long term. In addition, greater orlistat-induced body weight loss is also associated with greater reductions in cardiovascular risk factors such as total cholesterol, LDL, LDL/HDL ratio, blood pressure, fasting glucose and insulin levels, and glycated haemoglobin (HbA1c) after one year of treatment when compared to diet alone [27-30, 32]. Finally, orlistat is also able to reduce the incidence of type 2 diabetes by 37.3% after four years of treatment [31].

Another anti-obesity drug, lorcaserin, reduces appetite and food intake by selectively activating serotonin receptors in the hypothalamus that induce anorexigenic pro-opiomelanocortin signalling in the brain [33-36]. Similarly to orlistat, when combined with a hypocaloric diet it leads to a mean body weight loss of 5.8% after one year, compared to a mean body weight loss of 2.2%-2.8% after placebo treatment in non-diabetic subjects [33, 34]. Of these, 47.2%-47.5% of lorcaserin-treated subjects lose more than 5% of their initial body weight compared with 20.3%-25% of placebo-treated subjects, and 22.6% of lorcaserin-treated subjects lose more than 10% of their initial body weight compared with 7.7%-9.7% of placebo-treated subjects [33, 34]. In diabetic subjects, one-year lorcaserin treatment leads to a mean body weight loss of 4.5% compared to a 1.5% body weight loss after placebo treatment [35]. Of these, 37.5% of lorcaserin-treated subjects lose more than 5% of their initial body weight compared with 16.1% of placebo-treated subjects, and 16.3% of lorcaserin-treated subjects lose more than 10% of their initial body weight compared with 4.4% of placebo-treated subjects [35]. Greater lorcaserin-induced body weight loss is also associated with greater reductions in cardiovascular risk factors such as total cholesterol, LDL, triglycerides, blood pressure, fasting glucose and insulin levels, and HbA1c after one year of treatment when compared with diet alone [33, 36].

The combination therapy phentermine/topiramate decreases food intake and increases energy expenditure [37]. Similarly to orlistat and lorcaserin, when combined with a

hypocaloric diet it leads to a mean body weight loss of 9.8%-10.9% after one year, compared to a mean body weight loss of 1.2%-1.6% after placebo treatment [37, 38]. Of these, 66.7%-70% of treated subjects lose more than 5% of their initial body weight compared with 17.3%-21% of placebo, and 48% of treated subjects lose more than 10% of their initial body weight compared with 7% of placebo [37, 38]. Two years after start of treatment, mean weight loss in the treatment group is 10.5% from initial body weight compared with 1.8% in the placebo group [39], suggesting that phentermine/topiramate combination therapy is able not only to induce a greater body weight loss when compared with diet alone, but also to more successfully maintain this body weight loss in the longer term. In addition, the greater body weight loss is also associated with greater reductions in cardiovascular risk factors such as total cholesterol, LDL, triglycerides, blood pressure, fasting glucose and insulin levels, and HbA1c, as well as increased HDL levels after one or two years of treatment when compared with diet alone [37-39]. Finally, phentermine/topiramate treatment is also able to reduce the incidence of type 2 diabetes by 76% after two years of treatment [39].

The most recently approved anti-obesity drug, liraglutide, is a synthetic analogue of GLP-1, a gastrointestinal peptide hormone that stimulates pancreatic insulin secretion, delays gastric emptying, and inhibits food intake through vagal stimulation [40, 41]. After one year of liraglutide treatment combined with a hypocaloric diet, 73%-81.4% of liraglutide-treated subjects lose more than 5% of their initial body weight compared with 28%-48.9% of placebo-treated subjects, and 37% of liraglutide-treated subjects lose more than 10% of their initial body weight compared with 10% of placebo-treated subjects [40, 41]. In addition, liraglutide is able to induce a greater weight loss when directly compared with orlistat, which induces a 5% weight loss in only 44% of subjects (versus 73% with liraglutide treatment), and a 10% weight loss in only 14% of subjects (versus 37% with liraglutide treatment) in the same clinical trial after one year [40]. After two years of treatment, 52% of liraglutide-treated subjects maintain more than 5% of body weight loss compared with 29% of orlistat-treated subjects, and 26% of liraglutide-treated subjects maintain more than 10% of body weight loss compared with 16% of orlistat-treated subjects [40]. Interestingly, greater liraglutide-induced body weight loss is not associated with greater reductions in total cholesterol, LDL, and triglycerides after one year, but is associated with decreased blood pressure, fasting glucose, and HbA1c when compared with diet alone [40, 41]. In addition, liraglutide significantly increases HDL and decreases triglycerides, blood pressure, fasting

glucose, and HbA1c when compared with orlistat two years after start of treatment [40]. Finally, liraglutide is able to significantly reduce the prevalence of pre-diabetes when compared to both placebo and orlistat one and two years after start of treatment [40].

To summarize, adjunct pharmacological treatment of obesity is able to achieve significantly greater body weight loss and greater reductions in cardiovascular risk factors over a period of one year or more when compared with intensive lifestyle modification alone. However, despite improvements in cardiovascular risk factors, to date there are no studies demonstrating a beneficial effect of anti-obesity drugs on overall and cardiovascular mortality in the long term. In addition, pharmacological treatment of obesity is associated with specific side effects – increased gastrointestinal adverse events and decreased absorption of fat-soluble vitamins with orlistat [28]; headache, dizziness, and nausea with lorcaserin [33, 34, 36]; dry mouth, constipation, and insomnia with phentermine/topiramate [37, 38]; and nausea and vomiting with liraglutide [40, 42].

3.3.3 Bariatric surgery

Bariatric surgery is the common term for several gastrointestinal surgical procedures which are used to treat obesity by either restricting oral food intake or by reducing intestinal food absorption [43]. Currently surgical treatment of obesity is recommended to severely obese individuals with BMI>40 kg/m^2, or with BMI>35 kg/m^2 and an accompanying comorbidity such as type 2 diabetes, hypertension, or dyslipidemia, and which have been unsuccessful in reducing their body weight with conventional anti-obesity therapy [43]. Presently the most commonly performed procedures are Roux-en-Y gastric bypass (RYGB), vertical sleeve gastrectomy (VSG), and adjustable gastric banding (AGB) [44].

3.3.3.1 RYGB versus AGB and VSG

AGB is a restrictive and reversible procedure where an inflatable silicone band is implanted around the upper stomach to create a very small gastric pouch, therefore limiting stomach capacity and overall food intake; the size of the pouch can be individually adjusted by inflation of the gastric band with saline solution (Fig. 1A) [43]. VSG is an irreversible restrictive procedure where approximately 75% of the greater curvature of the stomach is removed, creating a small sleeve-like stomach that also limits overall food intake (Fig. 1B) [43]. RYGB, on the other hand, is a hybrid restrictive-bypass procedure where a very small

gastric pouch is created by cutting the uppermost part of the stomach and directly connecting it to the jejunum in the distal part of the small intestine; the rest of the stomach and the duodenum in the proximal intestine are bypassed and re-connected to the distal jejunum. This procedure creates a Y-shaped structure in the intestine where largely undigested food passes through the newly created gastric pouch and the so-called alimentary (or Roux) limb, while pancreatic juices and bile acids pass through the bypassed part of the duodenum, now called the biliopancreatic limb, before finally mixing in the distal part of the intestine, or the common channel (Fig. 1C). Therefore, RYGB not only restricts food intake by creating a smaller gastric pouch, but bypassing the proximal small intestine also results in changed gastrointestinal physiology (discussed in section 3.4.1.)[43].

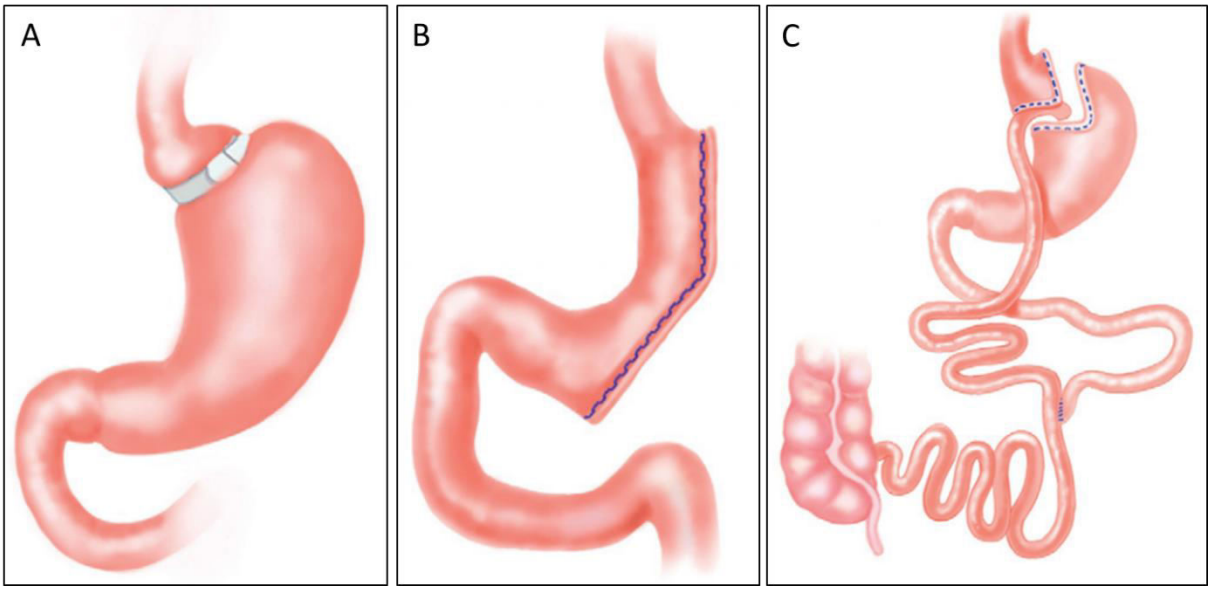

Fig. 1. Gastrointestinal anatomy of the three most commonly performed bariatric procedures. (A) Adjustable gastric banding**; (B)** Vertical sleeve gastrectomy**; (C)** Roux-en-Y gastric bypass. Adapted from Dixon *et al.* 2012 [45].

Bariatric surgery procedures are more effective than intensive lifestyle intervention and pharmacological therapy in inducing weight loss and in ameliorating cardiovascular risk factors for at least ten years of follow-up [46-50]. Bariatric surgery induces weight loss, decreases triglyceride, glucose, and HbA1c levels, and increases HDL levels significantly more than non-surgical treatment, and leads to a higher remission of type 2 diabetes and hypertension [46-50]. Currently the most commonly performed bariatric surgery is RYGB (45% of all bariatric procedures), followed by VSG (37% of all bariatric procedures) and AGB (10% of all bariatric procedures) [44]. Numerous clinical studies directly comparing RYGB and AGB have shown that RYGB is more effective than AGB in inducing weight loss and ameliorating obesity-associated comorbidities such as hypertension, dyslipidemia, and type 2 diabetes. One year after surgery, RYGB induces a 35% mean weight loss of initial weight and AGB induces only a 15% mean weight loss, which are maintained for up to three years after surgery [51]; ten years after surgery, 25% weight loss is maintained after RYGB and 13% after AGB [46]. This difference in weight loss becomes statistically significant already at one month [52] and three months after surgery [52-54]. Three years after surgery, RYGB results in significantly higher levels of complete or partial remission of type 2 diabetes, dyslipidemia, and hypertension than AGB [51, 54, 55]. VSG, on the other hand, is almost as effective as RYGB in inducing weight loss and in ameliorating obesity-associated comorbidities [56, 57]. Some studies show no difference in weight loss between RYGB and VSG one year after surgery [56], while others suggest that the weight loss effect of VSG is intermediate between RYGB and AGB [57]. Similarly, some studies show no difference in resolution of comorbidities between RYGB and VSG one year after surgery [56], while others suggest resolution of comorbidities is intermediate between RYGB and AGB [57]. Therefore, RYGB is currently considered the most effective treatment to induce weight loss, reduce cardiovascular risk factors, and ameliorate associated comorbidities in severely obese individuals.

3.3.3.2 RYGB and cardiovascular risk markers

More specifically, one year after surgery RYGB decreases total cholesterol by 12.5%-16%, triglycerides by 41.2%-63%, and LDL by 19.4%-31%, and increases HDL by 23.2%-39% compared to baseline levels [58, 59]; these differences in lipid levels become statistically significant already at three months [59] and six months after surgery [60], and are sustained

in the longer term [60, 61]. Five and six years after RYGB surgery, total cholesterol levels are lower by 5.2%-27%, triglycerides by 31.4%-47%, and LDL by 11.6%-40%, and HDL levels are higher by 12%- 33.7% compared to baseline levels [60, 61]. Systolic and diastolic blood pressure also decreases by respectively 14% and 11% one year after RYGB [62]. This decrease in cardiovascular risk factors results in complete resolution of type 2 diabetes in 45.8% of patients, dyslipidemia in 54.2% of patients, and hypertension in 37.5% of patients already at two months after surgery [63]. Six years after surgery, RYGB leads to 62% remission from type 2 diabetes and 42% remission from hypertension [47].

It has been suggested that increasing total HDL levels alone is not predictive of improved cardiovascular risk, and that HDL remodelling and functional properties are more important for maintaining cardiovascular health [64, 65]. In addition to its major anti-atherogenic role in mediating reverse cholesterol transport from peripheral tissues back to the liver, HDL also has other important endothelial functions – it can stimulate vasodilatory nitric oxide (NO) production from endothelial cells, protects them from inflammation and apoptosis, and has an anti-oxidative activity [64]. HDL functionality is dependent on HDL size and composition [66, 67]. Accordingly, it has been shown that six months and one year after surgery RYGB not only increases HDL levels, but also induces a shift in HDL remodelling towards more mature HDL particles [68, 69] with a higher anti-oxidative potential [69] and a higher content of the major anti-atherogenic apolipoprotein A-I [69, 70]. To date, however, the early and late changes in HDL functionality after RYGB surgery have not been extensively studied.

Another functional marker of cardiovascular risk is endothelial dysfunction, which plays an important role in the development of cardiovascular diseases such as atherosclerosis and hypertension [71, 72]. Endothelial function is impaired in obesity [73]. In patients it can be measured as flow-mediated dilation (FMD) of the brachial artery using ultrasound [74-76]. So far several studies have shown that bariatric surgery improves FMD [74], already at three months after surgery [75]. Another study has suggested that the improvement in FMD is associated with insulin levels and weight loss [76], but so far the exact mechanisms leading to improved endothelial function after RYGB are unknown.

3.3.3.3 Bariatric surgery and mortality

Overall, several systematic reviews and meta-analysis studies have shown that bariatric surgery leads to a complete or partial remission of type 2 diabetes in 73%-76.8% of obese patients, of dyslipidemia in 65%-71% of patients, and of hypertension in 61.7%-68% of patients after a mean follow-up of three to five years [77-79]. This is associated with a 30%-50% reduction of all-cause mortality [80-82] and a 53% reduction of total cardiovascular mortality [83]. Cause-specific mortality is decreased by 56% for CAD and by 92% for type 2 diabetes [81], and the incidence of myocardial infarction and stroke are also decreased by 54% and 51% respectively [82]. However, to date it has not been determined whether the reduced overall and cardiovascular mortality after bariatric surgery are a direct consequence of weight loss, or there are also weight loss-independent mechanisms involved [80, 81, 83].

To summarize, bariatric surgery, and in particular RYGB, is the only anti-obesity treatment to induce and maintain a >15% weight loss over ten years, to effectively resolve existing comorbidities such as type 2 diabetes, dyslipidemia and hypertension, and to reduce overall and cardiovascular mortality [83]. Currently, however, it is not known whether the reduced mortality risk after bariatric surgery is entirely mediated by weight loss [80, 81, 83].

3.4 Putative weight loss-independent mechanisms of RYGB

3.4.1 Role of GLP-1 in insulin resistance and RYGB

Remarkably, RYGB ameliorates or even resolves type 2 diabetes within days after surgery, before significant weight loss occurs [84], suggesting a weight loss-independent mechanism for improved insulin sensitivity and glucose metabolism. Indeed, hepatic insulin sensitivity, β-cell glucose sensitivity, and β-cell insulin secretion in response to nutrients significantly improve within one week after RYGB [85-87], and these improvements are maintained for at least two years after surgery [86, 88]. This effect is weight loss-independent because it is not observed in patients who lose equivalent weight with diet or AGB one week and one month after surgery [89, 90].

Interestingly, RYGB induces increased postprandial secretion of the gastrointestinal hormone GLP-1 one week and one month after surgery [86, 91, 92], and this effect is maintained for at

least two years after surgery [86, 88, 92]. GLP-1 is a peptide hormone secreted by enteroendocrine L cells in response to nutrients [93]. Its main functions are to act as an incretin, i.e. to stimulate pancreatic β-cell insulin synthesis and secretion, and to induce satiation and reduce food intake in the central nervous system through vagal stimulation [94]. Indeed, increased postprandial secretion of GLP-1 from one week to one year after RYGB is paralleled by improved β-cell glucose sensitivity and β-cell insulin secretion [86, 91, 92]. These improvements in glucose homeostasis are mainly due to an increased incretin effect as they are observed only after an oral glucose tolerance test and not after an equivalent intravenous glucose tolerance test in the same subjects [86, 91, 92]. Similarly, only oral feeding, but not gastric feeding through the bypassed stomach, increases postprandial GLP-1 and insulin secretion in the same subjects [95, 96]. Blocking GLP-1 signalling with the GLP-1 receptor antagonist exendin-9 significantly blunts the increased postprandial β-cell glucose sensitivity and insulin secretion after RYGB [97, 98], demonstrating that the GLP-1 incretin effect mediates the postprandial increase in β-cell glucose sensitivity and insulin secretion after RYGB. These increases in postprandial GLP-1 secretion and incretin effect after RYGB are weight loss-independent because they are not observed in patients who lose equivalent weight with diet or AGB from one week to one year after surgery [89-91, 99-101].

These conclusions from clinical studies are supported by *in vivo* animal experiments, which also show that three weeks and three months after surgery RYGB improves glucose tolerance and insulin sensitivity and increases plasma GLP-1 levels [102, 103]. In addition, a mixed-meal tolerance test, but not an intraperitoneal glucose tolerance test, increases postprandial GLP-1 and insulin excursions specifically in RYGB- and VSG-operated rats, but not in sham-operated pair-fed controls, and the GLP-1 receptor antagonist exendin-9 is able to blunt this effect on insulin [104]. In another study, chronic peripheral infusion of exendin-9 partially reverses the improved glucose tolerance after RYGB, indicating both GLP-1-dependent and weight-dependent effects of RYGB on glucose tolerance; in contrast, chronic exendin-9 does not affect food intake and weight loss [105]. Accordingly, GLP-1 receptor knockout mice lose the same amount of weight after RYGB or VSG surgery when compared to wild type mice [106-108]. Surprisingly, one study showed that VSG improves glucose tolerance to the same degree in wild type and in GLP-1 receptor knockout mice, but it lacked a body weight-matched control group to account for weight-dependent and weight–

independent changes in glucose tolerance [106]. Another study also showed that RYGB improves glucose tolerance and insulin sensitivity in GLP-1 receptor knockout mice to the same degree as in body weight-matched controls, but it lacked true wild type control groups to differentiate between GLP-1-dependent and weight-dependent effects [107]. Therefore, to date it is not known to what extent increased GLP-1 mediates the effects of RYGB on improved glucose tolerance and insulin sensitivity.

To summarize, RYGB surgery improves insulin resistance and β-cell glucose sensitivity and insulin secretion within days after surgery in a weight loss-independent manner. This effect could be mediated by increased incretin actions of GLP-1, whose postprandial secretion is increased after RYGB rapidly and independently of weight loss.

3.4.2 Role of JNK in insulin resistance and RYGB

Another crucial player linking obesity and insulin resistance is the c-jun N-terminal kinase (JNK) family of proteins [109]. There are three members in this family, JNK1 and JNK2, which are ubiquitously expressed, and JNK3, which is expressed mainly in the brain, heart, and testes [109]. JNK activation suppresses the insulin signaling pathway through phosphorylation of insulin receptor substrate-1 (IRS-1) at ser307, which inhibits IRS-1 activation and downstream cellular insulin signaling [110]. The first evidence that JNK could be involved in mediating obesity and obesity-induced insulin resistance was obtained in studies showing that total JNK activity is increased in liver, fat, and muscle in genetic (leptin-deficient *ob/ob* mice) and in diet-induced obesity [111]. Genetic deletion of JNK1 (JNK1-/-) in diet-induced obese mice results in less weight gain, lower levels of body adiposity, blood glucose and insulin, and in improved glucose tolerance and insulin sensitivity; these changes are associated with decreased total JNK activity in liver, muscle, and adipose tissue, and with reduced IRS-1 ser307 phosphorylation in the liver [111]. The protection against obesity and insulin resistance is not observed with JNK2-/- animals [111, 112], but it is present in JNK1+/-JNK2-/- animals, which also have decreased total JNK activity in the liver [112]. These results suggest that JNK2 also plays a role in obesity and that the balance of JNK1 and JNK2 and the resulting total JNK activation are critical for mediating these effects of JNK [112].

Interestingly, decreased activation of JNK and decreased IRS-1 ser307 phosphorylation in the liver has been demonstrated in type 2 diabetic rats two weeks after RYGB, and this is

associated with reduced hepatic lipotoxicity and oxidative stress, improved insulin sensitivity, and lower blood glucose and insulin [113]. Another type of metabolic surgery, the duodenal-jejunal bypass, shows improved glucose tolerance, insulin sensitivity, blood glucose levels and reduced liver and adipose tissue inflammation twelve weeks after surgery in type 2 diabetic rats [114]. These beneficial effects are again associated with decreased activation of JNK and decreased IRS-1 ser307 phosphorylation in the liver and adipose tissue [114].

Remarkably, JNK has also been shown to affect cardiovascular function and mediate cardiovascular disease. JNK2-/-ApoE-/- mice are protected from atherosclerosis [115], and JNK2-/- mice are protected from hypercholesterolemia-induced endothelial dysfunction and oxidative stress [116]. JNK2 has also been shown to directly regulate endothelial nitric oxide synthase (eNOS) by inhibitory phosphorylation [117]. In addition, vascular insulin resistance in spontaneously hypertensive rats is associated with increased JNK activation and increased IRS-1 ser307 phosphorylation in aortic tissue [118]. Finally, a recent study demonstrated that JNK mediates eNOS-dependent endothelial dysfunction in type 2 diabetic patients [119]. Thus, in addition to its role in obesity and hepatic insulin resistance, JNK has also been shown to negatively regulate both eNOS and insulin sensitivity in the vasculature.

To summarize, the JNK family of proteins mediates obesity-induced insulin resistance and hypercholesterolemia- and diabetes-induced vascular dysfunction, and might be involved in the rapidly improved glucose tolerance and insulin sensitivity after bariatric surgery.

4. Hypothesis, aims, and experimental design

4.1 Hypothesis

Based on previous clinical findings which show that bariatric surgery, and in particular RYGB, reduce cardiovascular risk factors, disease, and mortality, and that some of these effects might be weight loss-independent, we hypothesized that RYGB surgery also improves endothelial function and HDL endothelial protective properties rapidly and independently of weight loss. We further hypothesized that these improvements might be mediated by GLP-1- and JNK-dependent signalling pathways.

4.2 Aims and experimental design

Aim 1: To investigate whether RYGB surgery induces rapid and weight-independent improvement of endothelial function and HDL endothelial protective properties in a rat model of diet-induced obesity and in obese patients.

To study the rapid effects of RYGB on endothelial function, male Wistar rats were fed a high fat (60%) high cholesterol (1.25%) diet for 7 weeks to induce obesity prior to performing RYGB or sham surgery; animals were sacrificed 8 days after surgery and endothelial function was assessed by *ex vivo* isometric tension recordings of thoracic aorta. Weight-independent effects were studied by the use of a sham-operated control group which was body weight-matched to the RYGB-operated rats (Fig.2). HDL endothelial protective properties in obese rats and humans were assessed by functional *in vitro* assays with primary human aortic endothelial cells following HDL isolation from post-operative serum.

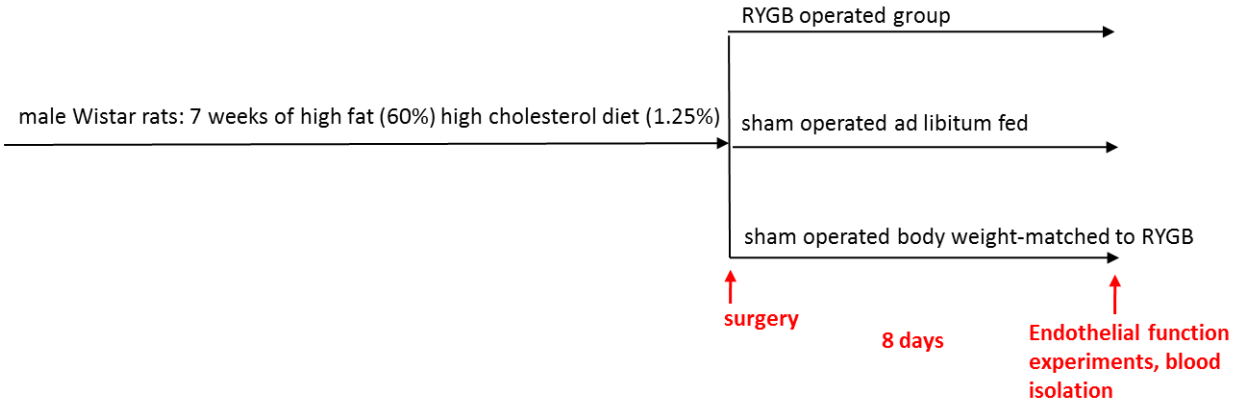

Fig. 2. Experimental design of Aim 1 – rapid and weight-independent effects of RYGB. After 7 weeks of high fat high cholesterol diet, male Wistar rats underwent RYGB or sham surgery, and were sacrificed 8 days later for *ex vivo* endothelial function experiments. RYGB-operated rats were compared to sham-operated ad libitum-fed control rats, and to sham-operated body weight-matched control rats to assess weight-dependent and independent effects of RYGB.

Aim 2: To investigate the role of GLP-1 in the molecular mechanisms underlying the rapid and weight-independent effects of RYGB on endothelial function and HDL properties in a rat model of diet-induced obesity.

To study the role of GLP-1 in mediating the beneficial effects of RYGB on endothelial function and HDL properties, we treated sham-operated ad libitum-fed rats with the GLP-1 analogue liraglutide, and RYGB-operated rats with the GLP-1 receptor antagonist exendin-9 *in vivo* for 8 days after surgery, and compared them with sham-operated ad libitum-fed control rats and RYGB-operated rats as described (Fig.3).

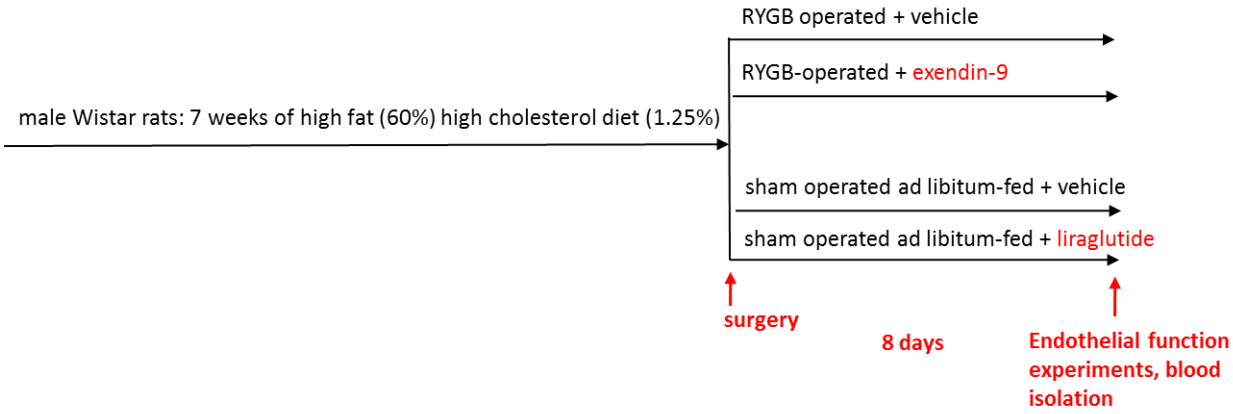

Fig. 3. Experimental design of Aim 2 – role of GLP-1 in mediating the rapid and weight-independent effects of RYGB. After 7 weeks of high fat high cholesterol diet, male Wistar rats underwent RYGB or sham surgery, and were sacrificed 8 days later for *ex vivo* endothelial function experiments. Sham-operated liraglutide-treated rats and RYGB-operated exendin-9-treated rats were compared to control sham-operated and RYGB-operated rats treated with vehicle.

Aim 3: To investigate the role of JNK in the molecular mechanisms underlying the rapid and weight-independent effects of RYGB on endothelial function in a rat model of diet-induced obesity.

To study the role of JNK in mediating the beneficial effects of RYGB on endothelial function, we treated sham-operated ad libitum-fed rats with two different JNK inhibitors *in vivo* for 8 days after surgery and compared them with sham-operated ad libitum-fed control rats and RYGB-operated rats as described (Fig. 4).

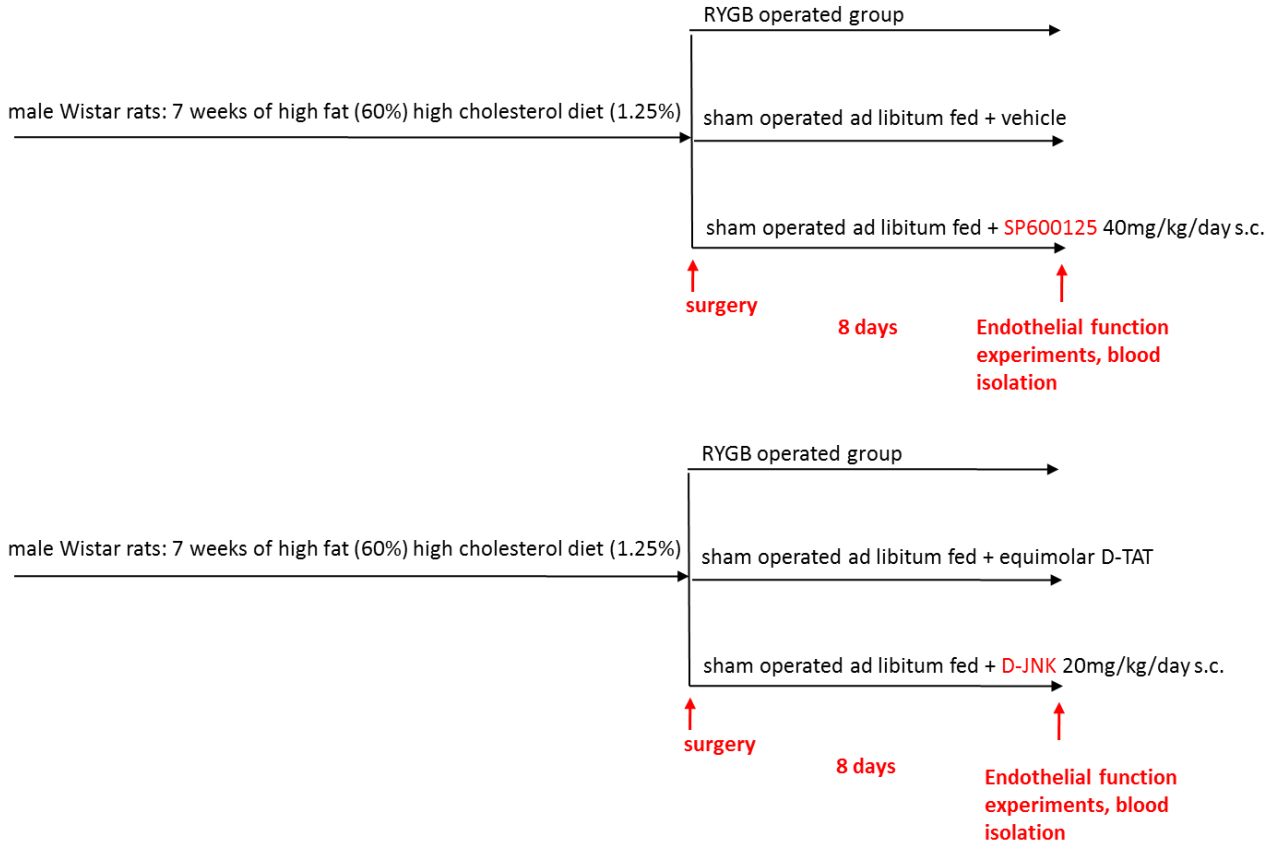

Fig. 4. Experimental design of Aim 3 - 2 – role of JNK in mediating the rapid and weight-independent effects of RYGB. After 7 weeks of high fat high cholesterol diet, male Wistar rats underwent RYGB or sham surgery, and were sacrificed 8 days later for *ex vivo* endothelial function experiments. Sham-operated rats treated with the JNK inhibitors SP600125 or D-JNK were compared to RYGB-operated rats and to control sham-operated rats treated with vehicle or the control peptide D-TAT, respectively.

5. Results

5.1 Original research article: “Rapid and Body Weight–Independent Improvement of Endothelial and High-Density Lipoprotein Function After Roux-en-Y Gastric Bypass: Role of Glucagon-Like Peptide-1”

This research article was published in *Circulation* in 2015 and contains part of the studies performed for the completion of the present PhD thesis. I share the first authorship of this article with Dr. E. Osto. My contributions to the published article include data acquisition, data analysis and interpretation, and revising the manuscript.

Rapid and Body Weight–Independent Improvement of Endothelial and High-Density Lipoprotein Function After Roux-en-Y Gastric Bypass

Role of Glucagon-Like Peptide-1

Elena Osto, MD, PhD*; Petia Doytcheva, MSc*; Caroline Corteville, MD; Marco Bueter, MD, PhD; Claudia Dörig, MSc; Simona Stivala, PhD; Helena Buhmann, MD; Sophie Colin, PhD; Lucia Rohrer, PhD; Reda Hasballa, MSc; Anne Tailleux, PhD; Christian Wolfrum, PhD; Francesco Tona, MD, PhD; Jasmin Manz, MSc; Diana Vetter, MD; Kerstin Spliethoff, DVM; Paul M. Vanhoutte, MD, PhD; Ulf Landmesser, MD; Francois Pattou, MD, PhD; Bart Staels, MD; Christian M. Matter, MD; Thomas A. Lutz, DVM, PhD*; Thomas F. Lüscher, MD*

Background—Roux-en-Y gastric bypass (RYGB) reduces body weight and cardiovascular mortality in morbidly obese patients. Glucagon-like peptide-1 (GLP-1) seems to mediate the metabolic benefits of RYGB partly in a weight loss–independent manner. The present study investigated in rats and patients whether obesity-induced endothelial and high-density lipoprotein (HDL) dysfunction is rapidly improved after RYGB via a GLP-1–dependent mechanism.

Methods and Results—Eight days after RYGB in diet-induced obese rats, higher plasma levels of bile acids and GLP-1 were associated with improved endothelium-dependent relaxation compared with sham-operated controls fed ad libitum and sham-operated rats that were weight matched to those undergoing RYGB. Compared with the sham-operated rats, RYGB improved nitric oxide (NO) bioavailability resulting from higher endothelial Akt/NO synthase activation, reduced c-Jun amino terminal kinase phosphorylation, and decreased oxidative stress. The protective effects of RYGB were prevented by the GLP-1 receptor antagonist exendin$_{9\text{-}39}$ (10 $\mu g \cdot kg^{-1} \cdot h^{-1}$). Furthermore, in patients and rats, RYGB rapidly reversed HDL dysfunction and restored the endothelium-protective properties of the lipoprotein, including endothelial NO synthase activation, NO production, and anti-inflammatory, antiapoptotic, and antioxidant effects. Finally, RYGB restored HDL-mediated cholesterol efflux capacity. To demonstrate the role of increased GLP-1 signaling, sham-operated control rats were treated for 8 days with the GLP-1 analog liraglutide (0.2 mg/kg twice daily), which restored NO bioavailability and improved endothelium-dependent relaxations and HDL endothelium-protective properties, mimicking the effects of RYGB.

Conclusions—RYGB rapidly reverses obesity-induced endothelial dysfunction and restores the endothelium-protective properties of HDL via a GLP-1–mediated mechanism. The present translational findings in rats and patients unmask novel, weight-independent mechanisms of cardiovascular protection in morbid obesity. **(*Circulation*. 2015;131:871-881. DOI: 10.1161/CIRCULATIONAHA.114.011791.)**

Key Words: bariatric surgery ■ endothelium ■ glucagon-like peptide-1 ■ lipoproteins ■ nitric oxide ■ obesity

Obesity is a worldwide health problem because of the associated increased morbidity and cardiovascular mortality.[1] Accompanying metabolic disorders such as insulin resistance and type 2 diabetes mellitus and risk factors such as dyslipidemia increase the disease risk linked to obesity. In particular, obesity induces endothelial dysfunction, which precedes atherosclerosis, but also contributes to insulin resistance in tissues

Editorial see p 845
Clinical Perspective on p 881

Received June 18, 2014; accepted December 29, 2014.

From Centre for Molecular Cardiology, University of Zurich and University Heart Center, Cardiology, University Hospital Zurich, Switzerland (E.O., P.D., S.S., J.M., U.L., C.M.M., T.F.L.); Institute of Veterinary Physiology, University of Zurich, Switzerland (P.D., C.C., C.D., H.B., K.S., T.A.L.); Department of Surgery (M.B., D.V.) and Institute of Clinical Chemistry (L.R., R.H.), University Hospital Zurich, Switzerland; Université Lille 2, INSERM UMR1011, EGID, Institut Pasteur de Lille, France (S.C., A.T., B.S.); Department of Health Sciences and Technology, ETH Zurich, Switzerland (C.W.); Department of Cardiac, Thoracic and Vascular Sciences, University of Padua, Italy (F.T.); State Key Laboratory for Pharmaceutical Biotechnology and Department of Pharmacology and Pharmacy, LKS Faculty of Medicine, University of Hong Kong, SAR (P.M.V.); and Department of Endocrine Surgery, Lille University Hospital, France (F.P.).

*Dr Osto, P. Doytcheva, Dr Lutz, and Dr Lüscher contributed equally.

The online-only Data Supplement is available with this article at http://circ.ahajournals.org/lookup/suppl/doi:10.1161/CIRCULATIONAHA.114.011791/-/DC1.

Correspondence to Elena Osto, MD, PhD, Centre for Molecular Cardiology, University of Zurich, Wagistrasse, 12, CH-8952 Schlieren, Switzerland. E-mail elena.osto@uzh.ch

involved in glucose and lipid metabolism.[2,3] Reduced nitric oxide (NO) bioavailability seems to be the primary defect that links obesity, insulin resistance, and endothelial dysfunction.[2,3]

Furthermore, obesity and insulin resistance result in proatherogenic dyslipidemia,[4] characterized by high low-density lipoprotein and triglyceride and low high-density lipoprotein (HDL) cholesterol plasma levels.[1,5] Abnormal HDL remodeling and maturation have been reported in obese subjects with an HDL profile similar to that of subjects with established cardiovascular disease.[5] In addition, pathological situations associated with obesity, in particular type 2 diabetes mellitus[6] and coronary artery disease,[7] impair the physiological protective properties of HDL, which preserves endothelial NO bioavailability and promotes vascular health.[8] Once dysfunctional, HDL may contribute to endothelial dysfunction.[8] Thus, assessing the properties of HDL is more informative than measuring its plasma levels alone.[8]

Roux-en-Y gastric bypass surgery (RYGB) induces sustained weight loss in contrast to the limited success of pharmacological or behavioral interventions.[9,10] Reductions in global and cardiovascular mortality[9,11] and obesity-related comorbidities[1,10,12,13] have been reported after RYGB.[1,11] The mechanisms underlying these beneficial effects are multiple.[1,11] Amelioration of insulin resistance[14] or even resolution of type 2 diabetes mellitus occurs within days after RYGB, before any substantial weight loss. These findings suggest that glycemic control is restored by mechanisms[15,16] related to the unique anatomic gut rearrangement and the altered flow of nutrients after RYGB,[10] rather than simply being a consequence of weight loss.[15,17] After RYGB, the modified enterohepatic circulation of bile acids increases their intraluminal and systemic concentrations. Thus, elevated levels of these acids and undigested chyme may modify the release of gastrointestinal hormones.[17] In particular, plasma levels of the gut hormone glucagon-like peptide-1 (GLP-1) increase rapidly after RYGB but not after dietary restriction despite a similar weight loss.[15,16,18] These observations raised the hypothesis that changes in GLP-1 levels mediate the rapid and surgery-specific metabolic improvement achieved after RYGB.[18,19] Drugs targeting the GLP-1 system are used in clinical practice as antidiabetic agents with potential weight-lowering effects.[20] Beyond its metabolic actions, GLP-1 exhibits multiple beneficial properties, in particular antioxidant and endothelium-protective effects.[19,21]

Therefore, the present study was designed to evaluate whether RYGB causes a rapid improvement in endothelial function and restores the protective properties of HDL. Moreover, the experiments examined whether increased GLP-1 levels mediate the rapid metabolic and cardiovascular improvements associated with RYGB and whether results of the procedure in obese rats can be translated to obese patients.

Methods

An expanded description of methods is available in the online-only Data Supplement.

Animals and Organ Chamber Experiments

Male Wistar rats were fed a high-fat, high-cholesterol diet containing 60% kcal fat and 1.25% cholesterol for 7 weeks before and after surgery to achieve diet-induced obesity. Two main experiments were performed (Figure I in the online-only Data Supplement): RYGB[22] and sham-operated rats either fed ad libitum (controls) or weight matched to RYGB and followed up for 8 days and rats randomized to 2 treatment groups for the 8 days of follow-up (controls treated with either vehicle or liraglutide 0.2 mg/kg twice daily and RYGB treated with either vehicle or exendin$_{9\text{-}39}$ 10 $\mu g \cdot kg^{-1} \cdot h^{-1}$). In addition, some rats were followed up for 1 month after surgery. All animal experiments were approved by the Zurich Cantonal Veterinary Office. Cumulative concentration-relaxation curves in response to insulin and GLP-1 were obtained in rings of thoracic aorta as described.[23]

Endothelium-Protective Properties of HDL

HDL was isolated from rat and patient serum by sequential density ultracentrifugation.[6,7] HDL-stimulated NO production by cultured human aortic endothelial cells (HAECs) was tested in vitro with the fluorescent probe 4,5-diaminofluorescein.[7] HDL antiapoptotic properties were assessed in HAECs.[24] Arylesterase activity of HDL-associated paraoxonase-1 (PON-1) was measured by ultraviolet spectrophotometry.[7] Endothelial protein expression of vascular cell adhesion molecule-1 (VCAM-1) was determined in tumor necrosis factor-α–stimulated (100pg/mL) HAECs treated with HDL.[7] NADPH oxidase activity was measured with a commercial assay kit.

Patient Population

The surgery group consisted of 29 patients undergoing primary laparoscopic proximal RYGB.[25] The body mass index (BMI)–matched group consisted of 29 obese patients matched for BMI, body weight, age, and sex to the RYGB group at week 12 after surgery. Moreover, 28 normal-weight volunteers matched for age and sex were enrolled. The local Research and Ethics Committee approved the study. All patients gave written consent

Statistical Analysis

Continuous variables with no or mild skew were presented as mean±SEM; skewed measures were presented as median and interquartile ranges. Discrete variables were summarized as frequencies and percentages. The distribution of the data was analyzed with a 1-sample Shapiro-Wilk test. Logarithmic transformation was performed to achieve normal distribution for skewed variables. Categorical variables were compared by use of the χ^2 test or Fisher exact test as appropriate. Continuous data were compared by use of the 2-tailed paired or unpaired t test (for normally distributed data sets) or the Mann-Whitney U or Wilcoxon signed-rank test (for skewed variables). We used a 2-way ANOVA with repeated measures to compare repeated measurements on the same animals. For studying the complete outcome of each variable over time, we applied the linear mixed model using an unstructured covariance matrix for quantitative variables. All tests were 2 sided, and statistical significance was accepted if the null hypothesis could be rejected at $P<0.05$.

The authors had full access to and take full responsibility for the integrity of the data. All authors have read and agree to the manuscript as written.

Results

GLP-1 and Bile Acid Plasma Levels Increase Rapidly After RYGB

Fasting circulating GLP-1 levels were significantly higher in RYGB than in sham-operated rats (Figure 1A and 1B and Figure IIA in the online-only Data Supplement). RYGB rats receiving exendin$_{9\text{-}39}$ had GLP-1 levels similar to those of RYGB rats (Figure 1B). Fasting plasma bile acid levels were increased after RYGB in all experiments (Figure 1C and 1D and Figure IIB in the online-only Data Supplement) and were not affected significantly by either liraglutide or exendin$_{9\text{-}39}$.

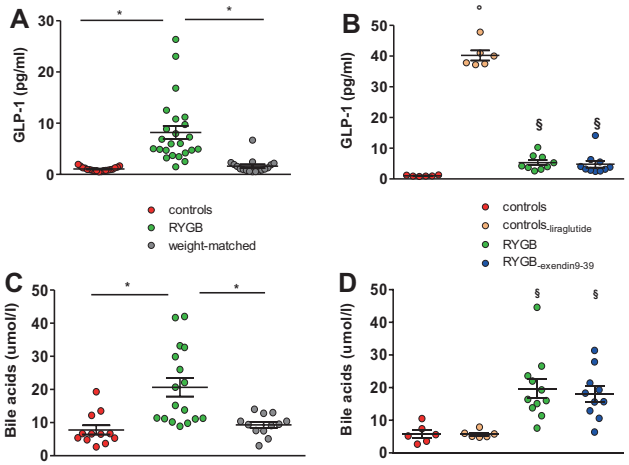

Figure 1. Plasma levels of glucagon-like peptide-1 (GLP-1; **A**) and total bile acids (**C**) in Roux-en-Y gastric bypass (RYGB) compared with sham-operated rats after surgery and after GLP-1 modulation for 8 days (**B** and **D**). The elevated GLP-1 concentrations measured in sham controls$_{\text{-liraglutide}}$ probably reflected a cross-reactivity of the assay with liraglutide. Results are shown as mean±SEM; n=10 to 15 per group. *P<0.0001, RYGB vs sham-operated rats, §RYGB and RYGB$_{\text{-exendin9-39}}$ vs controls and controls$_{\text{-liraglutide}}$; °controls vs controls$_{\text{-liraglutide}}$, P<0.002.

The Rapid Improvement of Vascular Function After RYGB Is Independent of Weight Loss

Physiologically, insulin and GLP-1 induce NO-mediated endothelium-dependent relaxations,[19,26] whereas decreased NO bioavailability in obesity impairs endothelial function.[2,3,26] Therefore, the impact of RYGB on relaxations in response to increasing concentrations of both hormones was tested. Preincubation of the aortic rings with the NO synthase (NOS) inhibitor N^{ω}-nitro-L-arginine methyl ester abolished endothelium-dependent relaxations in response to both hormones, indicating an NO-dependent mechanism (data not shown). The responses to insulin and GLP-1 improved significantly 8 days after RYGB but not in weight-matched rats (Figure 2A and 2B and Figure IIIA and IIIB in the online-only Data Supplement). The relaxing effect of GLP-1 was inhibited by incubation of the aortic rings with the specific GLP-1 receptor antagonist exendin$_{9\text{-}39}$ (10^{-5} mol/L; Figure IVA in the online-only Data Supplement).

Acetylcholine-induced relaxations were also restored rapidly after RYGB (Figure IVB in the online-only Data Supplement). One month after surgery, responses to both insulin and GLP-1 remained impaired in controls and weight-matched rats, but the acetylcholine-induced relaxation improved similarly in the aortas of weight-matched and RYGB rats (Figures IIIE, IIIF, IVD, and IVF in the online-only Data Supplement).

RYGB Improves Endothelial Function by a GLP-1 Receptor–Dependent Mechanism

To investigate the role of GLP-1 in the improved relaxation after RYGB, the GLP-1 receptor antagonist exendin$_{9\text{-}39}$ or the GLP-1 analog liraglutide was administered for 8 days after RYGB (RYGB$_{\text{-exendin9-39}}$) or to control (controls$_{\text{-liraglutide}}$) rats, respectively. The relaxations improved in response to insulin and GLP-1 in controls$_{\text{-liraglutide}}$ compared with controls, thus mimicking the effects of RYGB (Figure 2C and 2D). Instead, RYGB$_{\text{-exendin9-39}}$ rats had blunted relaxations to insulin and GLP-1 compared with RYGB; that is, they were not significantly different from controls (Figure 2C and 2D and Figure IIIC and IIID in the online-only Data Supplement). Relaxations to acetylcholine in RYGB$_{\text{-exendin9-39}}$ rats were similar to those in RYGB rats (Figure IVG in the online-only Data Supplement). Relaxations to the endothelium-independent vasodilator sodium nitroprusside were similar among all experimental groups (Figure IVC and IVH in the online-only Data Supplement).

Vascular GLP-1 Signaling Is Increased in RYGB Rats Independently of Weight Loss

Consistent with the improved relaxations to GLP-1 seen after RYGB, aortic GLP-1 receptor expression was increased in RYGB compared with sham-operated rats 8 days after surgery (Figure 3A).

Insulin and GLP-1 signaling in endothelial cells results in phosphorylation of protein kinase Akt at serine 473 (pSer^{473}-Akt), followed by phosphorylation of endothelial NOS (eNOS) on Ser1177 (pSer^{1177}eNOS), a well-known eNOS-activating pathway.[24,27] The phosphorylation level of pSer^{473}-Akt was significantly higher after RYGB compared with control rats (Figures 3B and 4A) and in controls$_{\text{-liraglutide}}$ compared with their controls, whereas it was reduced in RYGB$_{\text{-exendin9-39}}$ (Figure 4A).

Obesity increases c-Jun amino terminal kinase (JNK) activity, which in turn impairs insulin and GLP-1 signaling.[28,29] JNK phosphorylation was significantly reduced after RYGB compared with sham-operated groups (Figure 3C). Exendin$_{9\text{-}39}$ prevented the reduction in JNK phosphorylation after RYGB. Control$_{\text{-liraglutide}}$ rats had slightly decreased JNK activation compared with controls, but the degree of inhibition was lower than after RYGB (Figure 4B).

NO bioavailability was preserved after RYGB compared with the sham-operated groups as reflected by an increased pSer^{1177}eNOS and decreased inhibitory Thr^{495} phosphorylation of eNOS,[30] a higher eNOS dimer-to-monomer ratio, and an augmented aortic NO production (Figure 3D–3G). Moreover, in RYGB, we observed a lower eNOS glutathionylation, which impairs the enzyme function,[31] compared with weight-matched rats (Figure VA in the online-only Data Supplement). Despite an only slightly higher pSer^{1177}eNOS, pThr^{495} was reduced, and dimerization of eNOS and NO production were increased in control$_{\text{-liraglutide}}$ aortas to levels comparable to those in RYGB; in contrast, eNOS activation and NO production were reduced in RYGB$_{\text{-exendin9-39}}$. However, eNOS glutathionylation was not affected by GLP-1 modulation (Figure 4C–4F and Figure VB in the online-only Data Supplement).

Decreased Oxidative Stress Contributes to the Preserved NO Bioavailability After RYGB

High oxidative stress in obesity leads to NO inactivation by superoxide anions (O_2^-) and may impair endothelial NO availability. Concurrent with this notion, the addition of the free radical scavenger polyethylene glycol–superoxide dismutase significantly improved relaxations in response to insulin and GLP-1 in both sham-operated rats. In RYGB and in

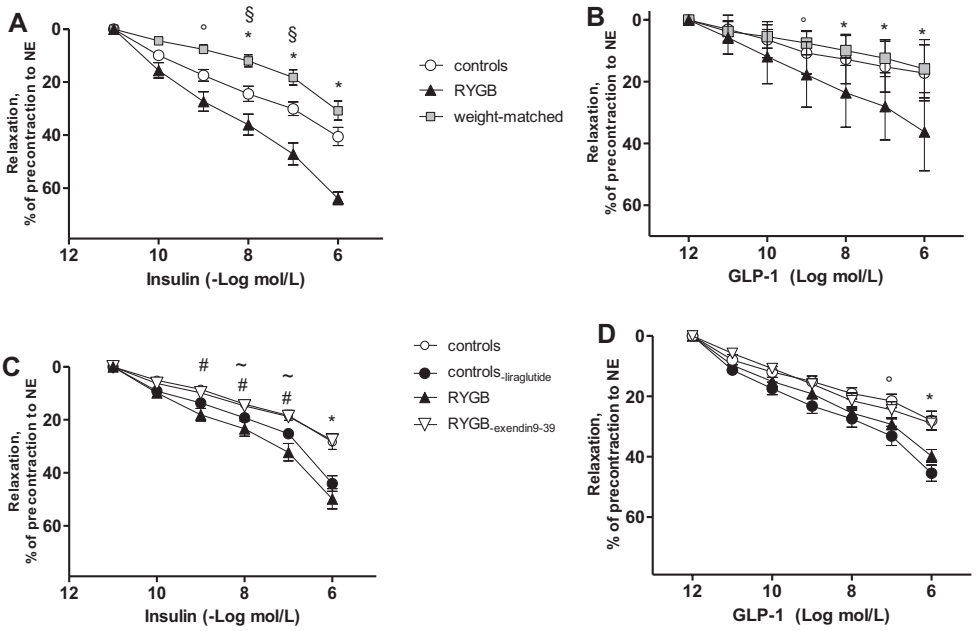

Figure 2. **A** and **B**, Relaxation of aortic rings isolated 8 days after Roux-en-Y gastric bypass (RYGB) compared with sham-operated rats. Concentration-response curves during submaximal contraction to norepinephrine (NE) in response to insulin (**A**) and glucagon-like peptide-1 (GLP-1; **B**). *Sham-operated rats vs RYGB, §controls vs weight-matched, °RYGB vs weight matched, $P<0.05$. **C** and **D**, Effect of GLP-1 modulation for 8 days on the relaxations to insulin (**C**) or GLP-1 (**D**). #RYGB vs controls, ~RYGB vs RYGB$_{\text{-exendin9-39}}$, °controls$_{\text{-liraglutide}}$ vs controls, *controls$_{\text{-liraglutide}}$ and RYGB vs other study groups, $P<0.05$; n=6 to 8 per group.

controls$_{\text{-liraglutide}}$, polyethylene glycol–superoxide dismutase did not modify relaxations, suggesting that the level of oxidative stress was reduced by the surgery and liraglutide. Instead, polyethylene glycol–superoxide dismutase was beneficial in RYGB$_{\text{-exendin9-39}}$, confirming the important vascular antioxidant effect of GLP-1 and analogs (Figure IVI–IVN in the online-only Data Supplement). In addition, O_2^- concentration and NADPH oxidase activity, which is a major oxidant enzyme system producing O_2^- in the vasculature,[6] were decreased in aortas of rats after RYGB compared with controls and weight-matched rats (Figure 5A–5C). In controls, treatment with liraglutide reduced aortic O_2^- concentration (Figure 5A and 5B) and, although to a lesser extent, aortic NADPH oxidase activity, mimicking RYGB; instead, exendin$_{9\text{-}39}$ treatment after RYGB did not counteract these antioxidant effects (Figure 5C).

Endothelium-Protective Properties of HDL Improve Rapidly After RYGB

Endothelium-protective properties of HDL and the role of the increased circulating GLP-1 levels as mediators of the observed changes were assessed. In parallel to the rat studies, similar experiments were performed with HDL obtained from patients before and 14 days and 12 weeks after RYGB and from the BMI-matched group. See Tables I and II in the online-only Data Supplement for patient characteristics.

HDL-Stimulated Endothelial NO Production Increases Rapidly After RYGB

HDL isolated from RYGB rats induced higher endothelial NO production in HAECs than HDL from controls (Figure 6A). Furthermore, HDL from control$_{\text{-liraglutide}}$ rats stimulated endothelial NO production in a fashion similar to HDL isolated after RYGB. This effect was independent of GLP-1 receptor activation because it was preserved in RYGB rats treated with exendin$_{9\text{-}39}$ (Figure 6D).

The capacity of HDL isolated from patients to stimulate NO production increased already at day 14 and was normalized 12 weeks after RYGB compared with the preoperative period (Figure 7A). The NO production stimulated by HDL isolated from the BMI-matched group was reduced compared with patients 12 weeks after RYGB. Accordingly, HAECs stimulated with HDL isolated from patients at day 14 and week 12 after RYGB exhibited improved eNOS dimerization relative to their preoperative HDL; eNOS dimerization was impaired in the BMI-matched group compared with patients 12 weeks after RYGB ($P<0.055$; Figure 7B).

HDL Reduces Endothelial Cell Apoptosis Rapidly After RYGB

Compared with controls, HDL isolated after RYGB markedly reduced endothelial apoptosis induced by serum and growth factors deprivation (Figure 6B). HDL from controls$_{\text{-liraglutide}}$ reduced endothelial apoptosis to a degree similar to the reduction after RYGB, but again, treatment with exendin$_{9\text{-}39}$ after RYGB did not influence this property of HDL (Figure 6E).

In patients, the capacity of HDL to inhibit endothelial apoptosis, which was impaired preoperatively, was restored after surgery and resembled that of healthy subjects. The antiapoptotic capacity of HDL was similar between patients 12 weeks after RYGB and their BMI-matched group (Figure 7C).

Anti-Inflammatory Properties of HDL Improve After RYGB

HDL isolated after RYGB reduced tumor necrosis factor-α–stimulated endothelial VCAM-1 expression significantly more than HDL from controls (Figure 6C). HDL from control$_{\text{-liraglutide}}$

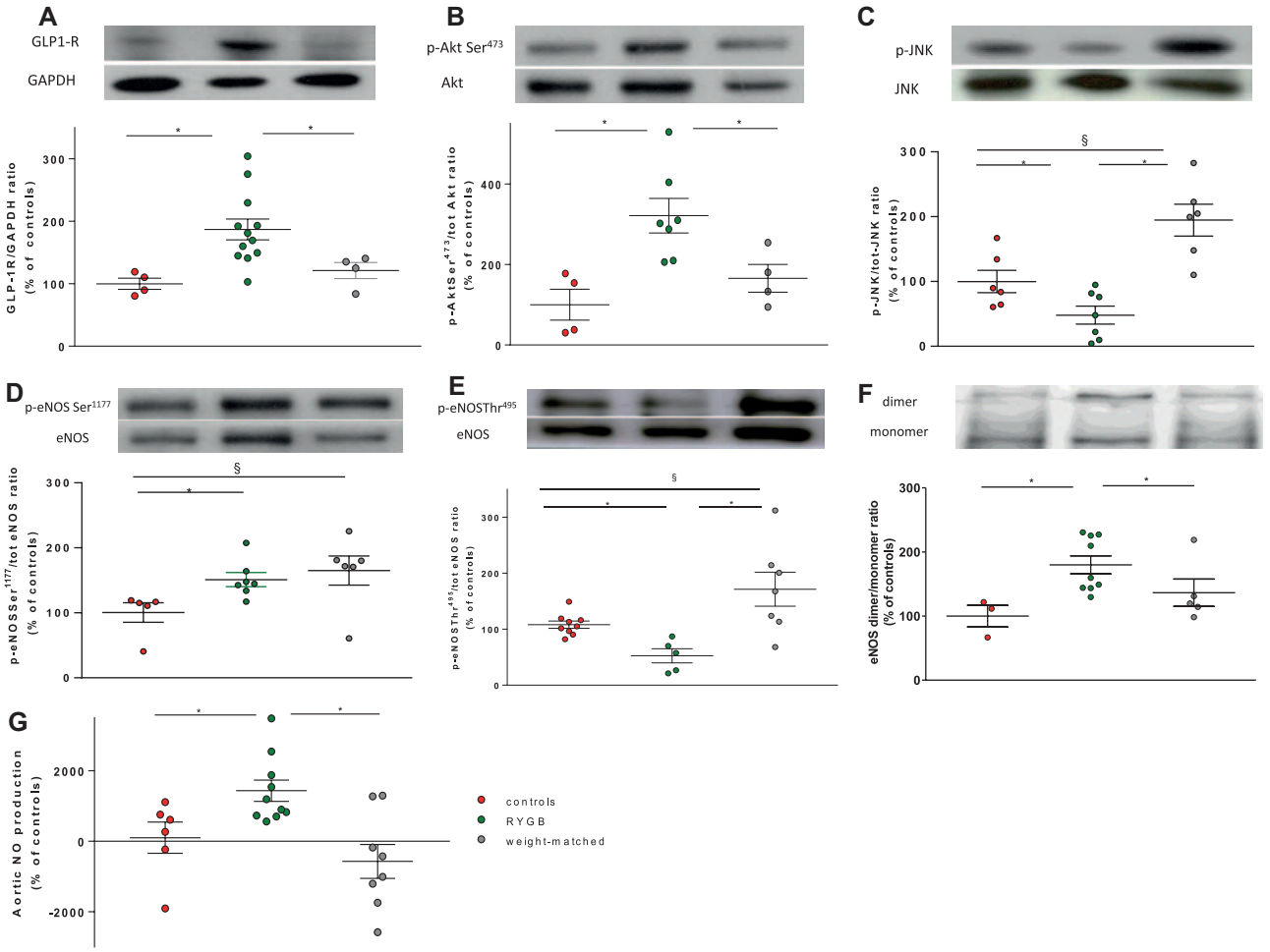

Figure 3. Glucagon-like peptide-1 receptor (GLP-1R; **A**), phosphorylated (p) Ser^{473}-Akt (**B**), and phosphorylated (p) c-Jun amino terminal kinase (JNK; **C**) protein expression from aortas isolated 8 days after Roux-en-Y gastric bypass (RYGB) compared with sham-operated rats. Endothelial nitric oxide (NO) synthase (eNOS) protein Ser^{1177} (**D**) and Thr^{495} (**E**) phosphorylation and eNOS dimerization (**F**). Representative Western blots and densitometric quantification are shown. **G**, Electron spin resonance spectroscopy analysis of aortic NO production. *RYGB vs other groups, §weight matched vs control, $P<0.05$; n=6 to 8 per group.

rats was similarly effective as HDL isolated after RYGB, whereas treatment of RYGB rats with exendin$_{9\text{-}39}$ had no effect. Hence, the increase in anti-inflammatory properties of HDL after RYGB is mimicked by the GLP-1 analog but does not involve the activation of the known GLP-1 receptor (Figure 6F). Endothelial VCAM-1 expression was reduced by HDL from patients 12 weeks after RYGB but not by HDL from BMI-matched subjects (Figure 7D).

PON-1 Activity Increases Rapidly After RYGB

PON-1 activity was increased after RYGB compared with controls. The improvement in PON-1 activity was surgery specific but independent of GLP-1 levels or signaling because treatment with liraglutide or exendin$_{9\text{-}39}$ did not modify it compared with the respective control groups (Figure VIA and VIC in the online-only Data Supplement). In patients, PON-1 activity improved progressively after RYGB; it was impaired in the BMI-matched group (Figure 7E).

RYGB Improves the Capacity of HDL to Stimulate Macrophage Cholesterol Efflux

HDL after RYGB increased cholesterol efflux from J774 macrophages compared with HDL from sham-operated rats. Instead, HDL from controls$_{\text{-liraglutide}}$ or RYGB$_{\text{-exendin9-39}}$ did not change this parameter compared with HDL from the respective controls, suggesting that the RYGB-induced effect is independent of changes in GLP-1 levels or signaling (Figure VIB and VID in the online-only Data Supplement). In patients 12 weeks after RYGB, HDL improved the cholesterol efflux capacity, in contrast to HDL from the BMI-matched group (Figure 7F).

RYGB Rapidly Restores the Endothelial Antioxidant Effects of HDL

In HAECs, stimulation with HDL isolated after RYGB or controls$_{\text{-liraglutide}}$ reduced NADPH oxidase activity compared with HDL from sham-operated animals; exendin$_{9\text{-}39}$ treatment after RYGB did not alter HDL antioxidant effects (Figure 5D). Endothelial NADPH oxidase activity was reduced by HDL from patients 12 weeks after RYGB but not by HDL from the BMI-matched group (Figure 5E).

Discussion

RYGB induces stable weight loss, improves obesity-associated comorbidities, and reduces cardiovascular mortality.[1,11] Here, we show that the beneficial metabolic and cardiovascular

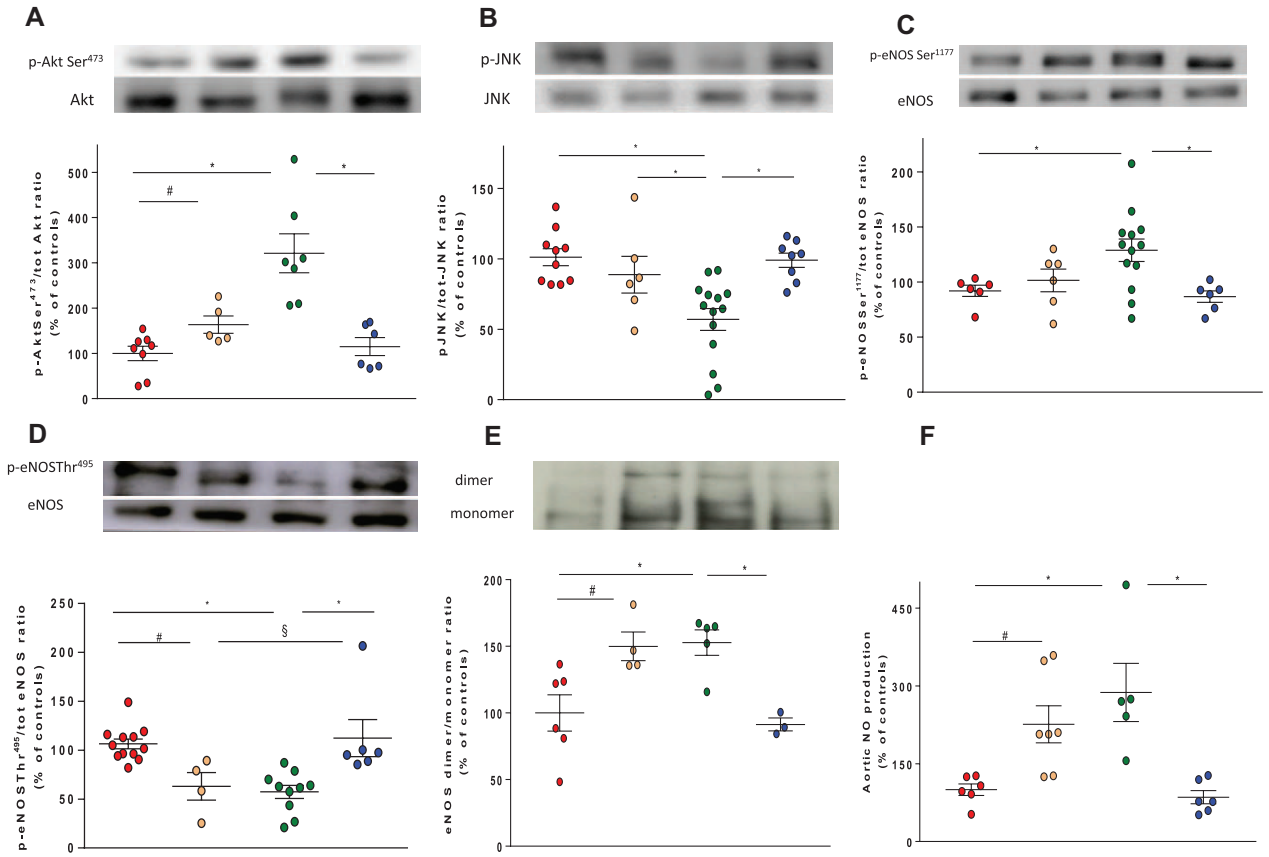

Figure 4. **A**, Phosphorylated (p) Ser[473]-Akt and (**B**) phosphorylated (p) c-Jun amino terminal kinase (JNK) protein expression from aortas isolated 8 days after glucagon-like peptide-1 (GLP-1) modulation. Endothelial nitric oxide (NO) synthase (eNOS) protein Ser[1177] (**C**) and Thr[495] (**D**) phosphorylation and eNOS dimerization (**E**). **F**, Electron spin resonance spectroscopy analysis of aortic NO production. *Roux-en-Y gastric bypass (RYGB) vs other groups, #controls$_{\text{-liraglutide}}$ vs controls, §controls$_{\text{-liraglutide}}$ vs RYGB$_{\text{-exendin9-39}}$, $P<0.05$; n=6 to 8 per group.

effects of RYGB likely result from changes in intestinal physiology rather than from weight loss alone. In particular, the gut hormone GLP-1, which increases rapidly after RYGB and restores glycemic homeostasis, may also contribute to the cardiovascular protection after surgery.[19,32] Indeed, we found in the present study that (1) in a rat model of RYGB, higher plasma levels of GLP-1 and bile acids were associated with increased aortic NO bioavailability, improved endothelium-dependent relaxation, and normalized endothelium-protective properties of HDL; (2) GLP-1–dependent signaling was selectively activated in rat aortas after RYGB and was independent of weight loss; (3) treatment of control rats with the GLP-1 analog liraglutide for 8 days improved both endothelial and HDL function, thus mimicking the effects of RYGB; and (4) in morbidly obese patients, increased plasma levels of GLP-1 and bile acids after RYGB were associated with a rapid improvement in the endothelium-protective properties of HDL. The major results and proposed underlying mechanisms are summarized in Figure 8 and Table III in the online-only Data Supplement.

Improved Endothelium-Dependent Relaxations After RYGB Involve a GLP-1–Dependent Mechanism

Beyond widespread metabolic actions, GLP-1 and its analogs affect the cardiovascular system,[33] in particular endothelial cells,[19,32] but also lipid metabolism.[32,34,35] GLP-1 exerts potent antioxidant effects[36] and possesses antiapoptotic and anti-inflammatory properties in endothelial cells.[24,37] The endothelial effects of GLP-1 are mediated by NO[38] and can be either dependent or independent of the activation of the known GLP-1 receptor.[33] Physiologically, GLP-1 promotes endothelial health indirectly by triggering insulin production[38] and by activating its own endothelial signaling pathways.[32,34,35]

The present findings demonstrate that increased plasma levels of GLP-1 after RYGB activate GLP-1 receptor–dependent intracellular signaling and induce a rapid restoration of endothelium-dependent relaxations. These beneficial effects were independent of weight because they were absent in rats that had a weight loss matched to RYGB. One month after surgery, relaxations to insulin and GLP-1 remained impaired in weight-matched compared with RYGB rats. This points out that weight loss achieved by food restriction is not sufficient to induce all the beneficial effects of RYGB. Moreover, the persistent impairment of insulin- and GLP-1–mediated endothelium-dependent relaxations suggests that the 2 hormones, which are partial agonists for the activation of endothelial NO release,[3] are a more sensitive tool compared with acetylcholine to investigate how metabolic modifications influence endothelial function.[3,26]

The endothelial Akt/eNOS pathway mediates GLP-1 receptor–dependent vascular effects and represents the major signaling cascade activated by insulin. This pathway was rapidly upregulated in aortas after RYGB and after liraglutide treatment in controls but was blunted by administration of the antagonist exendin$_{9\text{-}39}$ after RYGB.

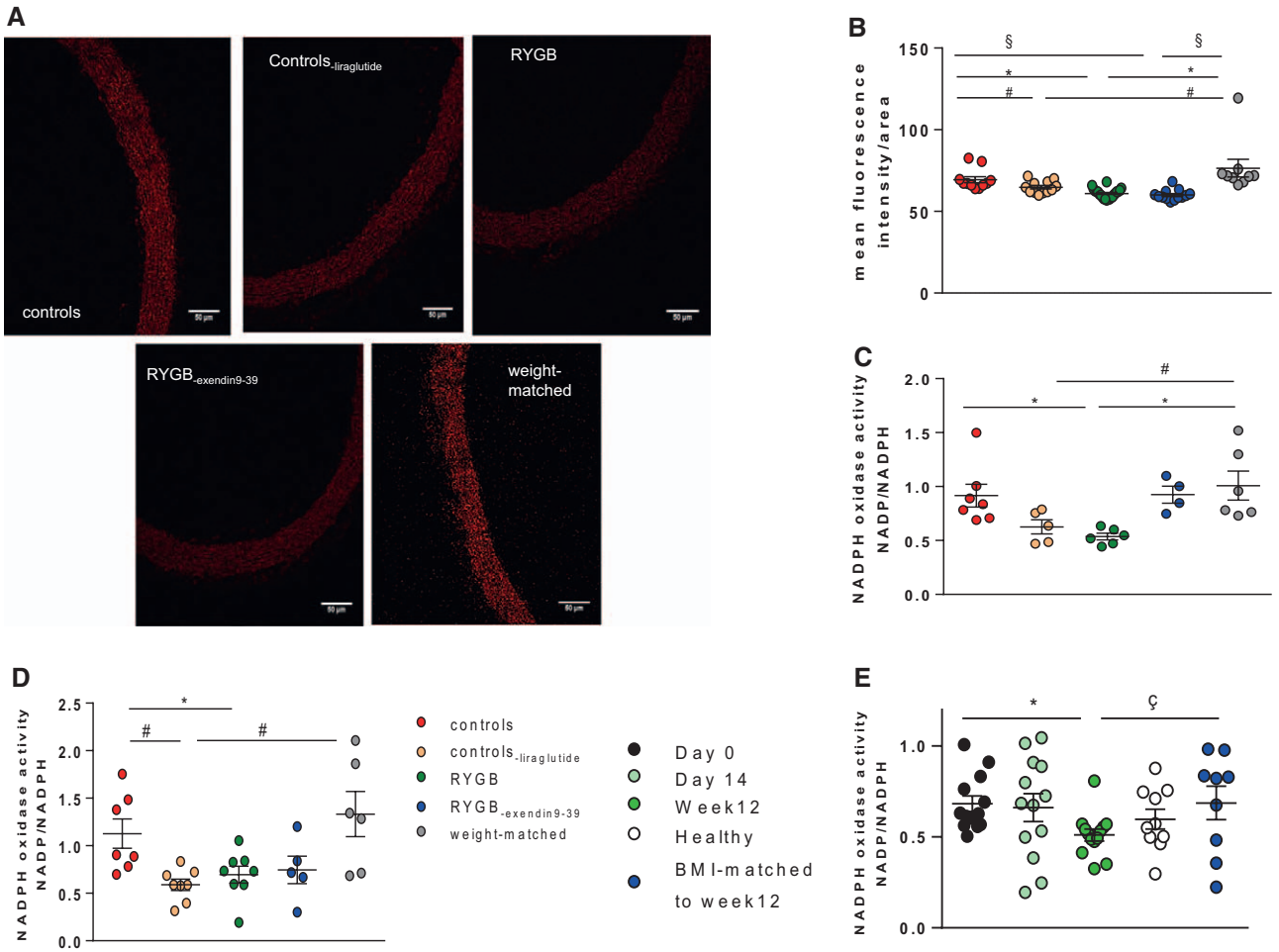

Figure 5. Fluorescence detection of superoxide anions in rat aortas labeled with red dihydroethidium staining (**A**) and relative quantification (**B**). NADPH oxidase activity was measured in rat aortas (**C**) and in human aortic endothelial cells (HAECs) after stimulation with high-density lipoprotein (HDL; **D**) isolated from rats after Roux-en-Y gastric bypass (RYGB) and after glucagon-like peptide-1 (GLP-1) modulation. *RYGB vs controls, §$RYGB_{-exendin9-39}$ vs sham-operated rats, $P \leq 0.05$; #$controls_{-liraglutide}$ vs sham-operated rats, $P<0.05$. **E**, NADPH oxidase activity in HAECs stimulated with HDL isolated preoperatively (D0), at day 14 (D14), and at 12 weeks (W12) after RYGB and in body mass index (BMI)–matched patients. *D0 vs W12, çW12 vs BMI matched, $P<0.05$; n=13 RYGB patients, 10 healthy subjects, and 9 body mass index (BMI)–matched patients.

Furthermore, the phosphorylation of JNK was reduced after RYGB and less potently so in $controls_{-liraglutide}$, but it was increased in $RYGB_{-exendin9-39}$. JNK is a crucial mediator of insulin resistance in obesity[29] and of endothelial dysfunction and oxidative stress.[23] Moreover, the inhibition of JNK signaling after the administration of GLP-1 analogs protects endothelial cells against lipotoxicity-induced apoptosis and "eNOS uncoupling."[24]

Indeed, obesity-induced oxidative stress impairs NO bioavailability.[3] This was confirmed by the significant improvement in relaxations with the free radical scavenger polyethylene glycol–superoxide dismutase in sham-operated rats but not in RYGB or $controls_{-liraglutide}$. Accordingly, NADPH oxidase activity and O_2^- concentration decreased rapidly after RYGB and in $controls_{-liraglutide}$. As a consequence of reduced aortic oxidative stress, eNOS uncoupling,[3,24] which causes dysfunction of the enzyme, was prevented in RYGB, as shown by higher dimerization and lower glutathionylation of eNOS. This explains the improved NO-dependent relaxations in RYGB compared with weight-matched or $exendin_{9-39}$–treated RYGB rats. As in RYGB, restored eNOS activity was paralleled by increased NO production after treatment with liraglutide. Hence, elevated GLP-1 levels and activation of GLP-1 receptor signaling play a key role in the improved endothelium-dependent vasodilatation after RYGB independently of weight loss.

Rapid Improvement of Endothelium-Protective Properties of HDL After RYGB Involves a GLP-1–Dependent Mechanism

Favorable lipid effects, that is, higher HDL cholesterol combined with lower low-density lipoprotein cholesterol and triglyceride levels, have been reported during long-term follow-up of patients after RYGB.[4,11] The hormonal changes after RYGB are likely to influence lipid metabolism in addition to the weight loss per se, as suggested by the persistence of a beneficial lipid profile even in the fate of weight regain after surgery.[39]

The present experiments demonstrate a specific effect of RYGB on HDL-mediated endothelial protection. HDL isolated after RYGB increased endothelial NO release and decreased

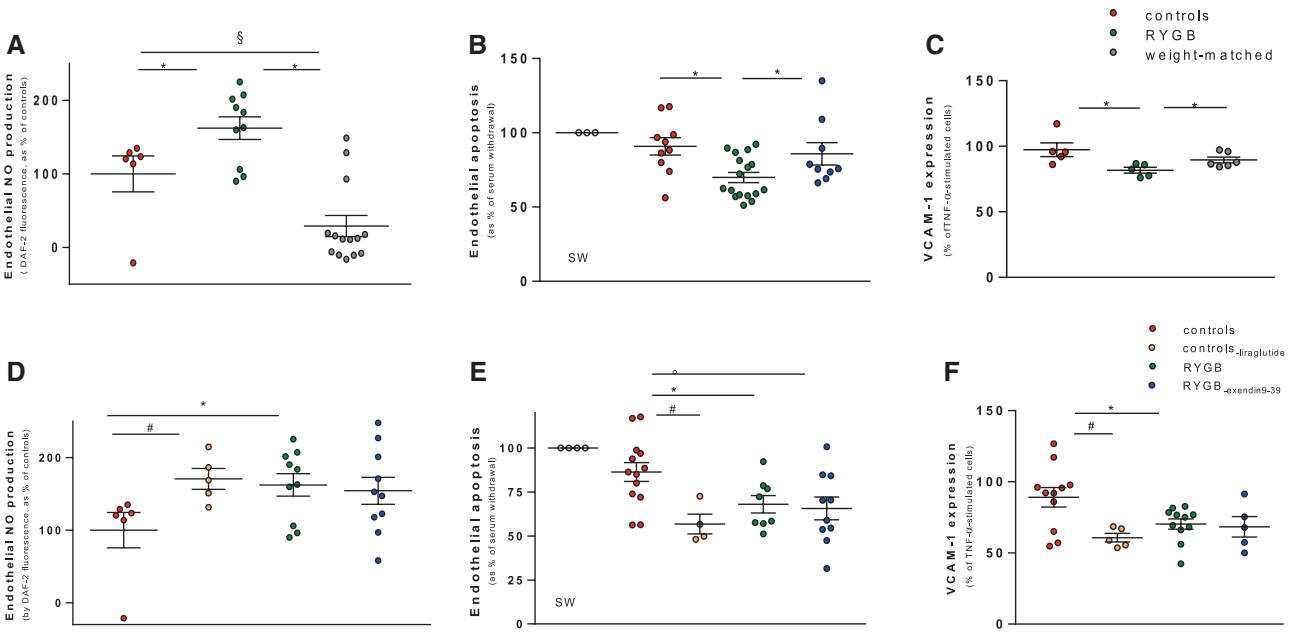

Figure 6. Endothelial nitric oxide (NO) production after human aortic endothelial cell stimulation with high-density lipoprotein (HDL) isolated after Roux-en-Y gastric bypass (RYGB; **A**) and after glucagon-like peptide-1 (GLP-1) modulation (**D**). Endothelial antiapoptotic effect (**B**) and endothelial anti-inflammatory effect (**C**) of HDL after RYGB and after GLP-1 modulation (**E** and **F**, respectively). *RYGB vs other groups, §control vs weight-matched group, #controls vs controls$_{-liraglutide}$, controls vs RYGB$_{-exendin9-39}$, $P<0.05$; n=8 to 10 per group. SW indicates serum withdrawal; and VCAM-1, vascular cell adhesion molecule-1.

endothelial apoptosis and the expression of the adhesion molecule VCAM-1. Furthermore, the antioxidant activity of HDL and the capacity of the lipoprotein to stimulate cholesterol efflux from macrophages were also potentiated. All these protective effects did not improve in weight-matched rats, suggesting a weight-independent effect of RYGB. The most likely explanation for these weight-independent effects is the activation of the endothelial Akt/eNOS pathway after RYGB, which is the main pathway involved in HDL-mediated NO release,[7] and its antiapoptotic,[40] antioxidant,[7] and anti-inflammatory properties.[6,8]

Likewise, HDL isolated from controls$_{-liraglutide}$ improved NO release and decreased endothelial apoptosis, oxidative stress, and VCAM-1 expression in a manner similar to HDL obtained from animals undergoing RYGB, suggesting a novel effect mediated by GLP-1. Hence, increased plasma levels of GLP-1 after RYGB exert protective endothelial effects via improved HDL cholesterol properties, direct activation of endothelial signaling pathways, and insulin-dependent vascular effects.

Despite the effect of RYGB on the properties of HDL, no difference was observed in total cholesterol concentrations in rats after RYGB. However, the cholesterol distribution profile was changed toward smaller HDL cholesterol particles compared with sham-operated groups in which cholesterol eluted in larger particles (Figure VII in the online-only Data Supplement), as described in animals fed a high-cholesterol diet.[41] These changes in cholesterol distribution profile may be linked directly to the improved properties of HDL after RYGB.

GLP-1 analogs favorably modulate lipid metabolism in enterocytes and hepatocytes.[42] Here, liraglutide treatment resulted in smaller HDL cholesterol particles, shifting the cholesterol distribution profile toward that seen after RYGB. Again, this effect does not seem to be mediated by the known GLP-1 receptor, as shown by the lack of effect of exendin$_{9-39}$.

Translational Relevance of the Rapid Improvement of Endothelial Protective Properties of HDL After RYGB

RYGB rapidly improved the endothelial protective properties of HDL in severely obese patients and thus conferred a translational relevance to the experimental animal data. Indeed, HDL isolated 14 days after RYGB improved endothelial NO release as a consequence of restored eNOS dimerization. Preserved NO bioavailability was paralleled by reduced endothelial NADPH oxidase activity, apoptosis, and VCAM-1 expression but also a higher PON-1 activity and HDL-stimulated cholesterol efflux capacity. In a previous study, HDL isolated from obese adolescents 1 year after RYGB did not improve pSer^{1177}eNOS.[43] This result may be related to the fact that eNOS activation was assessed by pSer^{1177}eNOS alone, whereas NO release measurement combined with eNOS dimerization, as performed here, may be more informative for assessing disturbances of NO bioavailability.[3] Results obtained in the present study appear to be applicable to both sexes, whereas previous reports involved mainly women.[5,44] Furthermore, the properties of HDL improved 12 weeks after RYGB to the level of healthy subjects, although the patients were still obese. Moreover, HDL properties were impaired in BMI-matched patients.

These observations suggest that the degree of weight and BMI loss induced by surgery is not sufficient or critical per se to improve the protective properties of HDL.[5,44] Diet-induced weight loss is not associated with increased circulating GLP-1 and does not improve HDL properties.[43,45] In future studies, it will be relevant to evaluate the impact on endothelial protective HDL properties of the other 2 most commonly performed bariatric surgery procedures: vertical sleeve gastrectomy and gastric banding.[1] Sleeve gastrectomy produces enhanced GLP-1 secretion and improvements in type 2 diabetes mellitus independently of weight loss, similar to RYGB. On the

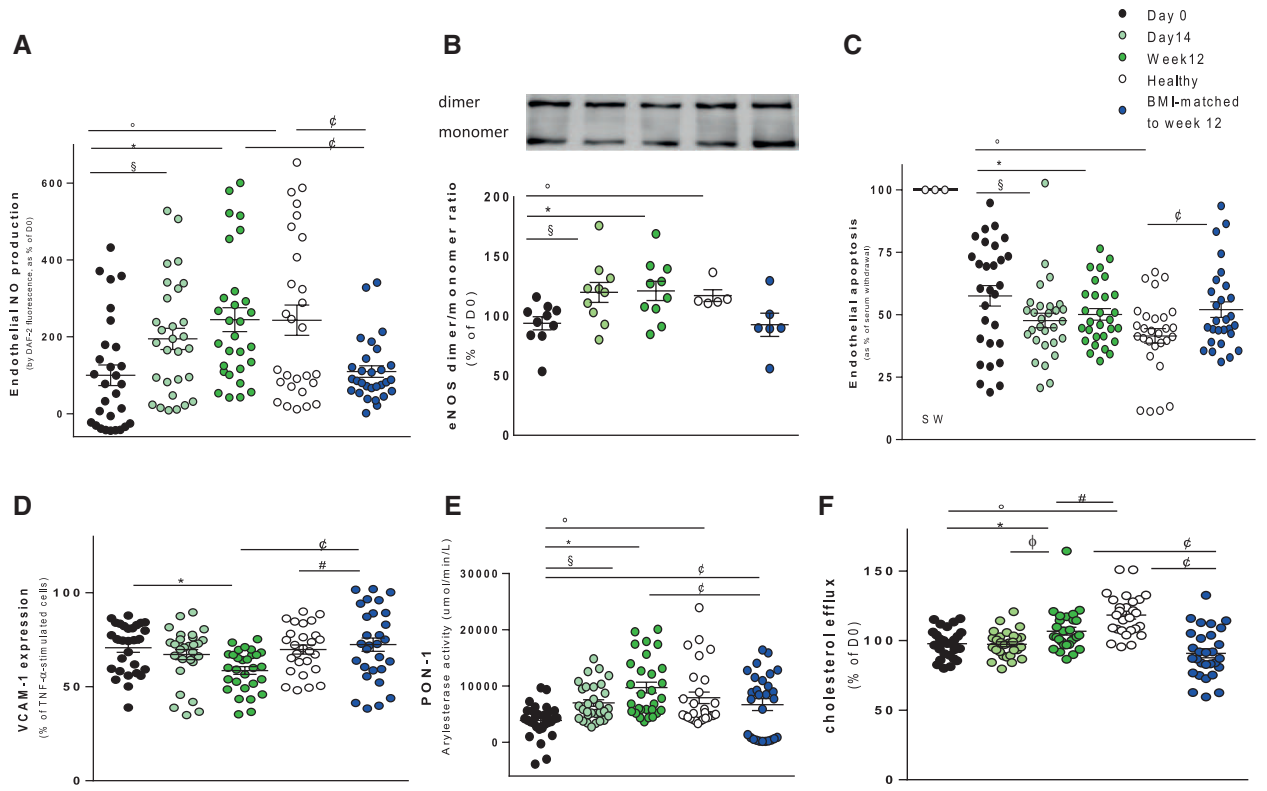

Figure 7. Endothelial nitric oxide (NO) production after human aortic endothelial cell (HAEC) stimulation with high-density lipoprotein (HDL) isolated preoperatively (D0), at day 14 (D14), and at 12 weeks (W12) after Roux-en-Y gastric bypass (RYGB) in body mass index (BMI)–matched patients and in healthy subjects (n=29 RYGB patients, 28 healthy subjects, 29 BMI matched; **A**); HDL-mediated endothelial NO synthase (eNOS) activation measured by eNOS dimerization (n=10 RYGB, 5 healthy, 6 BMI matched; **B**); endothelial antiapoptotic effect (n=29 RYGB, 28 healthy, 28 BMI matched; **C**); and anti-inflammatory effect of HDL on tumor necrosis factor-α–stimulated HAECs (n=29 RYGB, 27 healthy, 29 BMI matched; **D**). HDL-associated paraoxonase-1 (PON-1) activity (n=29 RYGB, 28 healthy, 28 BMI matched; **E**) and HDL-stimulated macrophage cholesterol efflux (n=28 RYGB, 28 healthy, 29 BMI matched; **F**). SW indicates serum withdrawal; and VCAM-1, vascular cell adhesion molecule-1. °D0 vs healthy, §D0 vs D14, *D0 vs W12, ΦD14 vs W12, #W12 vs healthy, ¢ W12 vs BMI matched, $P<0.05$.

other hand, adjustable gastric banding, which is a restrictive procedure, is associated with comparably smaller increases in circulating GLP-1 or in other gut hormones.[31]

Finally, RYGB normalized the fasting plasma levels of bile acids in patients, expanding a previous observation about the restoration of the postprandial rise in bile acids after RYGB.[46] Circulating bile acids, which were also elevated in the rats after RYGB, interact with the endothelium and induce NO production via Akt/eNOS activation[47]; they reduce endothelial VCAM -1 expression[47] and improve the ability of HDL to stimulate

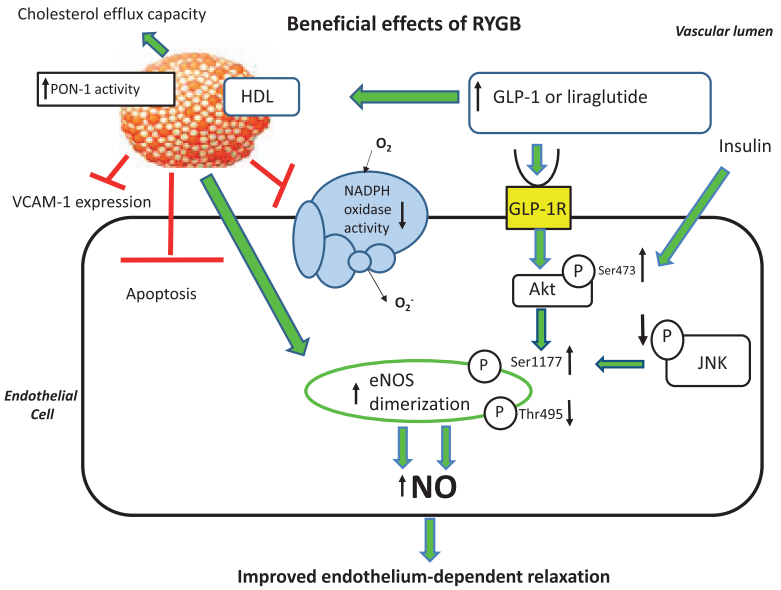

Figure 8. Proposed cellular mechanisms involved in the beneficial effects of Roux-en-Y gastric bypass (RYGB) on endothelial function and high-density lipoprotein (HDL) vasoprotective properties. The bioavailability of nitric oxide (NO) is decreased in obesity. Rapidly after RYGB, elevated glucagon-like peptide-1 (GLP-1) levels through the activation of the GLP-1 receptor (GLP-1R) activate the phosphorylated (P) Ser^{473}-Akt cascade, enhancing peNOSer^{1177}and endothelial NO synthase (eNOS) dimerization while reducing p-eNOSThr^{495}, c-Jun amino terminal kinase (JNK) phosphorylation, NADPH oxidase activity, and anion superoxide (O_2^-) production. This leads to higher NO levels and thus improved endothelial function. These effects are mimicked by liraglutide treatment in control rats and are blocked by exendin$_{9\text{-}39}$ after RYGB. RYGB surgery and liraglutide also improved HDL-mediated NO production and endothelial antiapoptotic, antioxidant, and anti-inflammatory properties. These properties are independent of the activation of the known GLP-1 receptor and are not blocked by exendin$_{9\text{-}39}$. HDL-associated paraoxonase-1 (PON-1) activity and cholesterol efflux improve after RYGB independently of GLP-1 modulation. VCAM-1 indicates vascular cell adhesion molecule-1.

cholesterol efflux. Therefore, bile acids may have contributed directly to the improved endothelial protective effects observed in the present study. However, because liraglutide treatment, in the absence of elevated bile acids levels, mimicked the beneficial metabolic effects of RYGB, GLP-1 signaling may be the dominating factor under the present experimental conditions.

A major strength of the present study is its translational nature. It highlights with the animal experiments that the cardiovascular effects of RYGB likely derive from more than simple weight loss and that increased GLP-1 signaling may play a critical role for some surgery-specific beneficial effects. The rapid improvement in the vascular protective properties of HDL also applies to morbidly obese patients undergoing RYGB.

Conclusions

The present study shows that RYGB exerts endothelium-protective effects beyond surgery-induced weight loss. These effects are mediated, at least in part, by GLP-1 and GLP-1 receptor signaling. These findings may allow the identification of less invasive treatment strategies targeting molecular cardiovascular and metabolic pathways affected by obesity.

Acknowledgments

We thank Markus Bachschmid, Melroy Miranda, Maja Franziska Müller, Silvija Radosavljevic, and Nicole Kachappilly for technical help.

Sources of Funding

This work was supported in part by grants of the Swiss National Research Foundation (grant 310030-135815), the Fondation Leducq, Paris (Transatlantic Network on HDL Dysfunction), the University of Zurich (Forschungskredit and Center of Integrative Human Physiology), the Swiss Heart Foundation, the Hartmann Müller Foundation, the European Union (RESOLVE), and the Foundation for Cardiovascular Research–Zurich Heart House, Zurich, Switzerland.

Disclosures

None.

References

1. Poirier P, Cornier MA, Mazzone T, Stiles S, Cummings S, Klein S, McCullough PA, Ren Fielding C, Franklin BA; American Heart Association Obesity Committee of the Council on Nutrition, Physical Activity, and Metabolism. Bariatric surgery and cardiovascular risk factors: a scientific statement from the American Heart Association. *Circulation*. 2011;123:1683–1701. doi: 10.1161/CIR.0b013e3182149099.
2. Sansbury BE, Cummins TD, Tang Y, Hellmann J, Holden CR, Harbeson MA, Chen Y, Patel RP, Spite M, Bhatnagar A, Hill BG. Overexpression of endothelial nitric oxide synthase prevents diet-induced obesity and regulates adipocyte phenotype. *Circ Res*. 2012;111:1176–1189. doi: 10.1161/CIRCRESAHA.112.266395.
3. Mauricio MD, Aldasoro M, Ortega J, Vila JM. Endothelial dysfunction in morbid obesity. *Curr Pharm Des*. 2013;19:5718–5729.
4. Bays HE, Toth PP, Kris-Etherton PM, Abate N, Aronne LJ, Brown WV, Gonzalez-Campoy JM, Jones SR, Kumar R, La Forge R, Samuel VT. Obesity, adiposity, and dyslipidemia: a consensus statement from the National Lipid Association. *J Clin Lipidol*. 2013;7:304–383. doi: 10.1016/j.jacl.2013.04.001.
5. Asztalos BF, Swarbrick MM, Schaefer EJ, Dallal GE, Horvath KV, Ai M, Stanhope KL, Austrheim-Smith I, Wolfe BM, Ali M, Havel PJ. Effects of weight loss, induced by gastric bypass surgery, on HDL remodeling in obese women. *J Lipid Res*. 2010;51:2405–2412. doi: 10.1194/jlr.P900015.
6. Sorrentino SA, Besler C, Rohrer L, Meyer M, Heinrich K, Bahlmann FH, Mueller M, Horváth T, Doerries C, Heinemann M, Flemmer S, Markowski A, Manes C, Bahr MJ, Haller H, von Eckardstein A, Drexler H, Landmesser U. Endothelial-vasoprotective effects of high-density lipoprotein are impaired in patients with type 2 diabetes mellitus but are improved after extended-release niacin therapy. *Circulation*. 2010;121:110–122. doi: 10.1161/CIRCULATIONAHA.108.836346.
7. Besler C, Heinrich K, Rohrer L, Doerries C, Riwanto M, Shih DM, Chroni A, Yonekawa K, Stein S, Schaefer N, Mueller M, Akhmedov A, Daniil G, Manes C, Templin C, Wyss C, Maier W, Tanner FC, Matter CM, Corti R, Furlong C, Lusis AJ, von Eckardstein A, Fogelman AM, Lüscher TF, Landmesser U. Mechanisms underlying adverse effects of HDL on eNOS-activating pathways in patients with coronary artery disease. *J Clin Invest*. 2011;121:2693–2708. doi: 10.1172/JCI42946.
8. Lüscher TF, Landmesser U, von Eckardstein A, Fogelman AM. High-density lipoprotein: vascular protective effects, dysfunction, and potential as therapeutic target. *Circ Res*. 2014;114:171–182. doi: 10.1161/CIRCRESAHA.114.300935.
9. Raffaelli M, Guidone C, Callari C, Iaconelli A, Bellantone R, Mingrone G. Effect of gastric bypass versus diet on cardiovascular risk factors. *Ann Surg*. 2014;259:694–699. doi: 10.1097/SLA.0b013e31829d6989.
10. Ikramuddin S, Korner J, Lee WJ, Connett JE, Inabnet WB, Billington CJ, Thomas AJ, Leslie DB, Chong K, Jeffery RW, Ahmed L, Vella A, Chuang LM, Bessler M, Sarr MG, Swain JM, Laqua P, Jensen MD, Bantle JP. Roux-en-Y gastric bypass vs intensive medical management for the control of type 2 diabetes, hypertension, and hyperlipidemia: the Diabetes Surgery Study randomized clinical trial. *JAMA*. 2013;309:2240–2249. doi: 10.1001/jama.2013.5835.
11. Adams TD, Davidson LE, Litwin SE, Kolotkin RL, LaMonte MJ, Pendleton RC, Strong MB, Vinik R, Wanner NA, Hopkins PN, Gress RE, Walker JM, Cloward TV, Nuttall RT, Hammoud A, Greenwood JL, Crosby RD, McKinlay R, Simper SC, Smith SC, Hunt SC. Health benefits of gastric bypass surgery after 6 years. *JAMA*. 2012;308:1122–1131. doi: 10.1001/2012.jama.11164.
12. Mingrone G, Panunzi S, De Gaetano A, Guidone C, Iaconelli A, Leccesi L, Nanni G, Pomp A, Castagneto M, Ghirlanda G, Rubino F. Bariatric surgery versus conventional medical therapy for type 2 diabetes. *N Engl J Med*. 2012;366:1577–1585. doi: 10.1056/NEJMoa1200111.
13. Brethauer SA, Heneghan HM, Eldar S, Gatmaitan P, Huang H, Kashyap S, Gornik HL, Kirwan JP, Schauer PR. Early effects of gastric bypass on endothelial function, inflammation, and cardiovascular risk in obese patients. *Surg Endosc*. 2011;25:2650–2659. doi: 10.1007/s00464-011-1620-6.
14. Faria G, Preto J, da Costa EL, Guimarães JT, Calhau C, Taveira-Gomes A. Acute improvement in insulin resistance after laparoscopic Roux-en-Y gastric bypass: is 3 days enough to correct insulin metabolism? *Obes Surg*. 2013;23:103–110. doi: 10.1007/s11695-012-0803-0.
15. Laferrère B, Reilly D, Arias S, Swerdlow N, Gorroochurn P, Bawa B, Bose M, Teixeira J, Stevens RD, Wenner BR, Bain JR, Muehlbauer MJ, Haqq A, Lien L, Shah SH, Svetkey LP, Newgard CB. Differential metabolic impact of gastric bypass surgery versus dietary intervention in obese diabetic subjects despite identical weight loss. *Sci Transl Med*. 2011;3:80re2. doi: 10.1126/scitranslmed.3002043.
16. Plum L, Ahmed L, Febres G, Bessler M, Inabnet W, Kunreuther E, McMahon DJ, Korner J. Comparison of glucostatic parameters after hypocaloric diet or bariatric surgery and equivalent weight loss. *Obesity (Silver Spring)*. 2011;19:2149–2157. doi: 10.1038/oby.2011.134.
17. Quercia I, Dutia R, Kotler DP, Belsley S, Laferrère B. Gastrointestinal changes after bariatric surgery. *Diabetes Metab*. 2014;40:87–94. doi: 10.1016/j.diabet.2013.11.003.
18. Laferrère B, Teixeira J, McGinty J, Tran H, Egger JR, Colarusso A, Kovack B, Bawa B, Koshy N, Lee H, Yapp K, Olivan B. Effect of weight loss by gastric bypass surgery versus hypocaloric diet on glucose and incretin levels in patients with type 2 diabetes. *J Clin Endocrinol Metab*. 2008;93:2479–2485. doi: 10.1210/jc.2007-2851.
19. Campbell JE, Drucker DJ. Pharmacology, physiology, and mechanisms of incretin hormone action. *Cell Metab*. 2013;17:819–837. doi: 10.1016/j.cmet.2013.04.008.
20. Wadden TA, Hollander P, Klein S, Niswender K, Woo V, Hale PM, Aronne L; NN8022-1923 Investigators. Weight maintenance and additional weight loss with liraglutide after low-calorie-diet-induced weight loss: the SCALE Maintenance randomized study. *Int J Obes (Lond)*. 2013;37:1443–1451. doi: 10.1038/ijo.2013.120.
21. Anagnostis P, Athyros VG, Adamidou F, Panagiotou A, Kita M, Karagiannis A, Mikhailidis DP. Glucagon-like peptide-1-based therapies and cardiovascular disease: looking beyond glycaemic control. *Diabetes Obes Metab*. 2011;13:302–312. doi: 10.1111/j.1463-1326.2010.01345.x.
22. Bueter M, Abegg K, Seyfried F, Lutz TA, le Roux CW. Roux-en-Y gastric bypass operation in rats. *J Vis Exp*. 2012:e3940.
23. Osto E, Matter CM, Kouroedov A, Malinski T, Bachschmid M, Camici GG, Kilic U, Stallmach T, Boren J, Iliceto S, Lüscher TF, Cosentino F.

c-Jun N-terminal kinase 2 deficiency protects against hypercholesterolemia-induced endothelial dysfunction and oxidative stress. *Circulation*. 2008;118:2073–2080. doi: 10.1161/CIRCULATIONAHA.108.765032.
24. Erdogdu O, Eriksson L, Xu H, Sjöholm A, Zhang Q, Nyström T. Exendin-4 protects endothelial cells from lipoapoptosis by PKA, PI3K, eNOS, p38 MAPK, and JNK pathways. *J Mol Endocrinol*. 2013;50:229–241. doi: 10.1530/JME-12-0166.
25. Weber M, Müller MK, Bucher T, Wildi S, Dindo D, Horber F, Hauser R, Clavien PA. Laparoscopic gastric bypass is superior to laparoscopic gastric banding for treatment of morbid obesity. *Ann Surg*. 2004;240:975–982.
26. Baron AD. Insulin resistance and vascular function. *J Diabetes Complications*. 2002;16:92–102.
27. Rask-Madsen C, Li Q, Freund B, Feather D, Abramov R, Wu IH, Chen K, Yamamoto-Hiraoka J, Goldenbogen J, Sotiropoulos KB, Clermont A, Geraldes P, Dall'Osso C, Wagers AJ, Huang PL, Rekhter M, Scalia R, Kahn CR, King GL. Loss of insulin signaling in vascular endothelial cells accelerates atherosclerosis in apolipoprotein E null mice. *Cell Metab*. 2010;11:379–389. doi: 10.1016/j.cmet.2010.03.013.
28. Zhang L, Yang M, Ren H, Hu H, Boden G, Li L, Yang G. GLP-1 analogue prevents NAFLD in ApoE KO mice with diet and Acrp30 knockdown by inhibiting c-JNK. *Liver Int*. 2013;33:794–804. doi: 10.1111/liv.12120.
29. Hirosumi J, Tuncman G, Chang L, Görgün CZ, Uysal KT, Maeda K, Karin M, Hotamisligil GS. A central role for JNK in obesity and insulin resistance. *Nature*. 2002;420:333–336. doi: 10.1038/nature01137.
30. Fleming I, Fisslthaler B, Dimmeler S, Kemp BE, Busse R. Phosphorylation of Thr(495) regulates Ca(2+)/calmodulin-dependent endothelial nitric oxide synthase activity. *Circ Res*. 2001;88:E68–E75.
31. Galougahi KK, Liu CC, Gentile C, Kok C, Nunez A, Garcia A, Fry NA, Davies MJ, Hawkins CL, Rasmussen HH, Figtree GA. Glutathionylation mediates angiotensin II-induced eNOS uncoupling, amplifying NADPH oxidase-dependent endothelial dysfunction. *J Am Heart Assoc*. 2014;3:e000731. doi: 10.1161/JAHA.113.000731.
32. Sivertsen J, Rosenmeier J, Holst JJ, Vilsbøll T. The effect of glucagon-like peptide 1 on cardiovascular risk. *Nat Rev Cardiol*. 2012;9:209–222. doi: 10.1038/nrcardio.2011.211.
33. Ban K, Noyan-Ashraf MH, Hoefer J, Bolz SS, Drucker DJ, Husain M. Cardioprotective and vasodilatory actions of glucagon-like peptide 1 receptor are mediated through both glucagon-like peptide 1 receptor-dependent and -independent pathways. *Circulation*. 2008;117:2340–2350. doi: 10.1161/CIRCULATIONAHA.107.739938.
34. Green BD, Hand KV, Dougan JE, McDonnell BM, Cassidy RS, Grieve DJ. GLP-1 and related peptides cause concentration-dependent relaxation of rat aorta through a pathway involving KATP and cAMP. *Arch Biochem Biophys*. 2008;478:136–142. doi: 10.1016/j.abb.2008.08.001.
35. Nyström T, Gonon AT, Sjöholm A, Pernow J. Glucagon-like peptide-1 relaxes rat conduit arteries via an endothelium-independent mechanism. *Regul Pept*. 2005;125:173–177. doi: 10.1016/j.regpep.2004.08.024.
36. Laviola L, Leonardini A, Melchiorre M, Orlando MR, Peschechera A, Bortone A, Paparella D, Natalicchio A, Perrini S, Giorgino F. Glucagon-like peptide-1 counteracts oxidative stress-dependent apoptosis of human cardiac progenitor cells by inhibiting the activation of the c-Jun N-terminal protein kinase signaling pathway. *Endocrinology*. 2012;153:5770–5781. doi: 10.1210/en.2012-1461.
37. Noyan-Ashraf MH, Shikatani EA, Schuiki I, Mukovozov I, Wu J, Li RK, Volchuk A, Robinson LA, Billia F, Drucker DJ, Husain M. A glucagon-like peptide-1 analog reverses the molecular pathology and cardiac dysfunction of a mouse model of obesity. *Circulation*. 2013;127:74–85. doi: 10.1161/CIRCULATIONAHA.112.091215.
38. Nyström T, Gutniak MK, Zhang Q, Zhang F, Holst JJ, Ahrén B, Sjöholm A. Effects of glucagon-like peptide-1 on endothelial function in type 2 diabetes patients with stable coronary artery disease. *Am J Physiol Endocrinol Metab*. 2004;287:E1209–E1215. doi: 10.1152/ajpendo.00237.2004.
39. Brolin RE, Bradley LJ, Wilson AC, Cody RP. Lipid risk profile and weight stability after gastric restrictive operations for morbid obesity. *J Gastrointest Surg*. 2000;4:464–469.
40. Riwanto M, Rohrer L, Roschitzki B, Besler C, Mocharla P, Mueller M, Perisa D, Heinrich K, Altwegg L, von Eckardstein A, Lüscher TF, Landmesser U. Altered activation of endothelial anti- and proapoptotic pathways by high-density lipoprotein from patients with coronary artery disease: role of high-density lipoprotein-proteome remodeling. *Circulation*. 2013;127:891–904. doi: 10.1161/CIRCULATIONAHA.112.108753.
41. Mahley RW, Weisgraber KH, Innerarity T, Brewer HB Jr, Assmann G. Swine lipoproteins and atherosclerosis: changes in the plasma lipoproteins and apoproteins induced by cholesterol feeding. *Biochemistry*. 1975;14:2817–2823.
42. Xiao C, Dash S, Lewis GF. Mechanisms of incretin effects on plasma lipids and implications for the cardiovascular system. *Cardiovasc Hematol Agents Med Chem*. 2012;10:289–294.
43. Matsuo Y, Oberbach A, Till H, Inge TH, Wabitsch M, Moss A, Jehmlich N, Völker U, Müller U, Siegfried W, Kanesawa N, Kurabayashi M, Schuler G, Linke A, Adams V. Impaired HDL function in obese adolescents: impact of lifestyle intervention and bariatric surgery. *Obesity (Silver Spring)*. 2013;21:E687–E695. doi: 10.1002/oby.20538.
44. Aron-Wisnewsky J, Julia Z, Poitou C, Bouillot JL, Basdevant A, Chapman MJ, Clement K, Guerin M. Effect of bariatric surgery-induced weight loss on SR-BI-, ABCG1-, and ABCA1-mediated cellular cholesterol efflux in obese women. *J Clin Endocrinol Metab*. 2011;96:1151–1159. doi: 10.1210/jc.2010-2378.
45. Aicher BO, Haser EK, Freeman LA, Carnie AV, Stonik JA, Wang X, Remaley AT, Kato GJ, Cannon RO 3rd. Diet-induced weight loss in overweight or obese women and changes in high-density lipoprotein levels and function. *Obesity (Silver Spring)*. 2012;20:2057–2062. doi: 10.1038/oby.2012.56.
46. Ahmad NN, Pfalzer A, Kaplan LM. Roux-en-Y gastric bypass normalizes the blunted postprandial bile acid excursion associated with obesity. *Int J Obes (Lond)*. 2013;37:1553–1559. doi: 10.1038/ijo.2013.38.
47. Kida T, Tsubosaka Y, Hori M, Ozaki H, Murata T. Bile acid receptor TGR5 agonism induces NO production and reduces monocyte adhesion in vascular endothelial cells. *Arterioscler Thromb Vasc Biol*. 2013;33:1663–1669. doi: 10.1161/ATVBAHA.113.301565.

CLINICAL PERSPECTIVE

Obesity is a public health priority because of the associated increase in morbidity and cardiovascular mortality. Currently, the most effective treatment for severe obesity is bariatric surgery, which induces sustained weight loss and is associated with a long-term reduction in obesity-associated comorbidity and cardiovascular mortality. The current understanding of the mechanisms underlying these beneficial effects suggests that a crucial role is played by the unique metabolic and hormonal changes after bariatric surgeries, in particular Roux-en-Y gastric bypass or vertical sleeve gastrectomy, rather than simply as the consequence of weight loss. The gut hormone glucagon-like peptide-1 (GLP-1), which increases rapidly after certain bariatric surgeries such as Roux en-Y gastric bypass and sleeve gastrectomy, but not after dietary restriction, seems to specifically mediate some metabolic benefits of bariatric surgery. In the present study, which uses a rat model of Roux-en-Y gastric bypass, higher plasma levels of GLP-1 were associated with increased aortic nitric oxide bioavailability, improved endothelium-dependent relaxation, and normalized endothelium-protective properties of high-density lipoprotein independently of weight loss. Furthermore, in morbidly obese patients, increased plasma levels of GLP-1 after Roux-en-Y gastric bypass were associated with a rapid improvement in the endothelium-protective properties of high-density lipoprotein, confirming the clinical relevance of the experimental animal findings. Thus, Roux-en-Y gastric bypass exerts rapid endothelium-protective effects beyond the surgery-induced weight loss. These effects are mediated, at least in part, by GLP-1 and GLP-1 receptor signaling. These findings may allow the identification of novel and less invasive treatment strategies targeting molecular cardiovascular and metabolic pathways affected by obesity.

Rapid and body weight-independent improvement of endothelial and HDL function after Roux-en-Y gastric bypass: role of glucagon-like peptide-1.

SUPPLEMENTAL MATERIAL

°Elena Osto, MD,PhD[1, *]; Petia Doytcheva, Msc[1,2*];Caroline Corteville, MD[2]; Marco Bueter, MD,PhD[3], Claudia Dörig, Msc[2], Simona Stivala, PhD[1], Helena Buhmann, MD[2], Sophie Colin, PhD[4], Lucia Rohrer, PhD[5]; Reda Hasballa Msc[5], Anne Tailleux, PhD[4], Christian Wolfrum PhD[6], .Francesco Tona, MD,PhD[7], Jasmin Manz Msc[1], Diana Vetter, MD[3], Kerstin Spliethoff DVM[2], Paul M. Vanhoutte MD, PhD[8], Ulf Landmesser, MD[1], Francois Pattou, MD,PhD[9], Bart Staels MD[4], Christian M. Matter, MD[1], Thomas A. Lutz DVM,PhD[2*], and Thomas F. Lüscher MD[1*].

1 Centre for Molecular Cardiology, University of Zurich and University Heart Center, Cardiology, University Hospital Zurich, Switzerland, 2Institute of Veterinary Physiology, University of Zurich, Switzerland, 3Department of Surgery, University Hospital Zurich, Switzerland, 4 Université Lille 2, INSERM UMR1011, EGID, Institut Pasteur de Lille, Lille, France , 5Institute of Clinical Chemistry, University Hospital Zurich, Switzerland,6 Department of Health Sciences and Technology, ETH Zurich, Switzerland, 7Department of Cardiac, Thoracic and Vascular Sciences, University of Padua, Italy ,8State Key Laboratory for Pharmaceutical Biotechnologies &Department of Pharmacology & Pharmacy, LKS Faculty of Medicine, The University of Hong Kong, 9Department of Endocrine Surgery, Lille University Hospital, France.

Running title: rapid effects of RYGB on endothelial and HDL function

Address for Correspondence °Elena Osto, M.D., Ph.D.

Centre for Molecular Cardiology

University of Zurich

Wagistrasse, 12

CH-8952 Schlieren, Switzerland

Tel: 41-44-635 6469

Fax: 41-44-635 6827

Email: elena.osto@uzh.ch

*These authors contributed equally.

Supplemental Materials and Methods

Animals and housing

Adult male Wistar rats obtained from Janvier, France, weighted 250-300g at arrival. We performed a pilot experiment in order to define 1) the appropriate diet (high fat high cholesterol (HFHC) versus high fat (HF) only) to achieve diet-induced obesity (DIO) and impaired endothelial dysfunction; 2) the earliest time point for tissue harvesting and HDL isolation after RYGB in order to avoid the acute phase reaction post-surgical trauma and 3) the approximate amount of food eaten by the RYGB rats for weight matching of sham-operated rats in the subsequent tests (see below). Seven weeks of HFHC diet induced endothelial dysfunction in contrast to HF diet alone (data not shown). The acute phase reaction after RYGB was resolved on post-operative day 8 (D8) as indicated by the time courses of Interleukin (IL)-1β, tumor necrosis factor (TNF)-α and IL-6 (data not shown). For all subsequent experiments, rats were transferred to a commercial HFHC containing 60% kcal fat and 1.25% cholesterol (Research Diets, New Brunswick NJ, USA) for a period of 7 weeks prior to surgery; the same diet was offered post-surgery. Rats were initially housed 4 per cage in Makrolon cages (Indulab, Gams, Switzerland). One week before surgery, they were single housed in wire mesh cages until the end of the experimental period. Rats were housed in a colony room with an average temperature of 23°C and a 12-hour light/dark cycle. The groups of animals used for the following two main experiments were: 1.) RYGB or sham-surgery fed ad libitum (controls) or weight- matched to RYGB and followed for a D8 period (SOM Fig.1A); 2.) RYGB or controls followed for a D8 period and simultaneous *in vivo* GLP-1 intervention (SOM Fig.1B). Some parameters were also assessed in RYGB and sham-operated rats that were followed up for one month after surgery. The Cantonal Zurich Veterinary Office approved all animal experiments.

Surgeries

Rats were randomly allocated to either RYGB or sham-operations. For the first experiment, 24 rats with an average body weight of 590g underwent RYGB surgery, and 24 underwent sham-surgery, of which 12 with an average body weight of 592g were controls, and 12 with average body weight of 593g were weight-matched to RYGB.

For the second experiment with simultaneous GLP-1 intervention, 22 rats with an average body weight of 502g underwent RYGB surgery and 12 rats with an average body weight of 500g underwent sham-surgery.

For the third experiment, 24 rats with an average body weight of 526g underwent RYGB surgery, and 24 rats underwent sham-surgery, of which 12 with an average body weight of 531g were controls and 12 with an average body weight of 532g were weight-matched.

Anesthesia was induced in a chamber filled with 5% isoflurane in room air (1 L/min). After an adequate depth of anesthesia was achieved, rats were shaved from sternum to pelvis followed by disinfection with Betadine scrub (Mundi Pharma, Basel, Switzerland). Rats were then placed in a supine position on a heating pad and positioned in a nose cone to maintain anesthesia (2%–3% isoflurane in room air, 0.8 L/min) for the duration of the surgery. All surgeries were conducted as previously described[1]. Briefly, a midline incision of approximately 4 cm starting just below the xiphoid process was performed. For the RYGB procedure, the proximal small bowel was transected approximately 20 cm distal to the pylorus of the stomach, creating a proximal and distal end of small bowel. The proximal end, being still continuous with the remaining portion of the stomach, constituted the biliopancreatic limb and was anastomosed to the distal small intestine, approximately 25–30 cm from the cecum, creating the common channel. For formation of the gastric pouch, the stomach was transected approximately 5 mm below the gastro-esophageal junction, creating a pouch of a size of less than 5% of original stomach size. The Roux-en-Y reconstruction was completed by connecting the distal end of the proximal small bowel to the gastric pouch, leading to

formation of the alimentary (Roux) limb. One single RYGB procedure lasted approximately 100 minutes. For sham operations, an anterior gastrostomy with subsequent closure was performed. One single sham procedure lasted approximately 30 minutes. The abdominal wall and the skin were closed in layers after both operations.

No RYGB rats died during surgery. Immediately following surgery, each rat received 5 mL of saline subcutaneously to compensate for fluid loss. Rats were then placed under indirect red light in a polycarbonate cage until they fully recovered from anesthesia, at which time they were returned to their home cages. Baytril 10mg/kg (Bayer, Germany) and Carprofen 5mg/kg (Norocarp, Norbrook Laboratories) were administered before surgery and for two days post-surgery. Post-operatively, rats were fed HFHC diet and body weight and food intake were measured daily. Sham rats were randomly divided into controls or weight-matched rats; the latter were food-restricted (approximately 9-10 g/day based on the pilot experiment). Hence, the weight-matched group had a controlled food intake in order to match their weight to RYGB rats, this allowed the distinction between RYGB-specific from weight-dependent effects, since the only difference between these two study groups was RYGB surgery. During three-days post-operatively the HFHC solid diet was mixed with water to facilitate swallowing.

In vivo GLP-1 interventions

For the second experiment, sham-operated and RYGB rats were randomized to one of the following treatment groups, respectively: controls were treated with phosphate-buffered saline (PBS) (vehicle, n=6) or with liraglutide (controls-$_{\text{liraglutide}}$; 0.2 mg/kg twice daily), n=6; RYGB were treated with vehicle (n=11) or RYGB exendin$_{9\text{-}39}$ (10ug/kg/h), n=11. Liraglutide (Victoza; Novo Nordisk, Bagsvaerd, Denmark) or PBS vehicle were administered twice daily via subcutaneous (s.c.) injections for the eight-days follow-up period starting immediately post-surgery, with one injection in the light phase and one in the dark phase. The liraglutide

dose was increased stepwise over the first two treatment days (0.05 mg/kg, 0.1 mg/kg, 0.15 mg/kg, 0.2 mg/kg) and then maintained at 0.2 mg/kg per injection. Exendin$_{9-39}$ (Bachem, Bubendorf, Switzerland) or its vehicle was administered s.c. via osmotic minipumps (Alzet model 2001, Charles River, Germany) for the eight-days follow-up period. Implantation of the osmotic minipumps was performed immediately following the RYGB surgery while rats were still under anesthesia; minipumps were inserted via an incision made in the midscapular region. Dosages of liraglutide and exendin$_{9-39}$ were selected based on previous *in vivo* results[2-4].

Rat blood collection

Preoperative plasma was collected on the day of surgery in Microvette EDTA vacutainers (Sarstedt, Nümbrecht, Germany) supplemented with protease inhibitor cocktail (Sigma-Aldrich, Saint Louis, Missouri,USA) and DPPIV inhibitor (Millipore, Darmstadt, Germany) and was kept on ice until centrifugation. Serum was collected in Microvette vacutainers (Sarstedt) and kept at room temperature until centrifugation. After centrifugation the supernatant was separated and stored at -80°C. Postoperative blood was collected at the time of euthanasia by heart puncture.

Tissue harvesting

Human insulin (10 mU/g; Humalog, Lilly, Indianapolis, Indiana, USA) or saline vehicle were injected intra-peritoneally for studying insulin signaling and action in subsequent *ex vivo* experiments as described[5]. Ten minutes after injection, rats were sacrificed and organs were harvested within 30 minutes; rats were anesthetized by isoflurane inhalation. The entire aorta from the heart to the iliac bifurcation was excised and placed immediately in cold modified Krebs-Ringer bicarbonate solution (pH 7.4, 37°C, 95% O2, 5% CO2) of the following composition (mmol/L): NaCl (118.6), KCl (4.7), CaCl2 (2.5), KH2PO4 (1.2), MgSO4 (1.2),

NaHCO3 (25.1), glucose (11.1), and calcium EDTA (0.026). The aorta was cleaned from adhering connective tissue under a dissection microscope and either snap-frozen in liquid nitrogen and stored at -80°C or used immediately for *ex vivo* organ chamber experiments.

Organ chamber experiments

For endothelial function experiments[6], 2-3 mm long aortic rings were connected to an isometric force transducer (Multi-Myograph 610M, Danish Myo Technology A/S, Aarhus, Denmark), suspended in an organ chamber filled with 5 mL Krebs-Ringer bicarbonate solution (37°C, pH 7.4), and bubbled with 95% O2, 5% CO2 at 37°C. Isometric tension was recorded continuously. After a 30-minutes equilibration period, rings were gradually stretched to the optimal point of their length-tension curve as determined by the contraction in response to potassium chloride (100 mmol/L). Concentration-response curves were obtained in a cumulative fashion. Responses to acetylcholine (10^{-9} to 10^{-6} mol/L; Sigma-Aldrich), GLP-$1_{(7–36)}$ amide (10^{-12}-10^{-6}mol/L; herein referred to as GLP-1; Bachem) and insulin (10^{-11} to 10^{-6} mol/L; Humalog, Lilly) were recorded during submaximal contraction to norepinephrine (10^{-6} mol/L, Sigma-Aldrich, USA) in the presence or absence of Nω-nitro-L-arginine methyl ester (L-NAME, 10^{-4} mol/L, Sigma-Aldrich), a non-selective nitric oxide (NO) synthase inhibitor or of the free radical scavenger polyethylene glycol–superoxide dismutase (SOD 150 U/mL, Sigma-Aldrich). The NO donor sodium nitroprusside (SNP, 10^{-10} to 10^{-5} mol/L; Sigma-Aldrich) was added to test endothelium-independent relaxation. Relaxations were expressed as a percentage of the pre-contraction. In order to study the direct effects of GLP-1 on vascular function, cumulative concentration-relaxation responses were obtained for the peptide GLP-$1_{(7-36)}$ amide (10^{-12} to 10^{-6} mol/L, Bachem) in the presence or absence of the highly specific GLP-1 receptor antagonist exendin$_{9-39}$ (10^{-5}mol/L 10 min before adding GLP-1) (Bachem), L-NAME or PEG-SOD.

Western blotting

Frozen aortae were pulverized and dissolved in lysis buffer (120 mmol/L sodium chloride, 50 mmol/L Tris, 20 mmol/L sodium fluoride, 1 mmol/L benzamidine, 1 mmol/L dithiothreitol, 1 mmol/L EDTA, 6 mmol/L EGTA, 15 mmol/L sodium pyrophosphate, 0.8 ug/mL leupeptin, 30 mmol/L *p*-nitrophenyl phosphate, 0.1 mmol/L phenylmethylsulfonyl fluoride, and 1% NP-40) for immunoblotting. The samples (30 ug) were subjected to SDS-PAGE gel for electrophoresis and incubated with SAPK/JNK and phospho-SAPK/JNK (Thr183/Tyr185) antibodies (Cell Signalling, Beverly, Massachusetts, USA), anti-eNOS/NOS Type III and anti-eNOS (pS1177) antibodies (BD Biosciences, San Jose, CA, USA), anti-eNOS (pT495) (BD Biosciences), Akt and phospho-Akt (Ser473) antibodies (Cell Signalling), anti-GLP-1-R antibody (Abcam, Cambridge, UK) and anti-GAPDH antibody (Millipore). The immunoreactive bands were detected by chemiluminescence (Amersham Biosciences, Buckinghamshire, UK) and quantified densitometrically with Image J software (National Institutes of Health, Bethesda, Maryland, USA). To assess eNOS dimer formation, non-denaturing low-temperature SDS-PAGE was employed. Aortas were lysed as described above, treated with 6x Laemmli`s buffer not containing β-mercaptoethanol, and immediately subjected to 6% SDS-PAGE without prior incubation at 99°C.

eNOS s-glutathionylation

Twenty mg of aortic tissue were lysed in lysis buffer supplemented with 25mM N-ethylmaleimide (NEM) (Sigma-Aldrich). eNOS was immunoprecipitated at 4°C overnight with NOS3 (C-20) agarose-conjugated antibody (Santa Cruz Biotechnology, Dallas, Texas, USA), eluted by two 10min 50°C 500rpm incubations with non-reducing 6xLaemmli`s buffer supplemented with 25mM NEM, and immediately subjected to non-reducing SDS-PAGE. S-glutathione was detected using anti-glutathione antibody (Virogen, Watertown, MA, USA) supplemented with 2.5mM NEM, and anti-eNOS/NOS Type III antibody (BD Biosciences).

DHE staining on rats aortae

Frozen 10 μm sections from aortae were cut with a Leica CM3050S cryostat and placed on positive-charged slides (Superfrost Plus, Thermo Scientific, Waltham, MA, USA). Dihydroethidium (Sigma Aldrich) was prepared as stock solution in DMSO, diluted in deoxygenated PBS (final concentration 5μM), and applied to frozen sections for 30 min at 37°C. Nuclei were counterstained with Hoechst 33258 (Sigma Aldrich, final concentration 1μg/ml). Slides were coverslipped and images taken on a SP8 microscope (10x/0.30 objective; Leica, Solms, Germany), and quantified (ImageJ, NIH). DHE fluorescence was calculated by subtracting the autofluorescence signal (green channel) from the DHE signal (red channel), and normalized to the total fluorescent area.

NADPH oxidase activity

NADPH oxidase activity was measured using a commercial NADP/NADPH assay kit (Abcam) according to the manufacturer`s instructions. To measure the effect of HDL on endothelial NADPH oxidase activity, HAECs were treated with HDL (50ug/ml) for one hour at 37°C, as described[7].

Serum bile acid measurements

Serum bile acids were measured with Cobas Integra 800 (Roche, Basel, Switzerland).

Plasma insulin and GLP-1 measurements

Customized rat and human duplex insulin/active GLP-1 Meso Scale Discovery 96-well plates were used to measure plasma insulin and GLP-1 concentrations, respectively, following the provided protocol (Meso Scale Discovery, Gaithersburg. MD, USA).

Serum HDL isolation by sequential density centrifugation

HDL was isolated from fresh, fasting plasma by density gradient ultracentrifugation (HDL: density 1.063 to 1.21 g/cm^3), as described[8, 9]. Potassium bromide (Merck KGaA, Darmstadt, Germany) was used to adjust the density. Purity of HDL was assessed by SDS-PAGE and subsequent Coomassie Blue staining of the gel.

Cell culture

Human aortic endothelial cells (HAEC) were obtained from (Lonza, Basel, Switzerland) and cultured in endothelial cell basal medium-2 (Lonza) supplemented with endothelial growth medium–SingleQuots as indicated by the manufacturer (37°C, 95% air / 5% CO2). HAECs were grown to sub-confluency and rendered quiescent before experiments by incubation in medium containing 0.5% fetal calf serum. For reverse cholesterol transport experiments, the murine macrophage cell line J774 was cultured on 75-cm2 flasks, in 10% FBS, 4.5g/l glucose RPMI medium 1640 (GIBCO, Life Technologies, Grand Island, NY, USA).

TNF α- induced VCAM 1 expression in HAEC stimulated with HDL

Expression of vascular cell adhesion molecule 1 (VCAM-1) was assessed in HAEC (passage 7-9) stimulated with TNF-α on 96-well black-wall clear-bottom plates (BD). HAECs were rendered quiescent before experiments and treated overnight with or without HDL (10-μg protein/mL), followed by four hours of stimulation with TNF-α (100pg/ml) before fixation. Blocking with Licor buffer and incubating cells with VCAM 1 (R&D Systems, Minneapolis, MN, USA). Washing and adding secondary antibody, anti-goat 800CW (green) with Draq-5 for normalization (680CW). For measurements the quantitative fluorescent imaging systems (LI-COR Odissey, Lincoln, Nebraska, USA) in channel 700CW and 800CW was used.

Measurement of endothelial cell NO production by 4,5-diaminofluorescein diacetate (DAF-2) staining.

Endothelial cell NO production was determined as described[10]. In brief, after overnight starvation HAEC were incubated for one hour at 37°C with HDL (60 μg/ml) and DAF-2 diacetate (1 μM; Cayman Chemical, Ann Arbor, Michigan, USA), that forms the fluorescent triazolofluorescein upon reaction with cellular NO. Following incubation, cells were transferred to a black microplate and fluorescence was measured on a Tecan Infinite M200 PRO reader (Tecan, Maennedorf, Switzerland) with excitation and emission wavelenghts of 485nm and 535nm, respectively.

Measurement of aortic NO production.

NO release in rat aortas was examined by electron spin resonance ESR spectroscopy analysis with the use of the spin-trap colloid Fe (DETC) 2 (Noxygen, Elzach, Germany), as described and validated previously[11, 12]. Briefly, Krebs-HEPES buffer (37°C), 500 μL of FeSO4 and DETC solution were added to each sample and incubated at 37°C for 60 minutes. Samples were frozen immediately in liquid nitrogen till recording with the use of NOX-E.5-ESR spectrometer (Bruker, Bremen, Germany). Signals were quantified by measuring the total amplitude after correction of baseline and subtraction of background signals.

PON-1 activity

Paraoxonase-1 (PON1) activity was determined using spectrophotometric measurement of rate of cleavage of phenylacetate (Sigma-Aldrich) to produce phenol in serum by monitoring the increase in absorbance at 270 nm at 25 °C, as described[13]. The resulting phenol concentration was calculated by the molar extinction coefficient, ε = 1,310 M–1 (pH 8.0). Each sample was run in duplicate. Activity of paraoxonase is expressed as umol/min/L.

In vitro apoptosis assay

HDL anti-apoptotic properties were assessed in HAEC by evaluating cytoplasmic DNA-histone complexes that increase after apoptosis associated DNA fragmentation, using the Cell Death Detection ELISA^{Plus} kit (Roche Biochemicals) according to the manufacturer's instructions.

In vitro reverse cholesterol transport capacity of HDL

J774 murine macrophages were seeded at a density of $1x10^6$ /well in 24-well plates and the next day labeled with 2 µCi/mL ^{3}H cholesterol for a minimum of 17 hours overnight in the presence of 2ug/ml acetyl-Coenzyme A acetyltransferase inhibitor (58-035, Sandoz Holzkirchen, Germany) in 500ul 0% FBS, 4.5g/l glucose RPMI 1640 medium (GIBCO, Life Technologies). The following day cells were washed 2x with PBS and equilibrated for six hours with 0.3mM 8-(4-bromophenylthio)-3'-5'-cyclic adenosine monophosphate (Sigma-Aldrich) in the presence of acetyl-Coenzyme A acetyltransferase inhibitor in 500ul 0% FBS 4.5g/l glucose RPMI medium. Apo B-depleted serum was obtained by polyethylene glycol precipitation, and 2.8% v/v Apo B-depleted serum was used as efflux acceptor for four hours in the presence of acetyl-Coenzyme A acetyltransferase inhibitor in 500ul 0% FBS MEM-25mM HEPES medium. As controls, 2.8% v/v Apo B-depleted healthy human serum or MEM-HEPES medium alone were used. Supernatants were collected and centrifuged during five minutes at 12 000 rpm and 250ul were used for ten minutes of liquid scintillation measurements (PerkinElmer, Boston, MA;USA). Cells were washed 1x with PBS and intracellular cholesterol was extracted twice sequentially with 500ul 3:2 hexane:isopropanol for thirty minutes and fifteen minutes respectively, evaporated under a N_2 flux and resuspended in 500ul isopropanol, from which 250ul were used for ten minutes liquid scintillation. Reverse cholesterol transport capacity of HDL was calculated as the ratio

between DPM counts of the supernatant vs. the intracellular ^{3}H cholesterol scintillation measurements.

Lipoprotein fractions

To assess the distribution of cholesterol over the different lipoprotein fractions, lipoproteins were separated by size exclusion chromatography followed by online determination of lipids[14] or by fast protein liquid chromatography (FPLC) using two Superose-6 FPLC columns in series (HR10/30) in PBS with 0.1 mM EDTA, pH 7.5 at 0.5 ml/min. Columns were calibrated using high and low molecular weight standards (Pharmacia, Stockholm, Sweden). 500 ul of serum was loaded on the column, the first 10 ml were discarded and afterwards 70 samples of 500 ul were collected for analysis. Cholesterol concentrations were measured using colorimetric and enzymatic methods with ready to use kits (Amplex red cholesterol kit, Life Technologies).

Patient population

Studies were performed according to the principles of the Declaration of Helsinki. The Local Research and Ethics committee approved the study (KEK-ZH-Nr. 2012-0260), and all patients gave written consent. The surgery group consisted of 29 patients undergoing primary laparoscopic proximal RYGB surgery. The RYGB procedure was performed as described[15]. All patients underwent a clinical, biochemical and pre-anesthetic evaluation, and all patients adhered to the study protocol and completed follow-up. Patients with unstable medical conditions such as recent coronary syndromes (within six months), congestive heart failure, systemic infection, acute illness, malignancy, or pregnancy, substance abuse, more than three alcoholic drinks per day, or psychiatric illness were excluded. Fasting blood samples were collected before (D0), at the first outpatient appointment two weeks (D14), and 12 weeks

(W12) post RYGB surgery. The BMI-matched group consisted of 29 obese patients, who were asymptomatic with no history of heart disease and not undergoing any cardiovascular conditioning program.

The BMI, body weight, age and gender of these patients were matched to the BMI of patients 12 weeks after RYGB. The control group consisted of 28 normal-weight volunteers matched for age and sex. They did not undergo any cardiovascular conditioning program. All control subjects were asymptomatic with no history of heart disease or accompanying disorders.

Blood sampling

Blood samples were obtained from fasting patients before RYGB (D0), in the morning of the first outpatient appointment two weeks after RYGB surgery (D14), and 12 weeks (W12) post RYGB surgery. Serum was collected in non-additive vacutainers, and plasma was collected in BD P800 vacutainers (containing DPPIV and protease inhibitors) that were kept at +4°C before and after blood collection. Blood samples were collected from fasting healthy subjects at the time of the study enrollment; plasma and serum were processed as described above.

Statistical Analysis

All analyses were performed with GraphPad Prism Software (version 5.0) or with SPSS software version 22.0 (Chicago, SPSS, Inc., Chicago, Illinois, USA).

Supplemental Results

RYGB reduces Food Intake and Body Weight compared to sham-operated controls

In the first experiment, RYGB reduced food intake (FI) and body weight relative to sham-operated *ad libitum* fed rats (controls) (SOM, Fig. 3 A-B). The body weight of the weight-

matched group was well matched to RYGB rats, thus allowing the discrimination of surgery-specific from weight-dependent effects since the only variable between these two study groups was the RYGB procedure. In the second experiment, FI and body weight were decreased to a similar extent in vehicle-treated RYGB versus sham-operated rats. Exendin$_{9-39}$ treatment in RYGB rat did not affect food intake or weight compared to the vehicle-treated RYGB (SOM, Fig. 3 C-D). Sham operated controls rats receiving liraglutide ate less initially, but they progressively increased their FI to a level similar to sham-operated controls on day 5 after surgery. The initial weight decrease in liraglutide-treated sham-operated rats was similar to that in RYGB rats, but liraglutide-treated rats started to regain some weight three to four days after treatment onset, as described[16] (SOM Fig.3 C-D). Some sham-operated and RYGB rats were followed up for one month in order to assess prolonged changes and compare weight-dependent effects (RYGB vs controls) with weight-independent effects (RYGB vs weight-matched). Sham-operated controls ate more compared to RYGB and weight-matched rats. The body weight of RYGB and weight-matched was well matched and remained stable around 470g after the initial weight loss (SOM Fig. 3 E-F).

The improvement of vascular function after RYGB is weight-independent.

Aortic contractions after norepinephrine (NE) were similar in sham-operated or RYGB rats (data not shown) in all experiments. Endothelium-independent relaxations in response to sodium nitroprusside (SNP) were equally preserved eight days after surgery (SOM Fig.4 C, H). Interestingly, one month after surgery, RYGB maintained a better relaxation in response to both insulin and GLP-1 with respect to sham-operated rats, whereas, acetylcholine-induced relaxation was restored in weight-matched equally to RYGB rats (SOM Fig. 4 D-F). Hence, although their weight was reduced as in the RYGB, weight-matched rats did not improve their relaxation upon stimulation with both hormones Because the response to acetylcholine one

month after surgery was similar in weight-matched and RYGB, insulin and GLP-1 are likely to be a more sensitive tools to investigate vascular function than muscarinic receptor-induced relaxation in this model of HFHC-induced obesity. After one month, endothelium-independent relaxations to sodium nitroprusside (SNP) (10^{-10}–10^{-5} mol/L) were similar in all groups (data not shown).

Improved HDL profile after RYGB

Despite similar plasmatic HDL-cholesterol concentrations among the study groups (SOM Fig 6 A), the analysis of the cholesterol distribution profile across all fast protein liquid chromatography (FPLC)-separated lipoprotein fractions revealed a clear shift towards smaller size and more uniformed HDL particle after RYGB (SOM Fig 6 B-C). The cholesterol distribution profile attributed to the HDL particles in sham-operated rats was similar to what has been described in animals fed high cholesterol diets[17]. Notably, sham-operated controls treated with liraglutide exhibited cholesterol attributed to smaller HDL particles similar to RYGB, whereas the absence of effect after exendin$_{9\text{-}39}$ compared to RYGB advocates an action independent of the classical GLP-1 receptor (SOM Fig.6 D).

Patient characteristics and follow-up after RYGB

The anthropometric characteristics, medications and lipid profile of obese patients undergoing RYGB surgery and those of the group BMI-matched to week 12 after RYGB are presented in SOM Table 1. All patients adhered to the study protocol and completed follow-up. The mean preoperative BMI was 45.44±1.0 kg/m2, n= six patients were super-obese (BMI> 50kg/m2). As expected, there was a high prevalence of obesity associated comorbidities at the time of study enrollment; T2DM was present in 20%; hypertension in 33% and obstructive sleep

apnea (OSAS) in 31% of the patients. There were five (17%) current smokers. At D14, the acute phase reaction post-surgical trauma was resolved as confirmed by the post-operative time course of IL-6, C-reactive protein (CRP) levels and leukocyte counting (data not shown); weight and BMI were reduced (42.20±1.0) (SOM Table 1), and decreased further at W12 (weight loss= 18.2%; mean BMI 37.13 kg/m2). RYGB patient at baseline had significantly lower concentrations of HDL-C and higher concentrations of TG than controls. Postoperative changes of HDL-C followed a U shaped curve: there was a significant decrease from baseline to D14 followed by an increase at 12 weeks, but HDL-C was lower than in controls. Triglycerides levels improved by RYGB but remained higher than in controls, even 12 weeks after RYGB; these levels were lower 12 weeks after surgery than in the BMI-matched group. As expected, age-matched, healthy subjects significantly differed from obese with respect to weight and BMI. As shown in SOM Table 2, RYGB was associated with a significant increase in fasting circulating GLP-1 and bile acids levels paralleled by a significant decrease in glucose, insulin levels and in Homeostatic model assessment for insulin resistance (HOMA).

Table 1: Clinical and Anthropometric Characteristics in Patients and Healthy Subjects

	RYGB D0	RYGB D14 (n=29)	RYGB 12W	BMI-matched to 12W RYGB (n=29)	Healthy (n =28)
Age, years	40.9 ± 1.7			42.7±2.1	37.8±2.4
Female gender, n (%)	17 (58.6%)			19 (65%)	14 (50%)
Height, m	1.7 ± 0.01			1.7± 0.01	1.7± 0.01
Body weight, kg	134.0 ± 3.7[a]	124.0 ± 3.4[ab]	109.3 ± 3.4[ac]	110.3±3.8[abc]	66.0±1.8
BMI (kg/m^2)	45.4 ± 1.0[a]	42.2 ± 1.0[ab]	37.0 ± 1.0[abc]	37.15±0.9[abc]	21.9±0.3
Current smokers (%)	5/29 (17%)	4/29 (14%)	3/29 (10%)	5/29 (17%)	
Diabetes, n (%)	6/29 (20.7%)	4/29 (13.8%)	0/29b (0%)b	2/29 (6.9%)	
OSAS	9/29 (31.0%)	7/29 (24.1%)	6/29 (20.7%)	10/29(34.5%)	
Lipid profile					
Total cholesterol (mmol/l)	4.8 ± 0.2	4.2 ± 0.2[ab]	4.0 ± 0.1[ab]	5.10± 0.20	4.89± 0.10
Log LDL (mmol/l)	1.04 ± 0.05	0.89 ± 0.06[b]	0.85 ± 0.05[b]	1.06± 0.07[bd]	0.98± 0.06
HDL (mmol/l)	0.97(0.82-1.21)	0.77 (0.67-0.97)	0.89 (0.82-1.02)	1.17 (1.01-1.46)[ab]	1.58 (1.29-1.88)
LDL/HDL	3.14±0.23[a]	3.35±0.24[a]	2.70±0.16[abc]	2.65±0.19	1.87±0.19
Log TG (mmol/l)	0.45±0.07[a]	0.53±0.06[a]	0.34±0.04	0.77±0.12[abc]	0.13±0.08
Medications					
Metformin, n (%)	3/29 (10.3%)	2/29 (6.9%)	0/29 (0%)[b]	2/29 (6.9%)	
ACEI (%)	2/29 (6.9%)	2/29 (6.9%)	0/29 (0%)	1/29 (3.4%)	
Sartans	2/29 (6.9%)	2/29 (6.9%)	2/29 (6.9%)	0/29	
B-blockers	5/29 (17.2%)	5/29 (17.2%)	1/29 (3.4%)[b]	0/29	
Statins	0/29 (0%)	0/29 (0%)	0/29 (0%)	6/29 (20.7%)[bcd]	
Ca-channels blockers	2/29 (6.9%)	2/29 (6.9%)	1/29 (3.4%)	0/29	
Diuretics	3/29 (10.3%)	2/29 (6.9%)	1/29 (3.4%)	1/29 (3.4%)	
Others (Gliptins)	1/29 (3.4%)	1/29 (3.4%)	0/29 (0%)	0/29	

Unless specified otherwise, values are means ± SE. Letters indicate statistically significant difference from : (a) Healthy, (b) D0, (c) D14, (d) 12W; (e) BMI-matched to 12W post RYGB; $p<0.05$.
For Log LDL: b vs. c, $p=0.001$; b vs. e, $p<0.0001$; d vs. e, $p=0.03$.
For HDL: $p<0.0001$ except for b vs. e, $p=0.01$
For Log TG: $p<0.0001$ except for c vs. e, $p=0.002$; b vs. e, $p=0.03$ and d vs. e, $p=0.003$.

BMI, body mass index. OSAS, obstructive sleep apnea syndrome. LDL, low density lipoprotein. HDL, high density lipoprotein. TG, triglycerides. ACEI, Angiotensin-converting-enzyme inhibitors.

Table 2: GLP-1, bile acids and glycemic profile in Patients and Healthy Subjects

	RYGB			BMI-matched to 12W RYGB	Healthy
	D0	D14	W12	(n=29)	(n =28)
		(n=29)			
Log GLP-1, pg/ml	-0.76±0.2[a]	0.69±0.1[b]	0.40±0.1[b]		0.29±0.13
Log Bile acids, umol/L	2.02±0.06[a]	2.19±0.05[ab]	2.39±0.06[bc]		2.4±0.06
Glucose, mmol/L	6.40±0.25[a]	5.39±0.11[b]	5.12±0.11[b]	5.49±0.27	5.29±0.15
Log Insulin, UI/ml	2.69±0.16[a]	2.49±0.09[ab]	2.28±0.1[b]	2.41±0.113[ac]	1.58±0.16
Log HOMA IR	0.69±0.15[a]	0.48±0.09[ab]	0.20±0.11[abc]	0.37±0.13[a]	-0.42±0.16

Unless specified otherwise, values are means ± SE. Letters indicate statistically significant difference from : (a) Healthy, (b) D0, (c) D14, (d) 12W, (e) BMI-matched to 12W post RYGB; $p<0.05$.
For Log GLP-1: $p<0.0001$.
For Log Bile acids: $p <0.0001$; except c vs. d, $p< 0.01$.
For Glucose: b vs. d 0.002
For Log Insulin: $p<0.0001$; except: c vs. d, $p< 0.03$; a vs. e, $p< 0.001$
Log HOMA IR: $p<0.0001$; except: b vs. d, $p< 0.01$; c vs. d, $p< 0.004$; a vs. d 0.004.

GLP-1, Glucagon-like peptide-1. HOMA IR, Homeostatic model assessment for insulin resistance.

Table 3. Overwiev of the RYGB-specific, weight-independent and GLP-1-mediated rapid effects on endothelial–mediated relaxation and HDL vaso-protective properties

	Rats eight days after RYGB			Patients after RYGB
	Improved after RYGB and weight-independent*	Improved by liraglutide in sham-operated controls†	Blocked by exendin$_{9-39}$ in RYGB‡	
Vasorelaxation in response to:				
Insulin	**YES**	**YES**	**YES**	
GLP-1	**YES**	**YES**	**YES**	
Acetylcholine	**YES**	**YES**		
HDL- mediated vaso-protective properties:				
NO production	**YES**	**YES**		**YES §**
Anti-apoptosis	**YES**	**YES**		**YES**
Anti-inflammatory	**YES**	**YES**		**YES §**
Anti-oxidant (NADPH oxidase activity)	**YES**	**YES**		**YES §**
PON-1 activity	**YES**			**YES §**
Cholesterol efflux	**YES**			**YES §**

*weight-independent effects are considered effects observed in RYGB but not in sham-operated weight-matched rats.

†Improved by liraglutide suggests effects involving GLP-1 activated signaling.

‡ Blocked by exendin$_{9-39}$ suggests effects mediated by the classical GLP-1 receptor.

§ protective HDL properties observed in patients 12 weeks after RYGB but not in the BMI-matched patients.

SOM Figure 1

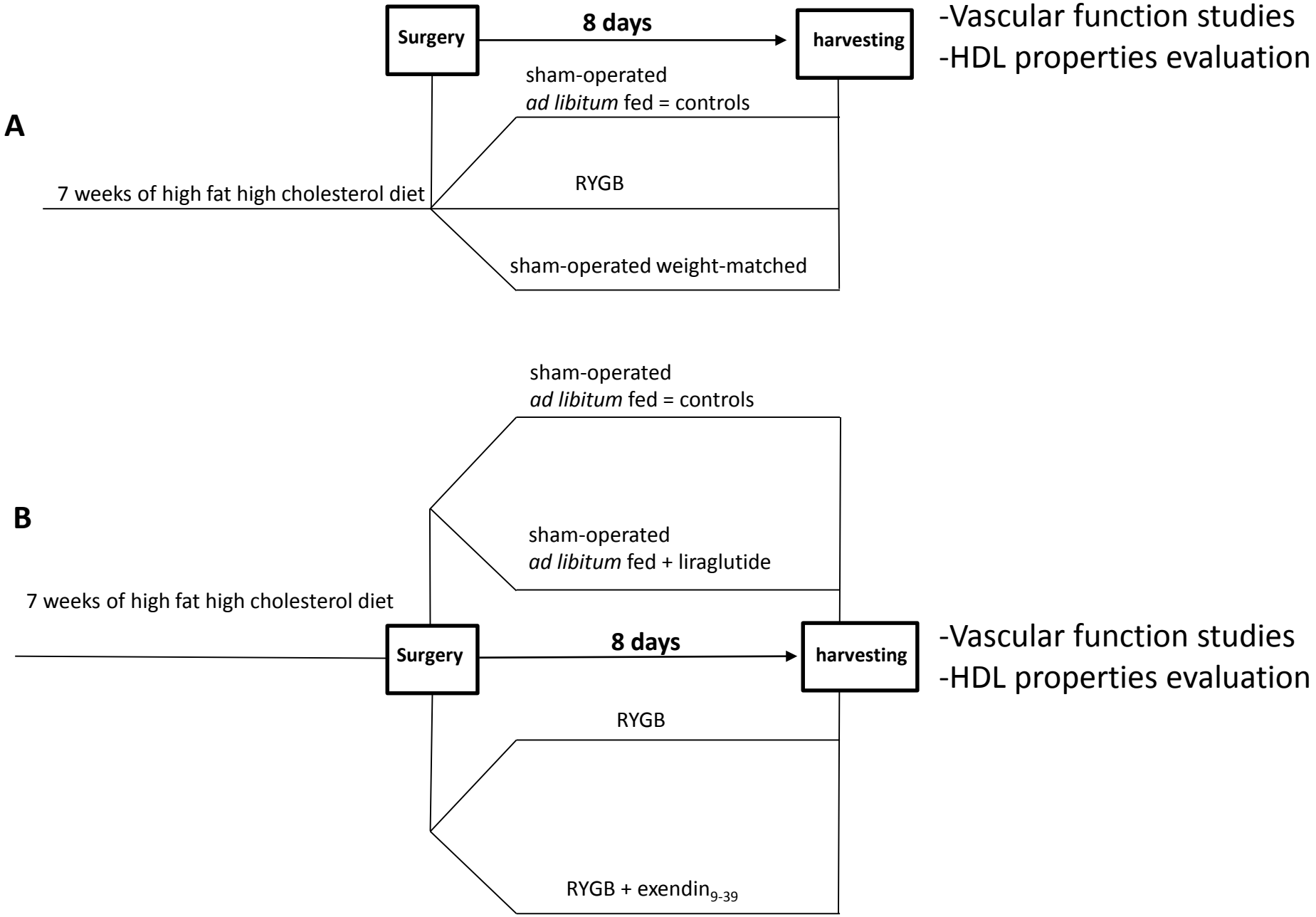
A
Surgery
8 days
harvesting
-Vascular function studies
-HDL properties evaluation
sham-operated
ad libitum fed = controls
7 weeks of high fat high cholesterol diet
RYGB
sham-operated weight-matched
B
sham-operated
ad libitum fed = controls
sham-operated
ad libitum fed + liraglutide
7 weeks of high fat high cholesterol diet
Surgery
8 days
harvesting
-Vascular function studies
-HDL properties evaluation
RYGB
RYGB + exendin$_{9-39}$

SOM Figure 2

A

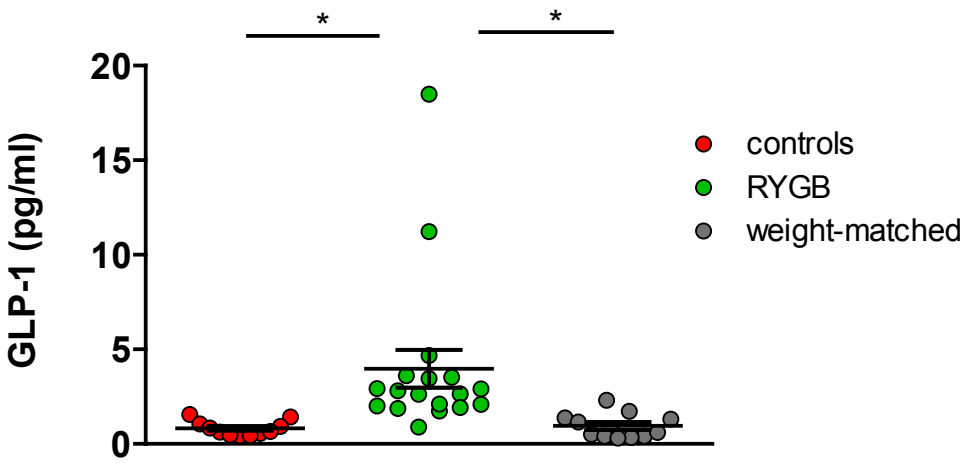

B

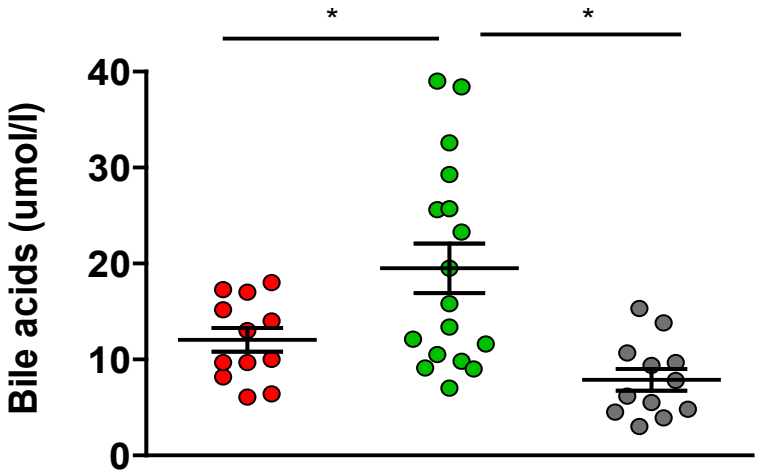

SOM Figure 3

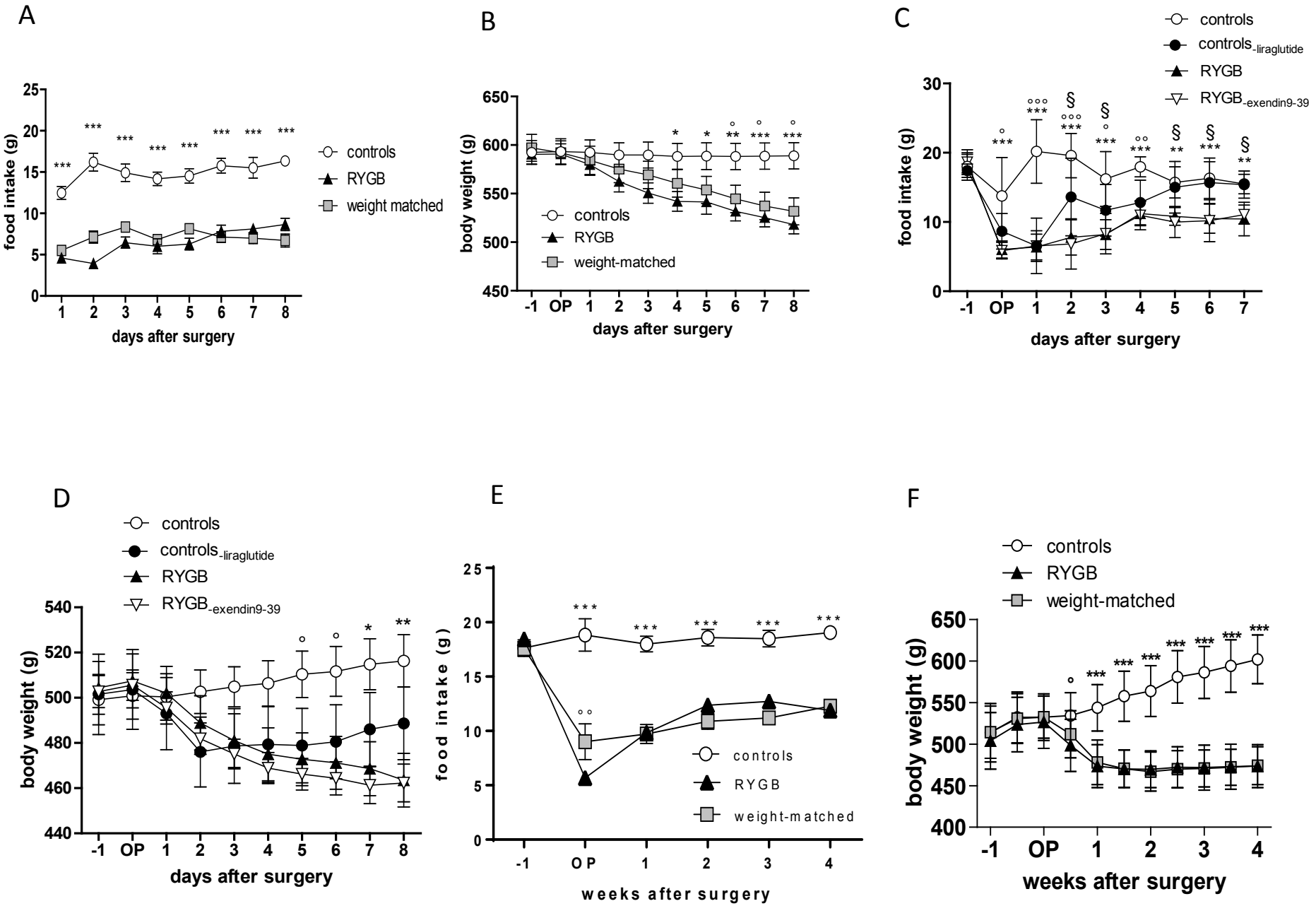
A
food intake (g)
days after surgery
controls
RYGB
weight matched
B
body weight (g)
days after surgery
controls
RYGB
weight-matched
C
food intake (g)
days after surgery
controls
controls-liraglutide
RYGB
RYGB-exendin9-39
D
body weight (g)
days after surgery
controls
controls-liraglutide
RYGB
RYGB-exendin9-39
E
food intake (g)
weeks after surgery
controls
RYGB
weight-matched
F
body weight (g)
weeks after surgery
controls
RYGB
weight-matched

SOM Figure 4

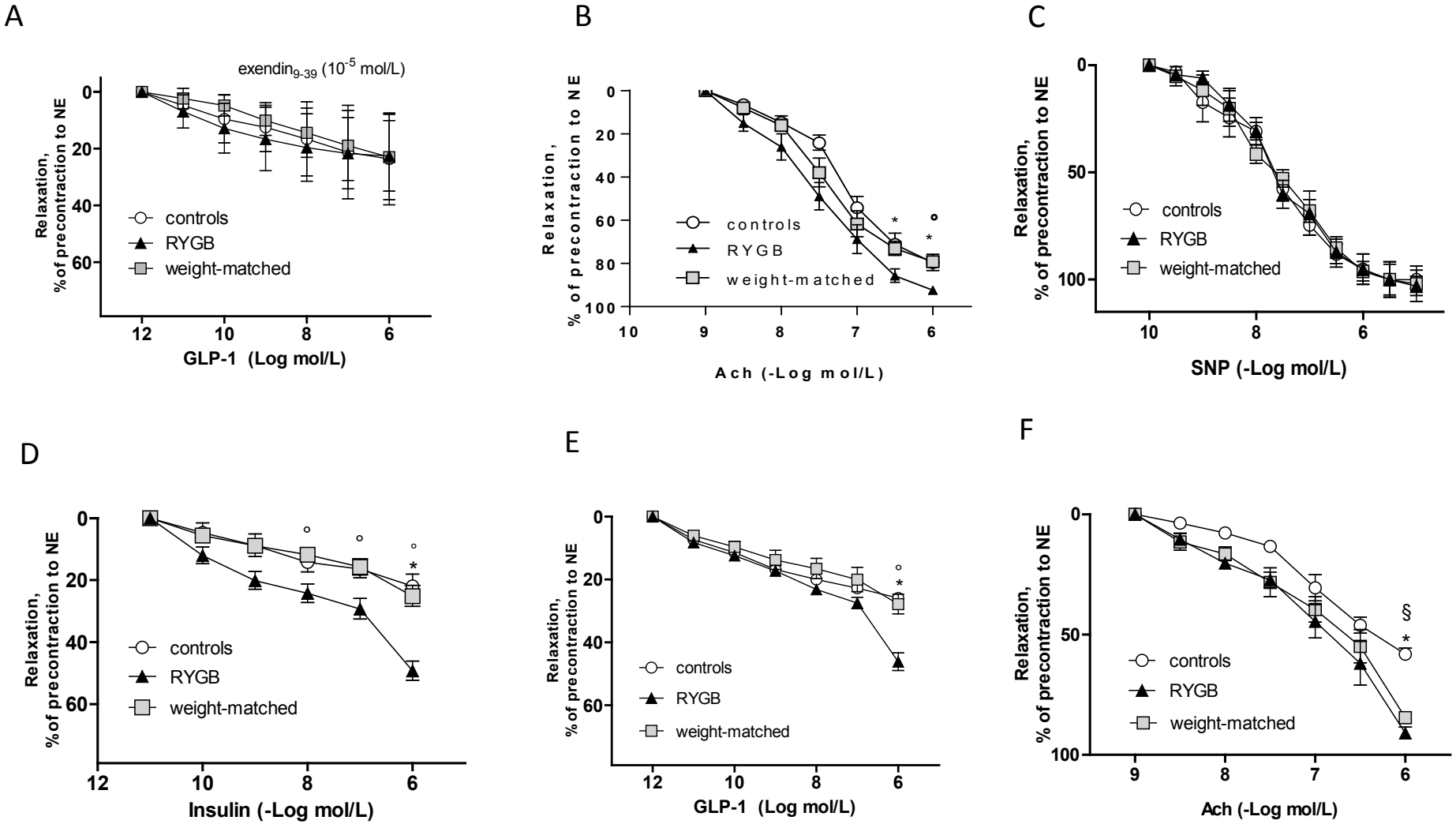
A
exendin9-39 (10-5 mol/L)
Relaxation, % of precontraction to NE
controls
RYGB
weight-matched
GLP-1 (Log mol/L)
B
Relaxation, % of precontraction to NE
Ach (-Log mol/L)
C
SNP (-Log mol/L)
D
Insulin (-Log mol/L)
E
GLP-1 (Log mol/L)
F
Ach (-Log mol/L)

SOM Figure 4

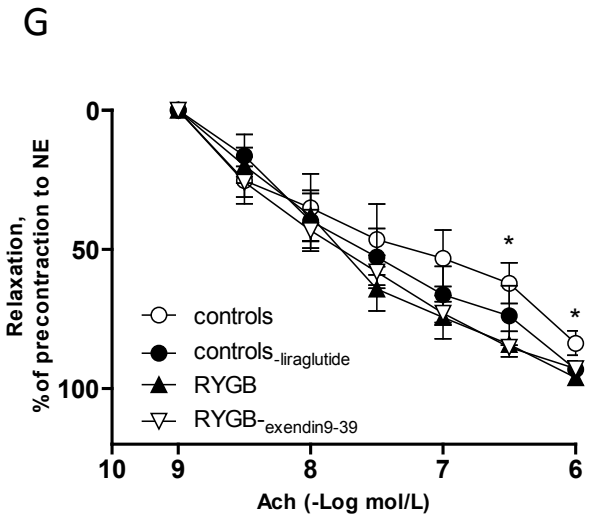
G
Relaxation, % of precontraction to NE
0
50
100
controls
controls-liraglutide
RYGB
RYGB-exendin9-39
*
*
10
9
8
7
6
Ach (-Log mol/L)

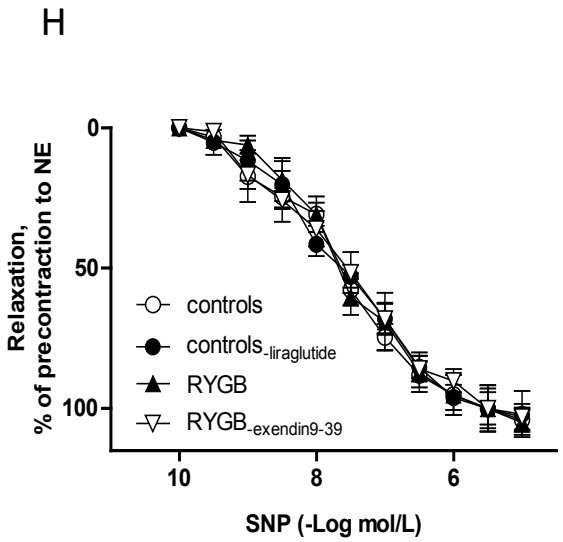
H
Relaxation, % of precontraction to NE
0
50
100
controls
controls-liraglutide
RYGB
RYGB-exendin9-39
10
8
6
SNP (-Log mol/L)

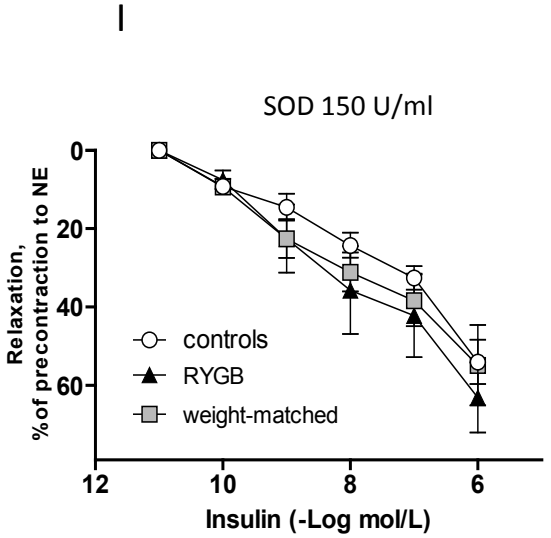
I
SOD 150 U/ml
Relaxation, % of precontraction to NE
0
20
40
60
controls
RYGB
weight-matched
12
10
8
6
Insulin (-Log mol/L)

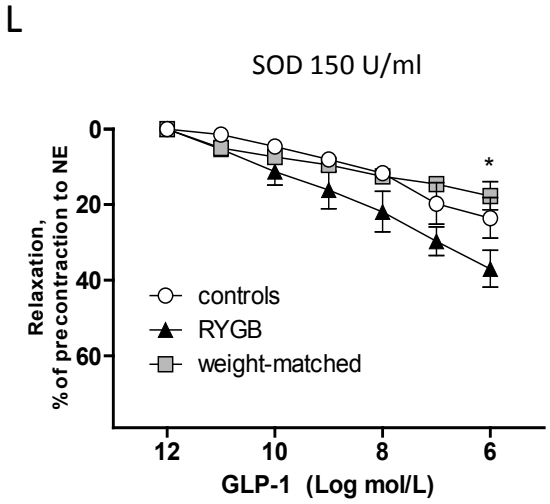
L
SOD 150 U/ml
Relaxation, % of precontraction to NE
0
20
40
60
controls
RYGB
weight-matched
*
12
10
8
6
GLP-1 (Log mol/L)

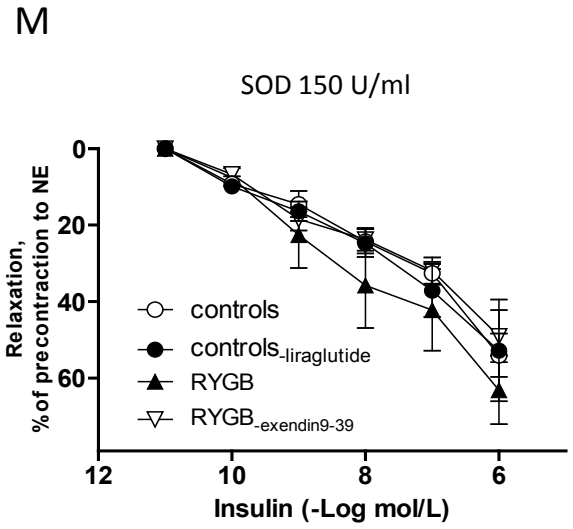
M
SOD 150 U/ml
Relaxation, % of precontraction to NE
0
20
40
60
controls
controls-liraglutide
RYGB
RYGB-exendin9-39
12
10
8
6
Insulin (-Log mol/L)

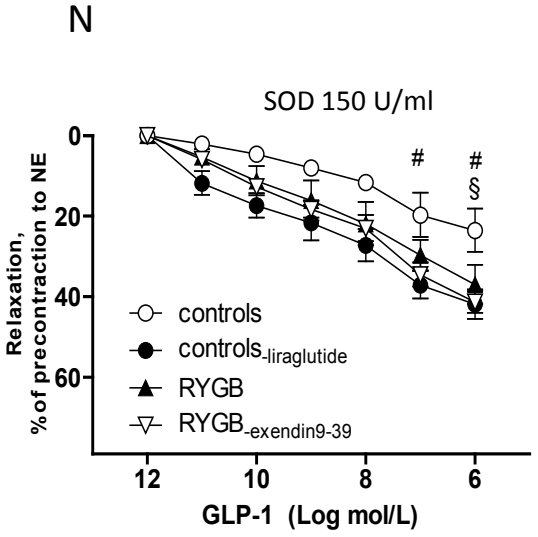
N
SOD 150 U/ml
Relaxation, % of precontraction to NE
0
20
40
60
#
#
§
controls
controls-liraglutide
RYGB
RYGB-exendin9-39
12
10
8
6
GLP-1 (Log mol/L)

SOM Figure 5

A

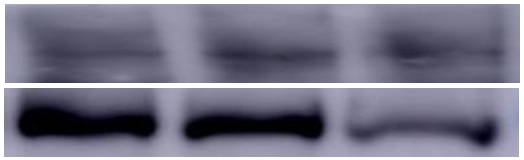

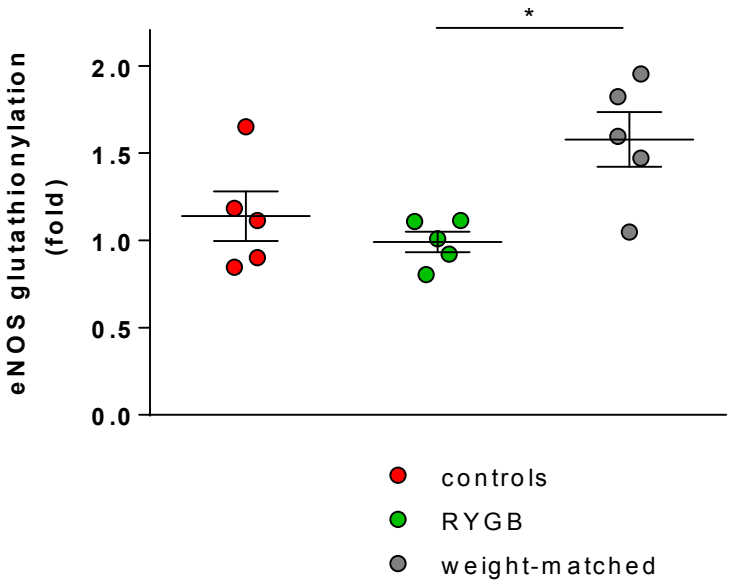

B

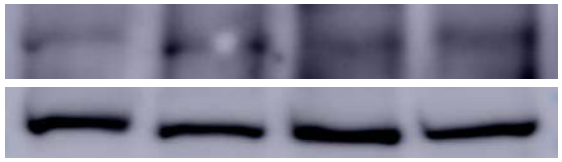

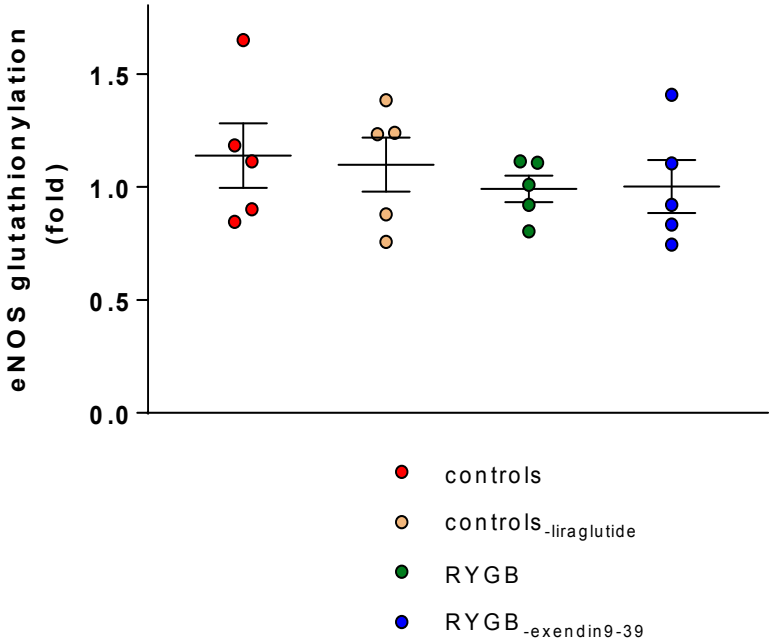

SOM Figure 6

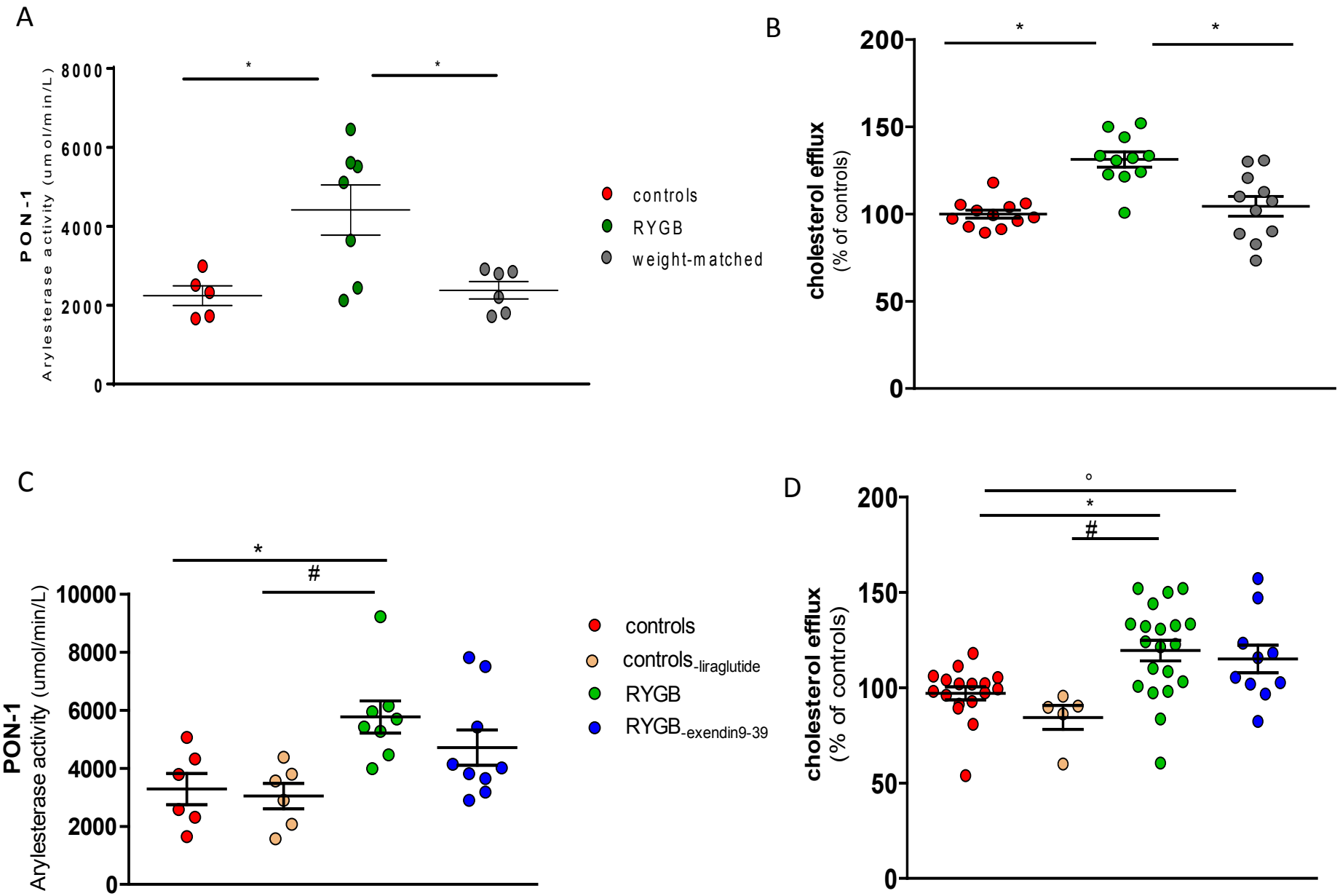
A
PON-1
Arylesterase activity (umol/min/L)
8000
6000
4000
2000
0
*
*
controls
RYGB
weight-matched
B
cholesterol efflux
(% of controls)
200
150
100
50
0
*
*
C
PON-1
Arylesterase activity (umol/min/L)
10000
8000
6000
4000
2000
0
*
#
controls
controls-liraglutide
RYGB
RYGB-exendin9-39
D
cholesterol efflux
(% of controls)
200
150
100
50
0
°
*
#

SOM Figure 7

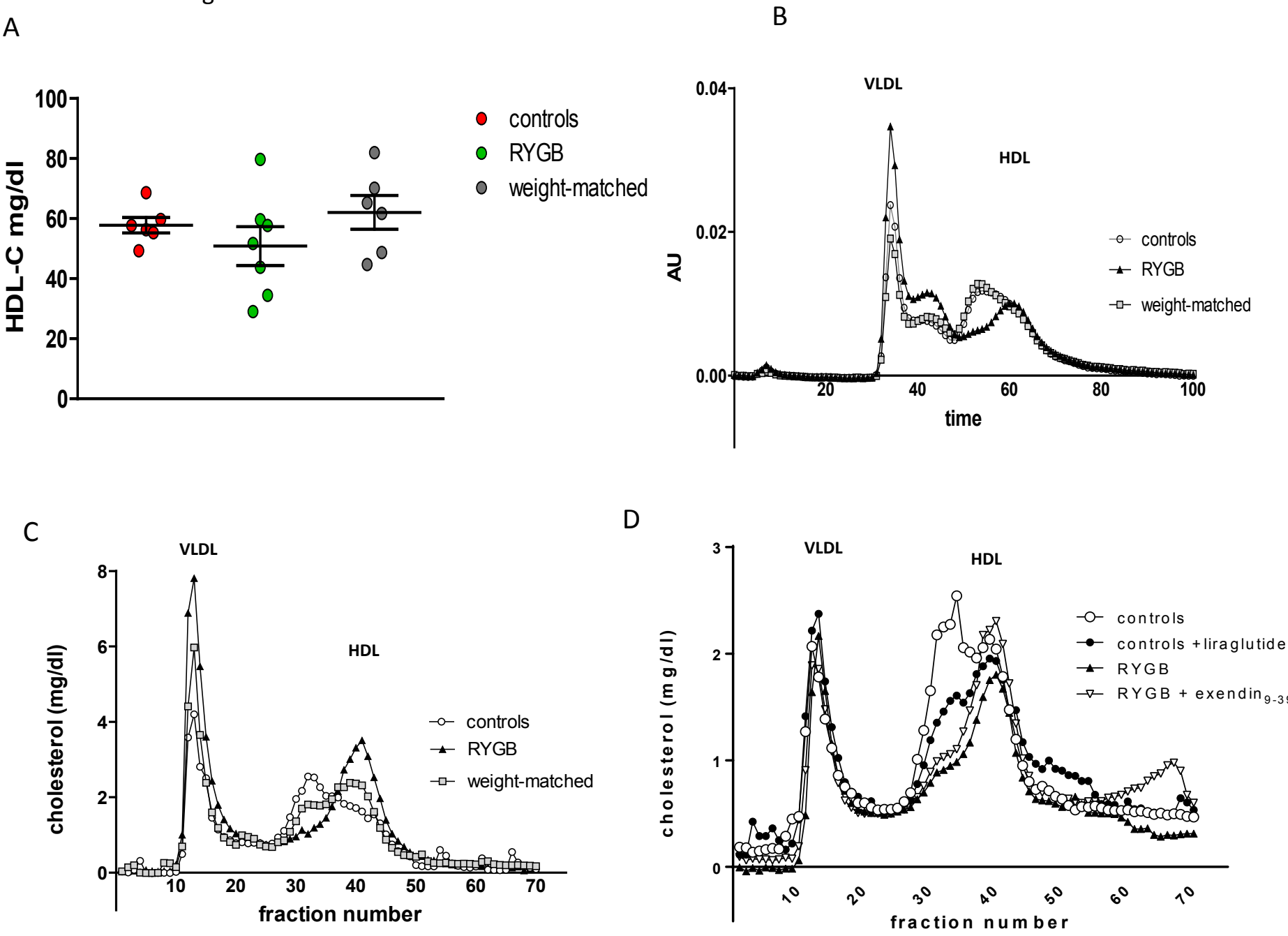
A
HDL-C mg/dl
100
80
60
40
20
0
controls
RYGB
weight-matched
B
VLDL
HDL
0.04
0.02
0.00
AU
20
40
60
80
100
time
controls
RYGB
weight-matched
C
VLDL
HDL
cholesterol (mg/dl)
8
6
4
2
0
10
20
30
40
50
60
70
fraction number
controls
RYGB
weight-matched
D
VLDL
HDL
cholesterol (mg/dl)
3
2
1
0
10
20
30
40
50
60
70
fraction number
controls
controls +liraglutide
RYGB
RYGB + exendin9-39

Supplemental Figure Legends

Figure 1.

Study design of the two main animal experiments (A) RYGB, sham-operated *ad libitum* fed (controls) or body weight- matched to RYGB rats followed up for eight days; (B) RYGB or sham-operated controls followed up for eight days with simultaneous *in vivo* pharmacological intervention.

Figure 2.

Plasma levels of GLP-1 (A) and total bile acids (B) in RYGB compared to sham-operated rats one month after surgery, (*RYGB vs controls and weight-matched, p=0.0001). Values are means ± SEM. n= 10-15 each group.

Figure 3.

A. Cumulative 24 hours-food intake in sham-operated controls (n=12), RYGB (n=17) and sham-operated weight-matched (n= 12) rats on the eight post-operative days. Average cumulative food intake was significantly higher in sham-operated controls vs. RYGB, and sham-operated weight-matched rats, (*** controls vs RYGB and weight-matched, p <0.001). No statistically significant difference was observed between RYGB and weight-matched rats.

B. Body weight before and eight days after surgery. Body weight was significantly higher in controls compared to RYGB rats starting from day 4; body weight did not differ between RYGB and weight-matched rats (*, **, *** controls vs RYGB; ° controls vs weight-matched, p<0.05, p<0.01, p<0.001, respectively). **C.** Cumulative 24 hours-food intake in controls (n=6), controls$_{\text{-liraglutide}}$ (n=6); RYGB (n=11), RYGB$_{\text{-exendin9-39}}$ (n=10). Average cumulative food intake was significantly higher in controls vs. RYGB and RYGB$_{\text{-exendin9-39}}$ rats (*, **, *** controls vs RYGB and RYGB$_{\text{-exendin9-39}}$; °,°°,°°° controls vs controls$_{\text{-liraglutide}}$, p

<0.05, p<0.01, p<0.001, resp.; § RYGB and RYGB$_{-exendin9-39}$ vs. controls$_{-liraglutide}$, p<0.05). There was no statistically significant difference between sham-operated controls and controls$_{-liraglutide}$ after post-operative day 5. **D.** Body weight increased progressively in sham-operated controls with statistically significant differences with RYGB$_{-exendin9-39}$ and RYGB (* controls vs RYGB and RYGB$_{-exendin9-39}$; p<0.05). **E.** Cumulative 24 hours-food intake in controls (n=12), RYGB (n=19) and sham-operated weight-matched (n= 12) rats during the 1 month postoperative period. Average cumulative food intake was significantly higher in sham-operated controls vs. RYGB, and weight-matched rats, (*** sham-operated controls vs RYGB and weight-matched, p <0.001). No statistically significant differences were observed between RYGB and weight-matched rats after surgery (°°RYGB vs weight-matched; p<0.01). **F.** Body weight after one month was significantly higher in controls rats compared to RYGB and sham-operated weight-matched (*** controls vs RYGB and weight-matched, p <0.001; °controls vs. RYGB, p<0.05). Results are presented as means ± SEM.

Figure 4.

A-C Endothelium-dependent relaxation (during submaximal contraction to norepinephrine (NE)) of aortic rings isolated eight days after RYGB compared to sham-operated rats (A) concentration-response curves in response to GLP-1 in the presence of the highly specific GLP-1 receptor antagonist exendin$_{9-39}$ (10^{-5} mol/l, 10 min before GLP-1). (B) Line graphs show concentration-response curves to acetylcholine (Ach). (C) Endothelium-independent relaxation to the NO donor sodium nitroprusside (SNP) across the experimental groups (*sham-operated controls rats vs RYGB; ° sham-operated weight-matched vs. RYGB, p<0.05).

D-F Endothelium-dependent relaxation one month after RYGB compared to sham-operated rats in response to insulin (D), GLP-1 (E) and (F) to acetylcholine (Ach) (*controls rats vs RYGB; ° weight-matched vs RYGB rats; § controls vs weight-matched, p<0.05 respectively).

G-H Effects of eight days treatment with liraglutide or exendin$_{9-39}$ in sham-operated controls and RYGB, respectively, on endothelium-dependent (G) relaxation to Ach and endothelium-independent response to SNP (H) (*sham-operated controls vs RYGB, $p<0.05$). Results are presented as means ± SEM. n=6 to 8 per group.

I-N Concentration-response curves in response to insulin and GLP-1 in the presence of the free radical scavenger polyethylene glycol–superoxide dismutase (SOD 150 U/mL) of aortic rings isolated eight days after RYGB and after GLP-1 modulation (* RYGB vs. sham-operated weight-matched; # controls vs. controls$_{-liraglutide}$; § controls vs. RYGB$_{-exendin9-39}$, $p<0.05$). Results are presented as means ± SEM. n=6 to 8 per group.

Figure 5.

(A-B) GSH immunoblotting of eNOS immunoprecipitated from rat aortae eight days after RYGB and after GLP-1 modulation (* RYGB vs. sham-operated weight-matched; $p<0.01$).

Figure 6.

HDL associated PON-1 activity. (A) Eight days after RYGB and after GLP-1 modulation (C). HDL-stimulated cholesterol efflux in J774 macrophages (as % of sham-operated controls); eight days after RYGB (B) and after GLP-1 modulation (D). (* RYGB vs. other groups; # sham-operated controls$_{-liraglutide}$ vs RYGB; ° sham-operated controls vs RYGB$_{-exendin9-39}$, $p<0.05$). Results are presented as means ± SEM n=8-10 in each group.

Figure 7.

The abnormal HDL particles size induced by high fat high cholesterol diet is reversed after RYGB and liraglutide treatment. Total HDL-cholesterol levels eight days after RYGB were unchanged (A). Cholesterol distribution profile across all fast protein liquid chromatography

(FPLC)-separated lipoprotein fractions from samples isolated eight days (B) and one month after surgery (C) and after liraglutide or exendin$_{9-39}$ treatment in sham-operated controls or RYGB rats, respectively (D). Results are presented as means ± SEM; n=5-7 per group.

Supplemental References

1. Bueter M, Abegg K, Seyfried F, Lutz TA, le Roux CW. Roux-en-y gastric bypass operation in rats. *J Vis Exp*. 2012:e3940
2. Gaspari T, Liu H, Welungoda I, Hu Y, Widdop RE, Knudsen LB, Simpson RW, Dear AE. A glp-1 receptor agonist liraglutide inhibits endothelial cell dysfunction and vascular adhesion molecule expression in an apoe-/- mouse model. *Diab Vasc Dis Res*. 2011;8:117-124
3. Noyan-Ashraf MH, Shikatani EA, Schuiki I, Mukovozov I, Wu J, Li RK, Volchuk A, Robinson LA, Billia F, Drucker DJ, Husain M. A glucagon-like peptide-1 analog reverses the molecular pathology and cardiac dysfunction of a mouse model of obesity. *Circulation*. 2013;127:74-85
4. Mells JE, Fu PP, Sharma S, Olson D, Cheng L, Handy JA, Saxena NK, Sorescu D, Anania FA. Glp-1 analog, liraglutide, ameliorates hepatic steatosis and cardiac hypertrophy in c57bl/6j mice fed a western diet. *Am J Physiol Gastrointest Liver Physiol*. 2012;302:G225-235
5. Rask-Madsen C, Li Q, Freund B, Feather D, Abramov R, Wu IH, Chen K, Yamamoto-Hiraoka J, Goldenbogen J, Sotiropoulos KB, Clermont A, Geraldes P, Dall'Osso C, Wagers AJ, Huang PL, Rekhter M, Scalia R, Kahn CR, King GL. Loss of insulin signaling in vascular endothelial cells accelerates atherosclerosis in apolipoprotein e null mice. *Cell Metab*. 2010;11:379-389
6. Osto E, Matter CM, Kouroedov A, Malinski T, Bachschmid M, Camici GG, Kilic U, Stallmach T, Boren J, Iliceto S, Luscher TF, Cosentino F. C-jun n-terminal kinase 2 deficiency protects against hypercholesterolemia-induced endothelial dysfunction and oxidative stress. *Circulation*. 2008;118:2073-2080
7. Sorrentino SA, Besler C, Rohrer L, Meyer M, Heinrich K, Bahlmann FH, Mueller M, Horvath T, Doerries C, Heinemann M, Flemmer S, Markowski A, Manes C, Bahr MJ, Haller H, von Eckardstein A, Drexler H, Landmesser U. Endothelial-vasoprotective effects of high-density lipoprotein are impaired in patients with type 2 diabetes mellitus but are improved after extended-release niacin therapy. *Circulation*. 2010;121:110-122
8. Riwanto M, Rohrer L, Roschitzki B, Besler C, Mocharla P, Mueller M, Perisa D, Heinrich K, Altwegg L, von Eckardstein A, Luscher TF, Landmesser U. Altered activation of endothelial anti- and proapoptotic pathways by high-density lipoprotein from patients with coronary artery disease: Role of high-density lipoprotein-proteome remodeling. *Circulation*. 2013;127:891-904
9. Besler C, Heinrich K, Rohrer L, Doerries C, Riwanto M, Shih DM, Chroni A, Yonekawa K, Stein S, Schaefer N, Mueller M, Akhmedov A, Daniil G, Manes C, Templin C, Wyss C, Maier W, Tanner FC, Matter CM, Corti R, Furlong C, Lusis AJ, von Eckardstein A, Fogelman AM, Luscher TF, Landmesser U. Mechanisms underlying adverse effects of hdl on enos-activating pathways in patients with coronary artery disease. *J Clin Invest*. 2011;121:2693-2708
10. Leikert JF, Rathel TR, Muller C, Vollmar AM, Dirsch VM. Reliable in vitro measurement of nitric oxide released from endothelial cells using low concentrations of the fluorescent probe 4,5-diaminofluorescein. *FEBS Lett*. 2001;506:131-134
11. Kleschyov AL, Munzel T. Advanced spin trapping of vascular nitric oxide using colloid iron diethyldithiocarbamate. *Methods Enzymol*. 2002;359:42-51

12. Khoo JP, Alp NJ, Bendall JK, Kawashima S, Yokoyama M, Zhang YH, Casadei B, Channon KM. Epr quantification of vascular nitric oxide production in genetically modified mouse models. *Nitric Oxide*. 2004;10:156-161
13. Bhattacharyya T, Nicholls SJ, Topol EJ, Zhang R, Yang X, Schmitt D, Fu X, Shao M, Brennan DM, Ellis SG, Brennan ML, Allayee H, Lusis AJ, Hazen SL. Relationship of paraoxonase 1 (pon1) gene polymorphisms and functional activity with systemic oxidative stress and cardiovascular risk. *JAMA*. 2008;299:1265-1276
14. Hesse D, Radloff K, Jaschke A, Lagerpusch M, Chung B, Tailleux A, Staels B, Schurmann A. Hepatic trans-golgi action coordinated by the gtpase arfrp1 is crucial for lipoprotein lipidation and assembly. *J Lipid Res*. 2014;55:41-52
15. Weber M, Muller MK, Bucher T, Wildi S, Dindo D, Horber F, Hauser R, Clavien PA. Laparoscopic gastric bypass is superior to laparoscopic gastric banding for treatment of morbid obesity. *Ann Surg*. 2004;240:975-982; discussion 982-973
16. Williams DL, Hyvarinen N, Lilly N, Kay K, Dossat A, Parise E, Torregrossa AM. Maintenance on a high-fat diet impairs the anorexic response to glucagon-like-peptide-1 receptor activation. *Physiol Behav*. 2011;103:557-564
17. Mahley RW, Weisgraber KH, Innerarity T, Brewer HB, Jr., Assmann G. Swine lipoproteins and atherosclerosis. Changes in the plasma lipoproteins and apoproteins induced by cholesterol feeding. *Biochemistry*. 1975;14:2817-2823

Rapid and Body Weight–Independent Improvement of Endothelial and High-Density Lipoprotein Function After Roux-en-Y Gastric Bypass: Role of Glucagon-Like Peptide-1

Elena Osto, Petia Doytcheva, Caroline Corteville, Marco Bueter, Claudia Dörig, Simona Stivala, Helena Buhmann, Sophie Colin, Lucia Rohrer, Reda Hasballa, Anne Tailleux, Christian Wolfrum, Francesco Tona, Jasmin Manz, Diana Vetter, Kerstin Spliethoff, Paul M. Vanhoutte, Ulf Landmesser, Francois Pattou, Bart Staels, Christian M. Matter, Thomas A. Lutz and Thomas F. Lüscher

Circulation. 2015;131:871-881; originally published online February 11, 2015;
doi: 10.1161/CIRCULATIONAHA.114.011791
Circulation is published by the American Heart Association, 7272 Greenville Avenue, Dallas, TX 75231

Print ISSN: 0009-7322. Online ISSN: 1524-4539

5.2 Original research article: "Inhibition of vascular JNK2 improves obesity-induced endothelial dysfunction after Roux-en-Y gastric bypass surgery"

This research article will be submitted to *Circulation* in May 2016 and contains part of the studies performed for the completion of the present PhD thesis. I am the first author of this article. Contributions to the manuscript include the study design, data acquisition, data analysis and interpretation, and writing and revising the manuscript.

Circulation, May 14th, 2016

Inhibition of vascular JNK2 improves obesity-induced endothelial dysfunction after Roux-en-Y gastric bypass surgery

Petia Doytcheva, MSc[1,2,3]; Thomas Bächler, MD[4]; Erika Tarasco, MSc[2,3]; Michael Engeli, BSc[1]; Giovanni Pellegrini, DVM, PhD[5]; Simona Stivala, PhD[1,3]; Lucia Rohrer, PhD[3,6], Paul M. Vanhoutte, MD, PhD[7]; Thomas F. Lüscher, MD[1,3]; Thomas A. Lutz, DVM, PhD[2,3]; *Elena Osto, MD, PhD[1,3,8]

[1]Center for Molecular Cardiology, University of Zurich and University Heart Center, Cardiology, University Hospital Zurich, Switzerland; [2]Institute of Veterinary Physiology, Vetsuisse Faculty University of Zurich, Winterthurerstrasse 260, 8057 Zurich, Switzerland; [3]Zurich Center for Integrative Human Physiology (ZIHP), University of Zurich, 8057 Zurich, Switzerland; [4]Department of Surgery, Cantonal Hospital Fribourg, Chemin des Pensionnats 2, 1708 Fribourg, Switzerland; [5]Laboratory for Animal Model Pathology, Institute for Veterinary Pathology, Vetsuisse Faculty University of Zurich, Winterthurerstrasse 260, 8057 Zurich, Switzerland; [6]Institute of Clinical Chemistry, University Hospital Zurich, 8001 Zurich, Switzerland; [7]State Key Laboratory for Pharmaceutical Biotechnologies &Department of Pharmacology & Pharmacy, LKS Faculty of Medicine, The University of Hong Kong; [8]Laboratory of Translational Nutrition Biology, Federal Institute of Technology Zurich ETHZ, Schorenstrasse 16, 8603 Schwerzenbach, Switzerland

Running title: *In vivo* JNK inhibition mimics endothelial benefits of RYGB

Word count: 7259

Address for correspondence: °Elena Osto, M.D., Ph.D.

Center for Molecular Cardiology

Wagistrasse, 12

CH-8952 Schlieren, Switzerland

Tel: 41-44-635 6469

Fax: 41-44-635 6827

Email: elena.osto@uzh.ch

Abstract

Background: Roux-en-Y gastric bypass surgery (RYGB) reduces body weight, obesity-associated co-morbidities, and cardiovascular mortality. Obesity-induced endothelial dysfunction is improved rapidly after RYGB independently from body weight loss. This effect is associated with reduced aortic activation of c-jun N-terminal kinase (JNK). In the present study we examined whether the RYGB-dependent improvement of endothelial function can be pharmacologically mimicked by *in vivo* JNK inhibition in diet-induced obese (DIO) rats. Furthermore, we investigated the specific contribution of JNK1 versus JNK2 in obesity-induced endothelial dysfunction and how RYGB modulates the activation of these JNK isoforms at the vascular level. **Methods and Results:** After seven weeks of high fat high cholesterol diet, DIO rats underwent RYGB or sham surgery, and sham-operated ad libitum-fed rats received either control peptide D-TAT or the JNK peptide inhibitor D-JNKi-1 (D-JNK; 20mg/kg/day s.c.) for 8 days post-surgery. Obesity was associated with increased aortic phosphorylation of JNK2, but not JNK1. Interestingly, *in vivo* D-JNK treatment completely mimicked the rapid improvement in endothelial function after RYGB, and this was associated with a selective blunting of aortic JNK2 phosphorylation after both RYGB surgery and D-JNK treatment. This was further accompanied by improved nitric oxide (NO) bioavailability resulting from reduced inhibitory phosphorylation of insulin receptor substrate-1 (IRS-1) and higher endothelial Akt/NO synthase activation in parallel with reduced anion superoxide levels. **Conclusions:** Obesity-induced endothelial dysfunction is associated with a specific increase of aortic JNK2 phosphorylation. *In vivo* JNK inhibition blunts aortic JNK2 activation and restores endothelial function, thus mimicking the rapid vaso-protective effects of RYGB. Our findings support a novel JNK2-dependent mechanism for the cardiovascular benefits of RYGB surgery.

Introduction

Severe obesity (BMI>35 kg/m^2) is a major worldwide health problem due to associated co-morbidities such as type 2 diabetes mellitus (T2DM) and dyslipidemia, which significantly increase cardiovascular disease risk and mortality.[1, 2] Obesity is characterized by a systemic chronic inflammation associated with endothelial dysfunction, oxidative stress, and insulin resistance.[2, 3] Bariatric surgery, and in particular Roux-en-Y gastric bypass (RYGB), is currently the single most effective treatment against morbid obesity, able to achieve not only sustained weight loss and significant long-term improvement of co-morbidities, but also a reduction of cardiovascular disease risk and mortality.[1, 4-8] RYGB has been shown to restore endothelial function and to normalize the lipid profile,[1, 4-8] and recent data suggest that in addition to weight loss, surgery-specific changes of gut hormones, i.e. glucagon-like peptide-1 (GLP-1), may be crucial contributors to these improvements.[9-12]

A crucial player linking obesity, insulin resistance, and endothelial dysfunction is the c-jun N-terminal kinase (JNK) family of proteins.[13] There are three genes in this family: JNK1 and JNK2 are ubiquitously expressed, while JNK3 expression is restricted to the brain, heart, and testes.[13] JNK activation suppresses the insulin signaling pathway through phosphorylation of insulin receptor substrate-1 (IRS-1) at ser307, which inhibits IRS-1 activation and downstream cellular insulin signaling.[14] The first evidence that JNK could play a role in obesity-induced insulin resistance was obtained in studies showing that total JNK activity is increased in liver, fat, and muscle in leptin-deficient *ob/ob* and in diet-induced obese (DIO) mice.[15] Deletion of JNK1 (JNK1-/-) in DIO mice reduced weight gain, decreased body adiposity, blood glucose and insulin, and improved glucose tolerance and insulin sensitivity; these changes were associated with decreased total JNK activity in liver, muscle, and adipose tissue, and with reduced IRS-1 ser307 phosphorylation in the liver.[15] In contrast to JNK1-/-, JNK2-/- mice were not protected against obesity and insulin resistance.[15, 16] Interestingly

however, JNK1+/-JNK2-/- mice showed a favorable metabolic profile similar to the JNK1-/- mice, with decreased total JNK activity in the liver.[16] This suggests that JNK2 may also play a relevant role in obesity, and that the balance between JNK1 and JNK2 activation is a critical determinant of overall JNK activity.[16] It is important to note that neither of these studies investigated the specific contribution of the different JNK isoforms to total JNK activity in tissues other than liver, muscle, and fat under obesogenic conditions.[15, 16] Hence, it is currently unknown which member of the JNK family plays a critical role in mediating obesity-induced insulin resistance in the vasculature.

JNK also contributes to the pathophysiology of cardiovascular disease. JNK2 directly inhibits endothelial nitric oxide synthase (eNOS),[17] and JNK2-/- mice were protected from hypercholesterolemia-induced endothelial dysfunction and oxidative stress.[18] Interestingly, both JNK2-/-apoE-/- mice[19] and JNK1-/-LDLR-/- mice[20] were resistant to atherosclerosis. In addition, vascular insulin resistance in spontaneously hypertensive rats was associated with increased total JNK activation and increased IRS-1 ser307 phosphorylation in aortic tissue.[21] Finally, JNK has been found to mediate endothelial dysfunction in T2DM subjects, but the relative contributions of JNK1 vs. JNK2 has not been investigated so far.[22]

The detrimental role of JNK activation in the vasculature is also supported by the favorable effect of JNK inhibitors against endothelial dysfunction and atherosclerosis. A four week-long treatment with the JNK inhibitor SP600125[23] reduced atherosclerotic plaque formation by 50% in apoE-/- mice.[19] *Ex vivo* SP600125 administration also inhibited vasoconstriction and induced dose-dependent relaxation in rat aortic rings.[24] Unfortunately, SP600125 is rather unspecific and also inhibits other kinases besides JNK,[25, 26] prompting the need for more specific inhibitors. The peptide inhibitor D-JNKi-1 (D-JNK), e.g., selectively blocks all three isoforms of JNK.[27] A two-week treatment of leptin receptor-deficient diabetic *db/db* mice

with the L-enantiomer L-JNK improved glucose tolerance and insulin sensitivity, increased Akt activation and decreased IRS-1 ser307 phosphorylation in liver, fat and muscle tissue.[28]

We previously demonstrated that in DIO rats RYGB improved endothelial vasodilation in response to insulin and to GLP-1, a major insulin-releasing peptide hormone with vasodilatory effects,[29] and the effect occurred rapidly and independently from body weight loss.[12] We also showed that RYGB activated the aortic Akt/eNOS signaling pathway and decreased total JNK phosphorylation and vascular oxidative stress, resulting in preserved nitric oxide (NO) bioavailability.[12] Therefore, in the present study we used pharmacological *in vivo* JNK inhibition in DIO rats to test whether this treatment mimics the protective endothelial effects of RYGB. Moreover, to gain further insights into the role of JNK activation in obesity-induced endothelial dysfunction, we investigated the specific aortic contribution of JNK1 versus JNK2 under obesogenic conditions and after RYGB surgery.

Materials and Methods

An expanded description of the methods is available in supplemental online materials (SOM).

Animals and organ chamber experiments

Male Wistar rats were fed a high fat high cholesterol diet containing 60% kcal fat and 1.25% cholesterol (HFHC) (Research Diets, New Brunswick NJ, USA) for seven weeks prior to surgery to achieve DIO; the same diet was given after surgery, as previously described.[12] Two main experiments were performed (SOM Fig. 1): 1.) RYGB group; sham-operated ad libitum-fed rats treated either with the peptide inhibitor D-JNKi-1 20mg/kg/day s.i.d. s.c. (D-JNK; H-dqsrpvqpflnlttprkprpprrrqrrkkrG-NH2, Pepscan, Lelystad, The Netherlands) or with an equimolar concentration (8.3 mg/kg) of the control peptide D-TAT s.i.d. s.c. (H-pprrrqrrkkrG-NH2, Pepscan) for 8 days ($controls_{D\text{-}TAT}$); 2.) RYGB group; sham-operated ad libitum-fed rats treated either with SP600125 40mg/kg/day s.i.d. s.c. (SP rats; Selleckchem, Houston TX, USA) or with vehicle (DMSO, Sigma-Aldrich, St. Louis, MO, USA) s.i.d. s.c. for 8 days ($controls_{DMSO}$). All results of the second experiment are reported in SOM.

Rats were randomly allocated to RYGB or sham surgery, and sham-operated rats were randomly allocated to the experimental or control treatment, respectively. Surgery was performed as previously described,[12] and the respective treatment started on the day after surgery. Rats were sacrificed 8 days after surgery. Non-operated male chow-fed Wistar rats of similar age were used as lean controls. A subset of DIO $controls_{D\text{-}TAT}$ and D-JNK rats were kept in metabolic cages to quantitatively assess water intake and urine excretion. Additionally, non-operated male chow-fed Wistar rats of similar age were also treated with D-JNK 20mg/kg/day s.i.d. s.c. and equimolar D-TAT s.i.d. s.c. for 8 days. The Cantonal Zurich Veterinary Office approved all animal experiments. Cumulative concentration-relaxation

curves in response to insulin and GLP-1 were obtained in rings of thoracic aorta, as described.[12]

Western blotting

Thoracic aorta was lysed as previously described[12] and subjected to SDS-PAGE gel for Western blotting. Membranes were incubated with SAPK/JNK (R&D Systems, Minneapolis, MN USA) and antibodies against: JNK1/2 (R&D Systems, Minneapolis, MN, USA) and phospho-JNK1/2 (Thr183/Tyr185) (Santa Cruz Biotechnology, Dallas TX, USA), IRS-1 and phospho-IRS-1 (Ser307) (Cell Signalling, Beverly, Massachusetts, USA), eNOS/NOS Type III and eNOS (pS1177) (BD Biosciences, San Jose, CA, USA), Akt and phospho-Akt (Ser473) (Cell Signalling, Danvers MA, USA), and GAPDH (Millipore, Darmstadt, Germany). The immunoreactive bands were detected by chemiluminescence (Amersham Biosciences, Buckinghamshire, UK) and quantified densitometrically with Image J software (National Institutes of Health, Bethesda, Maryland, USA). To assess eNOS dimer formation, non-denaturing SDS-PAGE was employed as previously described.[12]

NADPH oxidase activity and dihydroethidium (DHE) staining

NADPH oxidase activity in thoracic aorta was measured using a commercial NADP/NADPH assay kit (Abcam, Cambridge, UK) according to the manufacturer`s instructions. DHE staining was performed as previously described.[12]

GLP-1 measurements

Rat active GLP-1 Meso Scale Discovery 96-well plates were used to measure fasting plasma GLP-1 concentrations following the provided protocol (Meso Scale Discovery, Gaithersburg. MD, USA).

Statistical analysis

Data distribution was analyzed with Kolmogorov-Smirnov test. Normally distributed data was analyzed by an unpaired *t* test or by 1-way ANOVA followed by Bonferroni post hoc test where appropriate. We used a 2-way ANOVA with repeated measures to compare repeated measurements on the same animals. Non-normally distributed data was analyzed by 1-way ANOVA with Dunn`s multiple comparison test. All tests were two-sided and statistical significance was accepted if the null hypothesis could be rejected at $p<0.05$. All analyses were performed with GraphPad Prism Software (version 5.0). The authors had full access to and take full responsibility for the integrity of the data. All authors have read and agree to the manuscript as written.

Results

Additional results are available in SOM.

Diet-induced obesity increases JNK2, but not JNK1 activation in aorta

We first examined the specific activation of JNK isoforms 1 and 2 in the aorta under obesogenic conditions. JNK2 phosphorylation was significantly increased in DIO rats fed a HFHC diet compared to chow-fed controls, while JNK1 phosphorylation was not affected (Fig. 1A). This suggests that vascular JNK2 is specifically activated under obesogenic conditions, and that aortic JNK2 activation may play a role in obesity-induced endothelial dysfunction.

In vivo JNK inhibition improves endothelium-mediated vasodilation similar to RYGB surgery

We investigated the effect of 8-day *in vivo* JNK inhibition on obesity-induced endothelial dysfunction by treating DIO sham-operated ad libitum-fed rats with the JNK inhibitor D-JNK and comparing their endothelial-mediated vasodilation to RYGB-operated and controls$_{D\text{-}TAT}$ rats by *ex vivo* isometric tension recordings of thoracic aortic rings. As expected, RYGB surgery reduced food intake and body weight; D-JNK treatment also decreased food intake and body weight (see SOM). Endothelium-mediated vasodilation in response to GLP-1 and insulin improved in D-JNK-treated rats compared to controls$_{D\text{-}TAT}$ rats, mimicking the effects of RYGB surgery (Fig.1B-C); these relaxation responses were abolished by pre-incubation with the eNOS inhibitor Nω-nitro-L-arginine methyl ester (L-NAME), indicating an NO-dependent mechanism (SOM Fig. 5). A similar, but less pronounced effect was observed with the JNK inhibitor SP600125 (see SOM). Hence, JNK activation plays a crucial role in obesity-induced endothelial dysfunction, and the pharmacological inhibition of JNK has the potential to mimic the beneficial vascular effects of RYGB.

In vivo JNK inhibition improves endothelium-mediated vasodilation through a direct effect on aorta

To confirm that the improvement of vasodilation seen in D-JNK rats resulted from the specific vascular effects of the *in vivo* JNK inhibition rather than as a consequence of systemic metabolic benefits, we pre-incubated a subset of aortic rings isolated from D-JNK and controls$_{D\text{-}TAT}$ rats with 5 μM D-JNK for 30min *ex vivo*[24, 27] before performing endothelial function experiments. *Ex vivo* D-JNK treatment significantly improved insulin- and GLP-1-induced vasodilation in controls$_{D\text{-}TAT}$ aortas (Fig. 2A-B), while it did not further improve vasodilation in rats that had already received the *in vivo* chronic D-JNK treatment (Fig. 2C-D). This result strongly suggests that the improved vasodilation observed in rats after *in vivo* JNK inhibition is attributable to a direct protective effect on the aorta.

In vivo JNK inhibition and RYGB surgery reduce JNK2 activation in aorta

We then examined by Western blot analysis the impact of RYGB surgery and *in vivo* JNK inhibition on the aortic modulation of the different JNK isoforms. Interestingly, aortic JNK1 phosphorylation was not changed, while aortic JNK2 phosphorylation was significantly decreased in both RYGB and D-JNK rats compared to controls$_{D\text{-}TAT}$ rats (Fig. 3A). This suggests that RYGB surgery and chronic JNK inhibition specifically inhibit JNK2, but not JNK1, in the aorta of DIO rats.

Interestingly, and opposite to the aorta (Fig. 1A), hepatic JNK1, but not JNK2, phosphorylation was significantly increased in DIO rats compared to chow-fed controls (SOM Fig. 9A). Further, hepatic JNK2 phosphorylation was not changed in RYGB and D-JNK rats compared to controls$_{D\text{-}TAT}$ rats, while hepatic JNK1 phosphorylation was specifically reduced after RYGB (SOM Fig. 9B); D-JNK treatment did not affect hepatic JNK1 phosphorylation

compared to control rats (SOM Fig. 9B). Hence, obesity seems to affect the balance between JNK1 and JNK2 activation in a tissue-specific pattern.

In vivo JNK inhibition activates the vascular insulin-dependent Akt/eNOS signalling pathway similar to RYGB surgery

We performed Western blot analysis of the downstream vascular insulin-dependent signalling Akt/eNOS pathway, which is directly inhibited by JNK2.[14, 16, 17] Interestingly, RYGB and D-JNK similarly decreased the inhibitory phosphorylation of IRS-1 at ser307 and increased the activatory phosphorylation of Akt at ser473, which in turn lead to increased activatory ser1177 phosphorylation and dimerization of eNOS. (Fig.3B-E). Taken together, these results suggest that specific JNK2 inhibition in the aorta restores the insulin-dependent vascular signalling pathway which preserves NO bioavailability through increased eNOS activation.

In vivo JNK inhibition reduces vascular oxidative stress similar to RYGB surgery

JNK kinases enhance oxidative stress, which in turn impairs NO bioavailability and leads to endothelial dysfunction.[30, 31] We have shown that decreased oxidative stress contributes to the preserved NO bioavailability observed after RYGB.[12] Therefore, we investigated whether *in vivo* JNK inhibition also affects obesity-induced vascular oxidative stress. The addition of the free radical scavenger superoxide dismutase (SOD) significantly improved vasodilation in response to insulin and GLP-1 in controls$_{D\text{-}TAT}$ rats, while it did not further improve it in RYGB and D-JNK rats (Fig. 4 A-B). This suggests that *in vivo* JNK inhibition, similar to RYGB surgery, exerts potent antioxidant effects against endothelial dysfunction in obesity. Indeed, dihydroethidium (DHE) staining of aortic sections showed decreased anion

superoxide levels after RYGB surgery as well as after D-JNK treatment (Fig. 4C). NADPH oxidase activity, which contributes to the generation of radical superoxide anions,[30] was significantly decreased in RYGB rats as previously shown,[12] and also in D-JNK rats (Fig.4D). This suggests that *in vivo* JNK inhibition also mimics the protection of RYGB surgery against oxidative stress, therefore further contributing to preserve NO bioavailability.

Increased GLP-1 signalling might contribute to vascular JNK2 inhibition after RYGB surgery

Increased circulating GLP-1 seems to contribute to the beneficial cardiovascular effects of RYGB surgery,[12, 32] and GLP-1-dependent intracellular signalling inhibits JNK1 and JNK2 activation in various tissues through activation of protein kinase A (PKA).[33-37] In addition, GLP-1 can also activate the Akt/eNOS pathway via activation of PKA.[38, 39] Hence, we measured circulating GLP-1 levels and assessed aortic GLP-1-dependent signalling pathways controlling JNK activation by Western blot. In line with our previous results, RYGB surgery increased fasting plasma GLP-1 levels (Fig.5A). Surprisingly, D-JNK also significantly increased circulating GLP-1 levels in comparison to controls$_{D\text{-}TAT}$ rats, although to a lesser extent than RYGB (Fig.5A). Further, the increase in circulating GLP-1 in RYGB and D-JNK rats was accompanied by increased aortic expression of the GLP-1 receptor and by increased activation of downstream PKA and cAMP response element binding protein (CREB), which are known to negatively regulate JNK[33-37] (Fig.5B-D). Therefore, increased GLP-1 levels after RYGB surgery and systemic *in vivo* JNK inhibition seem to converge on JNK2 inactivation in the vasculature, thus restoring obesity-induced endothelial dysfunction.

Discussion

In the present study we investigated whether the RYGB-dependent improvement of endothelial function can be pharmacologically mimicked by *in vivo* JNK inhibition. In addition, we examined the specific contribution of JNK1 versus JNK2 in endothelial dysfunction under obesogenic conditions, and the impact of RYGB surgery and *in vivo* JNK inhibition on the modulation of these isoforms at the vascular level. Our major findings were: 1.) diet-induced obesity specifically increased JNK2, but not JNK1 phosphorylation in the aorta; 2.) chronic *in vivo* and acute *ex vivo* JNK inhibition significantly improved endothelial-mediated vasodilation, mimicking the rapid vascular effects of RYGB surgery; 3.) the increased JNK2 phosphorylation in the aorta of obese rats was blunted to the same extent by RYGB surgery and by *in vivo* pharmacological inhibition of JNK; 4.) as a consequence, after both RYGB surgery and *in vivo* JNK inhibition, the vascular insulin- and GLP-1-dependent intracellular signaling pathways converging on Akt/eNOS activation were restored; 5.) the two interventions similarly decreased vascular oxidative stress. Interestingly, *in vivo* JNK inhibition with D-JNK was associated with increased GLP-1 levels similar to RYGB surgery. GLP-1-dependent intracellular signaling is known to decrease JNK1 and JNK2 activation in different tissues including endothelial cells.[33-37] Together, our findings support a crucial role of JNK isoform 2 activation in obesity-induced endothelial dysfunction. RYGB and *in vivo* JNK inhibition specifically inhibit this isoform, directly at the aortic level and indirectly through increased GLP-1 signaling. This achieves a dual benefit - it decreases vascular oxidative stress and activates Akt/eNOS intracellular signaling pathways, both mechanisms leading to improved endothelial function.

Remarkably, in sham-operated rats treated with D-JNK, insulin- and GLP-1-mediated endothelial vasodilation improved to the same extent like in RYGB-operated rats. This effect could have been due to direct vascular JNK inhibition, or to improved systemic insulin

sensitivity following hepatic JNK inhibition.[15] To address this question, we additionally treated aortas with D-JNK *ex vivo*. Indeed, *ex vivo* D-JNK treatment significantly improved endothelial function in controls$_{D\text{-}TAT}$ animals, but it had no additional effect in D-JNK animals beyond the effect of the chronic *in vivo* D-JNK treatment. Therefore, D-JNK seems to improve endothelial-mediated vasodilation by a direct inhibition of aortic JNK.

Western blot analyses of aortic tissue supported this conclusion. First, we compared aortic JNK1 and JNK2 activation in chow-fed versus DIO rats, and we found that obesity specifically induced JNK2, but not JNK1, activation in aorta. Indeed, activation of JNK2, but not JNK1, was specifically decreased by both RYGB surgery and D-JNK treatment. D-JNK is able to efficiently inhibit all three isoforms of JNK, but isoform 3 has an expression profile limited to the heart, brain, and testes.[27] Hence, these results suggest that 1.) JNK2, but not JNK1, is specifically activated in aorta under obesogenic conditions; 2.) obesity-induced vascular JNK2 activation is reversed by RYGB surgery; 3.) *in vivo* JNK inhibition mimics the effect of RYGB surgery on vascular JNK2. Overall, our data highlight that JNK2 activation is critical in obesity-induced endothelial dysfunction, and that its inhibition plays a major role in the improvement of endothelium-mediated vasodilation seen after RYGB. In agreement with our results, specific aortic JNK2 activation has been demonstrated in both wild type mice fed a high cholesterol diet,[18] and in atherosclerosis-prone apoE-/- mice.[19]

Former studies have underlined the role of JNK1 as a mediator of obesity-induced insulin resistance in liver, muscle, and fat.[15, 16] In addition, a recent study demonstrated that RYGB surgery decreases JNK phosphorylation in the liver of diabetic rats, but it was not specified which JNK isoform was affected.[40] Interestingly, here we show that hepatic JNK1 activation, which is induced by obesity,[15, 16] was specifically decreased after RYGB, while hepatic JNK2 activation was not affected by the diet or the surgery. Therefore, our results highlight the

tissue-specific effects of obesity on JNK1 and JNK2 activation, and the relative importance of each isoform in different organs.

To further investigate the mechanisms underlying the improved endothelium-mediated vasodilation in response to insulin and GLP-1, we assessed by Western blot analysis the vascular signaling pathways which are activated by these two hormones and which lead to activation of eNOS. JNK2 is known to directly phosphorylate IRS-1 ser307,[14, 16] a critical player in the insulin signaling pathway, which in vascular tissue leads to the activation of eNOS.[41] In addition, JNK2 also directly regulates eNOS by inhibitory phosphorylation.[17] Accordingly, we observed decreased inhibitory IRS-1 ser307 phosphorylation, increased activatory phosphorylation of downstream Akt at ser473, and increased activatory phosphorylation at ser1177 and dimerization of eNOS after both RYGB and *in vivo* JNK inhibition. Hence, JNK2 inhibition in aorta may mediate the beneficial endothelial effects of RYGB surgery by activating downstream signaling pathways that lead to the activation of eNOS and the release of vasodilatory NO.

Increased intracellular oxidative stress can also contribute to endothelial dysfunction in different conditions such as T2DM, hypercholesterolemia and atherosclerosis.[18, 30, 42] Reactive oxygen species (ROS) such as superoxide anions impair NO bioavailability and lead to endothelial dysfunction.[30] The JNK family of proteins is known to be activated by and to mediate oxidative stress.[18, 31] Our results show that pre-treating thoracic aortic rings with the radical scavenger SOD improved insulin- and GLP-1-mediated vasodilation in controls$_{D\text{-}TAT}$ rats to the same extent like RYGB surgery and D-JNK treatment, confirming that oxidative stress contributes to the impaired endothelial function in obese rats. In line with this observation, the activity of NADPH oxidase, which contributes to the generation of radical superoxide anions,[30] was significantly lower in the aortas of RYGB and D-JNK rats. Indeed, DHE staining of rat aortas confirmed that anion superoxide levels were equally decreased

after RYGB surgery and D-JNK treatment. NADPH oxidase activity has been shown to be directly modulated by JNK in microvascular endothelial cells;[43] abrupt reoxygenation after hypoxia induced a NADPH-dependent increase in ROS, which was significantly blunted by treatment with the JNK inhibitor SP600125 or with dominant-negative JNK1.[43] Therefore, specific inhibition with dominant-negative JNK1 highlighted the role of JNK1 in reoxygenation-induced NADPH oxidase activation, but the role of JNK2 was not investigated in detail.[43] Our findings suggest that obesogenic conditions might differentially induce JNK2- rather than JNK1-dependent NADPH oxidase activation. Therefore, vascular JNK2 inhibition after RYGB surgery and *in vivo* JNK inhibition seems to contribute to improved endothelial function both by promoting NO production via eNOS, and by reducing NADPH oxidase activity and oxidative stress.

We observed a similar effect on endothelial function, oxidative stress, JNK2 inactivation, and activation of the Akt/eNOS signaling pathway with the other commonly used JNK inhibitor, SP600125, which also inhibits all three isoforms of JNK[23] (see SOM). The effect of SP600125 on endothelial function, however, was less pronounced than with D-JNK. SP600125 has been shown to inhibit multiple other kinases besides JNK,[25, 26] which may have interfered with the beneficial effects of JNK inhibition on endothelial function.

Finally, we aimed to investigate the upstream molecular pathways leading to vascular JNK2 inactivation after RYGB. We previously showed that increased GLP-1 levels mediate the improved endothelial function after RYGB in a GLP-1 receptor-dependent mechanism.[12] GLP-1 signaling is known to inhibit JNK in different tissues through activation of PKA.[33-37] More specifically, in human cardiac progenitor cells GLP-1 inhibited H_2O_2-induced activation of both JNK1 and JNK2,[35] and in human coronary artery endothelial cells the GLP-1 mimetic exendin-4 inhibited lipotoxicity-induced activation of JNK1 while JNK2 was not investigated.[36] In our DIO rat model 8-day *in vivo* treatment with the GLP-1 analogue

liraglutide seemed to mimic the effect of RYGB on aortic JNK2 inhibition in sham-operated rats, while *in vivo* treatment with the GLP-1 receptor antagonist exendin-9 blocked it in RYGB rats (SOM Fig. 10).[12] In other animal studies eight-week liraglutide treatment blocked both JNK1 and JNK2 activation in the pancreas of diabetic mice,[44] and four-week liraglutide treatment blocked JNK1 activation in the liver of HFHC-fed rats while JNK2 was not investigated.[45] These results suggest that GLP-1-dependent signaling is able to differentially modulate JNK isoforms in a tissue-dependent manner, and that it seems to selectively inhibit aortic JNK2 activation under obesogenic conditions. In addition, endothelial GLP-1 signaling can directly lead to eNOS activation and vasodilation through activation of PKA and Akt.[38, 39] Therefore, it is attractive to speculate that increased GLP-1 levels after RYGB could inhibit JNK2 in endothelial cells, leading to GLP-1- and insulin-dependent activation of eNOS and reduced oxidative stress, which translate into improved endothelial-mediated vasodilation (Fig. 6).

Interestingly, D-JNK also increased circulating GLP-1 levels and induced expression of the GLP-1 receptor and activation of PKA and CREB in aorta. We did not observe increased GLP-1 levels with SP600125, which could have been due to its less specific effects on JNK.[25, 26] To our knowledge, our study is the first one to show that chronic JNK inhibition is able to increase circulating GLP-1 levels, but the underlying molecular mechanisms are unknown and will require further investigations. This finding however suggests that systemic JNK inhibition is able to improve endothelial-mediated vasodilation both through a direct inactivation of aortic JNK2, and indirectly through increased GLP-1 signaling, which contributes to eNOS activation and JNK2 inactivation in endothelial cells (Fig. 6). Hence, our study demonstrates the potential of JNK2-targeted drugs to treat obesity-induced endothelial dysfunction and cardiovascular disease.

Finally, while we believe that our "proof of concept" data provide strong support for an important role of JNK2 in obesity-related vascular dysfunction, it is important to note that the currently available JNK inhibitors might not be directly suitable for the development of future anti-obesity JNK-targeted therapies. SP600125 is not very specific and has multiple other targets besides JNK,[25, 26] which makes it unsuitable for reliable *in vivo* studies and for clinical development. D-JNK, on the other hand, has a higher JNK specificity,[27] but in our model, and in agreement with *in vitro* studies,[46] it induced a typical carrier peptide-dependent kidney toxicity that appeared to be independent from its JNK inhibitory activity[46] (see SOM). The development of acute renal proximal tubule injury in both controls$_{D\text{-}TAT}$ and D-JNK rats, with an increased severity in the D-JNK rats, agrees with the published *in vitro* D-TAT and D-JNK intrinsic length-dependent, but sequence-independent cytotoxicity.[46] To our knowledge however, our study is the first to report that D-JNK can also induce cytotoxicity after *in vivo* systemic administration. Previously it had been shown that *in vivo* L-JNK treatment improved insulin sensitivity in diabetic *db/db* mice, but worsened diabetic albuminuria;[47] the latter might have been due to D-TAT carrier peptide-induced kidney toxicity independent from the JNK inhibition. Our results on D-JNK kidney toxicity also agree with published data on the accumulation and clearance of D-JNK in different organs after a single intraperitoneal administration in mice; D-JNK accumulated over time and showed the highest tissue concentrations in kidney, liver, spleen, and pancreas.[48] Interestingly, we did not observe histological signs of cytotoxicity in any other organ besides kidney. Finally, SP600125 treatment did not induce kidney toxicity, therefore further supporting the notion that the observed D-JNK kidney toxicity was independent of JNK inhibition. Hence, our data suggests that *in vivo* D-JNK treatment induces kidney-specific toxicity in a D-TAT-dependent but JNK-independent manner. The effect appeared to be more severe in rats on a high fat high

cholesterol diet than in chow-fed rats. A full toxicological examination of D-JNK, however, was beyond the scope of our study.

We believe that our study provides a very important proof-of-concept for the usefulness of JNK2 inhibition in the treatment of vascular dysfunction in obesity, although currently available JNK inhibitors are not suitable for the clinical development of JNK2-targeted therapies. Therefore, the development of novel non-peptide drugs able to maintain the same specific JNK inhibition while avoiding the current side effects,[49] may become a promising therapy against vascular dysfunction in obesity.

Conclusions

Obesity-induced activation of vascular JNK2 and the associated endothelial dysfunction were reversed by RYGB surgery, likely in part through a GLP-1-dependent signaling mechanism. These beneficial effects of RYGB were mimicked by *in vivo* JNK inhibition, demonstrating the potential of JNK2-targeted therapy against obesity-induced endothelial dysfunction.

Acknowledgments

We thank Sara Gobbato, Claudia Dörig and Dr. Helena Balke for technical help.

Funding Sources

This work was supported in part by grants of the Swiss National Science Foundation Ambizione Grant (EO), the Swiss Cardio-Onco-Grant - Alfred and Annemarie von Sick Grant (EO, TAL), the Swiss National Science Foundation (TAL), the European Union FP7 (Resolve; TAL), the Zurich Center of Integrative Human Physiology (TAL; EO), and the University of Zurich Forschungskredit (PD). The Fondation Leducq, Paris (Transatlantic

Network on HDL Dysfunction) (TFL, EO) and the Foundation for Cardiovascular Research–Zurich Heart House, Zurich, Switzerland are gratefully acknowledged.

Disclosures

None.

Figure legends

Figure 1.

(A) JNK1 and JNK2 phosphorylation in the aorta of chow-fed and DIO rats. Representative Western blots and densitometric quantification are shown (¢ $p<0.05$ normal chow vs. DIO, n=4-11 per group).

Ex vivo relaxation of aortic rings isolated 8 days after RYGB or sham surgery and start of treatment. Cumulative concentration–response curves after submaximal contraction to norepinephrine (NE) in response to **(B)** GLP-1 and **(C)** insulin in RYGB, $controls_{D\text{-}TAT}$ and D-JNK rats (*, *** $p<0.05$, $p<0.001$ RYGB vs. $controls_{D\text{-}TAT}$, °°° $p<0.001$ $controls_{D\text{-}TAT}$ vs. D-JNK, n=7-13 per group). Results are shown as mean ± SD.

Figure 2.

Ex vivo relaxation of aortic rings isolated 8 days after sham surgery/start of treatment with or without 30 min *ex vivo* pre-incubation with 5 μM D-JNK. Concentration–response curves after submaximal contraction to norepinephrine (NE) in response to **(A)** GLP-1 and **(B)** insulin in $controls_{D\text{-}TAT}$ rats, and to **(C)** GLP-1 and **(D)** insulin in D-JNK rats (##, ### $p<0.01$, $p<0.001$ $controls_{D\text{-}TAT}$ vs. D-TAT pre-incubated 30 min *ex vivo* with 5 μM D-JNK, n=3-6 per group). Results are shown as mean ± SD.

Figure 3.

Aortic **(A)** JNK1 and JNK2 phosphorylation, **(B)** IRS-1 ser307, **(C)** Akt ser473, **(D)** eNOS ser1177 phosphorylation and **(E)** eNOS dimerization in $controls_{D\text{-}TAT}$, RYGB, and D-JNK rats 8 days after surgery/start of treatment. Representative Western blots and densitometric quantification are shown (* $p<0.05$ RYGB vs. $controls_{D\text{-}TAT}$, °, °° $p<0.05$, $p<0.01$ $controls_{D\text{-}TAT}$ vs. D-JNK, n=6-13 per group). Results are shown as mean ± SD.

Figure 4.

Ex vivo relaxation of aortic rings isolated 8 days after RYGB or sham surgery/start of treatment after 30 min *ex vivo* pre-incubation with 150 U/ml superoxide dismutase (SOD). Concentration–response curves after submaximal contraction to norepinephrine (NE) in response to **(A)** GLP-1 and **(B)** insulin in $controls_{D\text{-}TAT}$, RYGB, and D-JNK rats (n=3-9 per group).

(C) *In vitro* dihydroethidium fluorescent staining of superoxide anions and relative quantification in aorta isolated from $controls_{D\text{-}TAT}$, RYGB and D-JNK rats 8 days after surgery/start of treatment. Representative pictures are shown. **(D)** *In vitro* NADPH oxidase activity in aorta isolated 8 days after surgery from $controls_{D\text{-}TAT}$, RYGB, and D-JNK rats (*, ** $p<0.05$, $p<0.01$ RYGB vs. $controls_{D\text{-}TAT}$, °, °°° $p<0.05$, $p<0.001$ $controls_{D\text{-}TAT}$ vs. D-JNK, n=7-10 per group). Results are shown as mean ± SD.

Figure 5.

(A) Fasting plasma GLP-1 levels in $controls_{D\text{-}TAT}$, RYGB, and D-JNK rats 8 days after surgery/start of treatment. Aortic **(B)** GLP-1 receptor expression, **(C)** PKA phosphorylation, and **(D)** cAMP response element binding protein (CREB) phosphorylation in $controls_{D\text{-}TAT}$,

RYGB, and D-JNK rats 8 days after surgery/start of treatment. Representative Western blots and densitometric quantification are shown (*, ** $p<0.05$, $p<0.01$ RYGB vs. $controls_{D\text{-}TAT}$, ° $p<0.05$ $controls_{D\text{-}TAT}$ vs. D-JNK, n=6-13 per group). Results are shown as mean ± SD.

Figure 6.

Proposed molecular signalling pathways underlying the rapid beneficial effects of RYGB surgery on endothelial function. RYGB surgery increases circulating GLP-1. GLP-1 activates the endothelial GLP-1 receptor and downstream PKA, which inhibits JNK2. JNK2 inactivation might also lead to increased expression of the GLP-1 receptor in a positive feedback mechanism. JNK2 directly inhibits eNOS and IRS-1 in the vascular insulin signalling pathway, and PKA and IRS-1 lead to Akt activation, which then directly activates eNOS, leading to increased NO and vasodilation. In parallel, JNK2 inactivation inhibits NADPH oxidase activity and decreases levels of anion superoxide, which further contributes to preserved NO bioavailability and vasodilation. Blue and red arrows indicate experimentally observed activation and inactivation, respectively, of proposed downstream mediators.

References

1. Poirier P, Cornier MA, Mazzone T, Stiles S, Cummings S, Klein S, McCullough PA, Ren Fielding C, Franklin BA, American Heart Association Obesity Committee of the Council on Nutrition PA, Metabolism. Bariatric surgery and cardiovascular risk factors: A scientific statement from the american heart association. *Circulation*. 2011;123:1683-1701
2. Meshkani R, Adeli K. Hepatic insulin resistance, metabolic syndrome and cardiovascular disease. *Clinical biochemistry*. 2009;42:1331-1346
3. Mauricio MD, Aldasoro M, Ortega J, Vila JM. Endothelial dysfunction in morbid obesity. *Current pharmaceutical design*. 2013;19:5718-5729
4. Raffaelli M, Guidone C, Callari C, Iaconelli A, Bellantone R, Mingrone G. Effect of gastric bypass versus diet on cardiovascular risk factors. *Annals of surgery*. 2014;259:694-699
5. Ikramuddin S, Korner J, Lee WJ, Connett JE, Inabnet WB, Billington CJ, Thomas AJ, Leslie DB, Chong K, Jeffery RW, Ahmed L, Vella A, Chuang LM, Bessler M, Sarr MG, Swain JM, Laqua P, Jensen MD, Bantle JP. Roux-en-y gastric bypass vs intensive medical management for the

control of type 2 diabetes, hypertension, and hyperlipidemia: The diabetes surgery study randomized clinical trial. *Jama*. 2013;309:2240-2249
6. Adams TD, Davidson LE, Litwin SE, Kolotkin RL, LaMonte MJ, Pendleton RC, Strong MB, Vinik R, Wanner NA, Hopkins PN, Gress RE, Walker JM, Cloward TV, Nuttall RT, Hammoud A, Greenwood JL, Crosby RD, McKinlay R, Simper SC, Smith SC, Hunt SC. Health benefits of gastric bypass surgery after 6 years. *Jama*. 2012;308:1122-1131
7. Mingrone G, Panunzi S, De Gaetano A, Guidone C, Iaconelli A, Leccesi L, Nanni G, Pomp A, Castagneto M, Ghirlanda G, Rubino F. Bariatric surgery versus conventional medical therapy for type 2 diabetes. *The New England journal of medicine*. 2012;366:1577-1585
8. Brethauer SA, Heneghan HM, Eldar S, Gatmaitan P, Huang H, Kashyap S, Gornik HL, Kirwan JP, Schauer PR. Early effects of gastric bypass on endothelial function, inflammation, and cardiovascular risk in obese patients. *Surgical endoscopy*. 2011;25:2650-2659
9. Faria G, Preto J, da Costa EL, Guimaraes JT, Calhau C, Taveira-Gomes A. Acute improvement in insulin resistance after laparoscopic roux-en-y gastric bypass: Is 3 days enough to correct insulin metabolism? *Obesity surgery*. 2013;23:103-110
10. Laferrere B, Reilly D, Arias S, Swerdlow N, Gorroochurn P, Bawa B, Bose M, Teixeira J, Stevens RD, Wenner BR, Bain JR, Muehlbauer MJ, Haqq A, Lien L, Shah SH, Svetkey LP, Newgard CB. Differential metabolic impact of gastric bypass surgery versus dietary intervention in obese diabetic subjects despite identical weight loss. *Science translational medicine*. 2011;3:80re82
11. Plum L, Ahmed L, Febres G, Bessler M, Inabnet W, Kunreuther E, McMahon DJ, Korner J. Comparison of glucostatic parameters after hypocaloric diet or bariatric surgery and equivalent weight loss. *Obesity*. 2011;19:2149-2157
12. Osto E, Doytcheva P, Corteville C, Bueter M, Dorig C, Stivala S, Buhmann H, Colin S, Rohrer L, Hasballa R, Tailleux A, Wolfrum C, Tona F, Manz J, Vetter D, Spliethoff K, Vanhoutte PM, Landmesser U, Pattou F, Staels B, Matter CM, Lutz TA, Luscher TF. Rapid and body weight-independent improvement of endothelial and high-density lipoprotein function after roux-en-y gastric bypass: Role of glucagon-like peptide-1. *Circulation*. 2015;131:871-881
13. Hotamisligil GS. Role of endoplasmic reticulum stress and c-jun nh2-terminal kinase pathways in inflammation and origin of obesity and diabetes. *Diabetes*. 2005;54 Suppl 2:S73-78
14. Aguirre V, Uchida T, Yenush L, Davis R, White MF. The c-jun nh(2)-terminal kinase promotes insulin resistance during association with insulin receptor substrate-1 and phosphorylation of ser(307). *The Journal of biological chemistry*. 2000;275:9047-9054
15. Hirosumi J, Tuncman G, Chang L, Gorgun CZ, Uysal KT, Maeda K, Karin M, Hotamisligil GS. A central role for jnk in obesity and insulin resistance. *Nature*. 2002;420:333-336
16. Tuncman G, Hirosumi J, Solinas G, Chang L, Karin M, Hotamisligil GS. Functional in vivo interactions between jnk1 and jnk2 isoforms in obesity and insulin resistance. *Proceedings of the National Academy of Sciences of the United States of America*. 2006;103:10741-10746
17. Park JH, Park M, Byun CJ, Jo I. C-jun n-terminal kinase 2 phosphorylates endothelial nitric oxide synthase at serine 116 and regulates nitric oxide production. *Biochemical and biophysical research communications*. 2012;417:340-345
18. Osto E, Matter CM, Kouroedov A, Malinski T, Bachschmid M, Camici GG, Kilic U, Stallmach T, Boren J, Iliceto S, Luscher TF, Cosentino F. C-jun n-terminal kinase 2 deficiency protects against hypercholesterolemia-induced endothelial dysfunction and oxidative stress. *Circulation*. 2008;118:2073-2080
19. Ricci R, Sumara G, Sumara I, Rozenberg I, Kurrer M, Akhmedov A, Hersberger M, Eriksson U, Eberli FR, Becher B, Boren J, Chen M, Cybulsky MI, Moore KJ, Freeman MW, Wagner EF, Matter CM, Luscher TF. Requirement of jnk2 for scavenger receptor a-mediated foam cell formation in atherogenesis. *Science*. 2004;306:1558-1561
20. Amini N, Boyle JJ, Moers B, Warboys CM, Malik TH, Zakkar M, Francis SE, Mason JC, Haskard DO, Evans PC. Requirement of jnk1 for endothelial cell injury in atherogenesis. *Atherosclerosis*. 2014;235:613-618

21. Sugita M, Sugita H, Kaneki M. Increased insulin receptor substrate 1 serine phosphorylation and stress-activated protein kinase/c-jun n-terminal kinase activation associated with vascular insulin resistance in spontaneously hypertensive rats. *Hypertension*. 2004;44:484-489
22. Breton-Romero R, Feng B, Holbrook M, Farb MG, Fetterman JL, Linder EA, Berk BD, Masaki N, Weisbrod RM, Inagaki E, Gokce N, Fuster JJ, Walsh K, Hamburg NM. Endothelial dysfunction in human diabetes is mediated by wnt5a-jnk signaling. *Arteriosclerosis, thrombosis, and vascular biology*. 2016;36:561-569
23. Bennett BL, Sasaki DT, Murray BW, O'Leary EC, Sakata ST, Xu W, Leisten JC, Motiwala A, Pierce S, Satoh Y, Bhagwat SS, Manning AM, Anderson DW. Sp600125, an anthrapyrazolone inhibitor of jun n-terminal kinase. *Proceedings of the National Academy of Sciences of the United States of America*. 2001;98:13681-13686
24. Zhou MS, Schulman IH, Chadipiralla K, Raij L. Role of c-jun n-terminal kinase in the regulation of vascular tone. *Journal of cardiovascular pharmacology and therapeutics*. 2010;15:78-83
25. Bain J, McLauchlan H, Elliott M, Cohen P. The specificities of protein kinase inhibitors: An update. *The Biochemical journal*. 2003;371:199-204
26. Bain J, Plater L, Elliott M, Shpiro N, Hastie CJ, McLauchlan H, Klevernic I, Arthur JS, Alessi DR, Cohen P. The selectivity of protein kinase inhibitors: A further update. *The Biochemical journal*. 2007;408:297-315
27. Bonny C, Oberson A, Negri S, Sauser C, Schorderet DF. Cell-permeable peptide inhibitors of jnk: Novel blockers of beta-cell death. *Diabetes*. 2001;50:77-82
28. Kaneto H, Nakatani Y, Miyatsuka T, Kawamori D, Matsuoka TA, Matsuhisa M, Kajimoto Y, Ichijo H, Yamasaki Y, Hori M. Possible novel therapy for diabetes with cell-permeable jnk-inhibitory peptide. *Nature medicine*. 2004;10:1128-1132
29. Oyama J, Higashi Y, Node K. Do incretins improve endothelial function? *Cardiovascular diabetology*. 2014;13:21
30. Salisbury D, Bronas U. Reactive oxygen and nitrogen species: Impact on endothelial dysfunction. *Nursing research*. 2015;64:53-66
31. Son Y, Kim S, Chung HT, Pae HO. Reactive oxygen species in the activation of map kinases. *Methods in enzymology*. 2013;528:27-48
32. Sivertsen J, Rosenmeier J, Holst JJ, Vilsboll T. The effect of glucagon-like peptide 1 on cardiovascular risk. *Nature reviews. Cardiology*. 2012;9:209-222
33. Ferdaoussi M, Abdelli S, Yang JY, Cornu M, Niederhauser G, Favre D, Widmann C, Regazzi R, Thorens B, Waeber G, Abderrahmani A. Exendin-4 protects beta-cells from interleukin-1 beta-induced apoptosis by interfering with the c-jun nh2-terminal kinase pathway. *Diabetes*. 2008;57:1205-1215
34. Natalicchio A, De Stefano F, Orlando MR, Melchiorre M, Leonardini A, Cignarelli A, Labarbuta R, Marchetti P, Perrini S, Laviola L, Giorgino F. Exendin-4 prevents c-jun n-terminal protein kinase activation by tumor necrosis factor-alpha (tnfalpha) and inhibits tnfalpha-induced apoptosis in insulin-secreting cells. *Endocrinology*. 2010;151:2019-2029
35. Laviola L, Leonardini A, Melchiorre M, Orlando MR, Peschechera A, Bortone A, Paparella D, Natalicchio A, Perrini S, Giorgino F. Glucagon-like peptide-1 counteracts oxidative stress-dependent apoptosis of human cardiac progenitor cells by inhibiting the activation of the c-jun n-terminal protein kinase signaling pathway. *Endocrinology*. 2012;153:5770-5781
36. Erdogdu O, Eriksson L, Xu H, Sjoholm A, Zhang Q, Nystrom T. Exendin-4 protects endothelial cells from lipoapoptosis by pka, pi3k, enos, p38 mapk, and jnk pathways. *Journal of molecular endocrinology*. 2013;50:229-241
37. Nagayama K, Kyotani Y, Zhao J, Ito S, Ozawa K, Bolstad FA, Yoshizumi M. Exendin-4 prevents vascular smooth muscle cell proliferation and migration by angiotensin ii via the inhibition of erk1/2 and jnk signaling pathways. *PloS one*. 2015;10:e0137960

38. Han L, Yu Y, Sun X, Wang B. Exendin-4 directly improves endothelial dysfunction in isolated aortas from obese rats through the camp or ampk-enos pathways. *Diabetes research and clinical practice*. 2012;97:453-460
39. Erdogdu O, Nathanson D, Sjoholm A, Nystrom T, Zhang Q. Exendin-4 stimulates proliferation of human coronary artery endothelial cells through enos-, pka- and pi3k/akt-dependent pathways and requires glp-1 receptor. *Molecular and cellular endocrinology*. 2010;325:26-35
40. He B, Piao D, Yu C, Wang Y, Han P. Amelioration in hepatic insulin sensitivity by reduced hepatic lipid accumulation at short-term after roux-en-y gastric bypass surgery in type 2 diabetic rats. *Obesity surgery*. 2013;23:2033-2041
41. Zeng G, Nystrom FH, Ravichandran LV, Cong LN, Kirby M, Mostowski H, Quon MJ. Roles for insulin receptor, pi3-kinase, and akt in insulin-signaling pathways related to production of nitric oxide in human vascular endothelial cells. *Circulation*. 2000;101:1539-1545
42. Sena CM, Pereira AM, Seica R. Endothelial dysfunction - a major mediator of diabetic vascular disease. *Biochimica et biophysica acta*. 2013;1832:2216-2231
43. Yu G, Peng T, Feng Q, Tyml K. Abrupt reoxygenation of microvascular endothelial cells after hypoxia activates erk1/2 and jnk1, leading to nadph oxidase-dependent oxidant production. *Microcirculation*. 2007;14:125-136
44. Zhao L, Guo H, Chen H, Petersen RB, Zheng L, Peng A, Huang K. Effect of liraglutide on endoplasmic reticulum stress in diabetes. *Biochemical and biophysical research communications*. 2013;441:133-138
45. Gao H, Zeng Z, Zhang H, Zhou X, Guan L, Deng W, Xu L. The glucagon-like peptide-1 analogue liraglutide inhibits oxidative stress and inflammatory response in the liver of rats with diet-induced non-alcoholic fatty liver disease. *Biological & pharmaceutical bulletin*. 2015;38:694-702
46. Cardozo AK, Buchillier V, Mathieu M, Chen J, Ortis F, Ladriere L, Allaman-Pillet N, Poirot O, Kellenberger S, Beckmann JS, Eizirik DL, Bonny C, Maurer F. Cell-permeable peptides induce dose- and length-dependent cytotoxic effects. *Biochimica et biophysica acta*. 2007;1768:2222-2234
47. Ijaz A, Tejada T, Catanuto P, Xia X, Elliot SJ, Lenz O, Jauregui A, Saenz MO, Molano RD, Pileggi A, Ricordi C, Fornoni A. Inhibition of c-jun n-terminal kinase improves insulin sensitivity but worsens albuminuria in experimental diabetes. *Kidney international*. 2009;75:381-388
48. Davoli E, Sclip A, Cecchi M, Cimini S, Carra A, Salmona M, Borsello T. Determination of tissue levels of a neuroprotectant drug: The cell permeable jnk inhibitor peptide. *Journal of pharmacological and toxicological methods*. 2014;70:55-61
49. Stebbins JL, De SK, Machleidt T, Becattini B, Vazquez J, Kuntzen C, Chen LH, Cellitti JF, Riel-Mehan M, Emdadi A, Solinas G, Karin M, Pellecchia M. Identification of a new jnk inhibitor targeting the jnk-jip interaction site. *Proceedings of the National Academy of Sciences of the United States of America*. 2008;105:16809-16813

A

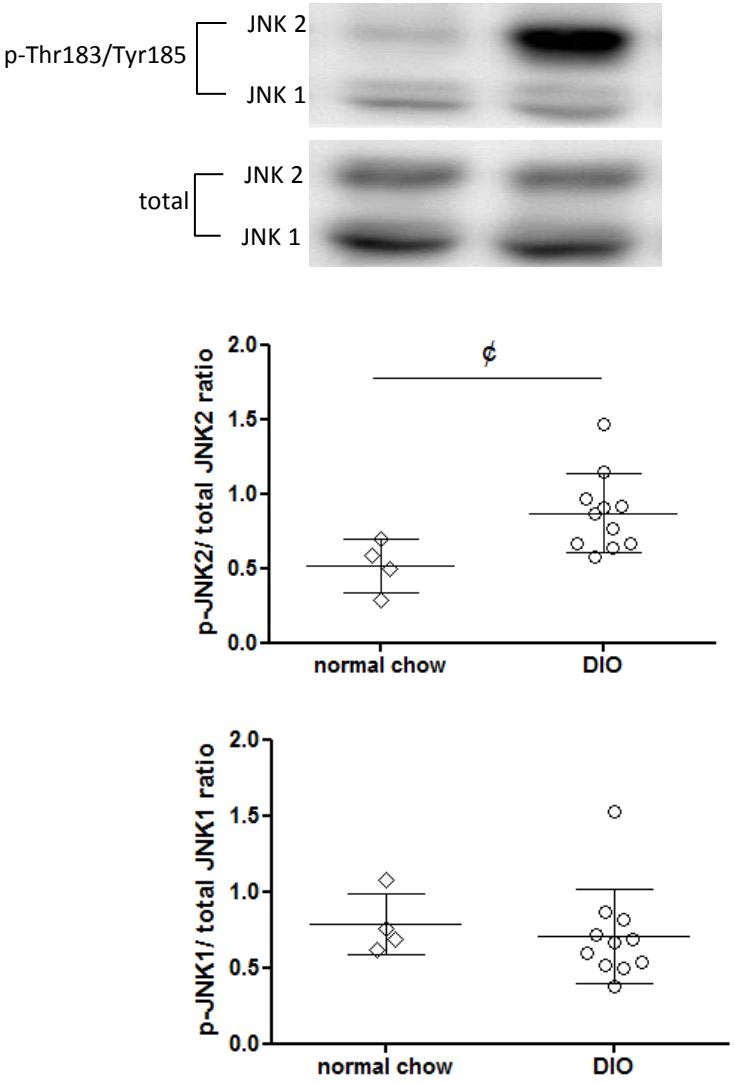
p-Thr183/Tyr185
JNK 2
JNK 1
total
JNK 2
JNK 1
p-JNK2/ total JNK2 ratio
¢
normal chow
DIO
p-JNK1/ total JNK1 ratio
normal chow
DIO

B

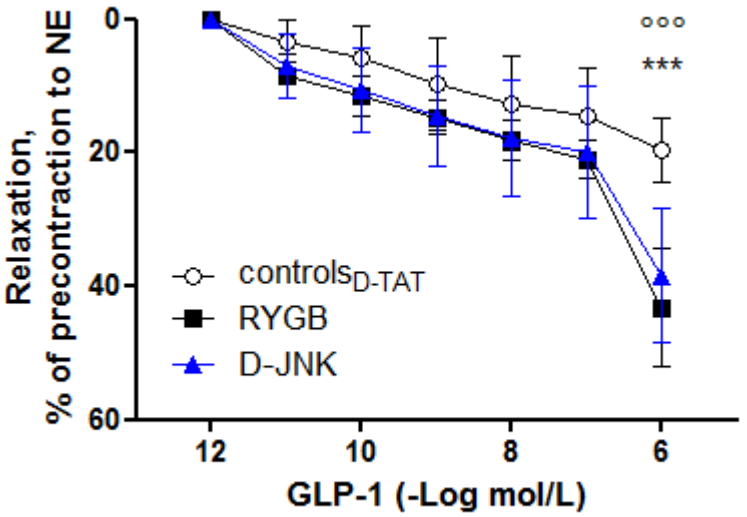
Relaxation, % of precontraction to NE
GLP-1 (-Log mol/L)
controls D-TAT
RYGB
D-JNK
°°°
***

C

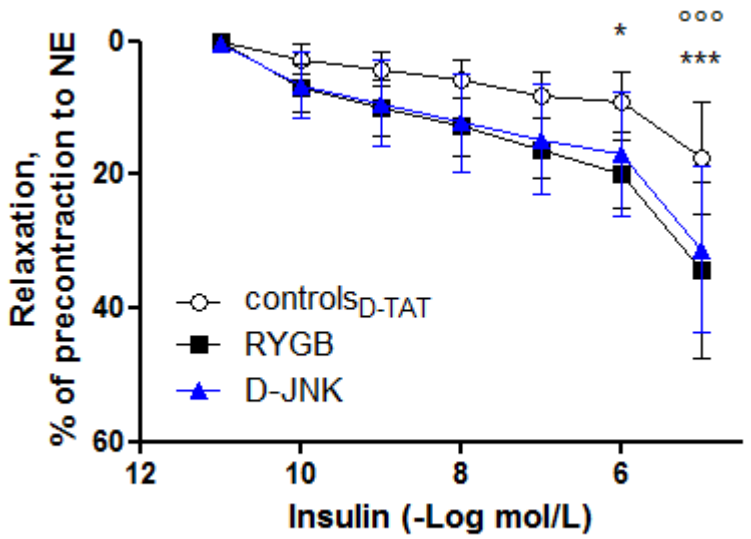
Relaxation, % of precontraction to NE
Insulin (-Log mol/L)
controls D-TAT
RYGB
D-JNK
*
°°°
***

Fig. 1

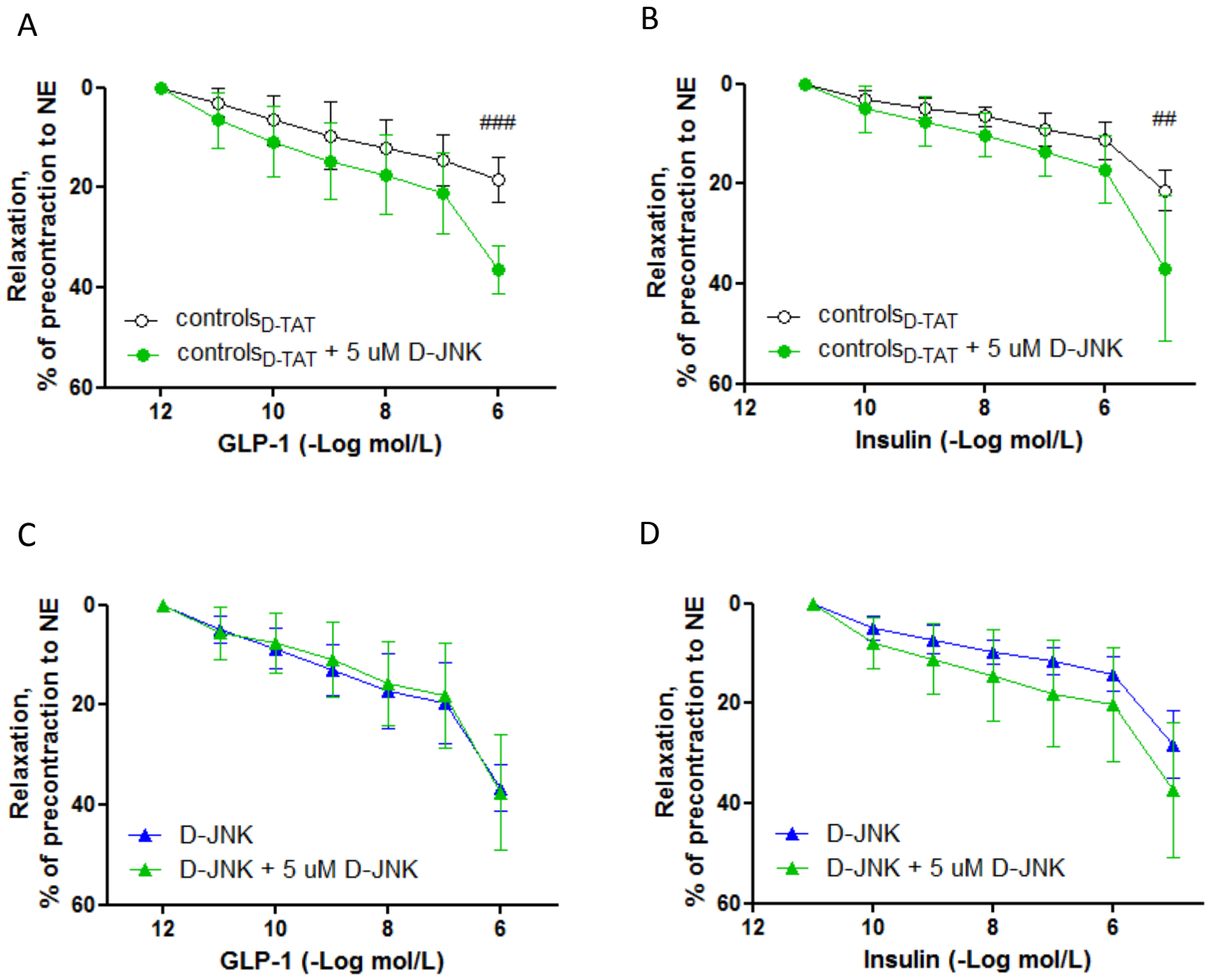
A
B
C
D
Relaxation, % of precontraction to NE
0
20
40
60
12
10
8
6
GLP-1 (-Log mol/L)
Insulin (-Log mol/L)
###
##
controls D-TAT
controls D-TAT + 5 uM D-JNK
D-JNK
D-JNK + 5 uM D-JNK

Fig. 2

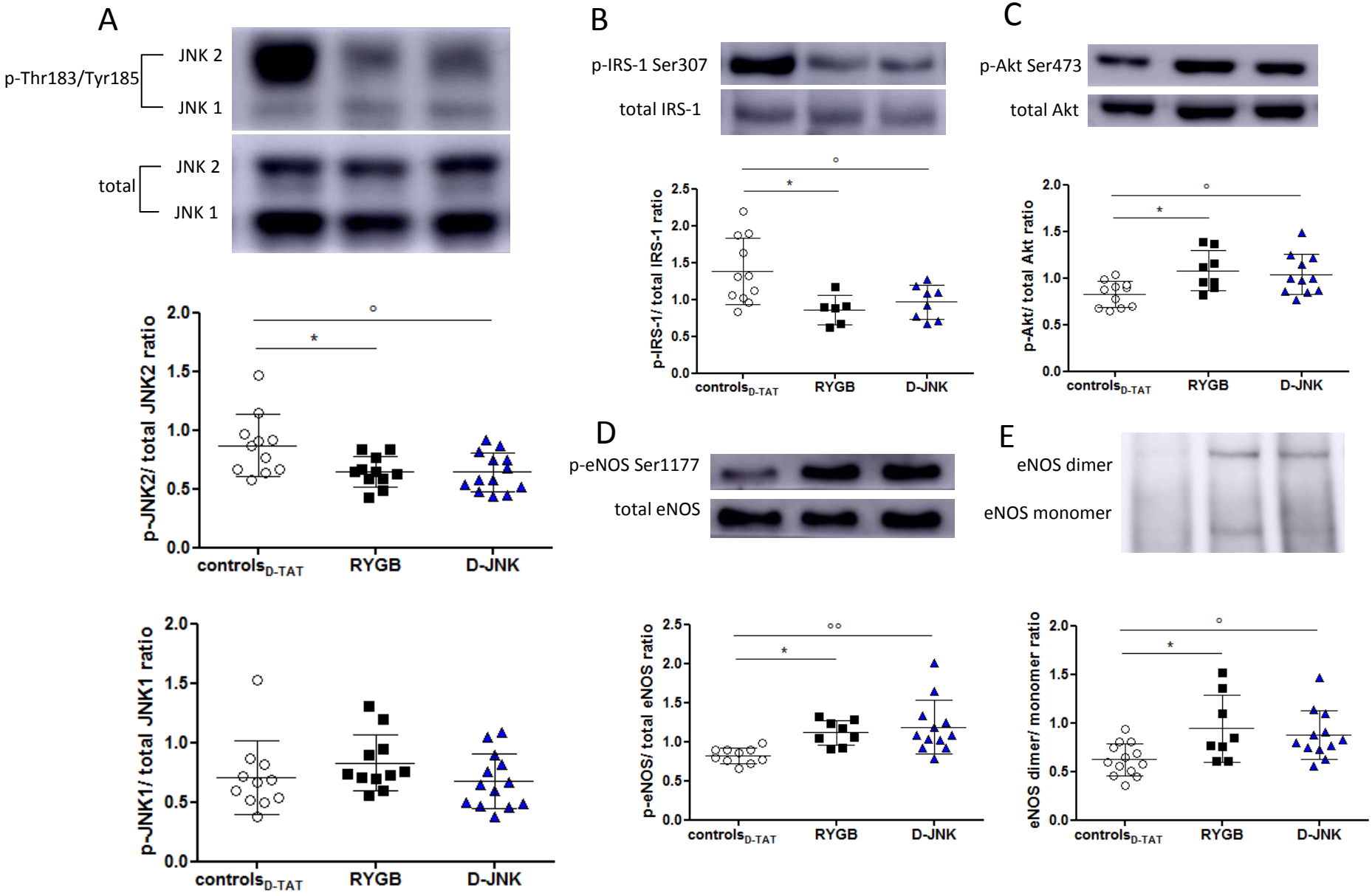
A
p-Thr183/Tyr185
JNK 2
JNK 1
total
JNK 2
JNK 1
p-JNK2/ total JNK2 ratio
p-JNK1/ total JNK1 ratio
controls D-TAT
RYGB
D-JNK
B
p-IRS-1 Ser307
total IRS-1
p-IRS-1/ total IRS-1 ratio
C
p-Akt Ser473
total Akt
p-Akt/ total Akt ratio
D
p-eNOS Ser1177
total eNOS
p-eNOS/ total eNOS ratio
E
eNOS dimer
eNOS monomer
eNOS dimer/ monomer ratio

Fig. 3

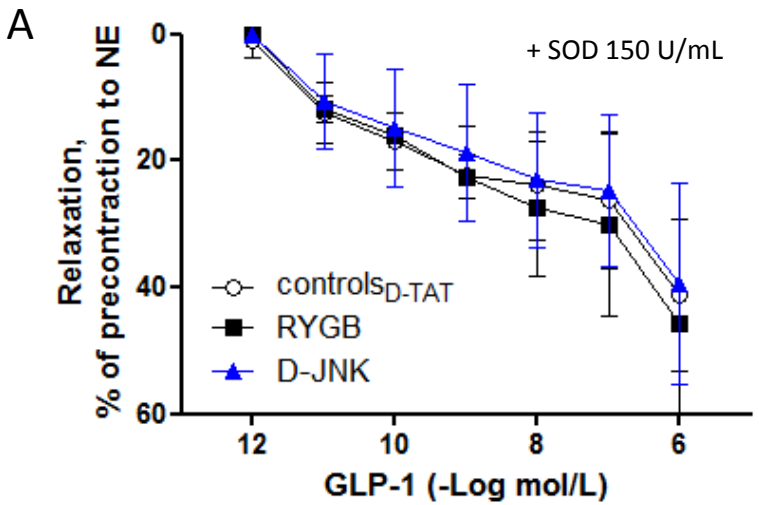
A
+ SOD 150 U/mL
Relaxation, % of precontraction to NE
0
20
40
60
12
10
8
6
GLP-1 (-Log mol/L)
controls D-TAT
RYGB
D-JNK

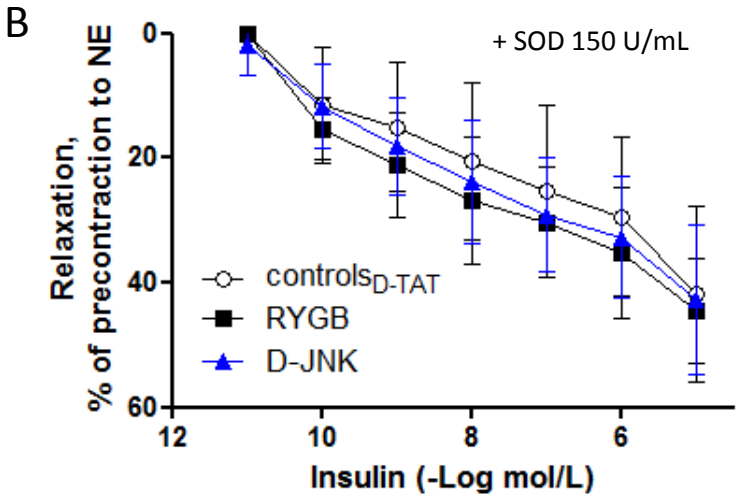
B
+ SOD 150 U/mL
Relaxation, % of precontraction to NE
0
20
40
60
12
10
8
6
Insulin (-Log mol/L)
controls D-TAT
RYGB
D-JNK

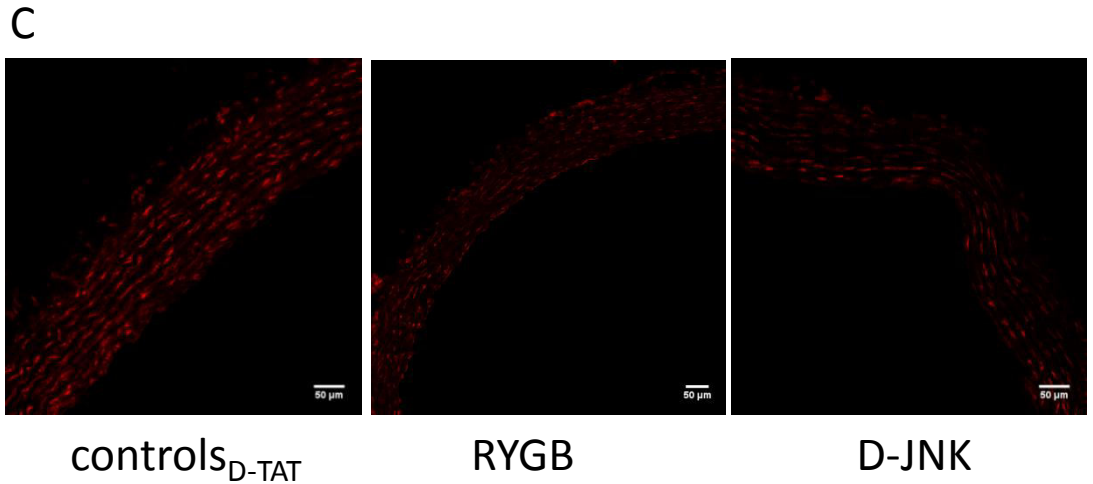
C
50 µm
50 µm
50 µm
controls D-TAT
RYGB
D-JNK

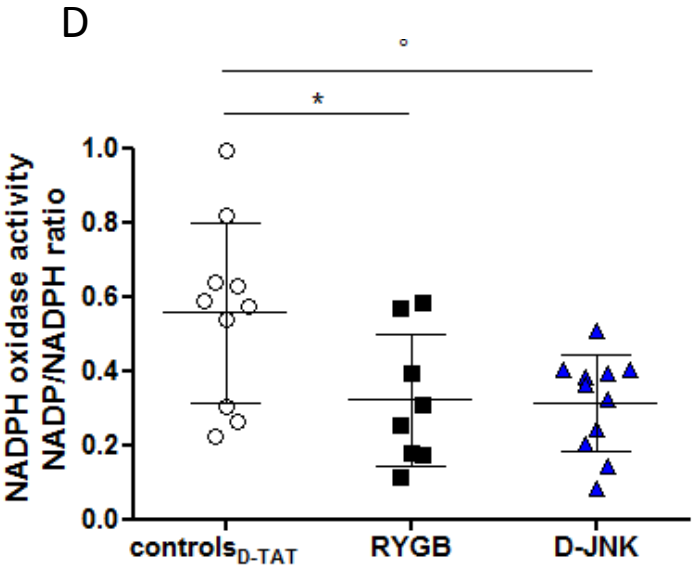
D
°
*
NADPH oxidase activity NADP/NADPH ratio
1.0
0.8
0.6
0.4
0.2
0.0
controls D-TAT
RYGB
D-JNK

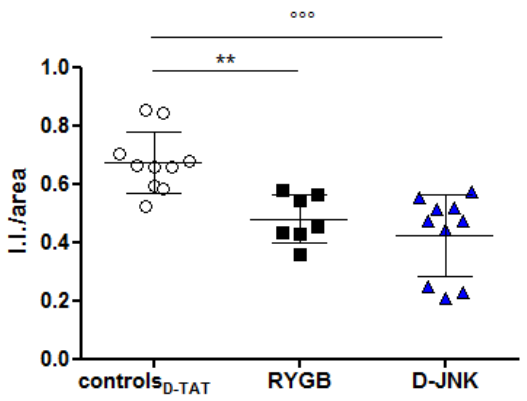
°°°
**
I.I./area
1.0
0.8
0.6
0.4
0.2
0.0
controls D-TAT
RYGB
D-JNK

Fig. 4

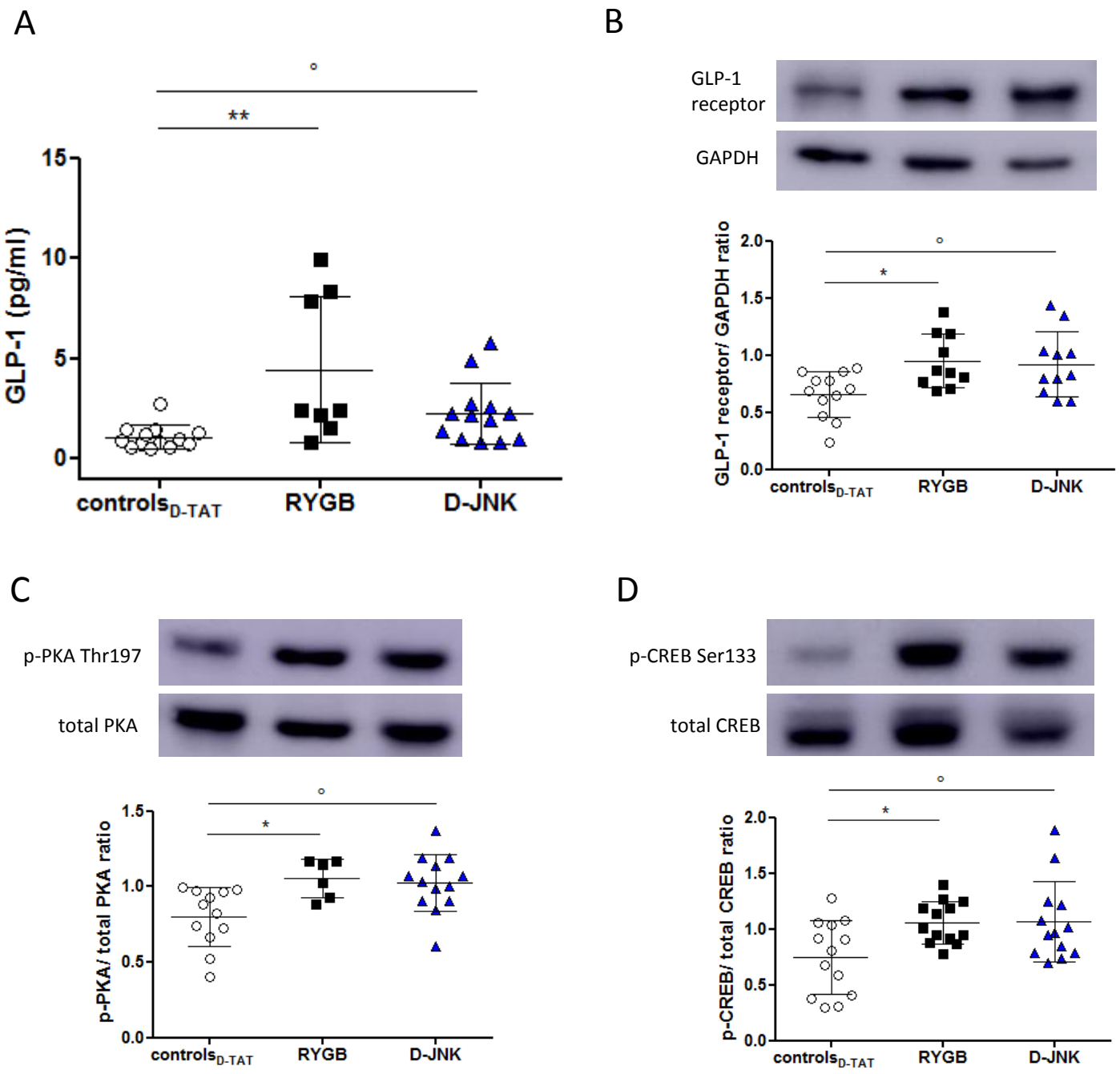
A
B
C
D
GLP-1 (pg/ml)
15
10
5
0
**
°
controls D-TAT
RYGB
D-JNK
GLP-1 receptor
GAPDH
GLP-1 receptor/ GAPDH ratio
2.0
1.5
1.0
0.5
0.0
*
p-PKA Thr197
total PKA
p-PKA/ total PKA ratio
p-CREB Ser133
total CREB
p-CREB/ total CREB ratio

Fig. 5

Endothelium-dependent mechanisms of improved vasodilation after RYGB

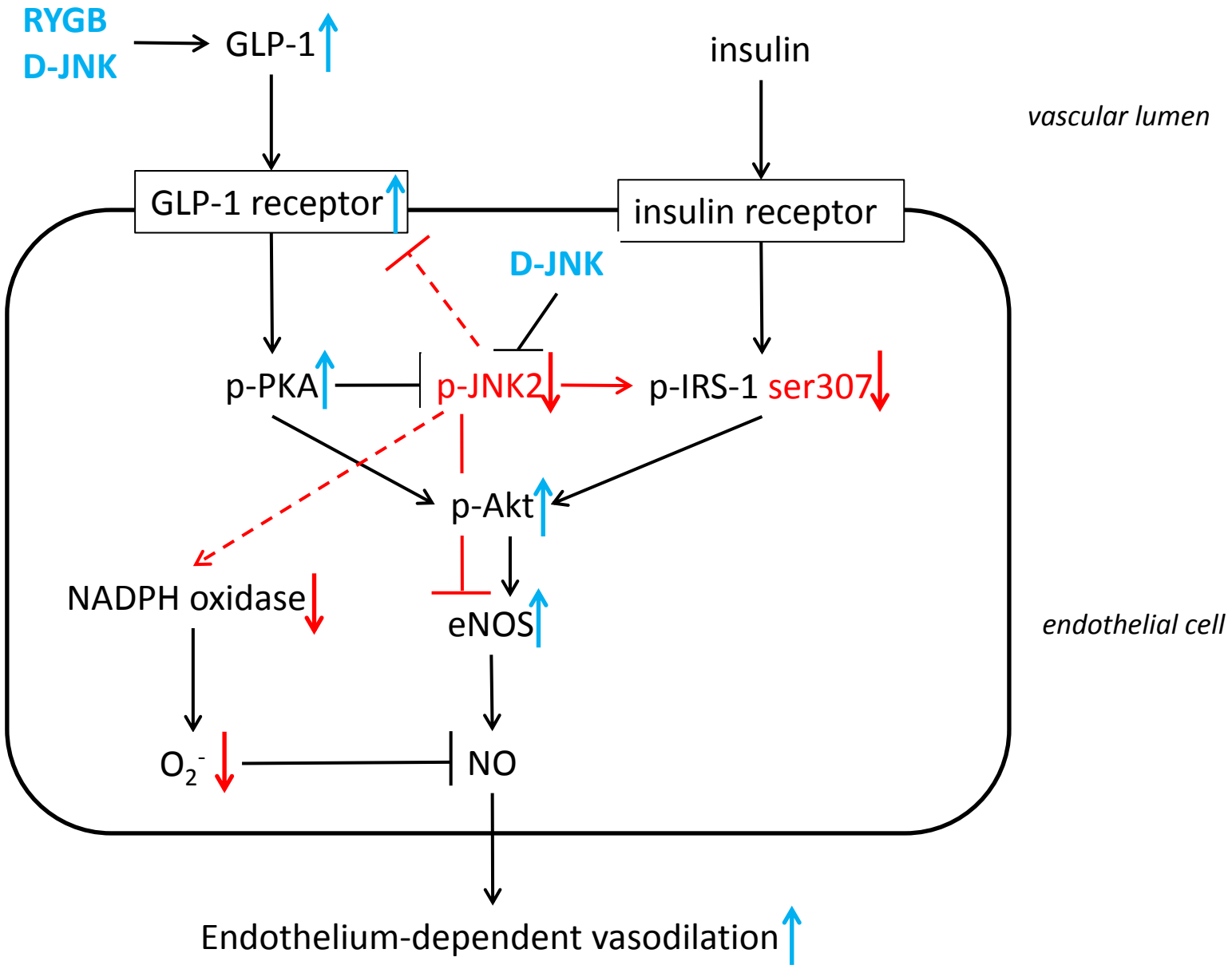

Fig. 6

SUPPLEMENTAL MATERIAL

Inhibition of vascular JNK2 improves obesity-induced endothelial dysfunction after Roux-en-Y gastric bypass surgery

Petia Doytcheva, MSc[1,2,3]; Thomas Bächler, MD[4]; Erika Tarasco, MSc[2,3]; Michael Engeli, BSc[1]; Giovanni Pellegrini, DVM, PhD[5]; Simona Stivala, PhD[1,3]; Lucia Rohrer, PhD[3,6], Paul M. Vanhoutte, MD, PhD[7]; Thomas F. Lüscher, MD[1,3]; Thomas A. Lutz, DVM, PhD[2,3]; *Elena Osto, MD, PhD[1,3,8]

[1]Center for Molecular Cardiology, University of Zurich and University Heart Center, Cardiology, University Hospital Zurich, Switzerland; [2]Institute of Veterinary Physiology, Vetsuisse Faculty University of Zurich, Winterthurerstrasse 260, 8057 Zurich, Switzerland; [3]Zurich Center for Integrative Human Physiology (ZIHP), University of Zurich, 8057 Zurich, Switzerland; [4]Department of Surgery, Cantonal Hospital Fribourg, Chemin des Pensionnats 2, 1708 Fribourg, Switzerland; [5]Laboratory for Animal Model Pathology, Institute for Veterinary Pathology, Vetsuisse Faculty University of Zurich, Winterthurerstrasse 260, 8057 Zurich, Switzerland; [6]Institute of Clinical Chemistry, University Hospital Zurich, 8001 Zurich, Switzerland; [7]State Key Laboratory for Pharmaceutical Biotechnologies &Department of Pharmacology & Pharmacy, LKS Faculty of Medicine, The University of Hong Kong; [8]Laboratory of Translational Nutrition Biology, Federal Institute of Technology Zurich ETHZ, Schorenstrasse 16, 8603 Schwerzenbach, Switzerland

Running title: *In vivo* JNK inhibition mimics endothelial benefits of RYGB

Address for Correspondence °**Elena Osto, M.D., Ph.D.**

Center for Molecular Cardiology

University of Zurich

Wagistrasse, 12

CH-8952 Schlieren, Switzerland

Tel: 41-44-635 6469

Fax: 41-44-635 6827

Email: elena.osto@uzh.ch

Supplementary Materials and Methods

Surgeries and postoperative care

Anesthesia was induced in a chamber filled with 5% isoflurane in room air (1 L/min). After adequate anesthesia was achieved, rats were shaved from sternum to pelvis followed by disinfection with Betadine scrub (Mundi Pharma, Basel, Switzerland). Rats were positioned in a supine position on a heating pad and maintained under anesthesia (2%–3% isoflurane in room air, 0.8 L/min) for the duration of the surgery. A midline incision of approximately 4 cm starting just below the xiphoid process was performed. For the RYGB procedure, the proximal small bowel was transected approximately 20 cm distal to the pylorus of the stomach, creating a proximal and distal end of small bowel. The proximal end, being still continuous with the remaining portion of the stomach, constituted the biliopancreatic limb and was anastomosed to the distal small intestine, approximately 25–30 cm from the cecum, creating the common channel. For formation of the gastric pouch, the stomach was transected approximately 5 mm below the gastro-esophageal junction, creating a pouch of a size of less than 5% of original stomach size. The Roux-en-Y reconstruction was completed by connecting the distal end of the proximal small bowel to the gastric pouch, leading to formation of the alimentary (Roux) limb. One single RYGB procedure lasted approximately 100 minutes. For sham operations, an anterior gastrostomy with subsequent closure was performed. One single sham procedure lasted approximately 30 minutes. The abdominal wall and the skin were closed in layers after both operations.

Immediately after surgery, rats received 5 mL of saline subcutaneously to compensate for fluid loss. Rats were then placed under indirect red light in a polycarbonate cage until they fully recovered from anesthesia and then returned to their home cages. Baytril 10mg/kg (Bayer, Leverkusen, Germany) and Carprofen 5mg/kg (Norocarp, Norbrook Laboratories, Corby, UK) were administered before and for three days post-surgery. Post-operatively body

weight and food intake were measured daily. During the first three post-operative days, the HFHC solid diet was mixed with water to facilitate swallowing. Postoperative RYGB mortality was between 30-50% mainly due to leakage of the lower anastomosis; sham mortality was 0%.

Terminal blood collection

Rats were fasted overnight and sacrificed by isoflurane anesthesia followed by heart exsanguination. For plasma analyses, blood was collected in Microvette EDTA vacutainers (Sarstedt, Nümbrecht, Germany) supplemented with a DPPIV inhibitor (Millipore, Darmstadt, Germany) and was kept on ice until centrifugation. For serum analyses, blood was collected in Microvette vacutainers (Sarstedt) and kept at room temperature until centrifugation. After centrifugation the supernatants (plasma or serum, respectively) were separated and stored at -80°C.

Tissue harvesting

Organs were harvested within 30 minute after exsanguination. A complete necropsy, including a thorough external and internal gross post mortem examination, was performed. The entire aorta from the heart to the iliac bifurcation was excised and placed immediately in cold modified Krebs-Ringer bicarbonate solution (pH 7.4, 37°C, 95% O2, 5% CO2) of the following composition (mmol/L): NaCl (118.6), KCl (4.7), CaCl2 (2.5), KH2PO4 (1.2), MgSO4 (1.2), NaHCO3 (25.1), glucose (11.1), and calcium EDTA (0.026). The aorta was cleaned from adhering connective tissue and either snap-frozen in liquid nitrogen and stored at -80°C or used immediately for *ex vivo* organ chamber experiments.

For Western blotting, frozen aortae were pulverized and dissolved in lysis buffer (120 mmol/L sodium chloride, 50 mmol/L Tris, 20 mmol/L sodium fluoride, 1 mmol/L benzamidine, 1 mmol/L dithiothreitol, 1 mmol/L EDTA, 6 mmol/L EGTA, 15 mmol/L

sodium pyrophosphate, 0.8 ug/mL leupeptin, 30 mmol/L p-nitrophenyl phosphate, 0.1 mmol/L phenylmethylsulfonyl fluoride, and 1% NP-40).

Organ chamber experiments

For endothelial function experiments, 2-3 mm long aortic rings were connected to an isometric force transducer (Multi-Myograph 610M, Danish Myo Technology A/S, Aarhus, Denmark), suspended in an organ chamber filled with 6 mL Krebs-Ringer bicarbonate solution (37°C, pH 7.4), and bubbled with 95% O2, 5% CO2 at 37°C. Isometric tension was recorded continuously. After a 30-minute equilibration period, rings were gradually stretched to the optimal point of their length-tension curve as determined by the contraction in response to potassium chloride (100 mmol/L). Concentration-response curves were obtained in a cumulative fashion. Responses to acetylcholine (10^{-9} to 10^{-6} mol/L; Sigma-Aldrich, St. Louis, MO, USA), GLP-$1_{(7–36)}$ amide (10^{-12}-10^{-6}mol/L; herein referred to as GLP-1; Bachem, Bubendorf, Switzerland) and insulin (10^{-11} to 10^{-5} mol/L; Humalog, Lilly, Indianapolis, IN, USA) were recorded during submaximal contraction to norepinephrine ($3x10^{-6}$ mol/L, Sigma-Aldrich) in the presence or absence of Nω-nitro-L-arginine methyl ester (L-NAME, 10^{-4} mol/L, Sigma-Aldrich), a non-selective nitric oxide (NO) synthase inhibitor or of the free radical scavenger polyethylene glycol–superoxide dismutase (SOD 150 U/mL, Sigma-Aldrich). To study the direct *ex vivo* effects of D-JNK on vascular function, a subset of aortic rings were incubated for 30 min with 5μM D-JNK prior to performing cumulative response curves to insulin and GLP-1. The NO donor sodium nitroprusside (SNP, 10^{-10} to 10^{-5} mol/L; Sigma-Aldrich) was added to test endothelium-independent relaxation. Relaxations were expressed as a percentage of the pre-contraction.

DHE staining on rats aortae

Frozen 10 µm sections from aortae were cut with a Leica CM3050S cryostat and placed on positive-charged slides (Superfrost Plus, Thermo Scientific, Waltham, MA, USA). Dihydroethidium (Sigma Aldrich) was prepared as stock solution in DMSO, diluted in deoxygenated PBS (final concentration 5µM), and applied to frozen sections for 30 min at 37°C. Nuclei were counterstained with Hoechst 33258 (Sigma Aldrich; final concentration 1µg/ml). Slides were coverslipped and images taken on a SP8 microscope (10x/0.30 objective; Leica, Solms, Germany), and quantified (ImageJ, NIH). DHE fluorescence was calculated by subtracting the autofluorescence signal (green channel) from the DHE signal (red channel), and normalized to the total fluorescent area.

qPCR analysis

Kidney expression of kidney injury molecule-1 (KIM-1) and lipocalin-2 (NGAL) was analyzed by qPCR of snap-frozen tissue. RNA was isolated from frozen kidneys with a miRNaeasy Mini Kit (Qiagen) and reverse transcribed with a Ready-To-Go You-Prime First-Strand Beads (GE Healthcare, Little Chalfont, UK). Rat-specific primers were used for KIM-1 (forward: GTGGGTCACCCTGTCACAAT, reverse: ATGTTGTATCGACCGCTGCT) and NGAL (forward: GATGAACTGAAGGAGCGATTC, reverse: TCGGTGGGAACAGAGAAAAC) (Microsynth, Balgach, Switzerland). CT results were normalized to GAPDH CT.

Histological analysis

Representative samples of aorta, liver, pancreas, kidneys, thyroid glands, inguinal white adipose tissue and interscapular brown adipose tissue were fixed in 10% neutral buffered formalin and embedded in paraffin. Sections (3-5 µm thick) were prepared, mounted on glass slides, deparaffinised in xylene, rehydrated through graded alcohols and stained with

haematoxylin and eosin (H&E) for the histological examination. All slides were scanned using digital slide scanner NanoZoomer-XR C12000 (Hamamatsu, Hamamatsu City, Japan) and images were taken using NDP.view2 viewing software (Hamamatsu).

Renal injury, characterized by tubular degeneration and regeneration and interstitial inflammation, was assessed by light microscopy in a blinded fashion (GP). A semi-quantitative scoring of 0-5 was employed, indicating normal histology (0), slight (1), mild (2), moderate (3), marked (4) or severe (5) renal damage.

Supplementary Results

D-JNK induces carrier peptide dependent kidney toxicity

SP600125 treatment did not affect food intake and body weight of sham-operated rats (SOM Fig. 2A-B). In a pilot experiment, the tolerability of D-TAT and D-JNK was assessed in non-operated, chow-fed rats; 8-day D-TAT and D-JNK treatment did not affect body weight (SOM Fig.2C). On the contrary, DIO sham-operated rats receiving D-JNK ate less and gradually lost body weight compared to controls$_{D\text{-}TAT}$, even though the differences in body weight were not significant (SOM Fig. 2D-E). To investigate whether this effect on weight loss was due to some kind of toxicity as opposed to an obesity-protective effect of JNK inhibition, we measured circulating markers of liver and kidney damage; of these, only creatinine and cystatin C levels were specifically elevated in the D-JNK group, suggesting potential kidney, but not liver, toxicity of D-JNK (data not shown). Further investigation demonstrated evidence for acute renal proximal tubular injury in both controls$_{D\text{-}TAT}$ and D-JNK rats as assessed by kidney histological analysis (SOM Fig. 3). Nephrotoxicity was characterized by ongoing tubular degeneration and necrosis, accompanied by prominent tubular regeneration and interstitial mixed, predominantly lymphohistiocytic cell infiltration.

Glomeruli were not affected. Renal injury occurred not only in D-JNK but also in controls$_{D\text{-}TAT}$ rats, and was generally moderate in controls$_{D\text{-}TAT}$ (approximately 50% tubules affected) or severe in D-JNK-treated rats (> 80% tubules affected) (SOM Fig. 3). These changes were accompanied by functional signs of impaired kidney function such as an increase in urinary excretion (SOM Fig. 4A-B) and a presumably compensatory increase in water intake in both controls$_{D\text{-}TAT}$ and D-JNK animals (SOM Fig. 4C-D); there was no statistical difference in urine excretion and water intake between controls$_{D\text{-}TAT}$ and D-JNK animals. Gene expression analysis of the acute kidney injury markers kidney injury molecule-1 (KIM-1) and neutrophil gelatinase-associated lipocalin/lipocalin 2 (NGAL) confirmed the severe kidney injury in the DIO D-JNK rats, while indicating milder damage in the DIO controls$_{D\text{-}TAT}$ rats and in the non-operated, normal chow-fed D-TAT and D-JNK treated animals from the pilot experiment (SOM Fig. 4E-F). Of note, SP600125 treatment did not affect KIM-1 and NGAL expression (SOM Fig. 4E-F).

There were no biochemical and histological signs of toxicity in controls$_{D\text{-}TAT}$ and D-JNK rats in other organs such as liver, pancreas, and aorta (data not shown). Previously it had been published that D-TAT-conjugated peptides such as D-JNK could induce cytotoxicity *in vitro* in a length-dependent but sequence independent manner, i.e. conjugation of the D-TAT carrier peptide with another peptide increased the cytotoxicity in proportion to the total peptide length, and not the specific sequence of the conjugated peptide.[1] To our knowledge, there are no previous studies demonstrating *in vivo* D-JNK toxicity. Therefore, the observed kidney toxicity was likely due to length-dependent intrinsic cytotoxicity of the D-TAT carrier peptide.[1] This would explain why signs of kidney toxicity were observed in both controls$_{D\text{-}TAT}$ and D-JNK rats, but the severity was higher in the D-JNK rats independently from the JNK inhibitory activity of D-JNK, and why we did not observe any toxicity with SP600125. The high-fat high-cholesterol diet seemed to worsen the observed kidney-specific toxicity.

In vivo JNK inhibition with SP600125 induces beneficial JNK2-dependent vascular effects similar to RYGB surgery

8-day treatment of DIO sham-operated ad libitum-fed rats with SP600125 tended to improve endothelium-mediated vasodilation in response to GLP-1 and insulin similar to RYGB surgery, although the difference to controls$_{DMSO}$ rats was not significant (SOM Fig. 6). *In vivo* SP600125 treatment also decreased aortic JNK2 and IRS-1 ser307 phosphorylation and increased Akt ser473 phosphorylation and eNOS dimerization similar to RYGB surgery and D-JNK (SOM Fig. 7). Additionally, *in vivo* SP600125 treatment also decreased aortic NADPH activity and anion superoxide levels similar to RYGB surgery (SOM Fig. 8A-B). Interestingly, SP600125 did not affect circulating GLP-1 levels (SOM Fig. 8C). These results with a different JNK inhibitor independently demonstrate the direct role of vascular JNK2 inactivation in decreasing oxidative stress and in activating eNOS signalling pathways that lead to improved endothelial function after RYGB surgery.

RYGB surgery decreases hepatic JNK1 activation

We observed increased activation of JNK1, but not JNK2, in the livers of DIO vs. chow-fed rats (SOM Fig. 9A). RYGB specifically reduced hepatic JNK1 activation 8 days after surgery compared with controls$_{D\text{-}TAT}$ and D-JNK rats; D-JNK had no effect compared to controls$_{D\text{-}TAT}$ (SOM Fig. 9B).

In vivo treatment with a GLP-1 analogue and a GLP-1 receptor antagonist seem to regulate JNK signalling in aorta

We previously treated sham-operated rats with the GLP-1 analogue liraglutide, and RYGB-operated rats with the GLP-1 receptor antagonist exendin-9 for 8 days post-surgery; *in vivo*

liraglutide treatment mimicked, and *in vivo* exendin-9 treatment blocked the improved endothelial function after RYGB.[2] To investigate whether GLP-1 receptor signalling regulates JNK isoform activation in aorta, we specifically looked at aortic JNK1 and JNK2 activation in the liraglutide- and exendin-9-treated rats from our previous study.[2] *In vivo* liraglutide treatment seemed to mimic the effect of RYGB on JNK2 inactivation in sham-operated rats, while *in vivo* exendin-9 treatment blunted this effect in RYGB-operated rats (SOM Fig. 10).

Supplementary figure legends

SOM Figure 1.

Experimental design of animal experiments. After 7 weeks of high fat high cholesterol diet, male Wistar rats underwent RYGB or sham surgery, and were sacrificed 8 days later for *ex vivo* endothelial function experiments. (**A**) RYGB-operated rats, sham-operated ad libitum-fed rats treated with the JNK inhibitor D-JNK, and control sham-operated rats treated with the control peptide D-TAT for 8 days post-surgery. (**B**) RYGB-operated rats, sham-operated ad libitum-fed rats treated with the JNK inhibitor SP600125, and control sham-operated rats treated with vehicle (DMSO) for 8 days post-surgery.

SOM Figure 2.

(A) 24-hour food intake and **(B)** body weight of AL, RYGB and SP rats before and after surgery and start of treatment (surgery/start of treatment was on day 0). **(C)** Body weight of non-operated, chow-fed rats treated with D-TAT and D-JNK for 8 days (n=4 per group)**. (D)** 24-hour food intake and **(E)** body weight of controls$_{D\text{-}TAT}$, RYGB and D-JNK rats before and after surgery and start of treatment (*, **, *** $p<0.05$, $p<0.01$, $p<0.001$ RYGB vs AL, SP,

and controls$_{D\text{-}TAT}$, $^{\&\&\&}$p<0.001 RYGB vs. D-JNK, $^{\circ\circ\circ}$ D-JNK vs. controls$_{D\text{-}TAT}$, n=8-13 per group). Results are shown as mean ± SD.

SOM Figure 3.

Histological analysis (hematoxylin and eosin stain) of the kidney from a **(A)** D-JNK rat and a **(B)** controls$_{D\text{-}TAT}$ rat euthanized 8 days after sham surgery/start of treatment. Representative micrographs of **severe** (A) and **moderate** (B) nephrotoxicity are shown, characterized by variable combinations of degenerating/necrotic (arrows) and regenerating (open arrows) tubules and interstitial inflammation (arrowheads). Only very few unaffected tubules (N) are displayed in A. Glomeruli (G) are unaltered in both examples.

SOM Figure 4.

24-hour urine excretion in **(A)** controls$_{D\text{-}TAT}$ rats and **(B)** D-JNK rats, and 24-hour water intake in **(C)** controls$_{D\text{-}TAT}$ rats and **(D)** D-JNK rats 1 day before and 7 and 8 days after surgery and start of treatment (#, ##, ### p<0.05, p<0.01, p<0.001 Day -1 vs. Day 7 and Day 8, n=6 per group). qPCR analysis of kidney expression of **(E)** KIM-1 and **(F)** NGAL 8 days after surgery and start of treatment ($^{\circ}$, $^{\circ\circ\circ}$ p<0.05, p<0.001 D-JNK vs. all other groups, n=4-7 per group). Results are shown as mean ± SD.

SOM Figure 5.

Ex vivo relaxation of aortic rings isolated 8 days after RYGB or sham surgery and start of treatment. Concentration–response curves after 30 min pre-incubation with 10^{-4} mol/L L-NAME and submaximal contraction to norepinephrine (NE) in response to **(A)** GLP-1 and **(B)**

insulin in controls$_{D\text{-}TAT}$, RYGB, and D-JNK rats (n=3 per group). Results are shown as mean ± SD.

SOM Figure 6.

Concentration–response curves after submaximal contraction to NE in response to **(A)** GLP-1 and **(B)** insulin in RYGB, controls$_{DMSO}$, and SP600125 rats (*, **, *** $p<0.05$, $p<0.01$, $p<0.001$ RYGB vs. controls$_{DMSO}$, $^{\&\&, \&\&\&}$ $p<0.01$, $p<0.001$ RYGB vs. SP600125, n=5-10 per group). Results are shown as mean ± SD.

SOM Figure 7.

Aortic **(A)** JNK1 and JNK2 phosphorylation, **(B)** IRS-1 ser307, **(C)** Akt ser473, **(D)** eNOS ser1177 phosphorylation and **(E)** eNOS dimerization in controls$_{DMSO}$, RYGB, and SP600125 rats 8 days after surgery/start of treatment. Representative Western blots and densitometric quantification are shown (*, **, *** $p<0.05$, $p<0.01$, $p<0.001$ RYGB vs. controls$_{DMSO}$, §, §§ $p<0.05$, $p<0.01$ controls$_{DMSO}$ vs. SP600125, n=5-11 per group). Results are shown as mean ± SD.

SOM Figure 8.

(A) *In vitro* dihydroethidium fluorescent staining of superoxide anions and relative quantification in aorta isolated from controls$_{DMSO}$, RYGB and SP600125 rats 8 days after surgery/start of treatment. Representative pictures are shown. **(B)** *In vitro* NADPH oxidase activity in aorta isolated 8 days after surgery from controls$_{DMSO}$, RYGB, and SP600125 rats. **(C)** Fasting plasma GLP-1 levels in controls$_{DMSO}$, RYGB, and SP600125 rats 8 days after

surgery/start of treatment (* $p<0.05$ RYGB vs. all other groups, § $p<0.05$ $controls_{DMSO}$ vs. SP600125, n=6-16 per group). Results are shown as mean ± SD.

SOM Figure 9.

Hepatic JNK1 and JNK2 phosphorylation in **(A)** normal chow-fed vs. DIO rats; **(B)** $controls_{D\text{-}TAT}$, RYGB, and D-JNK rats 8 days after surgery/start of treatment. Representative Western blots and densitometric quantification are shown (¢ $p<0.05$ normal chow vs. DIO, * $p<0.05$ RYGB vs. all other groups, n=4-13 per group). Results are shown as mean ± SD.

SOM Figure 10.

Aortic JNK1 and JNK2 phosphorylation in sham-operated rats treated with vehicle (controls) or liraglutide 0.2 mg/kg b.i.d. s.c. ($controls_{\text{-lira}}$) and RYGB-operated rats treated with vehicle (RYGB) or exendin-9 10 $\mu g \cdot kg^{-1} \cdot h^{-1}$ ($RYGB_{\text{-exe9}}$) 8 days after surgery and start of treatment; tissues were taken from rats of a previous study.[2] Representative Western blots and densitometric quantification are shown (** $p<0.05$ RYGB vs. all other groups, n=6-8 per group). Results are shown as mean ± SD.

Supplementary references

1. Cardozo AK, Buchillier V, Mathieu M, Chen J, Ortis F, Ladriere L, Allaman-Pillet N, Poirot O, Kellenberger S, Beckmann JS, Eizirik DL, Bonny C, Maurer F. Cell-permeable peptides induce dose- and length-dependent cytotoxic effects. *Biochimica et biophysica acta*. 2007;1768:2222-2234
2. Osto E, Doytcheva P, Corteville C, Bueter M, Dorig C, Stivala S, Buhmann H, Colin S, Rohrer L, Hasballa R, Tailleux A, Wolfrum C, Tona F, Manz J, Vetter D, Spliethoff K, Vanhoutte PM, Landmesser U, Pattou F, Staels B, Matter CM, Lutz TA, Luscher TF. Rapid and body weight-independent improvement of endothelial and high-density lipoprotein function after roux-en-y gastric bypass: Role of glucagon-like peptide-1. *Circulation*. 2015;131:871-881

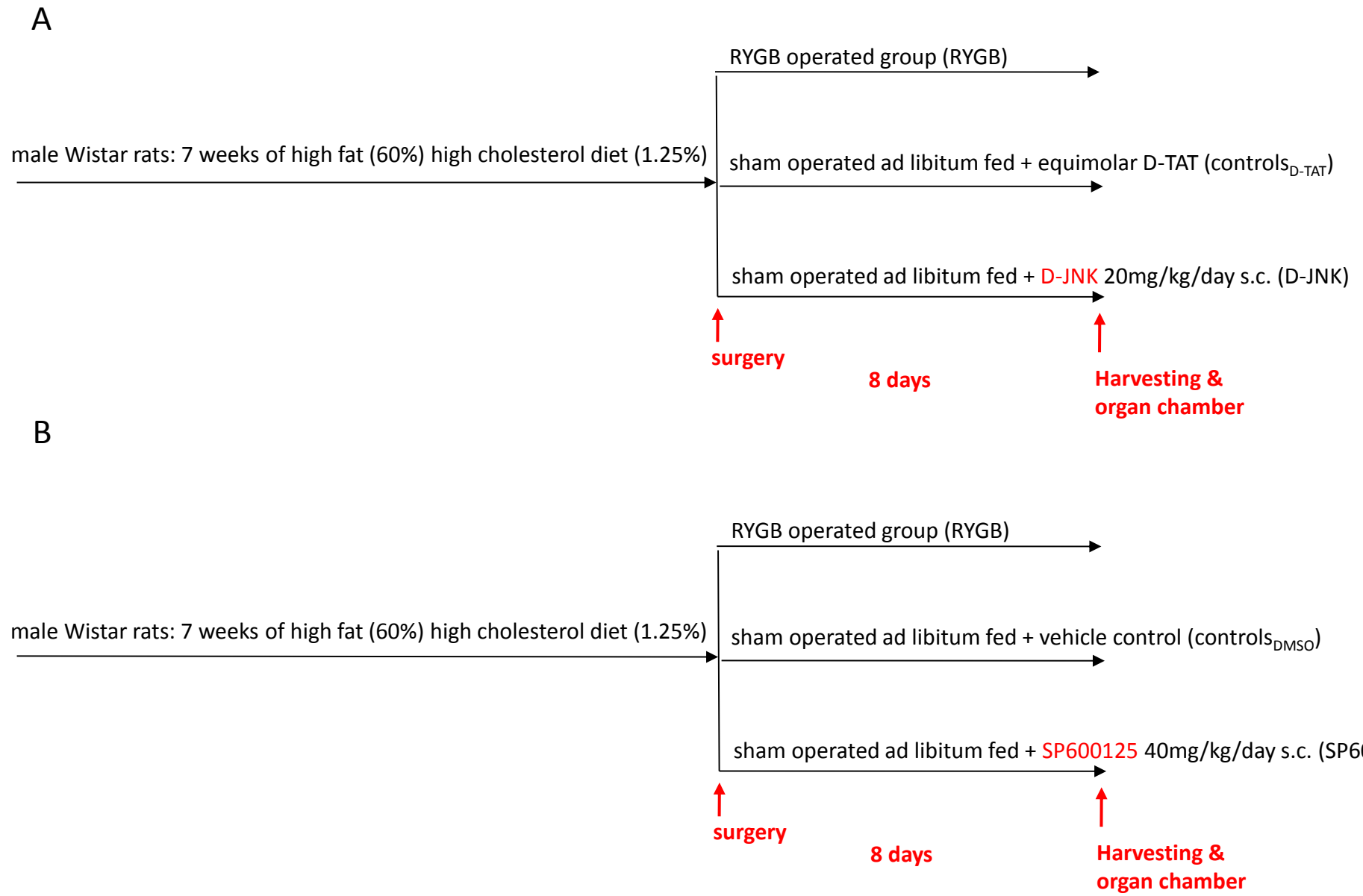
A
RYGB operated group (RYGB)
male Wistar rats: 7 weeks of high fat (60%) high cholesterol diet (1.25%)
sham operated ad libitum fed + equimolar D-TAT (controls$_{D-TAT}$)
sham operated ad libitum fed + D-JNK 20mg/kg/day s.c. (D-JNK)
surgery
8 days
Harvesting & organ chamber
B
RYGB operated group (RYGB)
male Wistar rats: 7 weeks of high fat (60%) high cholesterol diet (1.25%)
sham operated ad libitum fed + vehicle control (controls$_{DMSO}$)
sham operated ad libitum fed + SP600125 40mg/kg/day s.c. (SP600125)
surgery
8 days
Harvesting & organ chamber

SOM Fig. 1

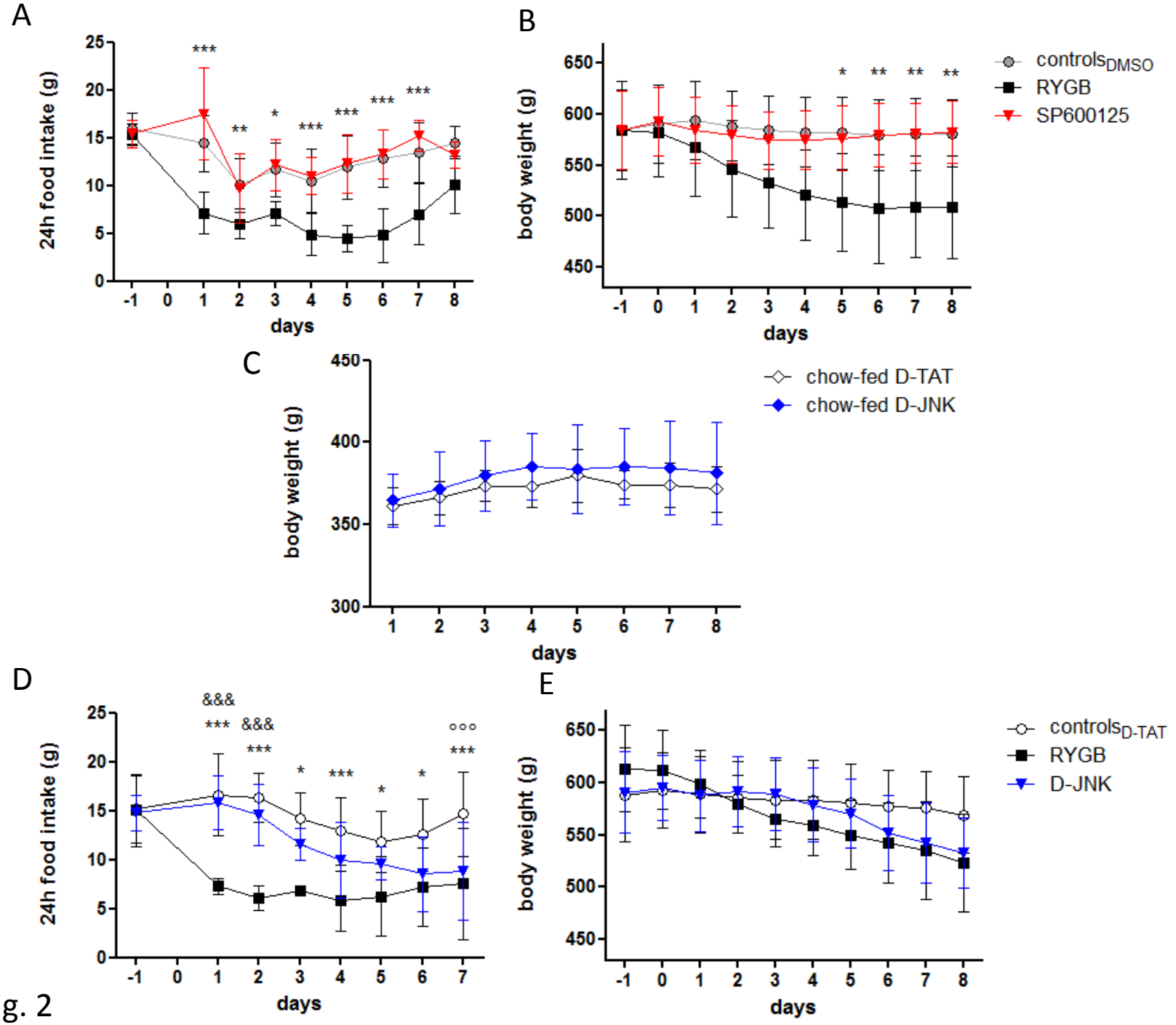
A
24h food intake (g)
days
B
body weight (g)
days
controls$_{DMSO}$
RYGB
SP600125
C
body weight (g)
days
chow-fed D-TAT
chow-fed D-JNK
D
24h food intake (g)
days
E
body weight (g)
days
controls$_{D-TAT}$
RYGB
D-JNK

SOM Fig. 2

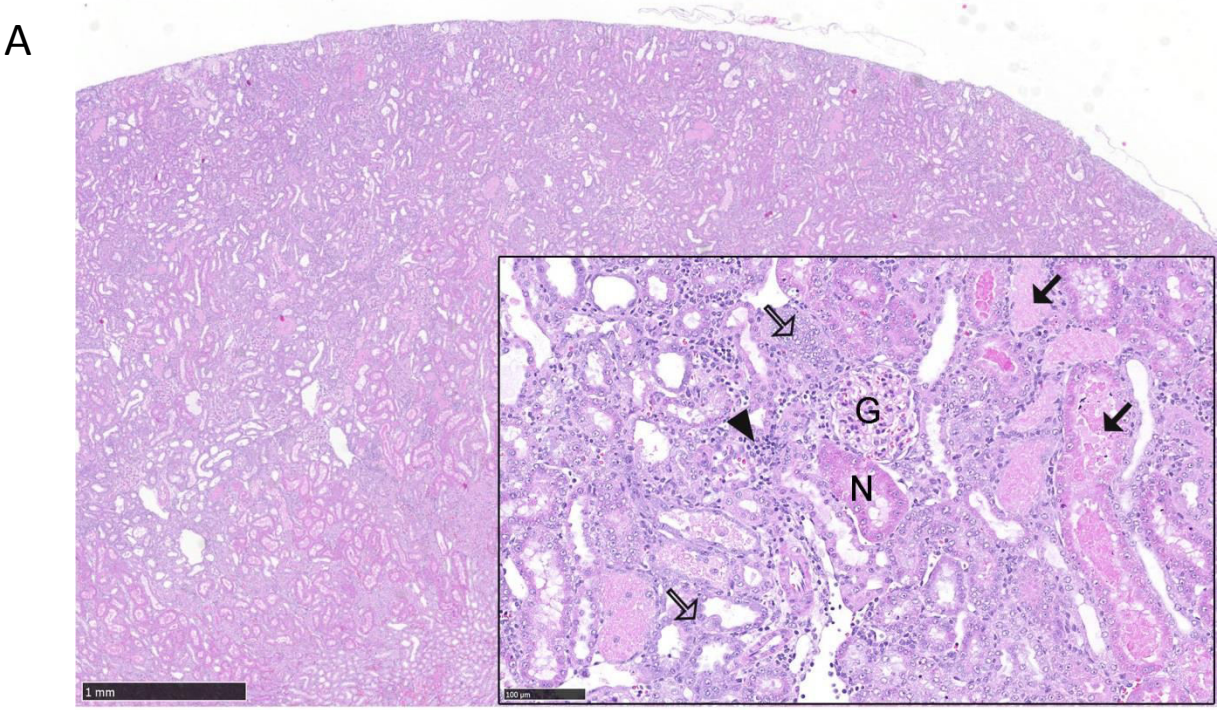

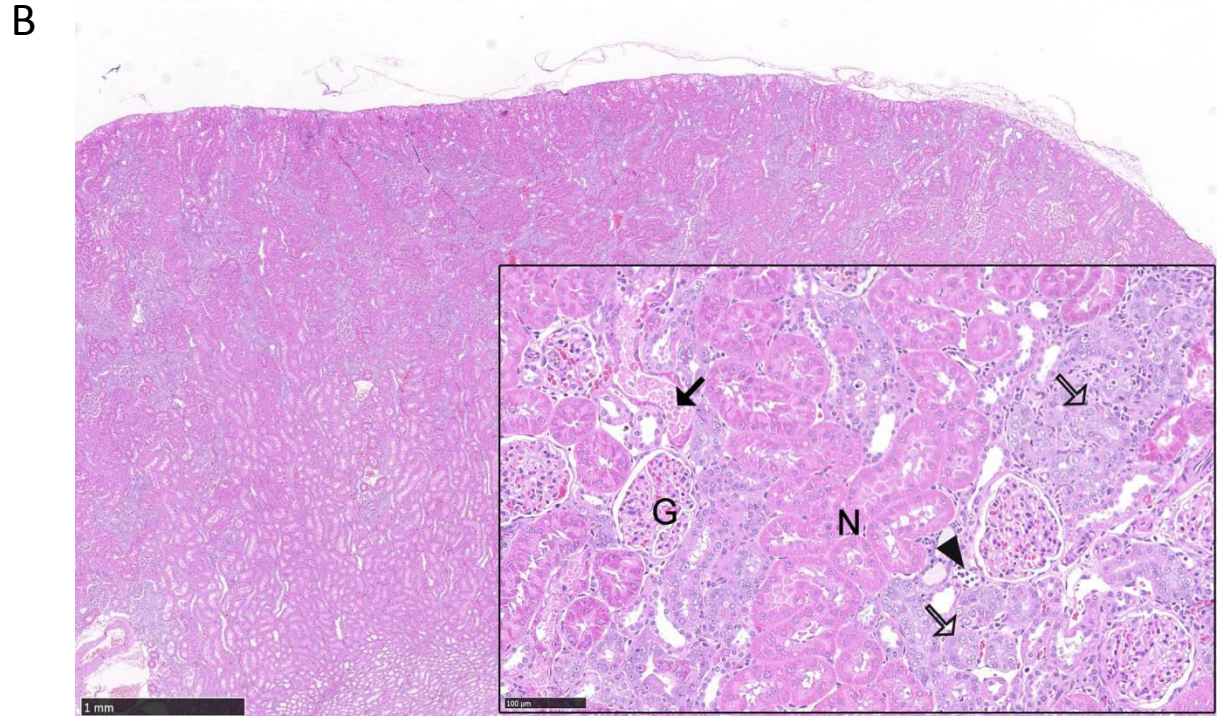

SOM Fig. 3

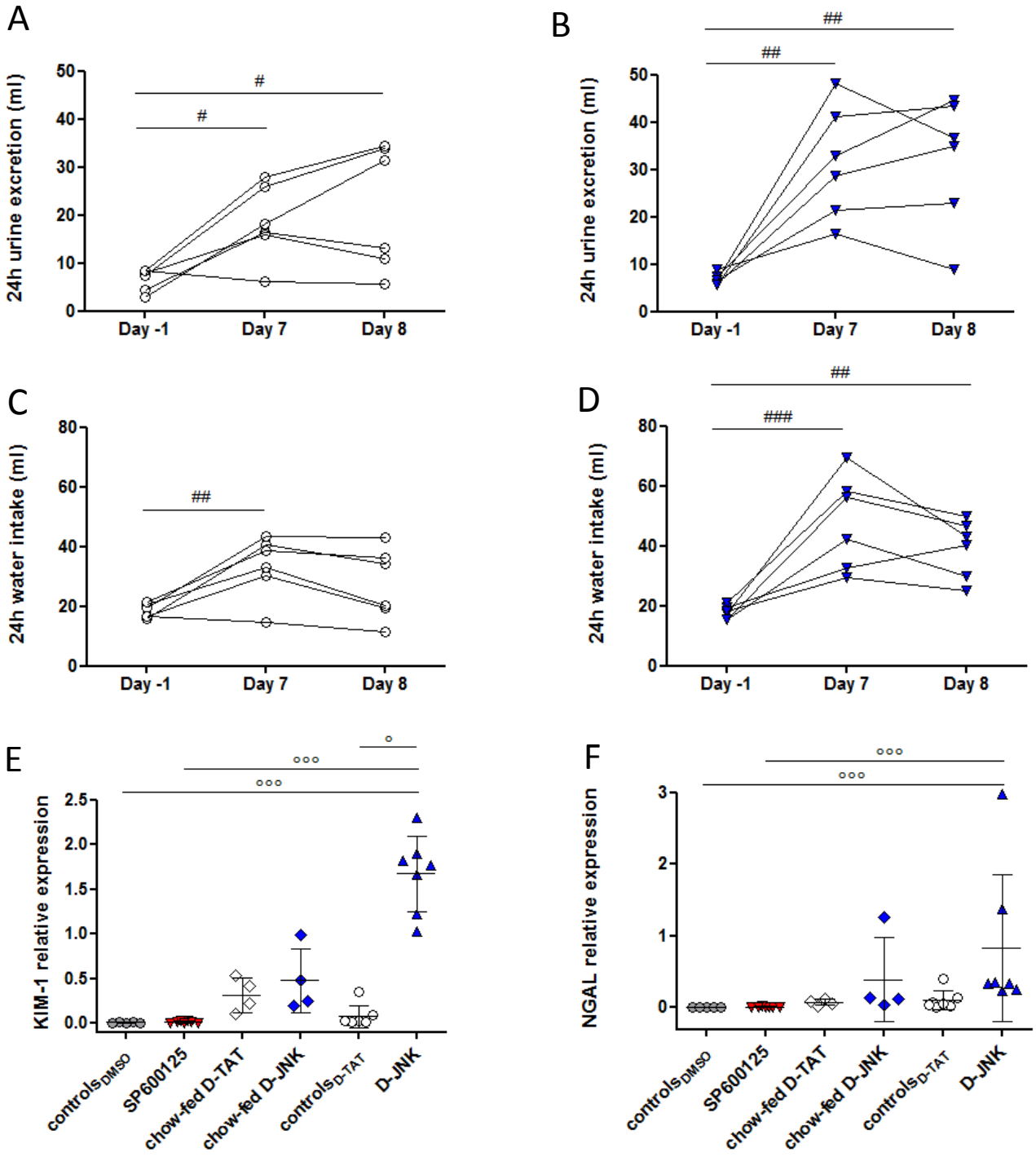
A
24h urine excretion (ml)
Day -1
Day 7
Day 8
#
#
B
24h urine excretion (ml)
##
##
C
24h water intake (ml)
##
D
24h water intake (ml)
###
##
E
KIM-1 relative expression
°°°
°°°
F
NGAL relative expression
°°°
°°°
controls DMSO
SP600125
chow-fed D-TAT
chow-fed D-JNK
controls D-TAT
D-JNK

SOM Fig. 4

A

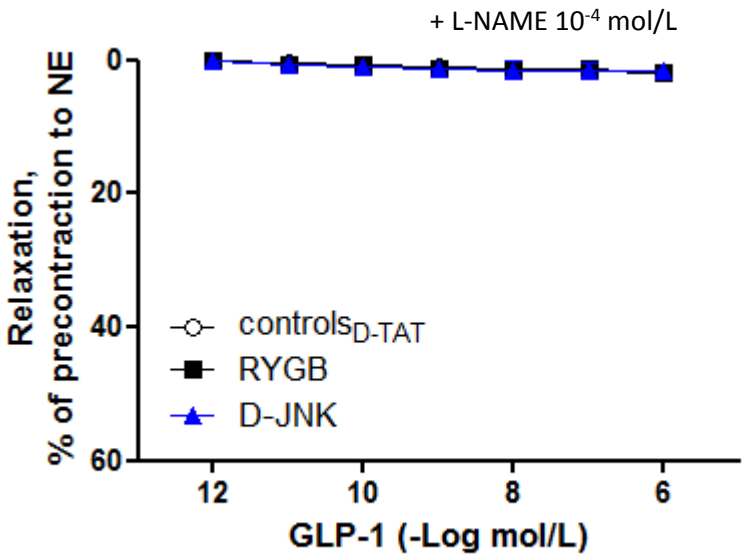
+ L-NAME 10-4 mol/L
Relaxation, % of precontraction to NE
0
20
40
60
12
10
8
6
GLP-1 (-Log mol/L)
controlsD-TAT
RYGB
D-JNK

B

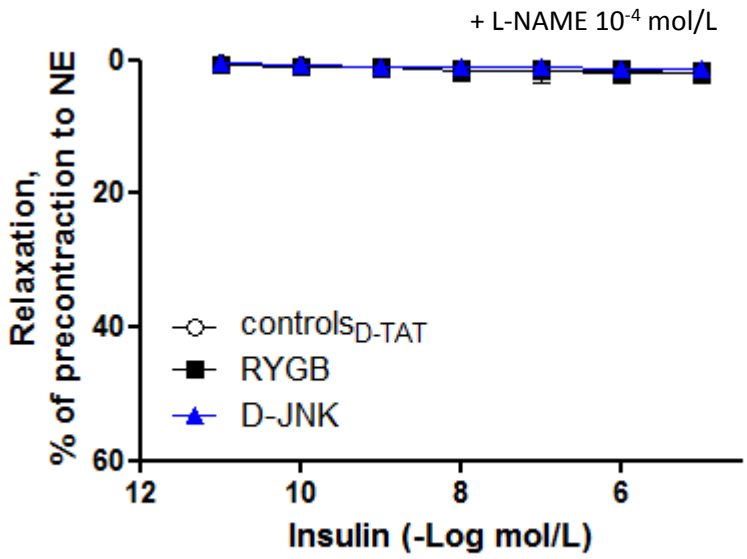
+ L-NAME 10-4 mol/L
Relaxation, % of precontraction to NE
0
20
40
60
12
10
8
6
Insulin (-Log mol/L)
controlsD-TAT
RYGB
D-JNK

SOM Fig. 5

A

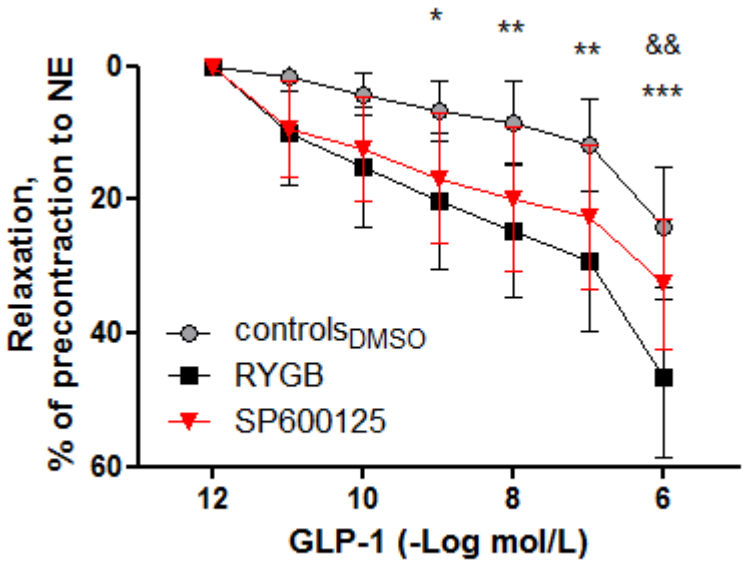
Relaxation,
% of precontraction to NE
0
20
40
60
12
10
8
6
GLP-1 (-Log mol/L)
controls$_{DMSO}$
RYGB
SP600125
*
**
**
&&
***

B

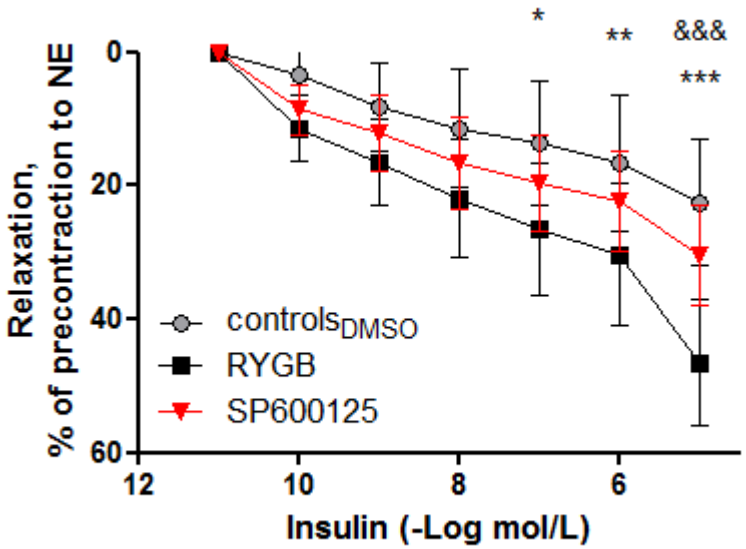
Relaxation,
% of precontraction to NE
0
20
40
60
12
10
8
6
Insulin (-Log mol/L)
controls$_{DMSO}$
RYGB
SP600125
*
**
&&&
***

SOM Fig. 6

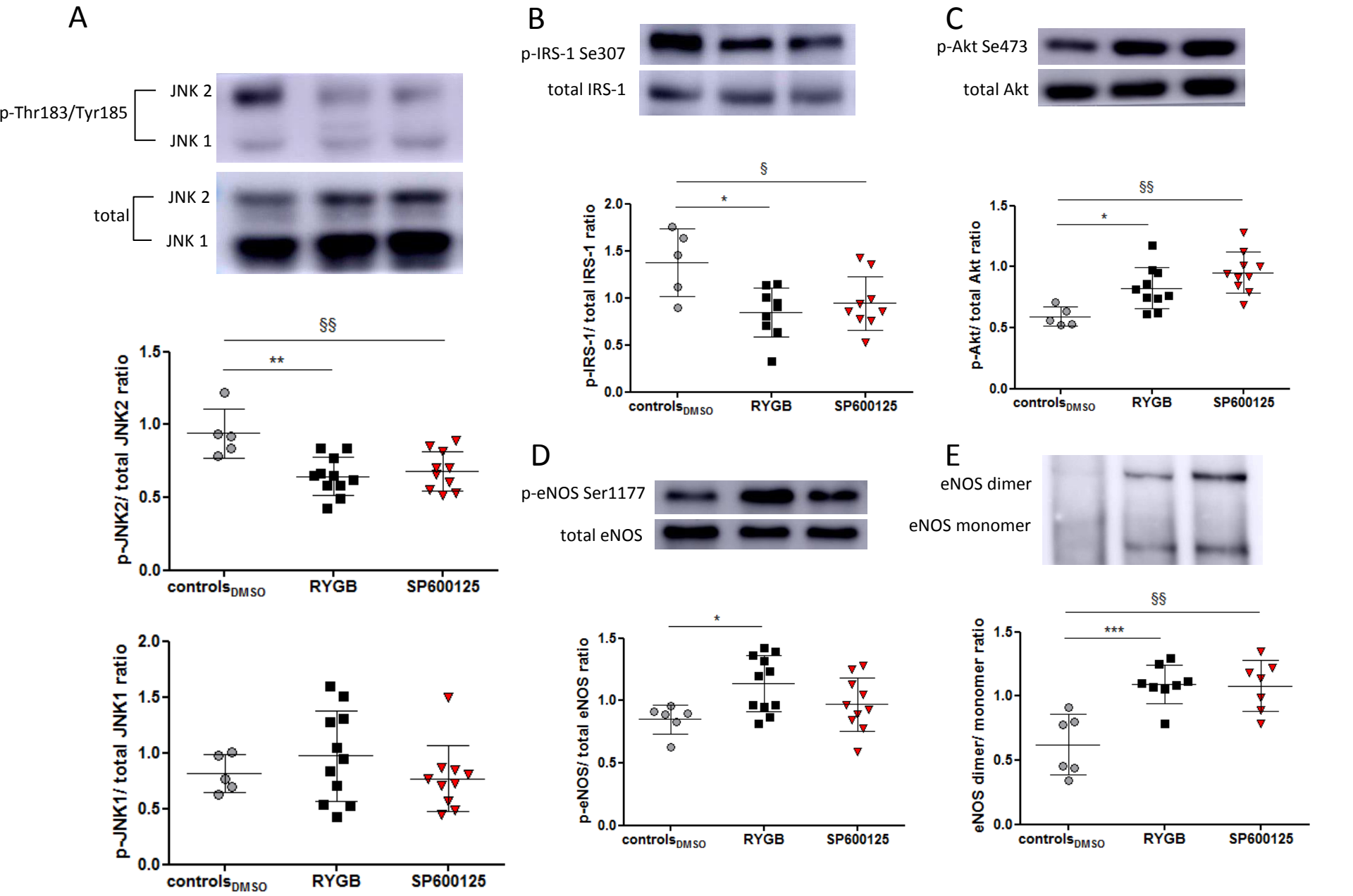
A
p-Thr183/Tyr185
JNK 2
JNK 1
total
JNK 2
JNK 1
p-JNK2/ total JNK2 ratio
§§
**
controls DMSO
RYGB
SP600125
p-JNK1/ total JNK1 ratio
controls DMSO
RYGB
SP600125
B
p-IRS-1 Se307
total IRS-1
p-IRS-1/ total IRS-1 ratio
§
*
controls DMSO
RYGB
SP600125
C
p-Akt Se473
total Akt
p-Akt/ total Akt ratio
§§
*
controls DMSO
RYGB
SP600125
D
p-eNOS Ser1177
total eNOS
p-eNOS/ total eNOS ratio
*
controls DMSO
RYGB
SP600125
E
eNOS dimer
eNOS monomer
eNOS dimer/ monomer ratio
§§
***
controls DMSO
RYGB
SP600125

SOM Fig. 7

A

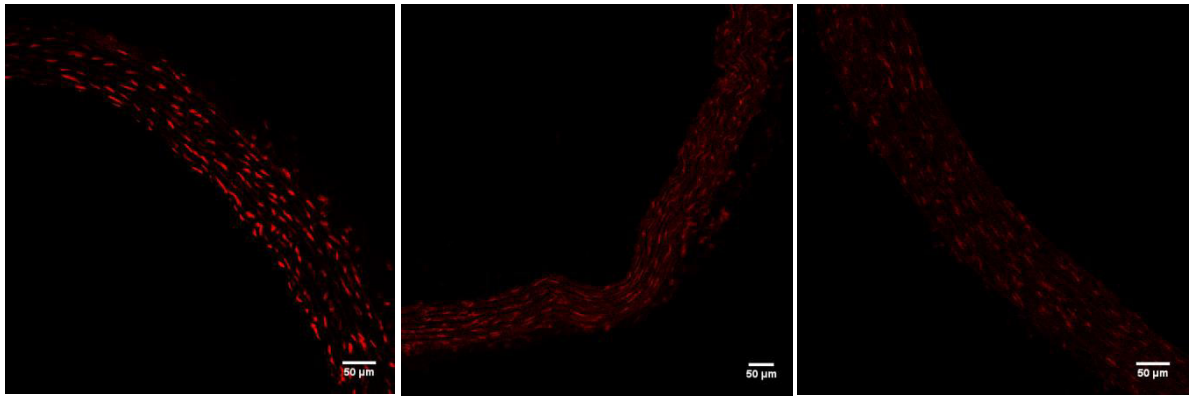

AL RYGB SP

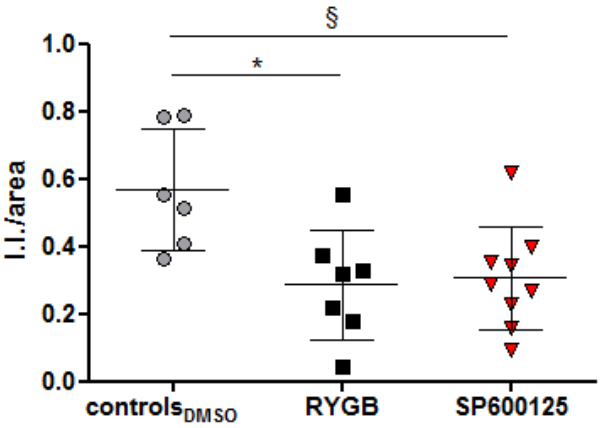

B

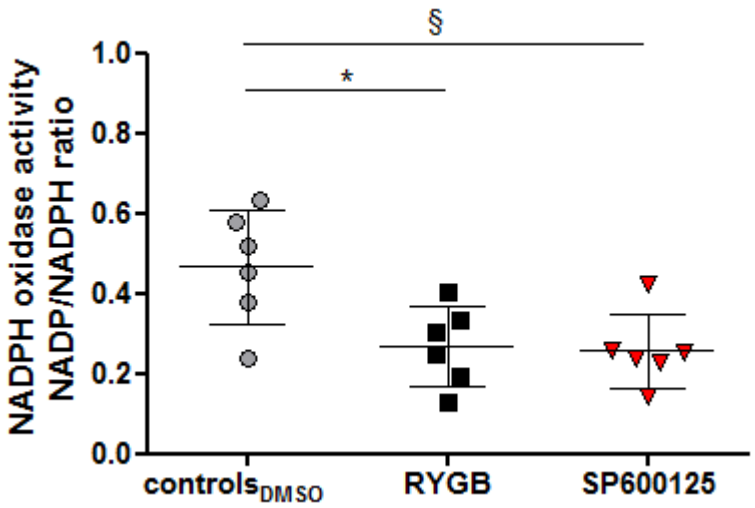

C

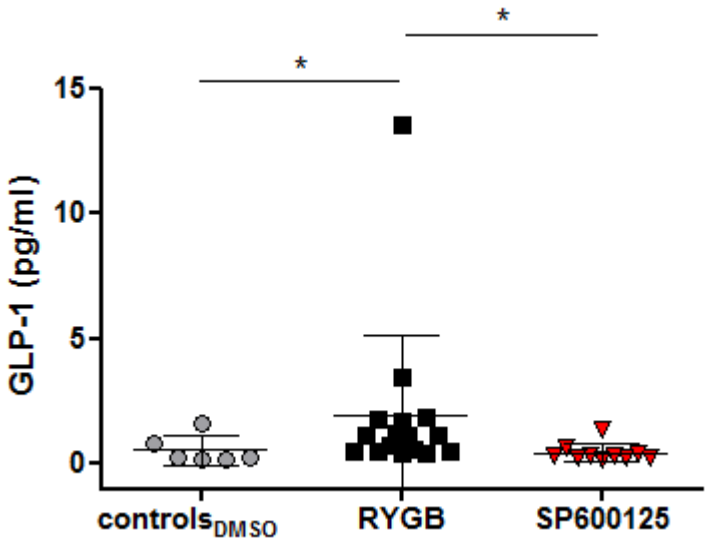

SOM Fig. 8

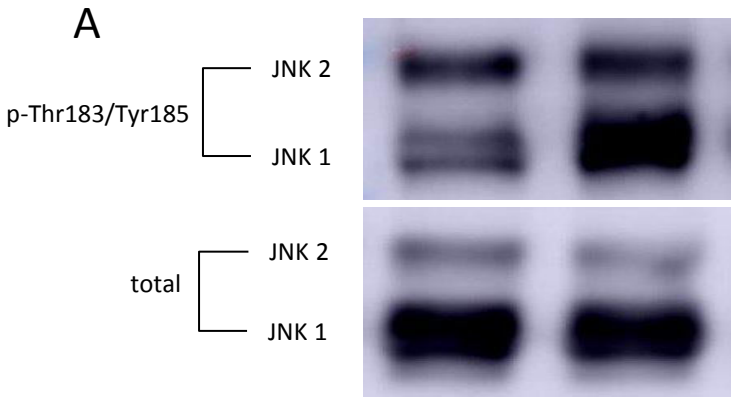
A
p-Thr183/Tyr185
JNK 2
JNK 1
total
JNK 2
JNK 1

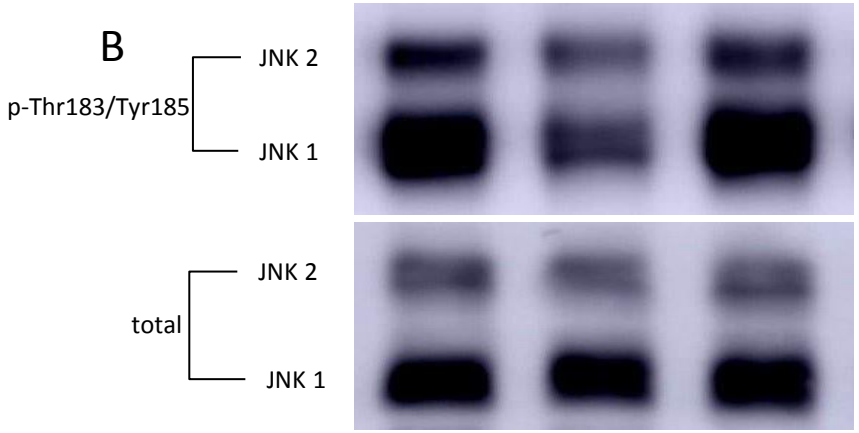
B
p-Thr183/Tyr185
JNK 2
JNK 1
total
JNK 2
JNK 1

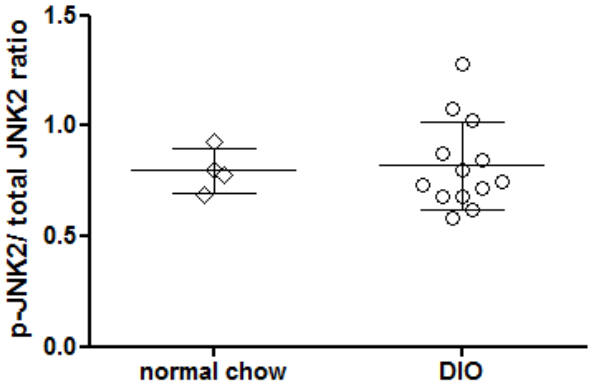
p-JNK2/ total JNK2 ratio
1.5
1.0
0.5
0.0
normal chow
DIO

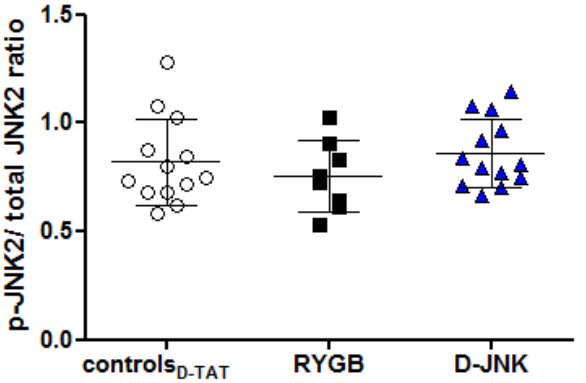
p-JNK2/ total JNK2 ratio
1.5
1.0
0.5
0.0
controls D-TAT
RYGB
D-JNK

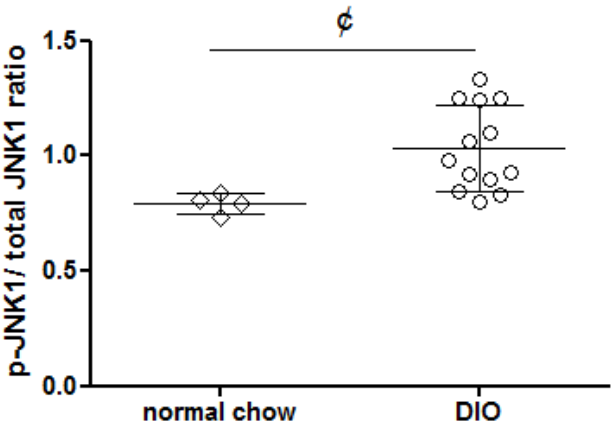
¢
p-JNK1/ total JNK1 ratio
1.5
1.0
0.5
0.0
normal chow
DIO

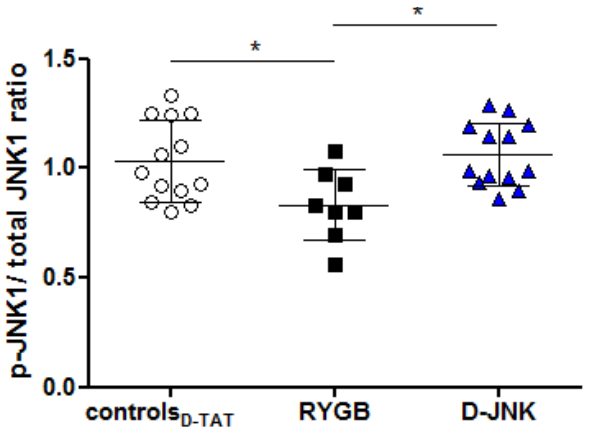
*
*
p-JNK1/ total JNK1 ratio
1.5
1.0
0.5
0.0
controls D-TAT
RYGB
D-JNK

SOM Fig. 9

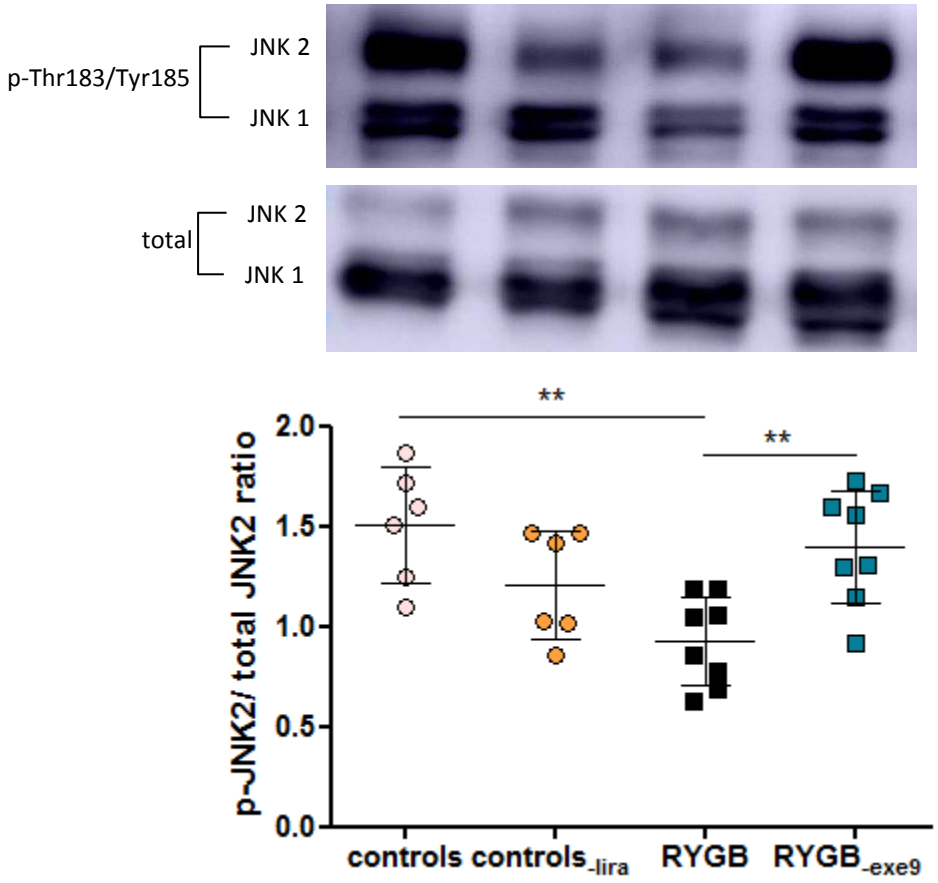
p-Thr183/Tyr185
JNK 2
JNK 1
total
JNK 2
JNK 1
**
**
p-JNK2/ total JNK2 ratio
2.0
1.5
1.0
0.5
0.0
controls
controls-lira
RYGB
RYGB-exe9
p-JNK1/ total JNK1 ratio
2.0
1.5
1.0
0.5
0.0
controls
controls-lira
RYGB
RYGB-exe9

SOM Fig. 10

6. Discussion

We investigated the rapid and weight loss-independent effects of RYGB on endothelial function and HDL endothelial protective properties in obesity, and the underlying molecular mechanisms. Using a rat model of diet induced-obesity, we showed that: 1.) RYGB improves endothelial-mediated vasodilation and HDL endothelial protective properties within 8 days in a weight-loss independent manner; 2.) the effects on vasodilation in the aorta are mediated by GLP-1 in a GLP-1 receptor- and JNK2-dependent mechanisms; 3.) some effects on HDL endothelial protective properties are likely mediated by a GLP-1-dependent, but GLP-1 receptor-independent mechanism.

6.1 RYGB improves endothelial function rapidly and independently of weight loss

Obesity is characterized by a systemic chronic inflammation, oxidative stress, and insulin resistance, which are crucial mechanisms contributing to endothelial dysfunction [73, 120]. Insulin signalling in the vasculature leads to activation of eNOS, which is the critical enzyme responsible for vasodilatory NO production [71, 121-123]. Therefore, obesity-induced vascular insulin resistance impairs eNOS activation, NO production, and blood vessel dilation [73, 122-124]. In addition, oxidative stress, which is characterized by increased levels of reactive oxygen species such as anion superoxide, also contributes to impaired blood vessel dilation by depleting NO; the anion superoxide radical reacts with NO to form peroxynitrite, and therefore decreases functional NO levels [72, 73, 125]. The resulting endothelial dysfunction is a major pathology contributing to the development of cardiovascular diseases such as atherosclerosis and hypertension [71, 72, 124]. Therefore, obesity-induced oxidative stress, vascular insulin resistance, and endothelial dysfunction are crucial mechanisms underlying the development of obesity-associated cardiovascular disease.

In the present study we show that RYGB surgery ameliorates vascular insulin resistance, oxidative stress, and endothelial dysfunction in diet-induced obese rats. Compared to sham-operated ad libitum-fed controls, RYGB induced aortic activation of Akt, an upstream activator of eNOS [71, 121-123], and activation of eNOS itself; in addition, RYGB decreased anion superoxide levels and increased NO in aortic tissue. *Ex vivo* endothelial function experiments with thoracic aorta demonstrated that RYGB surgery improved GLP-1- and insulin-mediated vasodilation (Fig. 5A-B); this improvement was eNOS-dependent as it was

blocked by the eNOS inhibitor Nω-nitro-L-arginine methyl ester (L-NAME). All of the these effects occurred rapidly within 8 days after surgery, and in a weight loss-independent manner as they were not observed in sham-operated rats body weight-matched to the RYGB rats. Therefore, RYGB surgery leads to improved endothelial function by activating eNOS signalling pathways, decreasing reactive oxygen species, and increasing NO in a weight loss-independent manner.

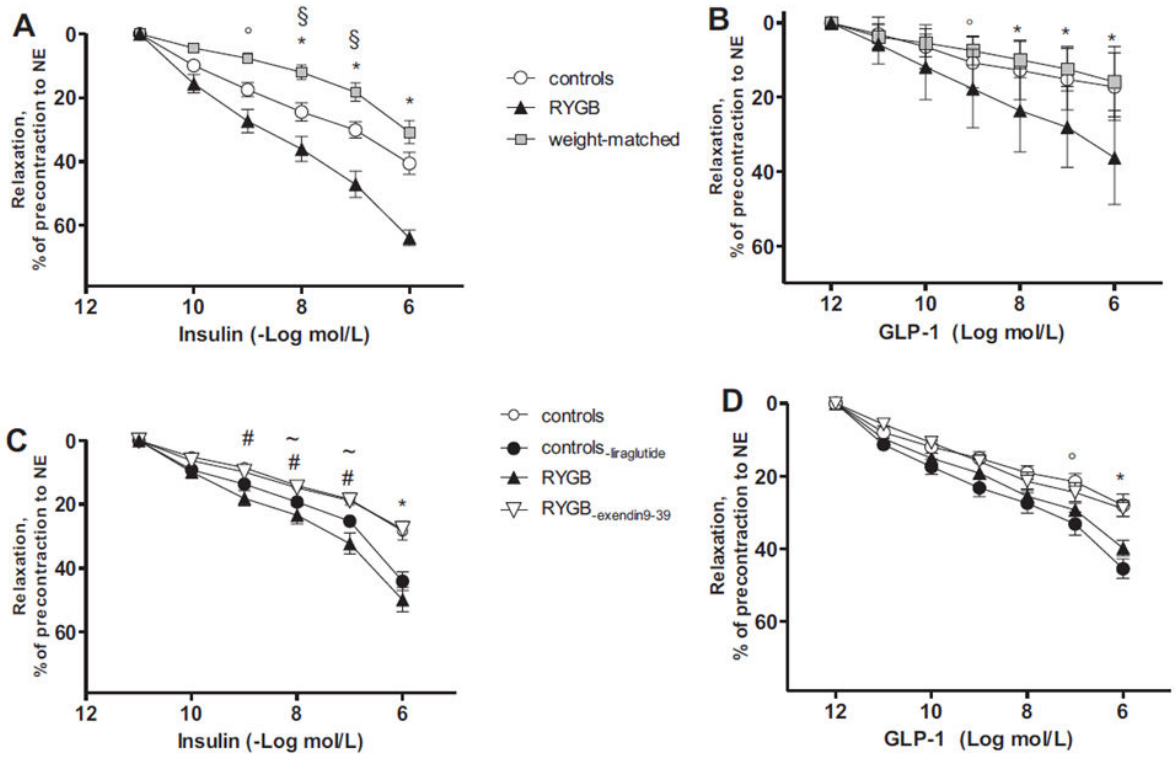

Fig. 5. ***Ex vivo*** **endothelial-mediated vasodilation of RYGB- and sham-operated rats 8 days after surgery. (A)** Insulin- and **(B)** GLP-1-induced vasodilation in RYGB and sham ad libitum-fed and body-weight matched controls (*Sham-operated rats vs RYGB, §controls vs weight-matched, °RYGB vs weight matched, P<0.05). **(C)** Insulin- and **(D)** GLP-1-induced vasodilation in RYGB rats treated with exendin-9 or vehicle, and sham rats treated with liraglutide or vehicle (#RYGB vs controls, ~RYGB vs RYGB-exendin9-39, °controls-liraglutide vs controls, *controls-liraglutide and RYGB vs other study groups P<0.05; n=6 to 8 per group).

6.1.1 Role of GLP-1 in mediating the effects of RYGB on endothelial function

Postprandial GLP-1 levels quickly rise after RYGB surgery and GLP-1 has been shown to mediate some of the weight-independent effects of RYGB on improved glucose metabolism, insulin sensitivity, and type 2 diabetes remission in obese patients [86, 89-92, 95-100]. Fasting plasma GLP-1 levels were increased rapidly and independently of weight loss in our rat RYGB model. Therefore, we hypothesized that increased GLP-1 levels might also mediate the rapid and weight-independent improvements in endothelial function after RYGB. To test this hypothesis, we treated obese sham-operated rats with the GLP-1 analogue liraglutide, and RYGB-operated rats with the GLP-1 receptor antagonist exendin-9 *in vivo* for 8 days after surgery. *In vivo* treatment of sham-operated rats with liraglutide improved GLP-1- and insulin-mediated vasodilation to the same extent like RYGB surgery, while *in vivo* treatment of RYGB-operated rats with exendin-9 blocked this improvement in endothelial function (Fig. 5C-D). These results were accompanied by respective activation/inhibition of Akt and eNOS, decreased/increased levels of anion superoxide, and increased/decreased levels of NO. Therefore, this experiment suggests that GLP-1 agonism is able to mimic the beneficial effects of RYGB on endothelial function in a GLP-1 receptor-dependent and body weight loss-independent mechanism. Indeed, we observed increased aortic expression of the GLP-1 receptor in RYGB rats compared to both sham-operated control rats and sham-operated rats body weight-matched to RYGB. Vascular activation of the GLP-1 receptor can lead to activation of Akt and eNOS and vasodilation [126-129]. Therefore, the rapid and weight-independent increase in GLP-1 levels after RYGB surgery could activate the endothelial GLP-1 receptor and downstream Akt and eNOS, leading to increased NO levels and improved vasodilation.

6.1.2 Role of JNK2 in mediating the effects of RYGB on endothelial function

In addition to activation of the vascular GLP-1-eNOS signalling pathway after RYGB, we also observed decreased activation of JNK, which is known to mediate insulin resistance in obesity by inhibiting IRS-1 of the insulin signalling pathway [110-112]; vascular JNK can also inhibit eNOS itself [117]. In addition, it has been shown that GLP-1 signalling can inhibit JNK in variety of tissues via activation of PKA and the transcription factor CREB [130-134]. Therefore, we hypothesized that vascular JNK inhibition also mediates the rapid and weight-independent beneficial effects of RYGB on endothelial function. To test this hypothesis, we

treated obese sham-operated rats with two different JNK inhibitors *in vivo* for 8 days after surgery. *In vivo* treatment of sham-operated rats with the SP600125 inhibitor tended to improve GLP-1- and insulin-mediated vasodilation in a weight loss-independent manner, while treatment with the D-JNK inhibitor completely mimicked the effect of RYGB surgery on improved vasodilation (Fig. 6). These results were accompanied by increased activation of Akt and eNOS and decreased levels of anion superoxide in both D-JNK- and SP600125-treated rats similar to RYGB surgery. Both RYGB surgery and *in vivo* JNK inhibition with D-JNK and SP600125 specifically decreased aortic activation of JNK2 and inhibitory phosphorylation of IRS-1 at ser307, the direct downstream target of JNK in the insulin signalling pathway [110, 112]. Therefore, this experiment suggests that specific JNK2 inhibition mediates the beneficial effects of RYGB on endothelial function by activating the vascular insulin signalling pathway that also leads to Akt and eNOS activation and vasodilation [71, 121-123]. As previously mentioned, GLP-1 signalling can inhibit JNK via activation of PKA and CREB [130-134]. Interestingly, while SP600125 treatment did not affect circulating GLP-1 levels in sham-operated rats, D-JNK treatment increased GLP-1 levels similar to RYGB surgery. This increase in GLP-1 was accompanied by increased expression of the GLP-1 receptor and increased activation of PKA and CREB in the aorta in both RYGB-operated and D-JNK-treated rats. In addition, liraglutide treatment in sham-operated rats seemed to decrease aortic JNK2 activation, while exendin-9 treatment in RYGB-operated rats blocked this effect.

Therefore, the rapid and weight-independent increase in GLP-1 levels after RYGB surgery could activate the endothelial GLP-1 receptor and downstream PKA, leading to inhibition of JNK2 and downstream activation of IRS-1, Akt and eNOS, increased NO levels, decreased oxidative stress, and improved vasodilation.

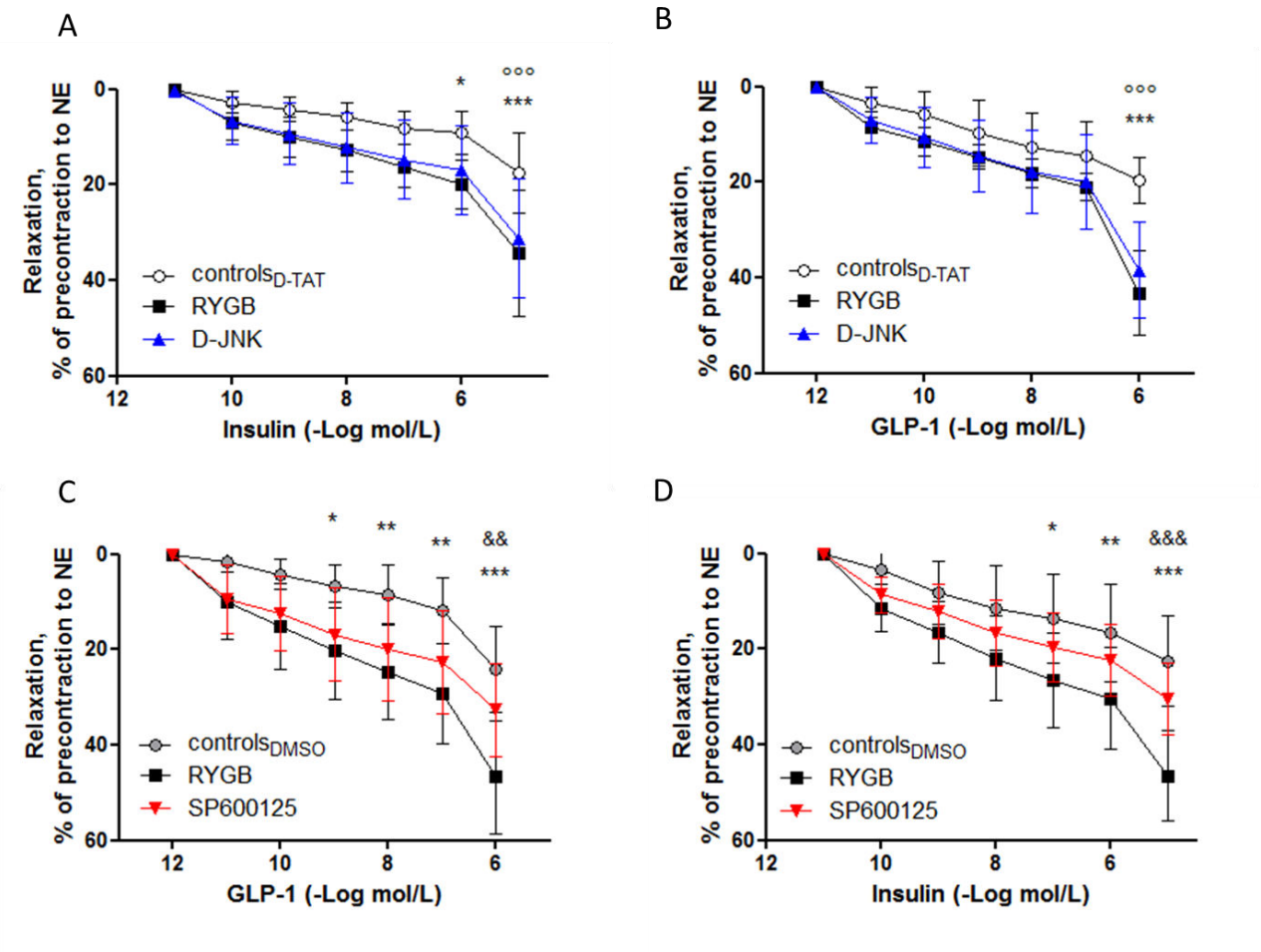

Fig. 6. *Ex vivo* endothelial-mediated vasodilation of RYGB and sham-operated rats 8 days after surgery and *in vivo* JNK inhibition. (A) Insulin- and **(B)** GLP-1-induced vasodilation in RYGB and sham rats treated with D-JNK or control peptide D-TAT (*, *** p<0.05, p<0.001 RYGB vs. $controls_{D\text{-}TAT}$, °°° p<0.001 $controls_{D\text{-}TAT}$ vs. D-JNK). **(C)** Insulin- and **(D)** GLP-1-induced vasodilation in RYGB and sham rats treated with SP600125 or vehicle (*, **, *** p<0.05, p<0.01, p<0.001 RYGB vs. $controls_{DMSO}$, &&, &&& p<0.01, p<0.001 RYGB vs. SP600125).

6.2 RYGB improves HDL properties rapidly and independently of weight loss

Obesity is also characterized by dyslipidemia, an imbalanced increase in triglycerides, total cholesterol, and pro-atherosclerotic LDL levels, and a decrease in anti-atherosclerotic HDL levels [15, 18]. In addition, pathological situations associated with obesity, in particular type 2 diabetes [135] and CAD [136], impair the physiological protective properties of HDL; hence, HDL's properties to preserve endothelial NO bioavailability and to promote vascular health are lost [64]. Once dysfunctional, HDL contributes to endothelial dysfunction [64]. Therefore, both endothelial dysfunction and altered HDL metabolism contribute to the increased

obesity-associated cardiovascular risk. The failure of HDL-raising treatments to prevent cardiovascular disease has highlighted the necessity to gain a deeper insight into HDL functioning in order to target HDL in a clinically relevant way to lower cardiovascular disease [64, 65]. Thus, assessing the properties of HDL is more informative than measuring HDL plasma levels alone [64].

In humans, RYGB is able to raise HDL levels and significantly ameliorate dyslipidemia [58-61]. We did not observe increased HDL levels in our rat RYGB model 8 days after surgery, but considering that functional HDL properties are more important than total HDL levels for cardiovascular health [64], we assessed the endothelial protective properties of HDL isolated from RYGB- and sham-operated rats using *in vitro* functional assays. Compared to sham-operated ad libitum-fed controls, RYGB surgery improved HDL cholesterol efflux capacity, HDL ability to stimulate endothelial NO production, and HDL anti-oxidative, anti-inflammatory, and anti-apoptotic properties. All of the these effects occurred rapidly within 8 days after surgery, and in a weight loss-independent manner as they were not observed in sham-operated rats body weight-matched to the RYGB rats. We also studied the role of increased GLP-1 levels in mediating the rapid and weight loss-independent effects of RYGB on endothelial protective HDL properties. *In vivo* treatment of sham-operated rats with liraglutide improved some of the HDL endothelial protective properties similar to RYGB surgery, while *in vivo* treatment of RYGB-operated rats with exendin-9 did not affect functional HDL properties. This result suggests that, unlike endothelial function, RYGB improves HDL functional properties in a GLP-1 receptor-independent mechanism. So far, cellular effects of GLP-1 independent from the classical GLP-1 receptor have been observed in several different organs, including the liver and the cardiovascular system, but the putative alternative GLP-1 receptors are still unknown [137]. Therefore, it is possible that some of the effects of RYGB surgery on HDL function are mediated by GLP-1 through a mechanism independent from the classical GLP-1 receptor.

Important for the translational validation of our rat study in humans, we also performed an *in vitro* functional analysis of HDL endothelial protective properties in obese patients before and after RYGB surgery. Similar to our rat RYGB model, in obese patients RYGB improved HDL cholesterol efflux capacity, its ability to stimulate endothelial NO production, and its anti-oxidative, anti-inflammatory, and anti-apoptotic properties; most of these effects

occurred within 2 weeks after surgery and in a weight loss-independent manner when compared to BMI-matched controls. A major limitation of the study design in humans was the lack of a diet- or calorie restriction-matched control group. Even though it has been shown that the early beneficial effects of RYGB surgery on insulin resistance and β-cell function are independent from weight loss [89, 90], other studies have suggested that severe caloric restriction, which is typical of the immediate RYGB post-operative period, is primarily responsible for the rapid improvements in insulin resistance and β-cell function after RYGB surgery [138-140]. Therefore, early caloric restriction prior to major weight loss might also be involved in the improvement of HDL functional properties after RYGB in humans; our data in rats does not support this hypothesis as the body weight-matched control group was calorie-restricted similar to the RYGB-operated group. Nevertheless, further investigations using not only BMI-matched, but also calorie intake-matched control groups in humans are needed to better differentiate between the weight loss- and calorie restriction-dependent and -independent effects of RYGB on HDL functional properties.

Interestingly, even though total HDL levels were not changed 8 days after RYGB surgery in our rat model, the cholesterol distribution profile shifted towards smaller HDL particles compared to both sham-operated ad libitum-fed rats and sham-operated rats body weight-matched to RYGB. It has been recently suggested that HDL size and molecular composition are crucial contributors to HDL cardiovascular protective effects [65-67]. Low concentrations of small HDL have been reported to be an independent risk factor for myocardial infarction and cardiovascular mortality [65]. Small HDL particles were also shown to be most efficient in stimulating the atheroprotective cholesterol efflux capacity in macrophages [66, 67], and in inhibiting LDL oxidation and endothelial apoptosis [67]. Accordingly, the improved functionality of smaller HDL particles was associated with their molecular composition, with a favorable role played by increased levels of the phospholipids phosphatidylcholine and phosphatidylserine, along with decreased levels of sphingomyelin, free cholesterol, cholesteryl esters, and triglycerides [67]. The observed improvement in HDL functional properties after RYGB might therefore be directly linked to changes in HDL molecular composition and distribution profile, which in rats was shifted towards smaller and potentially more protective HDL particles. In contrast, clinical studies have suggested that RYGB surgery in humans shifts the HDL distribution profile towards larger, more mature HDL particles [68, 69]. This discrepancy could be due to species-specific differences in HDL

remodelling and reverse cholesterol transport. Therefore, it will be important to further study the role of HDL remodelling in mediating the improved HDL functionality after RYGB in both obese patients and animal models, but the results of such additional investigations are beyond the scope of the present PhD thesis.

Therefore, the above results suggest that RYGB surgery improves HDL endothelial protective properties rapidly and independently of weight loss in both rats and humans; the exact molecular mechanisms are unknown but might be mediated by changed HDL size and composition in a GLP-1-dependent, but GLP-1 receptor-independent manner.

6.3 RYGB increases GLP-1 levels rapidly and independently of weight loss

Fasting plasma GLP-1 levels were increased rapidly and independently of weight loss in our rat RYGB model and mediated the improved endothelial function and some HDL properties after RYGB surgery. Currently there are two major hypotheses to explain the rapid and weight-independent increase in GLP-1 levels seen after RYGB: 1.) rapid increased delivery of undigested food to the alimentary limb and common channel, which leads to gut hypertrophy and stimulates the increased secretion of GLP-1 by enteroendocrine L cells [141-144]; 2.) rapid increased delivery of undiluted bile acids to the common channel, which can also stimulate increased secretion of GLP-1 by enteroendocrine L cells [145].

The unique anatomical rearrangement of the gastrointestinal tract after RYGB creates such conditions where largely undigested food passes from the gastric pouch directly into the small intestine; food cannot be properly digested and absorbed in the newly created alimentary limb because mixture with digestive pancreatic enzymes occurs only after the Y junction in the common channel. Indeed, RYGB surgery results in faster gastric pouch emptying, thus exposing enteroendocrine cells to nutrients more rapidly than under normal conditions [141, 144]; in RYGB patients faster gastric pouch emptying is associated with increased secretion of GLP-1 [141]. As an adaptive mechanism, it has been shown that RYGB surgery in rats leads to general hypertrophy of both the alimentary and common limbs, which is accompanied by a corresponding doubling of the total number of L cells [142, 143], and by an increase in preproglucagon gene expression [143]. Therefore, after RYGB surgery enteroendocrine L cells located throughout the alimentary limb and common channel are not only rapidly exposed to greater amounts of undigested nutrients than under normal

conditions, but their total numbers are also increased, resulting in increased secretion of GLP-1 .

Bile acids can also stimulate GLP-1 secretion from enteroendocrine L cells [146-148]. The unique anatomical gut rearrangement after RYGB also creates conditions where undiluted bile acids pass from the newly created biliopancreatic limb directly into the common channel [145]. Indeed, surgical drainage of endogenous bile into the distal ileum in rats is associated with increased levels of GLP-1 [145]. In humans, RYGB has been shown to increase both fasting and postprandial bile acid levels one and two years after surgery [149-152], and postoperative bile acid levels correlate with postprandial GLP-1 excursions [149, 153]. Some studies show that the increase in bile acids after RYGB occurs as early as one and three months after surgery with a concomitant increase in GLP-1 levels [145, 154], while other studies suggest that the increase in GLP-1 levels precedes the increase in bile acids, and that the latter occurs only after one-two years [151, 152]. Nevertheless, the observed increase in bile acids after RYGB occurs in a weight-loss independent manner as there is no change in bile acid levels with an equivalent weight loss after AGB surgery [145, 153]. Finally, the combination of food and bile acids is able to elicit a greater postprandial GLP-1 secretion than food or bile acids alone [145], and the mean preproglucagon gene expression per cell is specifically increased in the common channel after RYGB, reflecting the potential contribution of bile acids in stimulating GLP-1 secretion [143]. Therefore, it is likely that a weight loss-independent increase in bile acids after RYGB also contributes to increased secretion of GLP-1.

In agreement with this hypothesis, in our rat RYGB model we observed increased fasting plasma bile acid levels concomitant with increased fasting GLP-1 levels, which occurred within 8 days after surgery and in a weight loss-independent manner as they were not observed in sham-operated rats body weight-matched to the RYGB rats. Currently the exact mechanisms responsible for the increased bile acid levels after RYGB surgery are unknown, but is has been proposed that RYGB increases the enterohepatic circulation of bile acids by increasing their delivery to the ileum for reabsorption and recirculation back to the liver [153].

6.4 Conclusions and future perspectives

The present study suggests that RYGB surgery improves obesity-induced endothelial dysfunction in a GLP-1-dependent and JNK2-dependent mechanism, and in parallel improves HDL endothelial protective properties rapidly and independently of weight loss. The unique anatomical gut rearrangement after RYGB allows for increased and rapid delivery of nutrients and bile acids to the small intestine, which stimulates enteroendocrine L cells to secrete GLP-1 [91, 99, 101, 141, 145]. In endothelial cells GLP-1 activates the GLP-1 receptor and downstream PKA, Akt, and eNOS signalling, leading to increased production of vasodilatory NO [126-129]. GLP-1 receptor-dependent PKA signalling also inhibits JNK2 [130-134], thus activating IRS-1 and the downstream insulin signalling pathway that also leads to activation of Akt and eNOS [71, 121-123]. GLP-1-dependent JNK2 inhibition also decreases vascular oxidative stress and further contributes to increased NO levels, therefore leading to increased endothelial-dependent vasodilation and improved vascular function [72, 125]. In parallel, RYGB surgery induces HDL remodelling and increases HDL pro-vasodilatory, anti-atherogenic, anti-inflammatory, anti-oxidative, and anti-apoptotic properties [65-67], which further contribute to the improved endothelial function observed after surgery [64]. Improved endothelial function might then contribute to ameliorating obesity-associated cardiovascular disease risk after RYGB surgery [72, 124].

Experiments with GLP1 receptor knockout mice and JNK2 knockout mice would need to be performed in order to confirm the roles of GLP-1 and JNK2 in the improved endothelial function after RYGB surgery. If the proposed molecular mechanism is true, one should expect that GLP-1 receptor knockout mice, despite losing weight similarly to wild type mice [106-108], would not benefit from the endothelial protective effects of RYGB. JNK2 knockout mice, on the other hand, would be protected from obesity-induced endothelial dysfunction even though they are not protected from obesity [111, 112, 116], and RYGB surgery would not have an additional beneficial effect on endothelial function.

Understanding the weight loss-independent molecular mechanisms that lead to improved endothelial and HDL function after RYGB surgery will help to identify putative targets for future non-invasive anti-obesity pharmacological therapy that mimics the effects of RYGB. The present study identifies two such targets that mediate the beneficial effects of RYGB on vascular function – the intestinal hormone GLP-1 and the stress-activated kinase JNK.

Synthetic GLP-1 agonists and analogues such as liraglutide and exenatide are already in use to treat obesity and type 2 diabetes, and their effects on improved β-cell function and glucose tolerance in the pancreas, and on reduced food intake and increased satiation in the central nervous system have been extensively studied [40, 41, 94]. In our study, we additionally demonstrate that GLP-1 mediates weight-independent beneficial effects of RYGB on the cardiovascular system, which could be used to further tailor GLP-1-based therapies to treat or prevent obesity-associated cardiovascular disease. Similarly, pharmacological JNK-targeted therapy could be used to treat or prevent obesity-associated cardiovascular disease. Numerous *in vivo* animal studies have demonstrated the beneficial effects of several different JNK inhibitors on metabolic pathologies [155-157]; the present study adds the improvement of obesity-induced endothelial dysfunction to these beneficial effects. Unfortunately, however, we also demonstrate that pharmacological approaches might have undesirable and severe side effects, as in our case the D-JNK inhibitor resulted in unspecific but acute kidney toxicity. Future development of JNK-targeted or other anti-obesity therapies will require not only complete understanding of the molecular actions of the target, but also a complete understanding of the molecular actions of the developed drug.

7. Abbreviations

AGB – adjustable gastric banding

ApoE – apolipoprotein E

BMI – body mass index

CAD – coronary artery disease

CREB – cAMP response element binding protein

eNOS – endothelial nitric oxide synthase

FMD – flow-mediated dilation

GLP-1 – glucagon-like peptide-1

HbA1c – glycated haemoglobin, haemoglobin A1c

HDL – high-density lipoprotein

IRS-1 – insulin receptor substrate-1

JNK – c-jun N-terminal kinase

LDL – low-density lipoprotein

L-NAME - Nω-nitro-L-arginine methyl ester

NO – nitric oxide

PKA – protein kinase A

RYGB – Roux-en-Y gastric bypass

VSG – vertical sleeve gastrectomy

8. References

1. Ng, M., et al., *Global, regional, and national prevalence of overweight and obesity in children and adults during 1980-2013: a systematic analysis for the Global Burden of Disease Study 2013.* Lancet, 2014. **384**(9945): p. 766-81.
2. *Trends in adult body-mass index in 200 countries from 1975 to 2014: a pooled analysis of 1698 population-based measurement studies with 19·2 million participants.* The Lancet. **387**(10026): p. 1377-1396.
3. Calle, E.E., et al., *Body-mass index and mortality in a prospective cohort of U.S. adults.* N Engl J Med, 1999. **341**(15): p. 1097-105.
4. Adams, K.F., et al., *Overweight, obesity, and mortality in a large prospective cohort of persons 50 to 71 years old.* N Engl J Med, 2006. **355**(8): p. 763-78.
5. Prospective Studies, C., et al., *Body-mass index and cause-specific mortality in 900 000 adults: collaborative analyses of 57 prospective studies.* Lancet, 2009. **373**(9669): p. 1083-96.
6. Berrington de Gonzalez, A., et al., *Body-mass index and mortality among 1.46 million white adults.* N Engl J Med, 2010. **363**(23): p. 2211-9.
7. Fontaine, K.R., et al., *Years of life lost due to obesity.* JAMA, 2003. **289**(2): p. 187-93.
8. Brown, C.D., et al., *Body mass index and the prevalence of hypertension and dyslipidemia.* Obes Res, 2000. **8**(9): p. 605-19.
9. Wilson, P.W., et al., *Overweight and obesity as determinants of cardiovascular risk: the Framingham experience.* Arch Intern Med, 2002. **162**(16): p. 1867-72.
10. Global Burden of Metabolic Risk Factors for Chronic Diseases, C., et al., *Metabolic mediators of the effects of body-mass index, overweight, and obesity on coronary heart disease and stroke: a pooled analysis of 97 prospective cohorts with 1.8 million participants.* Lancet, 2014. **383**(9921): p. 970-83.
11. Kenchaiah, S., et al., *Obesity and the risk of heart failure.* N Engl J Med, 2002. **347**(5): p. 305-13.
12. Abdullah, A., et al., *The magnitude of association between overweight and obesity and the risk of diabetes: a meta-analysis of prospective cohort studies.* Diabetes Res Clin Pract, 2010. **89**(3): p. 309-19.
13. Wadden, T.A. and D.L. Frey, *A multicenter evaluation of a proprietary weight loss program for the treatment of marked obesity: a five-year follow-up.* Int J Eat Disord, 1997. **22**(2): p. 203-12.
14. Anderson, J.W., et al., *Long-term weight-loss maintenance: a meta-analysis of US studies.* Am J Clin Nutr, 2001. **74**(5): p. 579-84.
15. Curioni, C.C. and P.M. Lourenco, *Long-term weight loss after diet and exercise: a systematic review.* Int J Obes (Lond), 2005. **29**(10): p. 1168-74.
16. Look, A.R.G., *Eight-year weight losses with an intensive lifestyle intervention: the look AHEAD study.* Obesity (Silver Spring), 2014. **22**(1): p. 5-13.
17. Blackburn, G., *Effect of degree of weight loss on health benefits.* Obes Res, 1995. **3 Suppl 2**: p. 211s-216s.
18. Wing, R.R., R.W. Jeffery, and W.L. Hellerstedt, *A prospective study of effects of weight cycling on cardiovascular risk factors.* Arch Intern Med, 1995. **155**(13): p. 1416-22.
19. Dattilo, A.M. and P.M. Kris-Etherton, *Effects of weight reduction on blood lipids and lipoproteins: a meta-analysis.* Am J Clin Nutr, 1992. **56**(2): p. 320-8.
20. Stevens, V.J., et al., *Long-term weight loss and changes in blood pressure: results of the Trials of Hypertension Prevention, phase II.* Ann Intern Med, 2001. **134**(1): p. 1-11.
21. Tuomilehto, J., et al., *Prevention of type 2 diabetes mellitus by changes in lifestyle among subjects with impaired glucose tolerance.* N Engl J Med, 2001. **344**(18): p. 1343-50.
22. Ratner, R., et al., *Impact of intensive lifestyle and metformin therapy on cardiovascular disease risk factors in the diabetes prevention program.* Diabetes Care, 2005. **28**(4): p. 888-94.

23. Gregg, E.W., et al., *Association of an intensive lifestyle intervention with remission of type 2 diabetes.* JAMA, 2012. **308**(23): p. 2489-96.
24. Look, A.R.G., et al., *Cardiovascular effects of intensive lifestyle intervention in type 2 diabetes.* N Engl J Med, 2013. **369**(2): p. 145-54.
25. Uusitupa, M., et al., *Ten-year mortality and cardiovascular morbidity in the Finnish Diabetes Prevention Study--secondary analysis of the randomized trial.* PLoS One, 2009. **4**(5): p. e5656.
26. Li, G., et al., *The long-term effect of lifestyle interventions to prevent diabetes in the China Da Qing Diabetes Prevention Study: a 20-year follow-up study.* Lancet, 2008. **371**(9626): p. 1783-9.
27. Sjostrom, L., et al., *Randomised placebo-controlled trial of orlistat for weight loss and prevention of weight regain in obese patients. European Multicentre Orlistat Study Group.* Lancet, 1998. **352**(9123): p. 167-72.
28. Davidson, M.H., et al., *Weight control and risk factor reduction in obese subjects treated for 2 years with orlistat: a randomized controlled trial.* JAMA, 1999. **281**(3): p. 235-42.
29. Lindgarde, F., *The effect of orlistat on body weight and coronary heart disease risk profile in obese patients: the Swedish Multimorbidity Study.* J Intern Med, 2000. **248**(3): p. 245-54.
30. Rossner, S., et al., *Weight loss, weight maintenance, and improved cardiovascular risk factors after 2 years treatment with orlistat for obesity. European Orlistat Obesity Study Group.* Obes Res, 2000. **8**(1): p. 49-61.
31. Torgerson, J.S., et al., *XENical in the prevention of diabetes in obese subjects (XENDOS) study: a randomized study of orlistat as an adjunct to lifestyle changes for the prevention of type 2 diabetes in obese patients.* Diabetes Care, 2004. **27**(1): p. 155-61.
32. Aldekhail, N.M., et al., *Effect of orlistat on glycaemic control in overweight and obese patients with type 2 diabetes mellitus: a systematic review and meta-analysis of randomized controlled trials.* Obes Rev, 2015. **16**(12): p. 1071-80.
33. Smith, S.R., et al., *Multicenter, placebo-controlled trial of lorcaserin for weight management.* N Engl J Med, 2010. **363**(3): p. 245-56.
34. Fidler, M.C., et al., *A one-year randomized trial of lorcaserin for weight loss in obese and overweight adults: the BLOSSOM trial.* J Clin Endocrinol Metab, 2011. **96**(10): p. 3067-77.
35. O'Neil, P.M., et al., *Randomized placebo-controlled clinical trial of lorcaserin for weight loss in type 2 diabetes mellitus: the BLOOM-DM study.* Obesity (Silver Spring), 2012. **20**(7): p. 1426-36.
36. Chan, E.W., et al., *Efficacy and safety of lorcaserin in obese adults: a meta-analysis of 1-year randomized controlled trials (RCTs) and narrative review on short-term RCTs.* Obes Rev, 2013. **14**(5): p. 383-92.
37. Allison, D.B., et al., *Controlled-release phentermine/topiramate in severely obese adults: a randomized controlled trial (EQUIP).* Obesity (Silver Spring), 2012. **20**(2): p. 330-42.
38. Gadde, K.M., et al., *Effects of low-dose, controlled-release, phentermine plus topiramate combination on weight and associated comorbidities in overweight and obese adults (CONQUER): a randomised, placebo-controlled, phase 3 trial.* Lancet, 2011. **377**(9774): p. 1341-52.
39. Garvey, W.T., et al., *Two-year sustained weight loss and metabolic benefits with controlled-release phentermine/topiramate in obese and overweight adults (SEQUEL): a randomized, placebo-controlled, phase 3 extension study.* Am J Clin Nutr, 2012. **95**(2): p. 297-308.
40. Astrup, A., et al., *Safety, tolerability and sustained weight loss over 2 years with the once-daily human GLP-1 analog, liraglutide.* Int J Obes (Lond), 2012. **36**(6): p. 843-54.
41. Wadden, T.A., et al., *Weight maintenance and additional weight loss with liraglutide after low-calorie-diet-induced weight loss: the SCALE Maintenance randomized study.* Int J Obes (Lond), 2013. **37**(11): p. 1443-51.
42. Astrup, A., et al., *Effects of liraglutide in the treatment of obesity: a randomised, double-blind, placebo-controlled study.* Lancet, 2009. **374**(9701): p. 1606-16.

43. Poirier, P., et al., *Bariatric surgery and cardiovascular risk factors: a scientific statement from the American Heart Association.* Circulation, 2011. **123**(15): p. 1683-701.
44. Angrisani, L., et al., *Bariatric Surgery Worldwide 2013.* Obes Surg, 2015. **25**(10): p. 1822-32.
45. Dixon, J.B., et al., *Bariatric surgery for type 2 diabetes.* Lancet, 2012. **379**(9833): p. 2300-11.
46. Sjostrom, L., et al., *Lifestyle, diabetes, and cardiovascular risk factors 10 years after bariatric surgery.* N Engl J Med, 2004. **351**(26): p. 2683-93.
47. Adams, T.D., et al., *Health benefits of gastric bypass surgery after 6 years.* JAMA, 2012. **308**(11): p. 1122-31.
48. Gloy, V.L., et al., *Bariatric surgery versus non-surgical treatment for obesity: a systematic review and meta-analysis of randomised controlled trials.* BMJ, 2013. **347**: p. f5934.
49. Raffaelli, M., et al., *Effect of gastric bypass versus diet on cardiovascular risk factors.* Ann Surg, 2014. **259**(4): p. 694-9.
50. Cummings, D.E., et al., *Gastric bypass surgery vs intensive lifestyle and medical intervention for type 2 diabetes: the CROSSROADS randomised controlled trial.* Diabetologia, 2016. **59**(5): p. 945-53.
51. Courcoulas, A.P., et al., *Weight change and health outcomes at 3 years after bariatric surgery among individuals with severe obesity.* JAMA, 2013. **310**(22): p. 2416-25.
52. Weber, M., et al., *Laparoscopic gastric bypass is superior to laparoscopic gastric banding for treatment of morbid obesity.* Ann Surg, 2004. **240**(6): p. 975-82; discussion 982-3.
53. Kim, T.H., et al., *Early U.S. outcomes of laparoscopic gastric bypass versus laparoscopic adjustable silicone gastric banding for morbid obesity.* Surg Endosc, 2006. **20**(2): p. 202-9.
54. Cottam, D.R., et al., *A case-controlled matched-pair cohort study of laparoscopic Roux-en-Y gastric bypass and Lap-Band patients in a single US center with three-year follow-up.* Obes Surg, 2006. **16**(5): p. 534-40.
55. Puzziferri, N., et al., *Long-term follow-up after bariatric surgery: a systematic review.* JAMA, 2014. **312**(9): p. 934-42.
56. Peterli, R., et al., *Early results of the Swiss Multicentre Bypass or Sleeve Study (SM-BOSS): a prospective randomized trial comparing laparoscopic sleeve gastrectomy and Roux-en-Y gastric bypass.* Ann Surg, 2013. **258**(5): p. 690-4; discussion 695.
57. Carlin, A.M., et al., *The comparative effectiveness of sleeve gastrectomy, gastric bypass, and adjustable gastric banding procedures for the treatment of morbid obesity.* Ann Surg, 2013. **257**(5): p. 791-7.
58. Zlabek, J.A., et al., *The effect of laparoscopic gastric bypass surgery on dyslipidemia in severely obese patients.* Surg Obes Relat Dis, 2005. **1**(6): p. 537-42.
59. Nguyen, N.T., et al., *Resolution of hyperlipidemia after laparoscopic Roux-en-Y gastric bypass.* J Am Coll Surg, 2006. **203**(1): p. 24-9.
60. Jamal, M., et al., *Resolution of hyperlipidemia follows surgical weight loss in patients undergoing Roux-en-Y gastric bypass surgery: a 6-year analysis of data.* Surg Obes Relat Dis, 2011. **7**(4): p. 473-9.
61. Ties, J.S., et al., *The effect of laparoscopic gastric bypass on dyslipidemia in severely obese patients: a 5-year follow-up analysis.* Obes Surg, 2014. **24**(4): p. 549-53.
62. Hinojosa, M.W., et al., *Resolution of systemic hypertension after laparoscopic gastric bypass.* J Gastrointest Surg, 2009. **13**(4): p. 793-7.
63. Ali, M.R., W.D. Fuller, and J. Rasmussen, *Detailed description of early response of metabolic syndrome after laparoscopic Roux-en-Y gastric bypass.* Surg Obes Relat Dis, 2009. **5**(3): p. 346-51.
64. Luscher, T.F., et al., *High-density lipoprotein: vascular protective effects, dysfunction, and potential as therapeutic target.* Circ Res, 2014. **114**(1): p. 171-82.
65. Martin, S.S., et al., *HDL cholesterol subclasses, myocardial infarction, and mortality in secondary prevention: the Lipoprotein Investigators Collaborative.* Eur Heart J, 2015. **36**(1): p. 22-30.

66. Du, X.M., et al., *HDL particle size is a critical determinant of ABCA1-mediated macrophage cellular cholesterol export.* Circ Res, 2015. **116**(7): p. 1133-42.
67. Camont, L., et al., *Small, dense high-density lipoprotein-3 particles are enriched in negatively charged phospholipids: relevance to cellular cholesterol efflux, antioxidative, antithrombotic, anti-inflammatory, and antiapoptotic functionalities.* Arterioscler Thromb Vasc Biol, 2013. **33**(12): p. 2715-23.
68. Asztalos, B.F., et al., *Effects of weight loss, induced by gastric bypass surgery, on HDL remodeling in obese women.* J Lipid Res, 2010. **51**(8): p. 2405-12.
69. Zvintzou, E., et al., *Effects of bariatric surgery on HDL structure and functionality: results from a prospective trial.* J Clin Lipidol, 2014. **8**(4): p. 408-17.
70. Aminian, A., et al., *Exploring the impact of bariatric surgery on high density lipoprotein.* Surg Obes Relat Dis, 2015. **11**(1): p. 238-47.
71. Rask-Madsen, C., et al., *Loss of insulin signaling in vascular endothelial cells accelerates atherosclerosis in apolipoprotein E null mice.* Cell Metab, 2010. **11**(5): p. 379-89.
72. Sena, C.M., A.M. Pereira, and R. Seica, *Endothelial dysfunction - a major mediator of diabetic vascular disease.* Biochim Biophys Acta, 2013. **1832**(12): p. 2216-31.
73. Toda, N. and T. Okamura, *Obesity impairs vasodilatation and blood flow increase mediated by endothelial nitric oxide: an overview.* J Clin Pharmacol, 2013. **53**(12): p. 1228-39.
74. Lupoli, R., et al., *Effects of bariatric surgery on markers of subclinical atherosclerosis and endothelial function: a meta-analysis of literature studies.* Int J Obes (Lond), 2016. **40**(3): p. 395-402.
75. Nerla, R., et al., *Effect of bariatric surgery on peripheral flow-mediated dilation and coronary microvascular function.* Nutr Metab Cardiovasc Dis, 2012. **22**(8): p. 626-34.
76. Bigornia, S.J., et al., *Insulin status and vascular responses to weight loss in obesity.* J Am Coll Cardiol, 2013. **62**(24): p. 2297-305.
77. Heneghan, H.M., et al., *Effect of bariatric surgery on cardiovascular risk profile.* Am J Cardiol, 2011. **108**(10): p. 1499-507.
78. Vest, A.R., et al., *Bariatric surgery and cardiovascular outcomes: a systematic review.* Heart, 2012. **98**(24): p. 1763-77.
79. Buchwald, H., et al., *Bariatric surgery: a systematic review and meta-analysis.* JAMA, 2004. **292**(14): p. 1724-37.
80. Sjostrom, L., et al., *Effects of bariatric surgery on mortality in Swedish obese subjects.* N Engl J Med, 2007. **357**(8): p. 741-52.
81. Adams, T.D., et al., *Long-term mortality after gastric bypass surgery.* N Engl J Med, 2007. **357**(8): p. 753-61.
82. Kwok, C.S., et al., *Bariatric surgery and its impact on cardiovascular disease and mortality: a systematic review and meta-analysis.* Int J Cardiol, 2014. **173**(1): p. 20-8.
83. Sjostrom, L., et al., *Bariatric surgery and long-term cardiovascular events.* JAMA, 2012. **307**(1): p. 56-65.
84. Pories, W.J., et al., *Who would have thought it? An operation proves to be the most effective therapy for adult-onset diabetes mellitus.* Ann Surg, 1995. **222**(3): p. 339-50; discussion 350-2.
85. Wickremesekera, K., et al., *Loss of insulin resistance after Roux-en-Y gastric bypass surgery: a time course study.* Obes Surg, 2005. **15**(4): p. 474-81.
86. Jorgensen, N.B., et al., *Acute and long-term effects of Roux-en-Y gastric bypass on glucose metabolism in subjects with Type 2 diabetes and normal glucose tolerance.* Am J Physiol Endocrinol Metab, 2012. **303**(1): p. E122-31.
87. Bojsen-Moller, K.N., et al., *Early enhancements of hepatic and later of peripheral insulin sensitivity combined with increased postprandial insulin secretion contribute to improved glycemic control after Roux-en-Y gastric bypass.* Diabetes, 2014. **63**(5): p. 1725-37.
88. Griffo, E., et al., *Effects of Sleeve Gastrectomy and Gastric Bypass on Postprandial Lipid Profile in Obese Type 2 Diabetic Patients: a 2-Year Follow-up.* Obes Surg, 2015.

89. Kashyap, S.R., et al., *Acute effects of gastric bypass versus gastric restrictive surgery on beta-cell function and insulinotropic hormones in severely obese patients with type 2 diabetes.* Int J Obes (Lond), 2010. **34**(3): p. 462-71.
90. Pournaras, D.J., et al., *Remission of type 2 diabetes after gastric bypass and banding: mechanisms and 2 year outcomes.* Ann Surg, 2010. **252**(6): p. 966-71.
91. Laferrere, B., et al., *Incretin levels and effect are markedly enhanced 1 month after Roux-en-Y gastric bypass surgery in obese patients with type 2 diabetes.* Diabetes Care, 2007. **30**(7): p. 1709-16.
92. Bose, M., et al., *Weight loss and incretin responsiveness improve glucose control independently after gastric bypass surgery.* J Diabetes, 2010. **2**(1): p. 47-55.
93. Spreckley, E. and K.G. Murphy, *The L-Cell in Nutritional Sensing and the Regulation of Appetite.* Front Nutr, 2015. **2**: p. 23.
94. Campbell, J.E. and D.J. Drucker, *Pharmacology, physiology, and mechanisms of incretin hormone action.* Cell Metab, 2013. **17**(6): p. 819-37.
95. Dirksen, C., et al., *Postprandial diabetic glucose tolerance is normalized by gastric bypass feeding as opposed to gastric feeding and is associated with exaggerated GLP-1 secretion: a case report.* Diabetes Care, 2010. **33**(2): p. 375-7.
96. Lindqvist, A., et al., *Effects of ingestion routes on hormonal and metabolic profiles in gastric-bypassed humans.* J Clin Endocrinol Metab, 2013. **98**(5): p. E856-61.
97. Salehi, M., R.L. Prigeon, and D.A. D'Alessio, *Gastric bypass surgery enhances glucagon-like peptide 1-stimulated postprandial insulin secretion in humans.* Diabetes, 2011. **60**(9): p. 2308-14.
98. Jorgensen, N.B., et al., *Exaggerated glucagon-like peptide 1 response is important for improved beta-cell function and glucose tolerance after Roux-en-Y gastric bypass in patients with type 2 diabetes.* Diabetes, 2013. **62**(9): p. 3044-52.
99. Korner, J., et al., *Exaggerated glucagon-like peptide-1 and blunted glucose-dependent insulinotropic peptide secretion are associated with Roux-en-Y gastric bypass but not adjustable gastric banding.* Surg Obes Relat Dis, 2007. **3**(6): p. 597-601.
100. Korner, J., et al., *Prospective study of gut hormone and metabolic changes after adjustable gastric banding and Roux-en-Y gastric bypass.* Int J Obes (Lond), 2009. **33**(7): p. 786-95.
101. Laferrere, B., et al., *Effect of weight loss by gastric bypass surgery versus hypocaloric diet on glucose and incretin levels in patients with type 2 diabetes.* J Clin Endocrinol Metab, 2008. **93**(7): p. 2479-85.
102. Liu, Y., et al., *Roux-en-Y gastric bypass-induced improvement of glucose tolerance and insulin resistance in type 2 diabetic rats are mediated by glucagon-like peptide-1.* Obes Surg, 2011. **21**(9): p. 1424-31.
103. Shin, A.C., et al., *Meal-induced hormone responses in a rat model of Roux-en-Y gastric bypass surgery.* Endocrinology, 2010. **151**(4): p. 1588-97.
104. Chambers, A.P., et al., *Weight-independent changes in blood glucose homeostasis after gastric bypass or vertical sleeve gastrectomy in rats.* Gastroenterology, 2011. **141**(3): p. 950-8.
105. Carmody, J.S., et al., *Peripheral, but not central, GLP-1 receptor signaling is required for improvement in glucose tolerance after Roux-en-Y gastric bypass in mice.* Am J Physiol Endocrinol Metab, 2016: p. ajpendo 00412 2015.
106. Wilson-Perez, H.E., et al., *Vertical sleeve gastrectomy is effective in two genetic mouse models of glucagon-like Peptide 1 receptor deficiency.* Diabetes, 2013. **62**(7): p. 2380-5.
107. Mokadem, M., et al., *Effects of Roux-en-Y gastric bypass on energy and glucose homeostasis are preserved in two mouse models of functional glucagon-like peptide-1 deficiency.* Mol Metab, 2014. **3**(2): p. 191-201.
108. Ye, J., et al., *GLP-1 receptor signaling is not required for reduced body weight after RYGB in rodents.* Am J Physiol Regul Integr Comp Physiol, 2014. **306**(5): p. R352-62.

109. Hotamisligil, G.S., *Role of endoplasmic reticulum stress and c-Jun NH2-terminal kinase pathways in inflammation and origin of obesity and diabetes.* Diabetes, 2005. **54 Suppl 2**: p. S73-8.
110. Aguirre, V., et al., *The c-Jun NH(2)-terminal kinase promotes insulin resistance during association with insulin receptor substrate-1 and phosphorylation of Ser(307).* J Biol Chem, 2000. **275**(12): p. 9047-54.
111. Hirosumi, J., et al., *A central role for JNK in obesity and insulin resistance.* Nature, 2002. **420**(6913): p. 333-6.
112. Tuncman, G., et al., *Functional in vivo interactions between JNK1 and JNK2 isoforms in obesity and insulin resistance.* Proc Natl Acad Sci U S A, 2006. **103**(28): p. 10741-6.
113. He, B., et al., *Amelioration in hepatic insulin sensitivity by reduced hepatic lipid accumulation at short-term after Roux-en-Y gastric bypass surgery in type 2 diabetic rats.* Obes Surg, 2013. **23**(12): p. 2033-41.
114. Hu, C., et al., *Duodenal-Jejunal bypass improves glucose homeostasis in association with decreased proinflammatory response and activation of JNK in the liver and adipose tissue in a T2DM rat model.* Obes Surg, 2014. **24**(9): p. 1453-62.
115. Ricci, R., et al., *Requirement of JNK2 for scavenger receptor A-mediated foam cell formation in atherogenesis.* Science, 2004. **306**(5701): p. 1558-61.
116. Osto, E., et al., *c-Jun N-terminal kinase 2 deficiency protects against hypercholesterolemia-induced endothelial dysfunction and oxidative stress.* Circulation, 2008. **118**(20): p. 2073-80.
117. Park, J.H., et al., *c-Jun N-terminal kinase 2 phosphorylates endothelial nitric oxide synthase at serine 116 and regulates nitric oxide production.* Biochem Biophys Res Commun, 2012. **417**(1): p. 340-5.
118. Sugita, M., H. Sugita, and M. Kaneki, *Increased insulin receptor substrate 1 serine phosphorylation and stress-activated protein kinase/c-Jun N-terminal kinase activation associated with vascular insulin resistance in spontaneously hypertensive rats.* Hypertension, 2004. **44**(4): p. 484-9.
119. Breton-Romero, R., et al., *Endothelial Dysfunction in Human Diabetes Is Mediated by Wnt5a-JNK Signaling.* Arterioscler Thromb Vasc Biol, 2016. **36**(3): p. 561-9.
120. Meshkani, R. and K. Adeli, *Hepatic insulin resistance, metabolic syndrome and cardiovascular disease.* Clin Biochem, 2009. **42**(13-14): p. 1331-46.
121. Zeng, G., et al., *Roles for insulin receptor, PI3-kinase, and Akt in insulin-signaling pathways related to production of nitric oxide in human vascular endothelial cells.* Circulation, 2000. **101**(13): p. 1539-45.
122. Naruse, K., et al., *Activation of vascular protein kinase C-beta inhibits Akt-dependent endothelial nitric oxide synthase function in obesity-associated insulin resistance.* Diabetes, 2006. **55**(3): p. 691-8.
123. Wang, Y., et al., *APPL1 counteracts obesity-induced vascular insulin resistance and endothelial dysfunction by modulating the endothelial production of nitric oxide and endothelin-1 in mice.* Diabetes, 2011. **60**(11): p. 3044-54.
124. Baron, A.D., *Insulin resistance and vascular function.* J Diabetes Complications, 2002. **16**(1): p. 92-102.
125. Salisbury, D. and U. Bronas, *Reactive oxygen and nitrogen species: impact on endothelial dysfunction.* Nurs Res, 2015. **64**(1): p. 53-66.
126. Ban, K., et al., *Cardioprotective and vasodilatory actions of glucagon-like peptide 1 receptor are mediated through both glucagon-like peptide 1 receptor-dependent and -independent pathways.* Circulation, 2008. **117**(18): p. 2340-50.
127. Erdogdu, O., et al., *Exendin-4 stimulates proliferation of human coronary artery endothelial cells through eNOS-, PKA- and PI3K/Akt-dependent pathways and requires GLP-1 receptor.* Mol Cell Endocrinol, 2010. **325**(1-2): p. 26-35.
128. Ding, L. and J. Zhang, *Glucagon-like peptide-1 activates endothelial nitric oxide synthase in human umbilical vein endothelial cells.* Acta Pharmacol Sin, 2012. **33**(1): p. 75-81.

129. Han, L., et al., *Exendin-4 directly improves endothelial dysfunction in isolated aortas from obese rats through the cAMP or AMPK-eNOS pathways.* Diabetes Res Clin Pract, 2012. **97**(3): p. 453-60.
130. Ferdaoussi, M., et al., *Exendin-4 protects beta-cells from interleukin-1 beta-induced apoptosis by interfering with the c-Jun NH2-terminal kinase pathway.* Diabetes, 2008. **57**(5): p. 1205-15.
131. Natalicchio, A., et al., *Exendin-4 prevents c-Jun N-terminal protein kinase activation by tumor necrosis factor-alpha (TNFalpha) and inhibits TNFalpha-induced apoptosis in insulin-secreting cells.* Endocrinology, 2010. **151**(5): p. 2019-29.
132. Laviola, L., et al., *Glucagon-like peptide-1 counteracts oxidative stress-dependent apoptosis of human cardiac progenitor cells by inhibiting the activation of the c-Jun N-terminal protein kinase signaling pathway.* Endocrinology, 2012. **153**(12): p. 5770-81.
133. Erdogdu, O., et al., *Exendin-4 protects endothelial cells from lipoapoptosis by PKA, PI3K, eNOS, p38 MAPK, and JNK pathways.* J Mol Endocrinol, 2013. **50**(2): p. 229-41.
134. Nagayama, K., et al., *Exendin-4 Prevents Vascular Smooth Muscle Cell Proliferation and Migration by Angiotensin II via the Inhibition of ERK1/2 and JNK Signaling Pathways.* PLoS One, 2015. **10**(9): p. e0137960.
135. Sorrentino, S.A., et al., *Endothelial-vasoprotective effects of high-density lipoprotein are impaired in patients with type 2 diabetes mellitus but are improved after extended-release niacin therapy.* Circulation, 2010. **121**(1): p. 110-22.
136. Besler, C., et al., *Mechanisms underlying adverse effects of HDL on eNOS-activating pathways in patients with coronary artery disease.* J Clin Invest, 2011. **121**(7): p. 2693-708.
137. Cantini, G., E. Mannucci, and M. Luconi, *Perspectives in GLP-1 Research: New Targets, New Receptors.* Trends Endocrinol Metab, 2016.
138. Isbell, J.M., et al., *The importance of caloric restriction in the early improvements in insulin sensitivity after Roux-en-Y gastric bypass surgery.* Diabetes Care, 2010. **33**(7): p. 1438-42.
139. Lim, E.L., et al., *Reversal of type 2 diabetes: normalisation of beta cell function in association with decreased pancreas and liver triacylglycerol.* Diabetologia, 2011. **54**(10): p. 2506-14.
140. Lingvay, I., et al., *Rapid improvement in diabetes after gastric bypass surgery: is it the diet or surgery?* Diabetes Care, 2013. **36**(9): p. 2741-7.
141. Dirksen, C., et al., *Fast pouch emptying, delayed small intestinal transit, and exaggerated gut hormone responses after Roux-en-Y gastric bypass.* Neurogastroenterol Motil, 2013. **25**(4): p. 346-e255.
142. Mumphrey, M.B., et al., *Roux-en-Y gastric bypass surgery increases number but not density of CCK-, GLP-1-, 5-HT-, and neurotensin-expressing enteroendocrine cells in rats.* Neurogastroenterol Motil, 2013. **25**(1): p. e70-9.
143. Hansen, C.F., et al., *Hypertrophy dependent doubling of L-cells in Roux-en-Y gastric bypass operated rats.* PLoS One, 2013. **8**(6): p. e65696.
144. Chambers, A.P., et al., *Regulation of gastric emptying rate and its role in nutrient-induced GLP-1 secretion in rats after vertical sleeve gastrectomy.* Am J Physiol Endocrinol Metab, 2014. **306**(4): p. E424-32.
145. Pournaras, D.J., et al., *The role of bile after Roux-en-Y gastric bypass in promoting weight loss and improving glycaemic control.* Endocrinology, 2012. **153**(8): p. 3613-9.
146. Katsuma, S., A. Hirasawa, and G. Tsujimoto, *Bile acids promote glucagon-like peptide-1 secretion through TGR5 in a murine enteroendocrine cell line STC-1.* Biochem Biophys Res Commun, 2005. **329**(1): p. 386-90.
147. Parker, H.E., et al., *Molecular mechanisms underlying bile acid-stimulated glucagon-like peptide-1 secretion.* Br J Pharmacol, 2012. **165**(2): p. 414-23.
148. Thomas, C., et al., *TGR5-mediated bile acid sensing controls glucose homeostasis.* Cell Metab, 2009. **10**(3): p. 167-77.
149. Patti, M.E., et al., *Serum bile acids are higher in humans with prior gastric bypass: potential contribution to improved glucose and lipid metabolism.* Obesity (Silver Spring), 2009. **17**(9): p. 1671-7.

150. Ahmad, N.N., A. Pfalzer, and L.M. Kaplan, *Roux-en-Y gastric bypass normalizes the blunted postprandial bile acid excursion associated with obesity.* Int J Obes (Lond), 2013. **37**(12): p. 1553-9.
151. Steinert, R.E., et al., *Bile acids and gut peptide secretion after bariatric surgery: a 1-year prospective randomized pilot trial.* Obesity (Silver Spring), 2013. **21**(12): p. E660-8.
152. Dutia, R., et al., *Temporal changes in bile acid levels and 12alpha-hydroxylation after Roux-en-Y gastric bypass surgery in type 2 diabetes.* Int J Obes (Lond), 2015. **39**(5): p. 806-13.
153. Kohli, R., et al., *Weight loss induced by Roux-en-Y gastric bypass but not laparoscopic adjustable gastric banding increases circulating bile acids.* J Clin Endocrinol Metab, 2013. **98**(4): p. E708-12.
154. Nakatani, H., et al., *Serum bile acid along with plasma incretins and serum high-molecular weight adiponectin levels are increased after bariatric surgery.* Metabolism, 2009. **58**(10): p. 1400-7.
155. Kaneto, H., et al., *Possible novel therapy for diabetes with cell-permeable JNK-inhibitory peptide.* Nat Med, 2004. **10**(10): p. 1128-32.
156. Stebbins, J.L., et al., *Identification of a new JNK inhibitor targeting the JNK-JIP interaction site.* Proc Natl Acad Sci U S A, 2008. **105**(43): p. 16809-13.
157. Cho, H., et al., *Pharmacological characterization of a small molecule inhibitor of c-Jun kinase.* Am J Physiol Endocrinol Metab, 2008. **295**(5): p. E1142-51.

9. Acknowledgements

First of all, I would like to thank my supervisors Prof. Thomas Lutz and Dr. Elena Osto for giving me the great opportunity to work on this very interesting project. Thank you for the constant guidance and for pushing me well beyond my limits. Certainly this project would not have been realized without your expert supervision.

I would also like to thank Prof. Thomas Lüscher, Prof. Arnold von Eckardstein, Prof. Christian Wolfrum, and Prof. Bart Staels for the helpful and insightful discussions during lab meetings and PhD committee meetings. You gave me very good ideas and suggestions and also made me realize how little I still now about the subject, so that I make even more effort and push myself to do even better science.

I would like to thank all members of the Institute of Veterinary Physiology and the Center for Molecular Cardiology. In particular, I thank Claudia Dörig for helping with the animal experiments during my first year. I thank Dr. Caroline Corteville and Dr. Thomas Bächler for the excellent surgery work in rats. I very much thank Erika Tarasco for sharing with me the enormous workload of two parallel animal experiments in my second and third years – without you I would not have been able to manage them for sure! Thank you Dr. Giovanni Pellegrini for the excellent pathological expertise – without you we would be lost what to do with the unexpected JNK inhibitor kidney toxicity. I also very much thank Michael Engeli for doing my last western blot experiments for me – without your help I would not have been able to finish on time my second manuscript and the thesis itself!

On a personal note, I would to thank all the master and PhD students at the Center for Molecular Cardiology for making my everyday stay there so enjoyable. In particular, I would like to thank Julien Weber and Daniel Gaul for tolerating my constant talking, for always making me laugh, for listening to my personal problems, and for basically being the best colleagues one could ever ask for! Thank you also Daria Vdovenko, Remo Specha, and Martin Reiner for the all the jokes and the great company. Thank you Natacha Calatayud and Michael Engeli for being so nice and helpful master students. I cannot thank enough everyone personally. You all made my stay in the lab really enjoyable despite the long hours of hard work and failed experiments!

Outside the lab, I would like to thank my awesome Bulgarian folk dance group “Ludi Mladi” for providing a much needed stress outlet and social support. Thank you Albena, Nade, Silvi, Vladi, Rayna, Lilly for being such great dance companions and friends. Thank you Milena for your enormous efforts in doing everything you can for the group and for keeping us together, and thank you for always being there for me when I needed your support and advice for my personal problems! Thank

you Tyanko for never refusing a beer after a horrible day at work, and for always listening to me complaining about work! Thank you Pavka for being the best flatmate I could ever imagine, for putting up with my constant trolling, and for the tough but much needed and appreciated everyday support! Thank you Pencho, Kremi, Emi, Tyanko, Pavka for being the best friends ever in the entire world! You have no idea how much you have helped me throughout these three years – without you I would not have been able to survive through all the work stress! Finally, thank you Kristina Kakalacheva for helping me so much with my PhD application for this particular position – without your advice and support I probably would not be here at all!

Last, but not least, I would like to thank my family for always supporting me throughout these years. I apologize for not calling you more often as you wanted, but I needed other stress outlets and I didn`t want to bother you with my work problems. Thank you for still taking care of me even though I was physically not at home!

Petia Ivanova Doytcheva

Institute of Veterinary Physiology
University of Zurich - Winterthurerstrasse 260
8057 Zurich, Switzerland
+41 (0) 44 635 64 76 doytcheva@vetphys.uzh.ch

Nationality: **Bulgarian**
Date of Birth: **18/03/1986**

Education

01/2013 to date **University of Zurich, Switzerland**
PhD in Molecular Medicine with thesis topic "Molecular mechanisms of the rapid and weight loss-independent beneficial cardiovascular effects of Roux-en-Y gastric bypass surgery"

10/2008 – 09/2009 **Imperial College London, United Kingdom**
Merit M.Sc. in Molecular Medicine with thesis topic "Alternative splicing of Factor VIII in pulmonary endothelial cells"

09/2005 – 06/2008 **Jacobs University Bremen, Germany**
B.Sc. in Biochemistry and Cell Biology with thesis topic "Prokaryotic and eukaryotic protein-DNA interactions"

09/2000 – 05/2005 **American College of Sofia, Bulgaria**
Graduated with Summa Cum Laude with emphasis on English, literature and history

Practical Experience

09/2013 – 05/2015 **University of Zurich, Switzerland**
Teaching assistant in the Institute of Physiology's practical courses for medical students; responsible for helping and supervising second-year medical students with EKG, blood pressure, and blood flow Doppler measurements

09/2007 – 05/2008 **Jacobs University Bremen, Germany**
Teaching assistant in the Advanced Biochemistry and Molecular Biology I and II courses; responsible for correcting and grading second-year student homeworks and exams

Research and Project Experience

01/2011 – 12/2012 **European Institute of Oncology, IFOM-IEO Campus, Milan, Italy**
Research studentship in the group of Prof. Dr. Pier Giuseppe Pelicci
Project: Characterization of a novel p53-p66shc signalling pathway in oxidative stress and aging

09/2010 – 12/2010 **Institute of Cancer Research, London, United Kingdom**
Research internship in the group of Dr. Tomoyuki Sawado
Project: PCNA mutagenesis in mouse embryonic stem cells

06/2007 – 08/2007 **EMBL Molecular Medicine Partnership Unit, Heidelberg, Germany**
Research internship in the group of Dr. Gabriele Neu-Yilik
Project: Nonsense-mediated decay of p53 mRNA

Skills and Achievements

Languages: **English:** fluent **French:** working knowledge
Italian: basic knowledge **German:** basic knowledge

Workshops / Conferences:
> January 14-15, 2016 - Oral presentation at the Cardiovascular and Metabolic Research Meeting, Fribourg, Switzerland
> August 29-31, 2015 - Poster presentation at the European Society of Cardiology Congress, London, UK
> June 10-12, 2015 - Oral presentation at the Swiss Society of Cardiology Joint Annual Meeting, Zurich, Switzerland
> November 16-19, 2014 - Poster presentation at the American Heart Association Scientific Sessions, Chicago, USA

Publications: Osto E*, Doytcheva P* et. al. Rapid and body weight-independent improvement of endothelial and high-density lipoprotein function after Roux-en-Y gastric bypass: role of glucagon-like peptide-1. Circulation. 2015 Mar 10;131(10):871-81.

Awards: Best abstract 2015 - Topic Cardiovascular Biology
Swiss Society of Cardiology Joint Annual Meeting, June 10-12, 2015, Zurich